COUPLING FLAGELLAR GENE EXPRESSION TO FLAGELLAR ASSEMBLY IN *CAULOBACTER CRESCENTUS*

Christopher M. Birchall B.Sc. M.Res.

Thesis submitted in partial fulfillment of the requirements
of the regulations for the degree of Doctor of Philosophy

Newcastle University
Faculty of Medical Sciences
Institute for Cell and Molecular Biosciences
Centre for Bacterial Cell Biology
November 2011

Abstract

Bacterial flagellar filaments are long cell surface appendages that generate propulsion for movement. They also play key roles in surface attachment and host-bacterial interactions. The filament is made from a single protein species flagellin. Approximately 45 % of annotated flagellar systems possess multiple flagellin genes. We have investigated the ability of *Caulobacter crescentus* to build a flagellar filament using six flagellins: FljJ, FljK, FljL, FljM, FljN and FljO. Our analysis showed that this flagellar system exhibits extensive structural redundancy, in that one species of flagellin is sufficient to sustain motility. However, when that flagellin is FljJ cells are non motile.

Distinct flagellar assembly checkpoints are utilised by bacteria in order to coordinate and couple flagellar gene expression to the assembly pathway. One of these checkpoints, hook-basal-body completion, is sensed and overcome by the secretion of a flagellar-associated secretion substrate. This mechanism results in a system switch to the export of proteins, which are needed for filament assembly. In *C. crescentus* the post-transcriptional regulators FlbT and FlaF have been implicated to function at this switch. As the flagellins themselves are being secreted we asked the logical question: are the flagellins involved in subunit feedback control of the regulation of filament assembly? In a bacterial two-hybrid assay, FljJ was the only flagellin able to interact with FlbT and FlaF. Furthermore, FljJ along with FlbT was found to interact with flagellin mRNA.

In light of our data we a propose model for the regulation of flagellar filament assembly in *C. crescentus* and discuss the implications with respect to other flagellar systems

In loving memory

of

Rene Shepherd

Acknowledgements

I would like to begin by thanking my supervisor, Dr. Phillip Aldridge. Your help and support throughout this project has been tremendous. For the frequent moral encouragement whilst drinking a pint of beer or two: Cheers Phil. My friends Chrissie, Susie, Kritchai, Martin, Alex, Jonathon, Alison, Helen, Wendy and Tom: thank you for your great advice and always being willing to help. Thank you to everyone who resides on Level 2 of the Centre for Bacterial Cell Biology. Finally, a huge thank you goes to my family and the Imeson family, for their emotional and financial support.

I better not forget Emma, thank you. B402

Project funding: BBSRC

Research contributions: The following people have performed or assisted experiments in this thesis. Their names are referenced where appropriate: Dr. Phillip Aldridge, Dr. Alex Faulds-Pain, Dr. Wendy Smith, Dr. Shuichi Nakamura, Christine Aldridge, Giulia Grimaldi, Prof. Colin Harwood, Prof. Franz Narberhaus and Prof. James Gober.

Christopher M. Birchall

November 2011

"Any problem solved is a new problem made"

Karl Pilkington

(2008)

Table Of Contents

Table Of Figures

Table Of Tables

Abbreviations

α-helix	Alpha helix
A	Adenosine
Amp	Ampicillin
ANOVA	Analysis of variance (Statistical test)
APS	Ammonium persulfate
BSA	Bovine Serum Albumin
C	Cytosine
c-di-GMP	bis-(3',5')-cyclic diguanylic acid
C-ring	Flagellar cytoplasmic ring
C-terminus	Peptide carboxy terminus
$CaCl_2$	Calcium chloride
cAMP	Cyclic adenosine monophosphate
CAPS	*N*-cyclohexyl-3-aminopropanesulfonic acid
Co-IP	Coimmunoprecipitation
DIG	Digoxigenin
DNA	Deoxyribose nucleic acid
DMSO	Dimethyl sulphoxide
dNTP	Deoxyribonucleotide triphosphate
DNase	Deoxyribonuclease
DTT	DL-Dithiothreitol
EDTA	Ethylenediaminetetraacetic acid
EM	Electron microscopy
EPS	Extracellular polysaccharide
g	Gravity
G	Guanine
GFP	Green fluorescent protein
H_2O	Water
HBB	Flagellar hook basal body
HCl	Hydrochloric acid
His	Histidine
hr	Hours
IM	Inner membrane
IHF	Integration host factor

IPTG	Isopropyl β-D-1-thiogalactopyranoside
Kan	Kanamycin
KCl	Potassium chloride
L or l	Litre
L-ring	Flagellar Lipopolysacchride ring
LB	Luria Bertani
LC/MS	Liquid chromatography coupled mass spectrometry
M	Molar
MALDI-TOF	Matrix-Assisted Laser Desorption/Ionization Time of Flight
mA	Milli Amps
MCS	Multiple cloning site
$MgCl_2$	Magnesium chloride
min	Minutes
ml	Millilitre
mM	Millimolar
mRNA	Messenger ribonucleic acid
MW	Molecular weight
N-terminus	Peptide amino terminus
NaCl	Sodium chloride
nal	Naladixic acid
nM	Nanomolar
nm	Nanometer
OM	Outer membrane
ONPG	*ortho*-Nitrophenyl-β-galactoside
OD	Optical density
P-ring	Flagellar peptidoglycan ring
PAGE	Polyacrylamide gel electrophoresis
PBS	Phosphate buffered saline
PCR	Polymerase chain reaction
PD cell	Predivisonal cell
pmol	Picomoles
PYE	Peptone yeast extract
RNA	Ribose nucleic acid
RNase	Ribonuclease
RNAP	Ribose nucleic acid polymerase

rpm	Revolutions per minute
RT	Room temperature
SDS	Sodium dodecyl sulphate
SDS-PAGE	Sodium dodecyl sulphate polyacrylamide gel electrophoresis
sec	Seconds
ST cell	Stalked cell
SW cell	Swarmer cell
suc	Sucrose
T	Thymine
TAE	Tris-acetate ethylenediaminetetraacetic acid
TCS	Two component signal transduction system
TEMED	Tetramethylethylenediamine
tRNA	Transfer ribonucleic acid
TY	Tryptone yeast extract
T3S	Type three secretion
T3SS	Type three secretion system
U	Uracil
UV	Ultra violet
V	Volts
v/v	Percentage volume concentration
WHO	World Health Organisation
WT	Wild type
X-gal	5-bromo-4-chloro-3-indolyl-β-D-galactopyranoside
5’	5 prime end of DNA/RNA
3’	3 prime end of DNA/RNA
µl	Microlitre
µM	Micromolar
µm	Micrometer
λ	Wavelength

Chapter 1. Introduction

The ability of microorganisms to adapt to their surroundings and survive in the most inhospitable environments is remarkable. The metabolic versatility of the prokaryotes is an invaluable trait that has evolved through the ages of life. It has enabled one of their members, bacteria, to colonise the majority of environments under the earth's atmosphere; including those where no other organism can exist. This amazing feat has impacted our lives as human beings in both a positive and negative fashion. Vast amounts of money are spent each year on the treatment of microbial infections of both human, plant and animal. Equally, money is spent on scientific research to try to better understand the mechanisms that bacteria employ to avoid succumbing to antimicrobials we attack them with. For example, a 2010 report by the World Health Organisation estimated the global burden of Tuberculosis (*Mycobacterium tuberculosis*) in 2009 to be approximately 9.4 million incidences (WHO: 2010 report on global tuberculosis control). Furthermore, the amount of funding available for the control of Tuberculosis in 22 high-burden countries in 2011 was estimated to reach US$ 3.0 billion (WHO: 2010 report on global tuberculosis control). In stark contrast to the above, through years of developments in biotechnology we have engineered bacteria and utilised them to our advantage. Whether it is using them to efficiently produce biological products for the use in medicine, utilising their metabolic pathways in the production of biofuels, or simply exploiting their ability to improve the flavour of cheese (Chemier *et al*., 2009; Smit *et al*., 2005). Therefore, it is of great importance to our own lives that we continue to research and strive to understand how bacteria function and crucially how they survive.

1.1 Bacterial Survival: Sense and Respond

In order to survive in their environment and be successful different bacteria utilise an array of different survival strategies. Underpinning the various strategies is concept of being able to sense and respond. It may be sensing changes in the external environment and then responding by modulating metabolic pathways. It can also be sensing internally the different stages of cellular development and responding through regulation of the processes occurring. Bacteria have evolved and developed sophisticated mechanisms to do such tasks. Arguably, the most prevalent and key mechanism utilised by bacteria to do this is the two-component signal transduction

pathway. The main topic of this thesis is motility, specifically with respect to the bacterium *Caulobacter crescentus*. However, in order to discuss the mechanisms of motility, we need first to understand the concept of two-component signal transduction. Two-component systems (TCS) regulate diverse processes such as virulence, stress response, competence, motility and chemotaxis. TCS's were first characterised some 40 years ago and through years of research their involvement in the biology of a wide range of scientific fields has emerged time and time again. We will discuss specific examples of how TCS's are utilised in survival in the following sections, however, first we must define exactly what two-component signalling is and what components are involved. In the simplest and classical sense, a TCS will consist of one membrane-bound sensor kinase and a cognate cytoplasmic response regulator. Environmental or cellular stimuli are sensed by the sensor kinase and that information is then passed to the response regulator via protein phosphorylation. In doing so this activates the response regulator, which generally will then respond by modulating gene expression (Buelow and Raivio, 2010). The sensor kinase is comprised of two major domains: (i) an input, and (ii) a catalytic (Figure 1). The variable N-terminal input domain senses the signal and is located facing either the cytoplasm or extracellular environment. The conserved catalytic domain is located in the cytoplasm and houses an ATP-binding kinase and the site for phosphorylation (Gao *et al*., 2007). The response regulator is also comprised of two domains: (i) a receiver, and (ii) an output (Figure 1). The conserved N-terminal receiver domain is specific for its cognate sensor kinase. The variable C-terminal output domain functions to enforce the response that usually is the binding of DNA and regulating gene transcription. Signal detection results in the ATP-dependent autophosphorylation of a specific histidine residue in the catalytic domain of the sensor kinase. The phosphoryl group is then transferred from the histidine to a conserved aspartate residue on the receiver of the response regulator, which in turn alters the activity of its output domain triggering the response (Dutta *et al*., 1999; Parkinson, 1993). One specific regulatory mechanism that is pertinent to this thesis is that of σ^{54}-dependent gene expression. Here the activation of transcription by σ^{54} relies exclusively on a TCS partner. σ^{54} is a bacterial alternative sigma factor encoded by the *rpoN* gene (Reitzer *et al*., 1987). Unlike the housekeeping σ^{70} family of sigma factors that recognise a -35 -10 promoter region, σ^{54}-RNA polymerases recognise a -24 -12 consensus upstream of the transcriptional start site of a gene (Barrios *et al*., 1999; Malakooti *et al*., 1995). The σ^{54}-RNA polymerase is unique in that it cannot initiate the activation of gene expression solely by itself. Instead it requires an enhancer binding

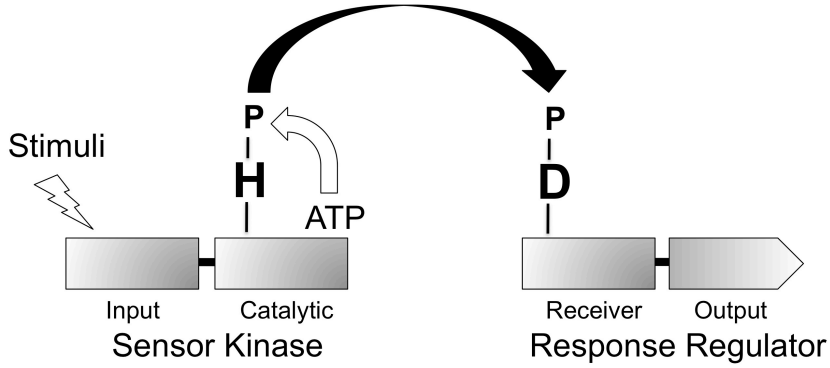

Figure 1: The bacterial two-component transduction system

A schematic illustrating the design of the classical two-component transduction system. Environmental or cellular stimuli activate a sensor kinase, which results in ATP-dependent autophosphorylation of a conserved histidine residue. The phosphoryl group is then transferred to a conserved aspartate on the cognate response regulator. The phosphorylated response regulator is now active to carry out the system response.

protein (EBP) that assists in the formation of open promoter complexes. These activators usually bind DNA approximately 80 to 150 nucleotide base pairs upstream of the promoter region and contact σ^{54}-RNA polymerase by looping out the DNA in between the two proteins (Osterberg *et al*., 2011). This mechanism provides a tight level of transcriptional control as the σ^{54} promoters will be silent when the EBP is inactive or absent. These proteins are typically comprised of three functional domains: an N-terminal receiver domain, a central ATPase, and a C-terminal DNA binding domain (Morett and Segovia, 1993). The receiver domain is phosphorylated by a cognate sensor histidine kinase. This activates ATPase activity, which leads to open complex formation in conjunction with RNA polymerase holoenzyme.

The abundance of different TCS's, all with different functions poses the question: how can a bacterial cell prevent detrimental cross-talk between TCS's? Recent work has shed light on this in revealing that cognate sensor kinase-response regulator pairs, co-evolve to maintain specificity (Skerker *et al*., 2008). The mutation of conserved amino acid residues in the catalytic domain of a sensor kinase resulted in it activating a response regulator with which it was normally incompatible. This simple model allows a bacterium to utilise TCS signalling in all cellular processes should it require to do so without the risk of a signal being lost. The classical TCS architecture is conserved in all systems, however, as more and more novel types are discovered it is becoming clear that in one particular TCS there may be great variation in: (a) the number of protein species involved and, (b) the structural and function of those proteins. We will now discuss important bacterial survival strategies that have been well characterised, and along the way highlight some key TCS that regulate those processes.

1.2 Survival Strategies: Staying Put

In a favourable environment rich with nutrients, sessile growth is a conventional way of life for many bacterial species. Being immobile and fixed in one place, sessile bacteria utilise a number of different mechanisms to secure survival.

1.2.1 *Sporulation: Bacillus subtilis*

The ability of a microorganism to exist as a spore, can be a vitally important strategy towards surviving adverse conditions. Not only has the process of sporulation been observed for many different species of bacteria, but also species of yeast and fungi (Piekarska *et al*., 2010; Ross and Abel-Santos, 2010; Yan *et al*., 2011). The

transformation from vegetative growth to the passive dormant state of a spore increases durability to detrimental environmental pressures, such as nutritional or chemical stresses. Furthermore, spores provide an effective way of cell dispersal relying simply on abiotic forces to disseminate them to new environments where the probability of survival might be increased. The latter example is crucial to sustaining intra-species genetic variation during the sexual or asexual life cycle of fungi (Roper *et al*., 2011). To be clear, the reference here to the dispersal of spores is not classified as motility, as the cells themselves are non-motile and cannot exclusively generate directional movement. There are, however, examples of bacterial spores that possess cell surface appendages used for motility (Uchida *et al*., 2011). Mechanisms of motility will be discussed in the following sections. Bacterial spores formed in response to stress can germinate and reinitiate vegetative growth upon being re-exposed to favourable conditions (Moir, 2006). This provides an outstanding biological mechanism utilised by bacteria in order to persevere through the 'bad times', and then proliferate during 'the good times'. Consequently, understanding bacterial sporulation has become a major focus of our efforts over the last couple of decades. Understanding the role of spores in human disease and how to control their spread is vital to public health (Mallozzi *et al*., 2010). But equally as important, understanding the intricate processes that occur during sporulation and collectively using them as a model to better understand cellular differentiation in bacteria and eukaryotes (Errington, 2010).

Actively growing cells of the Gram-negative bacterium, *Bacillus subtilis*, are induced to differentiate into endospores upon carbon or nitrogen starvation (Burkholder and Grossman 2000). At the heart of this process, from the sensing of nutrient depletion to the response of forming an endospore is, TCS signalling. If we consider just the induction of sporulation then: environmental signals result in the activation of the master transcriptional response regulator, Spo0A, via a phosphorelay of sensor kinases and intermediary response regulators (Burbulys *et al*., 1991). Activated Spo0A then begins the process of asymmetric cell division with an aim of producing a spore (forespore) and a mother cell, which is required for endospore formation (Piggot and Hilbert, 2004). There are five known sensor kinases involved in this system: KinABCDE. Each of them individually, have the ability to activate, Spo0F, a response regulator upstream in the process from Spo0A (Jiang *et al*., 2000). Spo0F activates Spo0B, which in turn phosphorylates and activates Spo0A. The accumulation of Spo0A~P then stimulates axial filament formation of chromatin across the cell body, polar septation leading to asymmetric division, and the expression of genes required for

cell-type-specific gene expression (Fujita and Losick, 2005). To complete the process it is crucial that different programs of gene expression occur within the mother cell and the forespore. This is achieved by the spatial compartmentalisation of cell specific sigma factors that direct the process of spore maturation. However, Spo0A continues to function as a mother cell-specific transcriptional regulator after it has initiated the beginning of the process (Fujita and Losick, 2003).

1.2.2 *Biofilms: Pseudomonas aeruginosa*

B. subtilis, along with other Gram-negative and Gram-positive species, is also capable of forming surface associated sessile multicellular communities known as biofilms (Branda *et al*., 2004; O'Toole *et al*., 2000). Like the process of sporulation: creating and living in a biofilm can protect a population of cells from environmental pressures. These communities can be tolerant to antimicrobials and therefore subsequently are responsible for many persistent and chronic bacterial infections of man (Costerton *et al*., 1999). They can be formed by a single bacterial species or multiple species and thus provide interesting opportunities to study mixed microbial communities (Yang *et al*., 2011).

Cells within the biofilm are contained within a self-produced matrix of exopolysaccharide polymers (EPS) that function as a protective barrier (Flemming, 2011). This presents a regulated and favourable environment in which to exist thus enhancing survival. Depending on the microorganism involved and other variables such as temperature and nutrient availability, the composition of the EPS can vary greatly (Flemming and Wingender, 2010). Extracellular DNA (eDNA) has been identified to exist within the EPS. It is thought to function somehow in stabilising the matrix and furthermore, it has been confirmed to be required for the initial biofilm establishment of some species (Conover *et al*., 2011; Whitchurch *et al*., 2002). In contrast, eDNA secreted by the dimorphic bacterium, *Caulobacter crescentus*, inhibits the ability of its motile cell type to settle in the biofilm (Berne *et al*., 2010). There is evidence available to suggest biofilms also promote increased genetic diversity among different species of bacteria through horizontal gene transfer as a result of close cell-cell contact and communication (Antanova and Hammer, 2011; Roberts and Mullany, 2010).

Much interest in biofilm research has focused on the opportunistic Gram-negative pathogen, *Pseudomonas aeruginosa*. Experimental studies have demonstrated the key role played by a multitude of TCS's in the stages of biofilm development and in the virulence of the bacterium (Chand *et al*., 2011; Petrova and Sauer, 2009). These

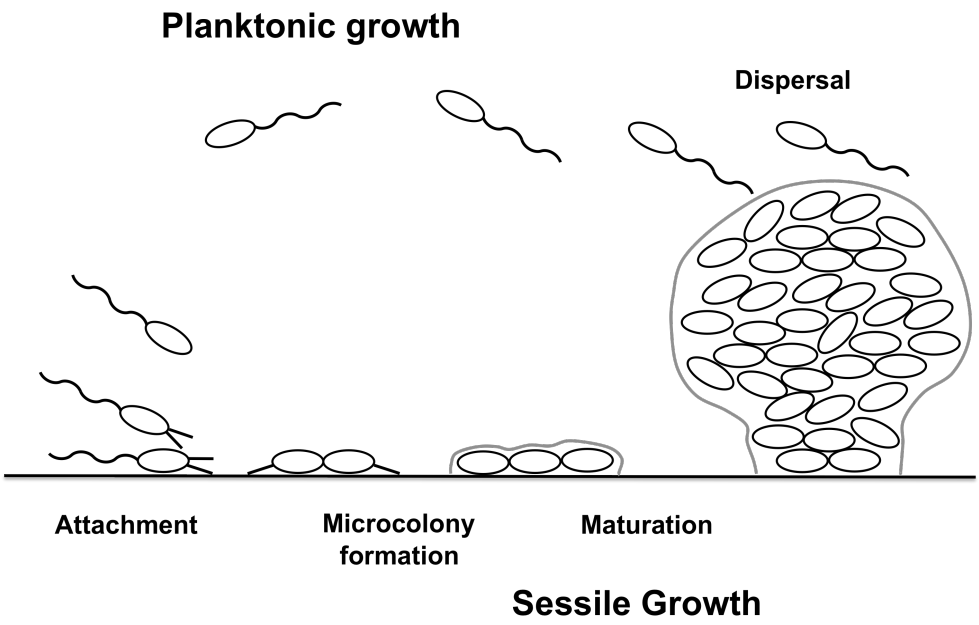

Figure 2: Bacterial biofilm formation

A schematic illustrating the various stages of development during biofilm formation. The extracellular polysaccharide matrix (EPS) is depicted in grey. The switch from a planktonic lifestyle to that of a sessile one begins with a motile bacterial cell settling on a surface. Both flagella and pili have been demonstrated to be important for attachment. Flagellar assembly/utilisation is then repressed and cells begin to move together using pili (see twitching motility). A monolayer biofilm is formed which can devlop into a mature complex biolfilm. Cells can re-enter a planktonic lifestyle by expressing flagella and swimming to disperse from the biofilm community.

biofilm developmental stages can be classified as: initial attachment, microcolony formation, maturation and finally dispersal (Figure 2) (Mikkelsen *et al*., 2011). Biofilm life is inextricably linked with a planktonic lifestyle. The entry into biofilm formation and the escape from rely on being able to move. *P. aeruginosa* has the ability to be motile: swimming in liquid environments by the means of a polar flagellum, and moving on surfaces utilising type IV pili (Dasgupta *et al*., 2003; Mattick, 2002). The flagellum and type IV pili are both bacterial cell surface appendages that will be discussed in more detail along with the concept of movement for survival in the following sections. We will instead here concentrate on the transition from a motile to sessile lifestyle within the biofilm. During this switch the flagellum is lost. It has been demonstrated that flagella are needed for the initial attachment to the surface on which the biofilm will develop (O'Toole and Kolter, 1998). Once attached, polar localised type IV pili are then required for the formation of a microcolony and early biofilm development. Importantly, however, for the biofilm to mature, flagella biogenesis has to be repressed. FleQ is the master transcriptional regulator of flagellar assembly in both P. aeruginosa (Arora *et al*., 1997). It is essential for the subsequent expression of a TCS (FleSR system) that couples flagellar gene expression to flagellar assembly: FleS is a sensor kinase and FleR is the cognate response regulator (Ritchings *et al*., 1995). FleQ has also been shown to repress the expression of the *pel* operon, which is involved in EPS synthesis, by binding the *pel* promoter (Hickman and Harwood, 2008). FleN, a flagellar protein that binds to and negatively regulates the activity of FleQ, reduces FleQ repression of the *pel* genes. However, maximal de-repression requires the ubiquitous bacterial secondary messenger molecule: bis-(3',5')-cyclic diguanylic acid (c-di-GMP) (Hickman and Harwood, 2008). The controlled synthesis and degradation of c-di-GMP and its influence on regulatory proteins affects a wide range of processes including motility and biofilm formation but also in cell cycle control (Jenal and Malone, 2006; Ross *et al*., 1991). So in *P. aeruginosa*, FleN/c-di-GMP regulation of FleQ provides a mechanism for the switching off TCS controlled motility and switching on the biofilm formation.

1.2.3 *Dimorphic bacteria: Caulobacter crescentus*

Both *P. aeruginosa* and *B. subtilis* have the ability to switch between planktonic and sessile growth. They do so in response to changing environmental signals. Other bacteria such as the dimorphic α-proteobacterium, *Caulobacter crescentus*, utilise an altogether different strategy, and undergo a major physical transformation every cell

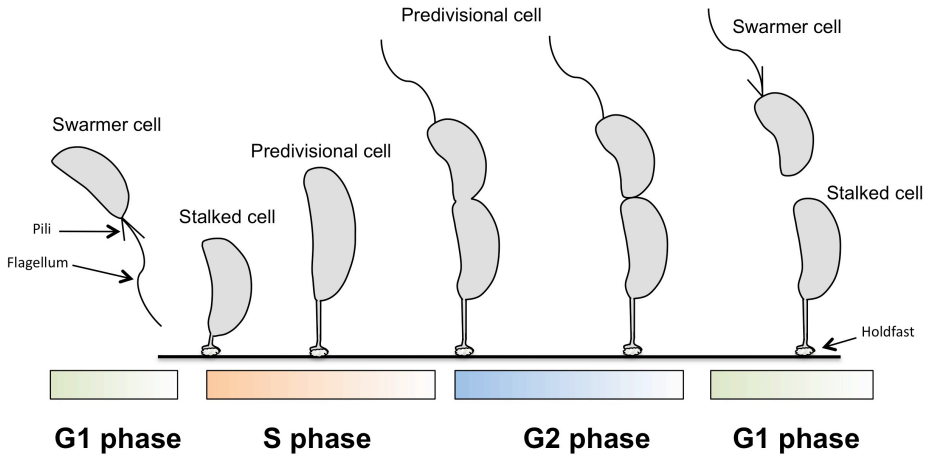

Figure 3: The life-cycle of *Caulobacter crescentus*

A schematic illustrating the dimorphic life cycle of *C. crescentus*. The *C. crescentus* swarmer cell (SW cell) is motile by means of a single polar flagellum. Upon differentiation into a stalked cell (ST cell), the flagellum is lost and replaced by a prostheca or stalk. At the tip of the stalk is an adhesive holfast, which anchors the cell to a surface. The ST cell initiates DNA replication and grows into a predivisional cell (PD cell). Differentiation of the new cell pole opposite the stalk begins with the assembly of a flagellum. Cell division produces two morphologically distinct daugther cells.

cycle. *C. crescentus* is a fascinating organism in that it inherently exploits both sessile and planktonic growth (Figure 3). Cell division in *C. crescentus* produces two cell types that are morphologically and behaviorally dissimilar to one another (Shapiro, 1976). One cell type is planktonic and referred to as the swarmer cell (SW cell). It is motile by means of a single polar flagellum and contains multiple pili at the same pole. The other cell type is sessile and known as the stalked cell (ST cell). Here the flagellum has been replaced by a long thin cytoplasmic extrusion of the cell called the stalk or prostheca. The ST cell is typically found attached to a surface via an adhesive polar organelle called the holdfast (Levi and Jenal, 2006; Ong *et al*., 1990). *C. crescentus* is a non-pathogenic gram-negative, oligotrophic α-proteobacterium found in freshwater environments (Poindexter, 1964). Presumably in the oligotrophic aquatic environments that *Caulobacter* spp. inhabit, anchorage to a surface provides a way of avoiding 'sinking' into the nutrient poor silt at the bottom of lakes/ponds. It is hypothesised that the stalk functions to extend the cell surface to help maximise efficiency of the translocation of nutrients (Poindexter 1981; Wagner *et al*., 2006; Wagner and Brun 2007).

Once the ST cell enters the S phase of its cell cycle, it becomes competent for DNA replication (Curtis and Brun, 2010). Replication and growth continues, as the cell becomes a predivisional cell (PD cell) entering G2 phase (Figure 3). At this time point, DNA replication is blocked and the cell begins to differentiate its cell poles. At the opposite pole to the stalk, a single flagellum is assembled. Subsequent cell division results in two morphologically distinct daughter cells, a SW cell and a ST cell. The SW cell is incompetent for DNA replication and thus cannot divide. It is therefore referred to exist in a separate and distinct life cycle phase: G1 phase (Figure 3). The sole purpose of the SW cell is to utilise cellular motility in order to disseminate away from the present location. After a fixed period of time, the swarmer cell undergoes a series of ordered events resulting in the loss of the flagellum and the cellular differentiation into a ST cell. The ST cell can then immediately begin a new round of cell division. The ST cell therefore makes use of a cyclic developmental program. In contrast, the SW cell undergoes non-cyclic development. The biological processes that occur in order to produce stable changes of cellular differentiation in *C. crescentus* have been researched extensively. For differentiation to ensue the generation of asymmetry during cell division is essential. This is achieved by the spatial and temporal regulation of key developmental proteins. Together these mechanisms permit the designation of the

separate fates of the two daughter cells. Importantly, TCS regulation is key to the cell cycle control of the creation of a SW cell and key to the removal of the flagellum.

CtrA is a global transcriptional response regulator that influences key events such as DNA replication, cell division and flagellar biogenesis (Quon *et al.*, 1996; Domian *et al.*, 1997). Through the direct activation or repression of approximately 95 genes, it regulates cell cycle and cell development in *C. crescentus* (Laub *et al.*, 2002). CtrA~P blocks the re-initiation of DNA replication in the PD cell. Additionally it switches on the expression of genes including those of the flagellar and pili regulon in order to begin cellular differentiation. Therefore, not surprisingly, CtrA has to be continually activated and deactivated during progression through the cell cycle. To ensure this happens correctly, it is subjected to strict temporal and spatial regulation within the cell. This is achieved through a variety of different regulatory mechanisms including proteolysis, protein phosphorylation and transcriptional control.

Activation of CtrA occurs via an essential phosphorelay exchange between the histidine kinase CckA and the phosphotransferase ChpT (Figure 4) (Biondi *et al*., 2006). ChpT phosphorylates CtrA and additionally the response regulator, CpdR (Figure 4). When in an unphosphorylated state, CpdR promotes the degradation of CtrA by the ClpXP protease (Iniesta *et al*., 2006). However, the phosphorylation of CpdR inactivates this function resulting in the stabilisation of CtrA. Therefore, when CckA is active it both activates CtrA and prevents CpdR-dependent degradation of CtrA. When the cell needs to re-initiate DNA replication, another essential response regulator, DivK, down regulates CckA kinase activity (Biondi *et al*., 2006) (Figure 4). DivK is a single domain response regulator, lacking an output domain. DivK~P controls CckA phosphorylation and thus CtrA, by interacting with and inhibiting the kinase responsible for CckA activation; DivL (Tsokos *et al*., 2011). DivK phosphorylation is controlled by two histidine sensor kinases, DivJ and PleC (Matroule *et al*., 2004). During S phase, DivK is phosphorylated by DivJ at the stalked pole and dephosphorylated by PleC at the swarmer pole (Figure 4): PleC is a bi-functional protein in that is can act both as a phosphatase (on DivK) and a kinase. By spatially controlling active DivK within the cell there exists a mechanism to allow differentiation to occur. *C. crescentus* not only has to time the production/removal of its flagellum in accordance with its cell cycle but also maintain polarity. Furthermore, the SW cell utilises pili and chemotaxis machinery located at the same pole as the flagellum. To create a flagellum at the SW cell pole (new pole) opposite the stalk, the asymmetric localisation of regulatory proteins is essential. Correct flagellum positioning at the SW cell pole relies on the protein TipN (Figure 5)

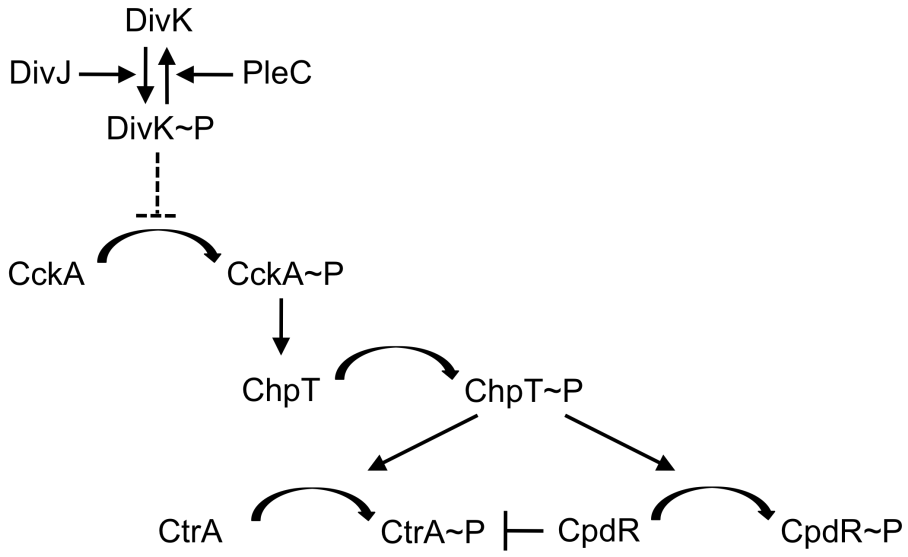

Figure 4: Two-component signal transduction regulation of CtrA (adapted from Bowers *et al.*, 2008)

The master cell cyle response regulator CtrA is activated by a two-component system (TCS) comprising of a phosphorelay exhange between the histidine sensor kinase CckA and the phosphotransferase ChpT. CtrA protein stability is sensitive the phosphorylation state of the response regulator CpdR. CckA activity is regulated by another TCS involving the response regulator DivK. The activity of DivK is modulated by the two sensor kinases, DivJ and PleC.

(Huitema *et al*., 2006). TipN is required for the polar localisation of a c-di-GMP phosphodiesterase protein, TipF (Figure 5). A deletion of *tipF* resulted in the decreased expression of flagellin protein and an absence of hook and flagellin secretion, indicating its involvement in flagellum biogenesis. Importantly, however, the absence of TipN resulted in the irregular positioning of flagella randomly across the cell surface (Huitema *et al*., 2006). TipN/TipF regulation of polar differentiation is thought to be a cyclic program. TipN and TipF exist in a SW cell at the pole opposite the flagellum and this localisation is maintained during the G1 to S phase transition (Figure 5). The ST cell initiates DNA replication becoming a PD cell and a flagellum is built at the TipN/F pole. Constriction of the division septum during cytokinesis, then results in TipN being localised to midcell followed by TipF. Thus, upon the completion of cell division TipN and TipF are localised such that they mark the site for flagellum assembly and SW pole differentiation (Figure 5) (Huitema *et al*., 2006).

The removal of the flagellum at the G1 to S phase transition is dictated by a special response regulator, PleD (Aldridge *et al*., 2003). Active PleD~P has diguanylate cyclase activity and catalyses the formation of c-di-GMP; which has been demonstrated to be influential in the switch from a planktonic to sessile life style in bacteria (See section 1.2.2) (Paul *et al*., 2004). PleD is phosphorylated by the kinase activity of PleC and DivJ. Surprisingly, it is actually DivK~P that controls PleC autokinase activity (Paul *et al*., 2008). In a SW cell both DivK and PleD are delocalised. As the G1 to S phase transition progresses, DivJ levels increase resulting in the phosphorylation of DivK and its localisation to the differentiating pole. It is thought that DivK and DivJ form a positive feedback loop leading to high DivK~P levels which result in the switch of PleC from phosphatase to kinase and the activation of PleD (Paul *et al*., 2008). PleD~P accumulates at the cell pole where as a result c-di-GMP levels rise and the flagellum is ejected by a yet uncharacterised mechanism (see later).

The ability to switch from a sessile life style to one that is planktonic is clearly advantageous. For example, in conditions of low nutrient availability, being able to swim allows colonisation of new niches preventing nutrient exhaustion. The sessile cells exploit the present location while the motile cells disperse in order to find new environments. *C. crescentus* cells have been shown to form both monolayer and complex biofilms. Pili are essential for forming the latter while it has been demonstrated that the SW cells being released from ST cell biofilm maintain a monolayer.

The concept of population heterogeneity is not unique to *C. crescentus* but occurs also in other non-related bacteria. For example, during normal growth *B. subtilis*

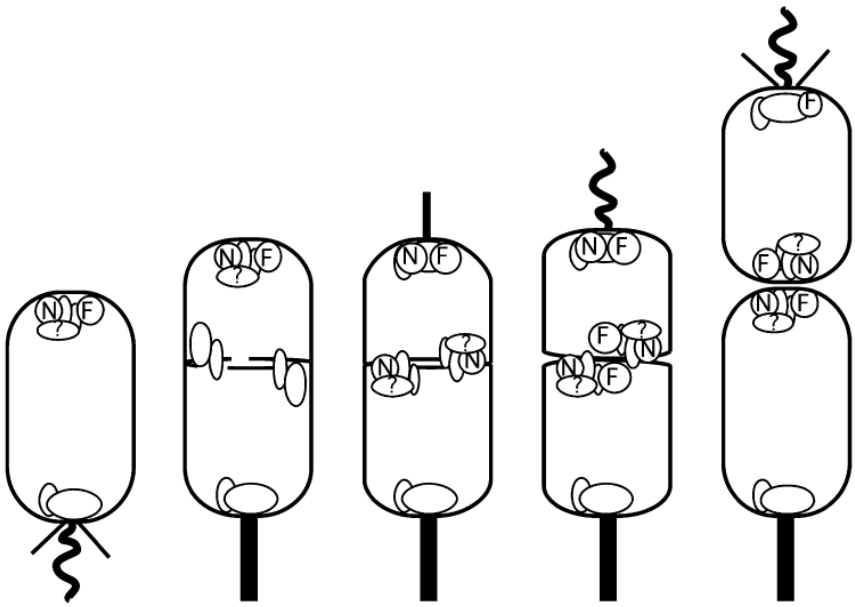

Figure 5: A proposed model for the TipN and TipF regulation swarmer pole differentation (taken from: Huitema *et al*., 2006)

TipN and TipF along with other unknown predicted proteins reside at the undifferentiated pole of the Swarmer cell (SW cell). TipN localises to midcell during cytokinesis and TipF follows. On completion of cell division both TipN and TipF are exclusively located at the pole where flagellum assembly will take place next. TipF is required for flagellar assembly, however, its exact function is yet to be determined.

cells exist concurrently in one of two morphologically distinct cell types: (i) motile and flagellated, or (ii) sessile and growing in long chains. It is the activity of the motility transcription factor, σ^D, that determines whether flagella are built and the cell swims (Helmann *et al*., 1988; Marquez *et al*., 1990). In an exponentially growing population, a proportion of the cells possess an active σ^D (motile) while other cells have an inactive σ^D (sessile) (Kearns and Losick, *et al*., 2005). As the population approaches stationary phase the prevalence of motile cells increases (Nishihara and Freese 1975). It has been recently shown that the transcriptional activator, SwrA, is required to modulate a higher proportion of the cell population to have an active σ^D (Kearns and Losick, *et al*., 2005). Furthermore, SwrA also stimulates hyper flagellation of a cell in preparation for swarming motility on a surface. Swarming is a form of flagellar mediated motility that occurs on surfaces (Fraser and Hughes, 1999). It has been suggested that the SwrA and σ^D regulation of motility is itself controlled by a bistable genetic switch that in responding to environmental signals specifically functions to maintain heterogeneity in the population (Kearns and Losick, 2005). This is in contrast, to *C. crescentus* where the generation of motility is a part of the normal life cycle of the bacteria. However, the reason for being motile in *C. crescentus* and *B. subtilis* is strikingly similar in that they both have a desire to maintain a heterogeneous population to enhance survival.

1.3 Bacterial Survival: Movement

For many bacteria, cellular motility is hugely important in enhancing survival. Motility driven by chemotaxis allows the bacteria to locate nutrients and occupy a preferred niche within the environment thus ensuring that movement isn't random. Chemotactic bacteria sense chemical gradients using chemoreceptor proteins that are part of the TCS family of proteins and located in clusters near the base of the flagella (Wadhams and Armitage, 2004). The chemical information is then relayed to the flagellar motor, which controls the direction of movement. We have already discussed the importance of motility in the establishment and release from a biofilm community. Here, one example is that, *P. aeruginosa* utilises two types of movement: flagellar-mediated and twitching motility. In fact movement in liquid environments or on solid surfaces is achieved by swimming, swarming, gliding, and twitching. These types of movement utilise a variety of different mechanisms (Jarrell and McBride, 2008). We will now discuss the different types of movement in more detail.

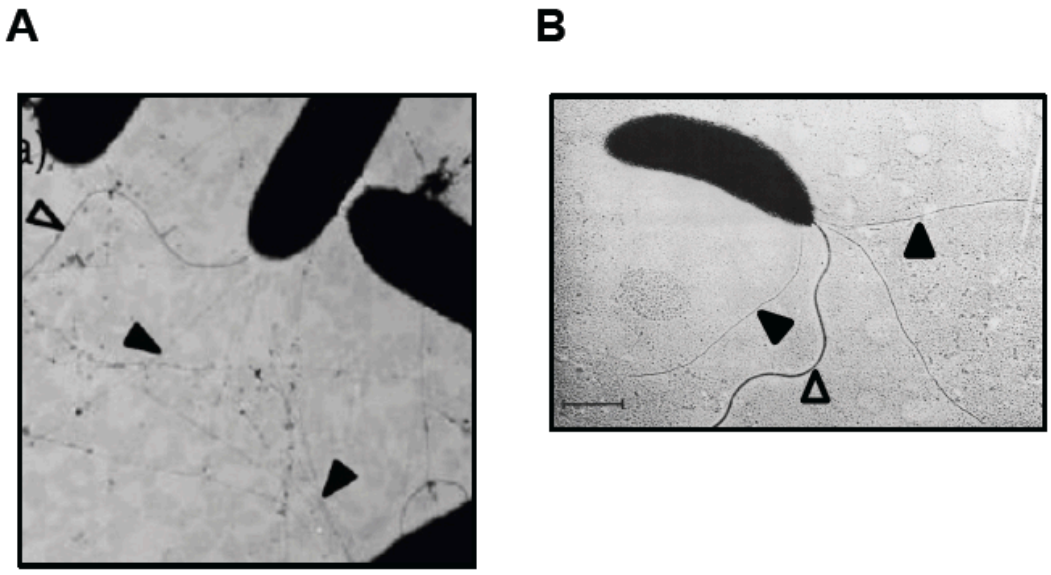

Figure 6: Bacterial cell surface appendages utilised during motility

Transmission electron micrographs showing bacterial Flagella and Type IV Pili. Filled arrows indicate pili and open arrows indicate flagella. **A.** *Pseudomonas aeruginosa* mPAO1 (taken from: Giltner *et al*., 2010). **B.** *Caulobacter crescentus* NA1000 (taken from: Sommer and Newton, 1988). Pili/Fimbrae are thinner than flagellar filaments, and are thus often referred to as hair-like.

1.3.1 *Twitching motility*

Twitching motility is a flagellar-independent form of bacterial movement over a surface (Mattick, 2002). This is a slow motion with movement of cells occurring at less than 1 μm/s (Harshey, 2003). It occurs on wet surfaces and is essential to establishment and development of a biofilm and also host colonisation by a number of plant and animal pathogens (Bocsanczy *et al*., 2011; Semmler *et al*., 1999; Taguchi and Ichinose, 2011). The mechanism relies on type IV pili. Pili are long thin surface appendages that are assembled and utilised by both Gram-positive and Gram-negative bacteria for conjugation (sex pilus), motility (type IV pili) and surface attachment (fimbrae/type IV pili) (Figure 6) (Kline *et al*., 2010; Schroder and Lanka, 2005). Type IV are unique amongst pili in that they can retract. It is the action of retracting, extending and retracting of the pili that provides the force to allow the bacterial cell to move. This physical motion has been visually observed in numerous bacteria, including *P. aeruginosa* where the extension and retraction of fluorescently labelled type IV pili was characterised (Skerker and Berg, 2001). From this particular study it was concluded that the cells moved by pulling themselves along the surface during a retraction, as opposed to pushing during an extension. It is predicted that the inherent flexibility of the structure does not provide enough strength to generate the force required to push a cell forward upon contact of the pilus with the surface (Skerker and Berg, 2001). The tip of the pili acts as an adhesin factor and facilitates surface binding (Lee *et al*., 1994). *pilA*, encodes the major structural subunit pilin, that polymerises to form the long pilus filament during the assembly process (Craig *et al*., 2003). The energy required for retraction comes from ATP hydrolysis, and is used to remove pilin subunits from the base of the pilus (Kaiser 2000). The removed subunits are then recycled during pilus assembly and extension. Its transcription is controlled by a TCS comprised of PilS/PilR (Hobbs *et al*., 1993). PilR belongs to a large family of Nitrogen regulatory protein C - σ^{54} transcriptional activators (NtrC) (Hobbs *et al*., 1993). It functions as the response regulator that activates *pilA* transcription in a σ^{54}-dependent manner. PilR is activated by its cognate membrane-bound sensor kinase PilS (Boyd, 2000). The signal that allows PilS to activate PilR is currently unknown, however upon activation, PilR binds upstream of the *pilA* promoter and turns on its the expression in conjunction with σ^{54} (Jin *et al*., 1994).

1.3.2 *Gliding motility*

Gliding motility is the movement of cells on solid surfaces without the use of flagella. This form of movement is very slow in comparison to other forms such as flagellar mediated motility, with cells moving around 1 or 2 μm/min (Harshey, 2003). Cells capable of moving in this way possess type IV pili, which they utilise during one form of gliding motility, Social motility (S-motility), as well as twitching. S-motility functions in a similar way to twitching motility and involves pilus retraction and extension resulting in the coordinated movement of groups of cells. However, while twitching motility occurs in a localised area, cells utilising S-motility cover larger distances. A second mechanism of gliding motility, Adventurous motility (A-motility), requires no flagella or pili and involves the oscillation of helical bacterial cytoskeleton filaments (Nan *et al*., 2011). Gliding motility is utilised by a wide range of bacteria that colonise many different environments, such as the Myxobacteria (Myxococcales) and the Cyanobacteria (Hoiczyk, 2000; Nan and Zusman, 2010). Gliding motility is an important survival mechanism for the cells of *Myxococcus xanthus* as they lack flagella and cannot swim. *M. xanthus* cells use gliding to discover nutrients in the soil environment, in which they inhabit (Berleman and Kirby, 2009). Furthermore, movement enables them to find prey microorganisms, which they 'kill' (digest) in order to provide a source of nutrients (Berleman and Kirby, 2009).

1.3.3 *Flagellar motility*

Flagella are complex biological macromolecular machines used for bacterial locomotion. A single flagellum comprises of a basal membrane-embedded molecular motor that produces the power to rotate a filamentous axial substructure, which concludes in a long filament extension. The filament works like a propeller to generate propulsion for movement. Flagellum-mediated motility has been studied extensively in a number of organisms, particularly the enteric bacteria (which we define here as *E. coli* and *S.* Typhimurium), and is associated with both swimming and swarming. Swimming motility occurs in liquid environments while swarming involves a coordinated migration of hyper-flagellated cells across a solid surface (Fraser and Hughes, 1999). Astonishingly, genes encoding for flagellar systems are present in 45 % of annotated bacterial genomes and thus flagellar-mediated motility can be considered a major form of movement within the bacterial kingdom (Faulds-Pain *et al*., 2011). For some pathogenic bacteria flagellar motility and chemotaxis is an essential virulence factor for host colonisation and infection. *Helicobacter pylori* is a major human gastric pathogen

associated with gastric ulcers and gastric cancers (Lopez-Vidal *et al*., 2008). *H. pylori* cells swim by the means of a cluster of 4-6 polar flagella (Douillard *et al*., 2010). Nonchemotactic mutants of *H. pylori* are greatly reduced in initial infection of mice and are outcompeted by wild type cells (Terry *et al*., 2005). Furthermore, the mutants are unable to colonise all regions of the stomach. *H. pylori* needs motility in order to remain in the mucus layer close to the stomach epithelial cells. Without motility it is likely that bacteria will be carried away into the lumen by the rapid turnover of mucus that is being continuously secreted from mucosal glands (Schreiber *et al*., 2004).

There are examples of non-pathogenic bacteria too that require to ability to swim in order to be successful. *Vibrio fischeri* is a bacterium that exists in a remarkable symbiotic relationship with the Hawaiian bobtail squid (*Euprymna scolopes*). *V. fischeri* colonises juvenile squid and produce light by means of bioluminescence (Ruby and Asato, 1993). This process helps to prevent the squid from casting a dark shadow on the ocean floor during moonlit nights and increases its survival (Visick and McFall-Ngai, 2000). *V. fischeri* is motile by means of 1-5 polar flagella (Millikan and Ruby, 2004). Flagellar-mediated motility is essential for initiating the colonistation of the squid's internal light organ and it also increases the retention of bacterial cells (Millikan and Ruby, 2004).

One striking observation among these different types of motility is that they all generate quite widely varying speeds of movement. For example, single cells of *P. aeruginosa* exhibiting twitching motility have been recorded moving at speeds up to 0.2 μm/s (Skerker and Berg, 2001). Individual *Myxococcus xanthus* cells moving by the mechanism of gliding motility do so only at approximately 2 μm/min (Mauriello *et al*., 2010). This is in complete contrast to some of the recorded swimming speeds generated by flagellar motility. *Vibrio* spp., *C. crescentus* and *Bdellovibrio bacteriovorus* move at speeds up to: 60 μm/s, 55 μm/s, and 160 μm/s respectively (Faulds-Pain *et al*., 2011; Lambert *et al*., 2006; McCarter 2001). Both twitching and gliding motility occurs on a surface whereas flagellar mediated swimming is in liquid environments so it may be no surprise that the latter mechanism generates faster speeds. However, individual cells utilising flagella for swarming motility on a surface can move at speeds of up to 10 μm/sec, which is significantly faster than other surface motility (Harshey, 2003). These observations suggest that regardless of the environment, if a bacterium needs to move quickly then utilising flagella to do so is the best way to go. So why do swimming bacteria move at different speeds if they are all utilising the same mechanism: i.e. Flagella? One answer could be differences in the number of flagella per cell. It would

be sensible to think that the greater the number of flagella the greater the speed. However, *Salmonella enterica* serovar Typhimurium typically possesses 6-8 flagella per cell and swims at speeds around 20-50 μm/s (Magariyama *et al*., 2001), where as *C. crescentus* generates one polar flagellum per cell and swims much faster at speeds approximately 55 μm/s (Faulds-Pain *et al*., 2011). The multiple flagella of *S.* Typhimurium have to bundle together and it is possible that the thickness of the bundle causes resistance as the cell moves. Therefore, it is likely that differences in the number, localisation, and the structure of flagella play all influence swimming speed.

1.4 Flagella Distribution and Numbers

The number and distribution of flagella differs between bacterial species (Figure 7). Monotrichous bacteria such as *C. crescentus* and *P. aeruginosa* use a single polar flagellum for swimming (Figure 6 and 7) (Poindexter 1964; Dasgupta *et al*., 2003). *Salmonella* spp. typically produce six to eight peritrichous flagella that are distributed over the whole cell surface. The symbiotic bioluminescent bacterium, *Vibrio fischeri*, is lopotrichous with a cluster of up to five flagella co-located at the pole of the cell (Figure 7) (Millikan and Ruby, 2004). Some bacteria that swim by means of a polar flagellum will, under certain conditions, switch to a separate lateral flagellar system that allows for swarming on solid surfaces (Sar *et al*., 1990; Wilhelms *et al*., 2011). Some research has been carried out to investigate how a bacterial cell regulates the placement of a flagellum on the cell surface. In the polar flagellar systems of *Pseudomonas* spp. and *Vibrio* spp., flagellar placement has been shown to require the GTP-binding protein FlhF (Bange *et al*., 2007; Kusumoto *et al*., 2006; Kusumoto *et al*., 2008). Deletion of the *flhF* gene in *P. aeruginosa* results in the decreased expression of flagellar genes and the assembly of flagella at nonpolar locations (Murray and Kazmierczak, 2006). FlhF localises to the cell pole where it plays a role in the regulation of flagellum biogenesis at that location. A model for FlhF-dependent flagella placement has recently been suggested based on work carried out in *V. cholerae*. FlhF intrinsically localises to the cell pole, where it directly recruits FliF, the earliest flagellar structural protein (Green *et al.*, 2009). It is likely that the GTPase activity of the protein plays an important role in its function. However, it is important to note that in some species FlhF is essential for flagella assembly, while in others it is not (Brown *et al*., 2009). In complete contrast, a deletion of *flhF* in peritrichous flagellar system of *B. subtilis* does appear to affect

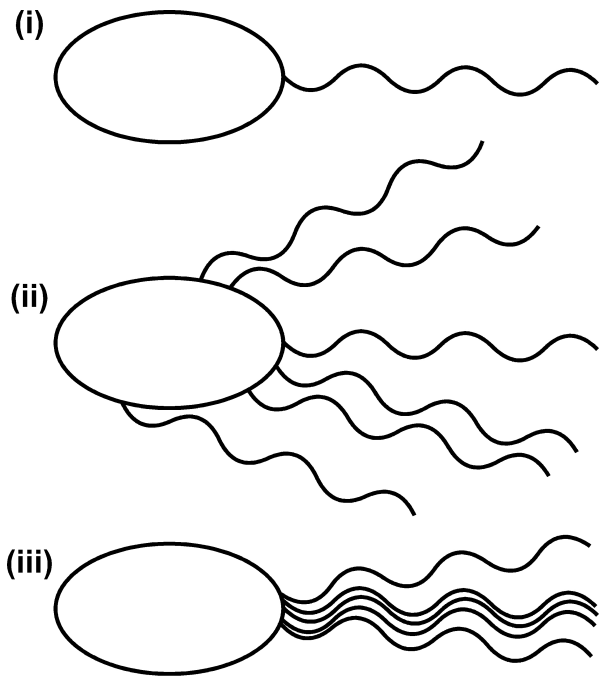

Figure 7: The spatial arrangement of flagella on the cell surface

(i) Monotrichous with a single polar flagellum; e.g. *Caulobacter* spp. **(ii)** Peritrichous with numerous flagellar distributed across the cell; e.g. *Salmonella* spp. **(iii)** Lopotrichous with numerous polar flagellar e.g. *Vibrio fischeri*.

flagella assembly in any way (Zanen *et al*., 2004). The *flhF* gene is absent from the enteric bacteria (Kanehisa *et al*., 2008). A second protein, FlhG, has been shown to reduce the polar localisation of FlhF through a direct protein-protein interaction (Kusumoto *et al* 2008). It is speculated that this acts as a mechanism to prevent the accumulation of FlhF at the cell pole, thus regulating the number of flagella produced. This hypothesis is consistent with the finding that FlhG negatively regulates the expression of the flagellar master regulator in *Vibrio* spp. (Correa *et al*., 2005; Kusumoto *et al*., 2006). In *C*. *crescentus*, correct flagellum positioning at the cell pole relies on the protein, TipN. Loss of *tipN* results in the mis-localisation of flagella (Huitema *et al*., 2006). Furthermore, TipN is required for the polar localisation of, TipF, a protein outside the flagellar regulon which has however been shown to required for flagellar assembly.

1.5 Flagellar Power Source

The flagellar motor at the base of the flagellum generates the torque required to rotate the structure and propel the cell forward. Torque being defined as a twisting force which causes rotation.. There are differences in the way bacteria generate the power required to rotate the flagellum. Both *E*. *coli* and *S*. Typhimurium couple proton (H^+) flow through the motor to power the flagellum (Berg, 1995). However, the H^+ driven motor is not exclusive among flagellar systems. Some bacterial species, including *V. alginolyticus, Vibrio cholerae* and certain members of the genus *Bacillus* (although not *Bacillus subtilis)* require sodium (Na^+) for motility (Atsumi *et al*., 1990; Imae and Atsumi, 1989; Kojima *et al*., 1999; Tokuda and Unemoto, 1982). Interestingly, *Vibrio parahaemolyticus* has evolved to possess two separate and independent flagellar systems, one utilising a H^+ motor and the other a Na^+ motor (McCarter 1999). It is likely that the ability to utilise more than one power source provides a selective advantage to certain bacteria in changing environmental conditions. This is consistent with observations of swimming cells of *Shewanella oneidensis*, where a single polar flagellum is powered by a Na^+-dependent motor but at low concentrations of sodium is supported by a H^+-dependent motor (Thormann and Paulick, 2010).

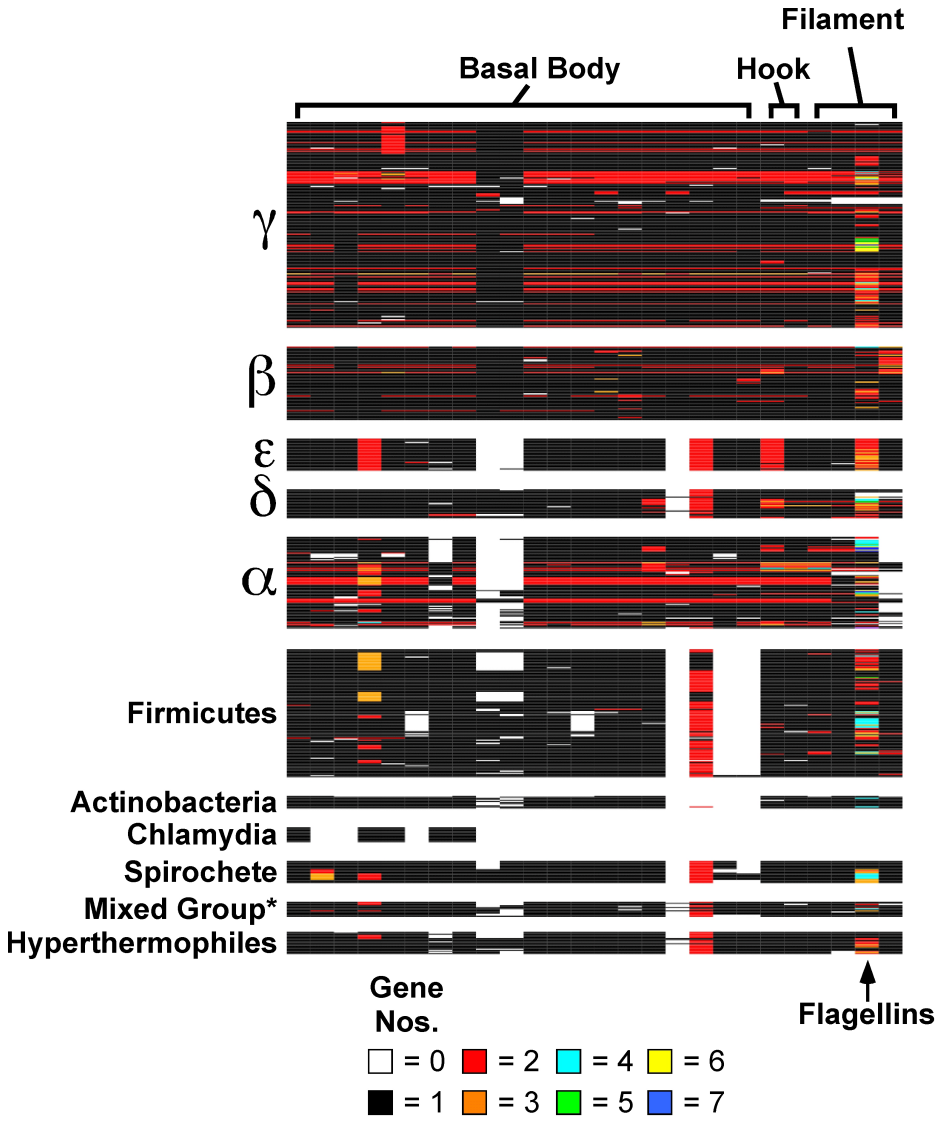

Figure 8: Bioinformatic analysis of flagellar gene dosage of annotated bacterial genomes in the KEGG database (taken from Faulds-Pain *et al.*, 2011)

To be included in the analysis the bacterial genome had to possess the *fliF* gene, which encodes for one of the earliest structural proteins built in the flagellum. 1,144 annotated bacterial genomes were used in this analysis and of those 607 contained *fliF*. The genes are organised according to their approximate location in the flagellum structure, beginning with *fliF* at the left and finishing with *fliD* (the filament cap) on the right. Bacterial classes are listed at the side. * The mixed group of bacteria includes species belonging to: *Acidobacteria*, *Verrucomicrobia*, *Gemmatimonadetes*, *Planctomycetes*, *Synergistetes*, and the green nonsulfur bacteria. A key feature of this evaluation is the variation in gene dosage observed for flagellin genes. 45 % of the 607 genomes contained multiple flagellin genes.

1.6 Flagellar Gene Dosage: Multiple Flagellins

Other than differences in flagella number, localisation and motor power, there is also a slight variation in the number and presence of flagellar-specific structural proteins. A bioinformatical analysis of flagellar gene dosage based on annotated bacterial genomes in the KEGG database reveals some striking features amidst a generally conserved picture (Figure 8) (Faulds-Pain *et al*., 2011). When considering gene dosage, the structural components of the flagellum exhibit a significant degree of conservation in that one or two copies of a gene per genome is present (Figure 8) (Pallen and Matzke, 2006; Faulds-Pain *et al.*, 2011). However, the majority of genomes that possess two copies of a gene, have two flagellar systems. For example, *V*. *parahaemolyticus* utilises a polar flagellum for swimming and a separate system of lateral flagella to swarm over surfaces (Sar *et al*., 1990). Novel secondary flagellar systems have also now been predicted for *E*. *coli* and *Yersinia enterocolitica* (Bresolin *et al*., 2008; Ren *et al*., 2005). For the majority of bacteria outside the classes of β- and γ-proteobacteria the flagellar specific genes *fliO* and *fliJ* are missing (Figure 8). Both *fliO* and *fliJ* encode proteins involved in the flagellar specific export machinery. Another striking observation is the lack of a *fliD* gene in the α-proteobacteria. *fliD* encodes for the HAP2 protein or the Flagellar Filament Cap, as it is commonly known (Figure 8). This protein is fairly well conserved at the sequence level and is also essential for flagellar assembly. Therefore, its absence in this group of bacteria is even more intriguing suggesting that either a different protein of as yet unknown, could contribute to flagellar assembly in these bacteria. Finally and most strikingly, a high level of diversity is observed when considering the number of flagellin genes per genome: 45 % of annotated flagellar systems possess multiple flagellin genes (Figure 8) (Faulds-Pain *et al*., 2011). Flagellin is the major structural protein that polymerises to form the flagellar filament, which is the long extracellular appendage. The numbers can vary widely between bacterial species. For example, *S*. Typhimurium has two flagellin genes, *C*. *crescentus* has seven and *Bdellovibrio bacteriovorus* has six. Remarkably, genome sequencing has revealed that *Magnetococcus* sp. MC-1 possesses 15 flagellin genes (Schubbe *et al*., 2009). *S*. Typhimurium is capable of phase variation between flagellins and consequently utilises only one flagellin species at a time during filament assembly (Bonifield and Hughes, 2003). In other bacteria, such as *B*. *bacteriovorus* and *C*. *crescentus* there is strong evidence that all the flagellins are utilised (Ely *et al*., 2000; Lambert *et al*., 2006).

Some recent studies into multiple flagellin systems have highlighted a number of common features shared between all that have been investigated. Firstly, all flagellins genes on a genome encode flagellin proteins that possess molecular weights that differ by only 1-5 kDa from each other. FlaA and FlaB of *Campylobacter jejuni* are both 59 kDa, while the six flagellins of *Vibrio fischeri* are all approximately 40 kDa (Nuijten *et al.*, 1990; Millikan and Ruby, 2004). Secondly, expression of individual flagellins occurs from monocistronic operons that are differentially regulated by one or more alternate sigma factors (See later). Two of the flagellin genes of the spirochete *Brachyspira hyodysenteriae* are regulated in response to the flagellar-specific sigma factor σ^{28} while two are regulated by the general house keeping sigma factor, σ^{70} (Li *et al*., 2010). Of the five flagellin genes of *V*. *cholerae*, the expression of four is controlled by σ^{28} and one flagellin is regulated by the alternate sigma factor σ^{54} (Klose and Mekalanos, 1998). Thirdly, flagellin redundancy has been observed. Though in some systems one or more flagellin is essential for filament assembly and has therefore been defined as the major flagellin. For example, *flaA* from *V*. *cholerae* and *fliC*3 from *B*. *bacterivorus* are both essential genes in a redundant system (Klose and Mekalanos, 1998; Lambert *et al*., 2006). The final common feature is that there is evidence available to suggest ordered assembly of the flagellins in the filament (Driks *et al.*, 1989; Bardy *et al.*, 2002). The order in the filament of *B*. *bacteriovorus* has been determined to be, proximal to distal: FliC3, FliC5, FliC1, FliC2 then FliC6 (Iida *et al*., 2009). FliC4 was detected in low levels and its location was not determined. *C*. *crescentus* also possess six flagellin genes, *fljJ*, *fljK*, *fljL*, *fljM*, *fljN*, *fljO* (Nierman *et al*., 2001). Prior to *fljM-O* being identified order was determined in the filament, with FljJ and FljL located proximally followed by FljK (Driks *et al.*, 1989).

Our current understanding of filament structure, regulation of assembly and the wide range of habitats colonised by bacteria possessing multiple flagellin flagellar systems, does not sufficiently explain why having them is an advantage. It has been suggested that multiple flagellin genes are there to provide a mechanism for antigenic variation (McCarter 2001). This is consistent with the differing antigenic properties of the flagellins of *Campylobacter jejuni* and *E*. *coli* (Harris *et al.,* 1987; Pallen and Matzke, 2006). In terms of antigenic variation it is becoming increasingly clear that posttranslational modification of flagellins is playing an important role. Glycosylation of flagellins has been observed for many species including *Pseudomonas* spp., *C*. *jejuni*, *C*. *crescentus* and *Clostridium difficle* (Faulds-Pain *et al*., 2011; Ewing *et al*., 2009; Taguchi *et al*., 2010; Twine *et al*., 2009; Verma *et al*., 2006). A recent study suggested

that flagellin glycosylation is required for virulence in the plant pathogen *Pseudomonas syringae* pv. *tabaci* 6605; the causal agent of wildfire disease on tobacco plants (Taguchi *et al*., 2010). In contrast, flagellin glycosylation in *C. jejuni* and *Helicobacter pylori* is essential for filament assembly (Goon *et al*., 2003; Schirm *et al*., 2003). In *C. crescentus* it has been shown that glycosylation is required to maintain the intracellular stability of flagellins prior to secretion (Faulds-Pain *et al*., 2011). Posttranslational methylation and phosphorylation of flagellin has also been reported (Burnens *et al*., 1997; Kelly-Wintenberg *et al*., 1993). As well as antigenic variation, phase variation of flagellin has been shown to be important in murine infection of *S.* Typhimurium, by allowing bacteria to survive better in the spleen of the animal (Ikeda *et al*., 2001). Importantly, in these experiments, no differences were observed between the wild type strain and the two phase variants ability to invade epithelial cells, survive in macrophages or influence gastroenteritis. This strongly suggests that here the use of multiple flagellins is environment specific.

All things considered there are still some general questions unanswered with respect to the use of multiple flagellins: (1) Why do so many bacteria utilise multiple flagellins? and (2) How is the production and their incorporation into the filament regulated? Thus far we have discussed several observable differences between assembled flagella and that these differences may be playing a role in the different observed swimming speeds of bacteria. We have also highlighted how significant this mechanism of motility is and furthermore, how widespread it actually is. Because of this, we believe that flagella research is extremely important. Investigating how different flagellar systems work from top to bottom will enable us to better understand and control the survival of bacteria. Let us now consider how a flagellum is actually created and how that process is regulated.

1.7 Flagella Biogenesis

The flagellum is a self-assembling organelle. It is comprised from numerous different structural proteins and a multitude of additional factors. The construction spans both the cytoplasmic and outer membranes of a Gram-negative bacterial cell. It is composed of three major structural sections; the basal body which includes the motor and the switch, the hook and the filament (Figure 9). A flagellar-specific type 3 secretion system (T3SS) is employed to facilitate secretion of structural subunits bound for the outside of the cell across the periplasm (Figure 9).

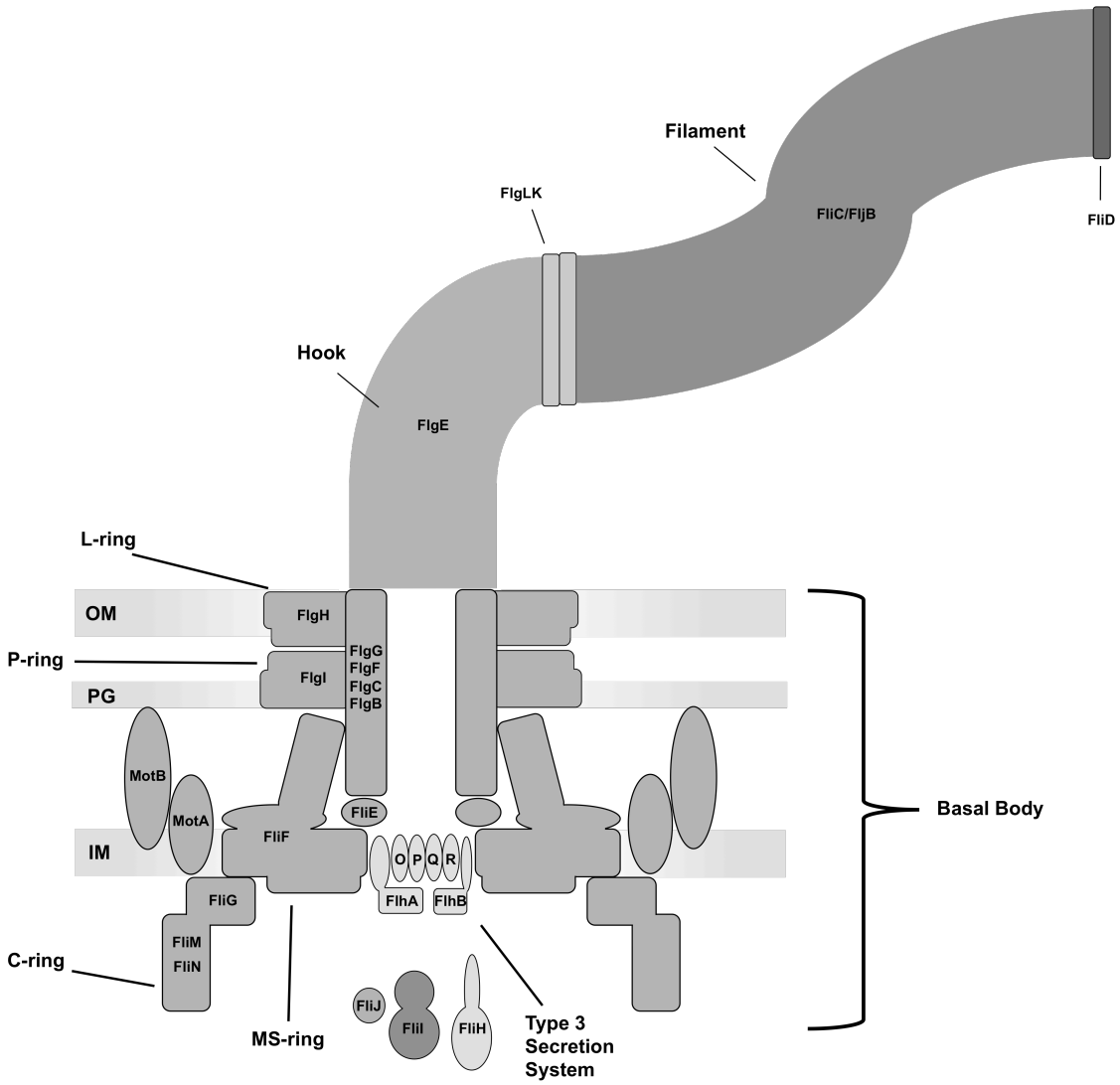

Figure 9: The Gram-negative bacterial flagellum (adapted from Minamino *et al.*, 2008)

The schematic illustrates the structure of the *E. coli* and *S.* Typhimurium flagellum. The drawing is not to scale. Known structural proteins are indicated. The structure can be split into three distinct sections: the basal-body, the hook, and the filament. FliJ, FliI and FliH are cytoplasmic components of the flagellar type 3 secretion system.

1.7.1 *Flagellum structure and mechanism of assembly*

Flagellar biogenesis is a principal feature of cellular differentiation during the life cycle of *C. crescentus*. Electron microscopy has shown that the polar flagellum of *C. crescentus* possesses a structure similar to flagella from the enteric bacteria (Stallmeyer *et al*., 1989). The focus of attention in this project is studying flagellar assembly in *C. crescentus,* however, it is important to understand the enteric data in order to understand flagellar structure. Many of the genes encoding structural components of the enteric flagellum, have been to shown to have homologs in the *C. crescentus* flagellar system. At least 48 genes are involved in flagellar assembly in *C.* crescentus, of which approximately 20 are predicted to be structural (Ely and Ely, 1989). Extensive studies into the molecular structure of the gram-negative γ-proteobacteria, *S.* Typhimurium and *E. coli* flagella, has led to creation of a recognised structural paradigm to which all other flagellated species are compared (Figure 9). Therefore, in the following section, flagellar structure will be discussed based on the findings and investigations in the enteric bacteria, however, where possible known differences in *C. crescentus* and other species will be highlighted.

1.7.1.1 *The basal body*

The basal body is the first substructure to be assembled and can be considered the "engine house". It provides secure anchorage for the flagellum in the cell envelope (Figure 9). Furthermore, it generates the power required to rotate the filament. Electron microscopy has revealed a complexity of multi-ring structures embedded in the cell envelope, and at a central axis, a rod traversing the periplasm (Hosogi *et al*., 2011; Sosinsky *et al*., 1992). The rings are named according to their relative location: L-ring (lipopolysaccharide), P-ring (peptidoglycan), C-ring (cytosol) and the MS-ring (cytoplasmic and supramembranous) (Figure 9) (Blair, 2006). It has been suggested that the flagellum of *C. crescentus* contains an additional ring, the E-ring, located between the P- and the S-ring. It is hypothesised that the E-ring is involved in the process of flagellar ejection during cellular differentiation, thus explaining why such a structure is absent in the enteric bacteria (Stallmeyer *et al*., 1989). However, as of yet no gene encoding for the structure has been located and its existence has been recently disputed (Kanbe *et al*., 2005). The polar flagellum of *Vibrio alginolyticus* has also been shown to contain additional rings. The T-ring and H-ring are located in the outer membrane and the peptidoglycan layer. The T-ring has been shown to be essential for motility (Terashima *et al*., 2006). Mutation of the H-ring results in a severe impairment in

motility (Terashima *et al*., 2010). It is thought that they function to provide added reinforcement to the structure thus preventing against physical breaking of the basal body during rotation (Terashima *et al*., 2010). This is because it has been demonstrated that the rotational speed of the *V. alginolyticus* motor is approximately four times faster than that of *E. coli* (Magariyama *et al*., 1994). It has been shown that the fast swimming speed of wild type *C. crescentus* is due to increased motor velocity when compared to *E. coli* and *V. alginolyticus* (Li and Tang, 2006). It would be tempting to suggest that the *C. crescentus* E-ring may contribute in someway to fast swimming, however, this would require investigation.

The MS-ring comprises of 26 individual copies of FliF embedded in the inner membrane (Figure 9) (Aizawa *et al*., 1985; Ueno *et al*., 1994; Kubori *et al*., 1997). The oligomerisation of FliF provides a platform on which to build the C-ring. The C-ring is made from the switch proteins FliG, FliM and FliN (Figure 9) (Francis *et al*., 1994). The switch-protein complex forms the moving rotor module of the flagellar motor. The integral membrane proteins, MotA and MotB, form the stationary stator complexes; which together with the rotor function to regulate the direction of rotation (Figure 9). The stator complexes operate by forming a channel through which occurs the conduction of proton (H^+) flow across a gradient. The flow of H^+ subsequently generates torque used for the rotation (Nakamura *et al*., 2009). The complexes are anchored into the cell wall by the C-terminal domain of MotB, via a peptidoglycan-binding motif (Van Way *et al.*, 2000). MotA is responsible for proton conduction and although it is essential for flagellar rotation, is not essential for flagellar assembly (Blair and Berg, 1990). The C-terminal domain of MotA interacts with the switch protein FliG. The flow of protons through the channel results in a conformational change in MotA, pushing the FliG proteins resulting in rotation of the C-ring (Zhou *et al.*, 1998). PomA and PomB (orthologues of MotA and MotB) in *V. alginolyticus* form a complex to channel Na^+ into the cell and couple this to rotation in a similar way to the H^+ motor (Asai *et al*., 1997; Sato and Homma, 2000).

Connected to the C-ring is a filamentous rod which functions as a drive shaft through which the power generated by the motor is transmitted to the hook and the filament. The rod is hollow thus allowing it to be utilised by the T3SS for the translocation of the external subunits outside the cell for incorporation into the growing flagellum. It is comprised of two sections; FlgB, FlgC and FlgF are components of the proximal section, while FlgG forms the distal section (Figure 9) (Homma *et al.*, 1990). The rod subunits are secreted into the periplasm, via the T3SS, where the assembly

process takes place under the direction of the capping protein, FlgJ (Hirano *et al*., 2001). Interestingly, FlgJ in *S.* Typhimurium has been shown to possess muramidase activity, which is thought to assist rod assembly through the peptidoglycan layer (Hirano *et al*., 2001; Nambu *et al*., 1999). Muramidases are enzymes that break down the bacterial cell wall.

The P ring (FlgI) and the L ring (FlgH) act as bushings to protect for the rod in the peptidoglycan layer and outer membrane (Figure 9) (Jones *et al*., 1987, 1989; Khambaty and Ely, 1992). Although it is possible that the rings form a conduit in order to allow the axial components of the flagellum to spin freely. Unlike rod subunits, FlgI and FlgH are secreted via the Sec-secretion pathway (Homma *et al*., 1987). It has been shown that the P-ring is required to stabilise the formation of the L-ring (Mohr *et al*., 1996).

FlhE is a flagellar protein that appears to play no role in assembly; however, strains that are deficient are defective in flagellar-associated swarming (Stafford and Hughes, 2007). FliE, is thought to act as a junction protein between the MS-ring and the rod (Figure 9) (Minamino *et al*., 2000a; Muller *et al*., 1992). Homologues of the rod and ring proteins have been identified in *C. crescentus* and some have been characterised (Boyd and Gober, 2001, Dingwall *et al*., 1992; Hahnenberger and Shapiro, 1987; Nierman *et al*., 2001).

In *S.* Typhimurium an additional protein associated with the basal body, FliL, has been shown to provide the rod with protection against increased torsional stress during swarming motility (Attmannspacher *et al.*, 2008). In contrast, FliL in *C. crescentus* is essential for swimming motility (Jenal *et al*., 1994). However, it is not required for flagellar assembly. Recently a model has emerged for the involvement of FliL in c-di-GMP regulation of motility (Christen *et al*., 2007). It is predicted that c-di-GMP levels modulate FliL levels and subsequently regulate flagellar rotation. Furthermore, FliL is required for the efficient degradation of FliF, leading to removal of the flagellum; an essential process of the life cycle of *C. crescentus* cells (Aldridge and Jenal, 1999).

1.7.1.2 *The flagellar type 3 secretion system*

As the majority of the flagellum is presented outside of the cell, there is a requirement for a protein secretion system. The T3SS is located at the base of the flagellum and consists of six integral membrane proteins (FlhA, FlhB, FliO, FliP, FliQ, and FliR) and three soluble cytoplasmic proteins (FliH, FliI, FliJ) (Figure 9) (Minamino and Macnab,

1999). The flagellar T3SS is homologous to that of those systems used by animal and plant pathogens to translocate virulence factors into eukaryotic hosts (Galan *et al.*, 1992). FliQ and FliR of *C. crescentus* exhibit significant homology to virulence factor export proteins of *Erwinia carotovora*, *Shigella flexneri* and *Yersinia pestis* (Zhuang and Shapiro, 1995). FlhA of *C. crescentus* has also been shown to be homologous to the *Yersinia enterocolitica* T3S protein LcrD (Sanders *et al*., 1992).

T3S substrate recognition relies on a N-terminal signal peptide. Unlike the Sec-pathway, this signal is not cleaved during secretion (Macnab, 2004). Twenty amino acids in the N-terminus of hook protein have been shown to be all that is essential for hook subunit secretion in *C. crescentus* (Kornacker and Newton, 1994). The intrinsic self-assembling nature of filamentous proteins means there exists a requirement for a mechanism to prevent polymerisation and aggregation of these subunits prior to secretion (Bennett and Hughes, 2000). Furthermore, due to the narrow channel diameter (approximately 2 nm) of the whole flagellar axial substructure, subunits have to be secreted in a partially unfolded state (Shaikh *et al*., 2005; Yonekura *et al*., 2003). The system achieves these two objectives by using T3S chaperones. FliS is one example of such a flagellar-T3S chaperone, that itself has been shown to facilitate the secretion of FliC (flagellin protein) in *S.* Typhimurium (Yokoseki *et al*., 1995). FliS binds to the C-terminus of FliC preventing premature interactions between flagellin proteins in the cytoplasm (Auvray *et al*., 2001). Other flagellar specific T3SS chaperones have been identified based on chaperone properties. Interestingly, an increasing number of these proteins also play a secondary role in the regulation of flagellar assembly (Aldridge *et al*., 2006; Yamamoto and Kutsukake, 2006). FliI is an ATPase that has similarities to F_0F_1-ATPsynthase (Imada *et al*., 2007). It uses the energy from the hydrolysis of ATP to drive protein export (Fan and Macnab, 1996; Minamino and Namba, 2008). It currently is believed that FliI forms an oligomeric ring like structure, assembling on a platform provided by the membrane components FlhA and FlhB (Claret *et al*., 2003; Minamino *et al*., 2006; Zhu *et al*., 2002). Importantly, the ATPase activity exhibits a positive cooperativity which suggests that this oligomerisation is an important feature of the export system. FliH is proposed to act as a negative regulator of FliI to prevent it from hydrolysing ATP before export is needed (Minamino and Macnab, 2000b). It has been proposed that FliJ is acting as a general T3S chaperone (Minamino and Macnab, 2000c). There is evidence available to suggest that it may facilitate the export of rod-hook and filament substrates by bringing them in close contact with the T3SS (Fraser *et al*., 2003; Minamino *et al*., 2000). However, a recent study has indicated that the role of

FliJ may lie in the recruitment of other T3S chaperones and the transfer of them to secretion substrates, thereby reprocessing free chaperones after substrate release (Evans *et al*., 2006). Importantly, ATPase activity of FliI is not essential for secretion. Flagellar proteins of *S.* Typhimurium are still exported in a *fliI* mutant (Minamino and Namba, 2008). Furthermore, the loss of *fliI* and *fliH* does not inhibit flagellar assembly and motility. It is now accepted that the ATPase activity of the T3SS functions only to make secretion more efficient. The energy required for the unfolding of secretion substrates and their export from the cytoplasm is provided solely by proton motive force (PMF) (Minamino *et al*., 2008).

1.7.1.3 *The hook*

The hook functions as a universal joint connecting the flagellum base to the filament giving the whole structure a necessary degree of flexibility. It is comprised of approximately 120 monomers of a single structural protein, FlgE (Figure 9) (Samatey *et al*., 2004; Sheffery and Newton, 1979; Ohta *et al*., 1982). The structure of both the *S.* Typhimurium and *C. crescentus* hook are essentially the same (Shaikh *et al*., 2005). However, FlgE in *C. crescentus* is predicted to have a higher molecular weight. A central channel through the hook allows for the export of subunits for assembly into the flagellum. The size of the channel diameter has lead to the prediction that hook subunits must be in a partially unfolded state to pass through (Morgan *et al*., 1993). It is the action of the scaffolding protein, FlgD, that caps the hook and co-ordinates the assembly of the hook subunits underneath itself (Ohnishi *et al*., 1994; Mullin *et al*., 2001). During hook-basal body (HBB) assembly, the flagellar T3SS specifically exports only the subunits required for assembly of the rod and the hook (Minamino and Macnab, 1999). When the hook reaches a length of approximately 55 nm a secretion substrate specificity switch occurs that changes the flagellar T3SS system to accept late flagellar proteins of the filament (Hirano *et al*., 1994; Williams *et al*., 1996).

1.7.1.4 *The filament*

Hook length control and hook completion corresponds with the switching of secretion substrates from the rod-hook components to the late flagellar proteins. The hook-associated proteins, HAP1 and HAP3 (FlgK, FlgL) are secreted and assemble to make the hook-filament junction (Figure 9) (Homma *et al*., 1984; Homma and Iino, 1985; Ikeda *et al*., 1987). Another hook-associated protein, HAP2 (FliD), then co-ordinates the assembly of each flagellin (FliC) into the growing filament between itself and HAP3

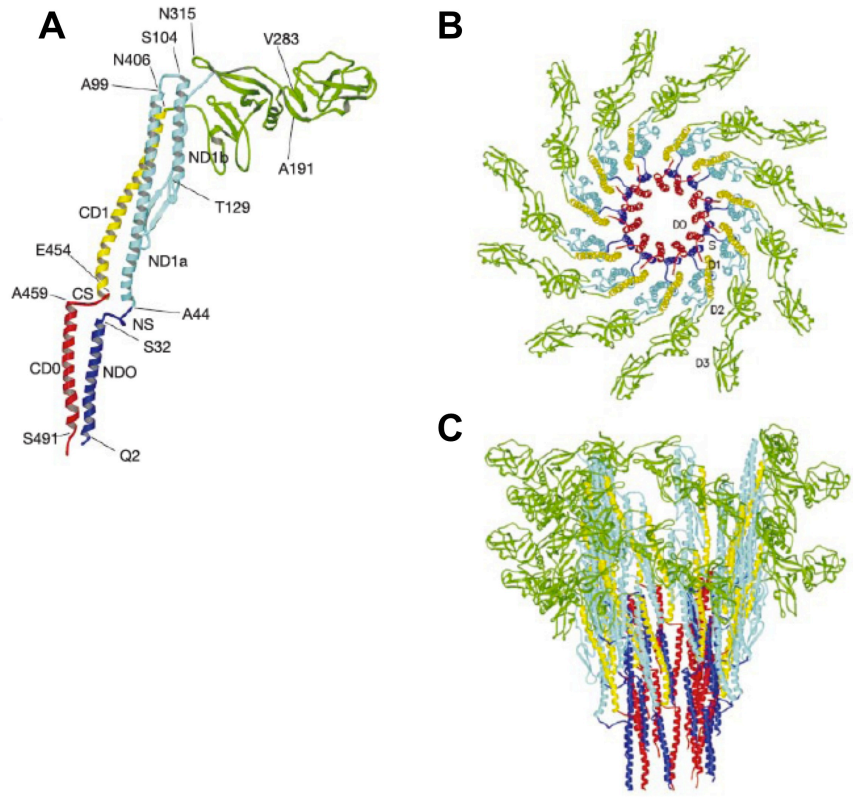

Figure 10: Structural analysis of the flagellar filament (taken from Yonekura *et al.*, 2003)

A. The atomic model of a single flagellin protein (FliC). **B.** A model of flagellin assembly into the helical flagellar filament. Viewed from the top, 11 flagellin subunits are displayed. **C.** A side on view of the organisation of flagellin subunits in the filament. The four flagellin structural domains are indicated. D0 and D1 form the central channel, while D2 and D3 are exposed to the surface.

(Figure 9) (Yonekura *et al.*, 2000). HAP2 is also referred to as the filament cap protein. A mutant lacking HAP2 will form a basal-body-hook structure, capped by HAP1 and HAP3, but does not however form a filament (Homma and Iino, 1985). Instead the mutant secretes unassembled flagellin monomers into the external environment (Homma *et al*., 1984). Purified HAP2 can be added to the culture medium in order to recover filament assembly, however purified flagellin added to the culture medium can not assemble on the distal end of a wild type filament capped by HAP2 suggesting that filament assembly can only occur under a filament cap (Homma *et al*., 1986; Ikeda *et al*., 1993; Imada *et al*., 1998). HAP2 is predicted to form a pentameric structure that has the ability to flex and rotate to incorporate the self-assembling flagellin monomers beneath it (Imada *et al*., 1998; Yonekura *et al*., 2000; Yonekura *et al*., 2003). The *fliD* the gene that encodes HAP2 is absent from many α-proteobacterial genomes, including *C. crescentus*.

Assembly of flagellin occurs in a helical fashion with 11 subunits per 2 helical turns (Figure 10) (Samatey *et al.*, 2001; Yonekura *et al.*, 2003). Consequently, the organisational structure can be described as being composed of 11 protofilaments. The filament itself can form two configurations: 1) Left-handed helix and 2) Right-handed helix. These are created due to filament supercoiling, which is caused by a mixture of two types of protofilament conformation: L- and R-type. When all of the protofilaments exist in the same configuration a straight filament is produced (Yonekura *et al*., 2003). During swimming in *S.* Typhimurium and *E. coli*, the individual flagellar filaments, in the Left-handed configuration, bundle tight together and rotate in the same direction (Macnab and Ornston, 1977). Chemotactic signals can then result in a sudden change in the direction of flagellar motor rotation, which causes the filaments to switch from Left-handed to Right-handed, which in turn causes the bundle of flagella to fall apart and the cell to tumble (Larsen *et al*., 1974). This allows the bacteria to change direction. The 3-D structure of the flagellin protein FliC in *Salmonella* has been solved by X-ray crystallography (Samatey *et al.*, 2001; Yonekura *et al.*, 2003). The protein comprises of four domains D0, D1, D2 and D3 (Figure 10). D0 and D1 represent the N and C termini of the protein and form a α-helical coiled coil facing the central channel of the filament. The interactions that are made by amino acids in D0/D1 stabilize the whole filament structure and are thus essential for polymerisation (Kitao *et al*., 2006). Therefore, it is not surprising that D0 and D1 are highly conserved throughout bacterial species (Beatson *et al.*, 2006). D2 and D3 represent the central part of the protein and are surface exposed. Because of this these domains are important factors in host-bacterial

interactions, which results in a selective pressure for the amino acid sequence to vary. Divergence is observed across bacterial species in D2/D3 to the point that D3 is sometimes absent from the flagellin of some bacteria, such as in *C. crescentus* and *Bacillus cereus* (Beatson *et al.*, 2006).

Flagellar filament lengths vary between different organisms. For example the average length of the *Salmonella* filament is approximately 10 microns where as the filament of *C. crescentus* is approximately 6 microns (Yonekura *et al.*, 2000; Li and Tang, 2006). It is estimated that a single flagellar filament of *S.* Typhimurium utilises up to 30,000 flagellin monomers (Chevance and Hughes, 2008). Essential for the functionality of the flagellum; the flagellins are also a major recognition target for host defense systems or predators. Toll-like receptors (TLR) are a family of proteins that play a key role in the innate immune response (Kawai and Akira, 2011). One member of the family, TLR5 has been shown to recognise flagellin via direct binding resulting in activation of the host immune system (Smith and Ozinsky, 2002). Site-directed mutagenesis analysis has mapped the recognition site on flagellin to a discrete 13 amino acid site in the D1 domain (Smith *et al.*, 2003). Remarkably, although D1 is evolutionally conserved among most bacteria, divergence at this site has occurred in some, such as *Helicobacter pylori*. This has resulted in the bacteria not being recognised by TLR5 and thus evading TLR5 directed immune responses (Galkin *et al.*, 2008). *S.* Typhimurium actually produces two species of flagellin, FliC and FljB although only one species is found in the filament at any given time. The bacteria can switch between the two in a process called phase variation. FljB is co-transcribed with FljA, a transcriptional and translational repressor of *fliC*. An inversion of the *fljB* promoter switches off the expression of *fljAB* and *fliC* begins (Bonifield and Hughes, 2003). FljB and FliC are antigenically different which suggests phase variation plays a role in evasion of the host cell immune system (Ikeda *et al.*, 2001).

In contrast, *C. crescentus* is not a pathogenic organism and does not exhibit phase variation of its flagellins. It has been shown that the flagellar filament is the specific target of a number of bacteriophages that can infect *C. crescentus* (Guerrero-Ferreira *et al*., 2011). The phage head binds directly to the filament and is pulled down towards the cell by flagellar rotation. It would be interesting to see if changes in flagellin composition in the filament affect phage infection.

1.8 Coupling flagellar gene expression to flagellar assembly

Bacterial flagellar assembly is a complex and highly ordered process. Temporal regulation of flagellar gene expression ensures that the structural proteins of the flagellum are produced at the correct time during assembly. The backbone of this temporal control is a transcriptional regulatory cascade consisting of regulatory proteins and RNA polymerase sigma factor subunits (Figure 11). It is the action of these regulators that couple flagellar gene expression with flagellar assembly. The general regulatory architecture coupling gene expression to assembly is highly conserved in all bacteria (Figure 11) (Brown *et al*., 2009). Flagellar genes from every characterised flagellar regulon are always located in distinct clusters together on the genome. These clusters are organised in a way that they correspond to the temporal requirement of different components during flagellar assembly (Aldridge and Hughes, 2002). The genes as a result can be classified as early, middle and late flagellar genes. In every system, early genes consist of regulatory proteins that function to initiate the process of flagellar assembly. Middle genes encode structural proteins that form the basal-body and the hook. Finally, the filament proteins are classified to late flagellar genes. As more and more flagellar systems are characterised, we are developing a better understanding of system-specific regulators that are involved.

1.8.1 *Flagellar assembly checkpoints*

Distinct flagellar assembly checkpoints are utilised by bacteria in order to coordinate and couple flagellar gene expression to the assembly pathway (Figure 11). All flagellar systems utilise the assembly checkpoint of hook completion. This coincides with the correct time for late flagellar gene production and a secretion substrate switch. Others use an additional second intermediate assembly checkpoint of rod initiation/assembly. It is plausible that this second and earlier checkpoint is being used as a marker for the activation of T3S. This is consistent with investigations into two checkpoint flagellar systems, of which will be discussed later.

Assembly begins with the construction of the MS-ring, the C-ring and the T3SS (Figure 11). Two flagellar specific proteins, FlhB and FliK, are involved in the regulation of hook length control. FlhB is an integral membrane component of the flagellar T3SS (Minamino *et al*., 2008). A number of elegant models have been proposed to explain exactly how FliK and FlhB achieve this control. The molecular ruler model states that FliK, in a partially unfolded state, is exported by the flagellar

T3SS during hook assembly (Minamino *et al*., 1999; Mizuno *et al*., 2011). The N-terminal region of FliK ($FliK_N$) then measures the length of the growing hook by directly binding to the hook cap protein (Moriya *et al.*, 2006). When $FliK_N$ is fully extended at 55nm, the C-terminal region, which remains in the cytoplasm, is able to interact with FlhB, catalyzing FlhB self-cleavage and a subsequent substrate specificity switch (Erhardt *et al*., 2011; Minamino and Macnab, 2000a; Mizuno *et al*., 2011; Moriya *et al.*, 2006). This elegant model is consistent with the mechanism behind needle length control of the T3S bacterial injectisome. The hollow needle structure is required for the translocation of virulence factors out of the bacterial cell. In *Yersina* spp. it is proposed that the T3S-specific protein YscP acts as a molecular ruler in a similar way to FliK in the flagellar system (Journet *et al*., 2003).

1.8.2 *Enteric flagellar systems*

The temporal expression of flagellar genes in the enteric bacteria is responsive to progression of flagellar assembly. However, as the majority of these systems make between four and eight flagella per cell, the regulation of assembly is often discussed in terms of the initiation and completion of a flagellum as opposed to flagella. We will discuss flagellar regulation in *S*. Typhimurium and *E*. *coli* and then after consider the mechanisms used to maintain a discrete number of flagella per cell.

The enteric bacteria utilise only the hook completion checkpoint to coordinate flagellar gene expression with flagellar assembly (Figure 11A). The expression of flagellar genes in these systems are driven by three promoter classes: Class 1-3. A single Class 1 promoter that drives the expression of the early genes that encode the enteric master transcriptional regulator, *flhD* and *flhC* (Kutsukake *et al.*, 1990). FlhD and FlhC form a hetero-hexameric protein complex, $FlhD_4C_2$, and together with the σ^{70} activate Class 2 promoters that transcribe middle genes such as those that encode for HBB subunits and regulatory factors (Figure 11A) (Chilcott and Hughes, 2000; Wang *et al*., 2006). $FlhD_4C_2$, unlike other flagellar master regulators, some of which will be discussed later, is not a member of the TCS family of transcriptional activators. Studies of flagellar gene expression have shown that FlhC is responsible for DNA binding and FlhD is required to stabilise the protein:DNA complex (Claret and Hughes, 2000). Its own transcription i.e. Class 1 promoter, is likely to be controlled by a plethora of global regulators, some of which have been identified and characterised (Clarke and Sperandio, 2005; Kutsukake, 1997; Wei *et al*., 2001). Examples of TCS involved in the activation/repression of *flhDC* can be found in the literature. The QseBC TCS has been

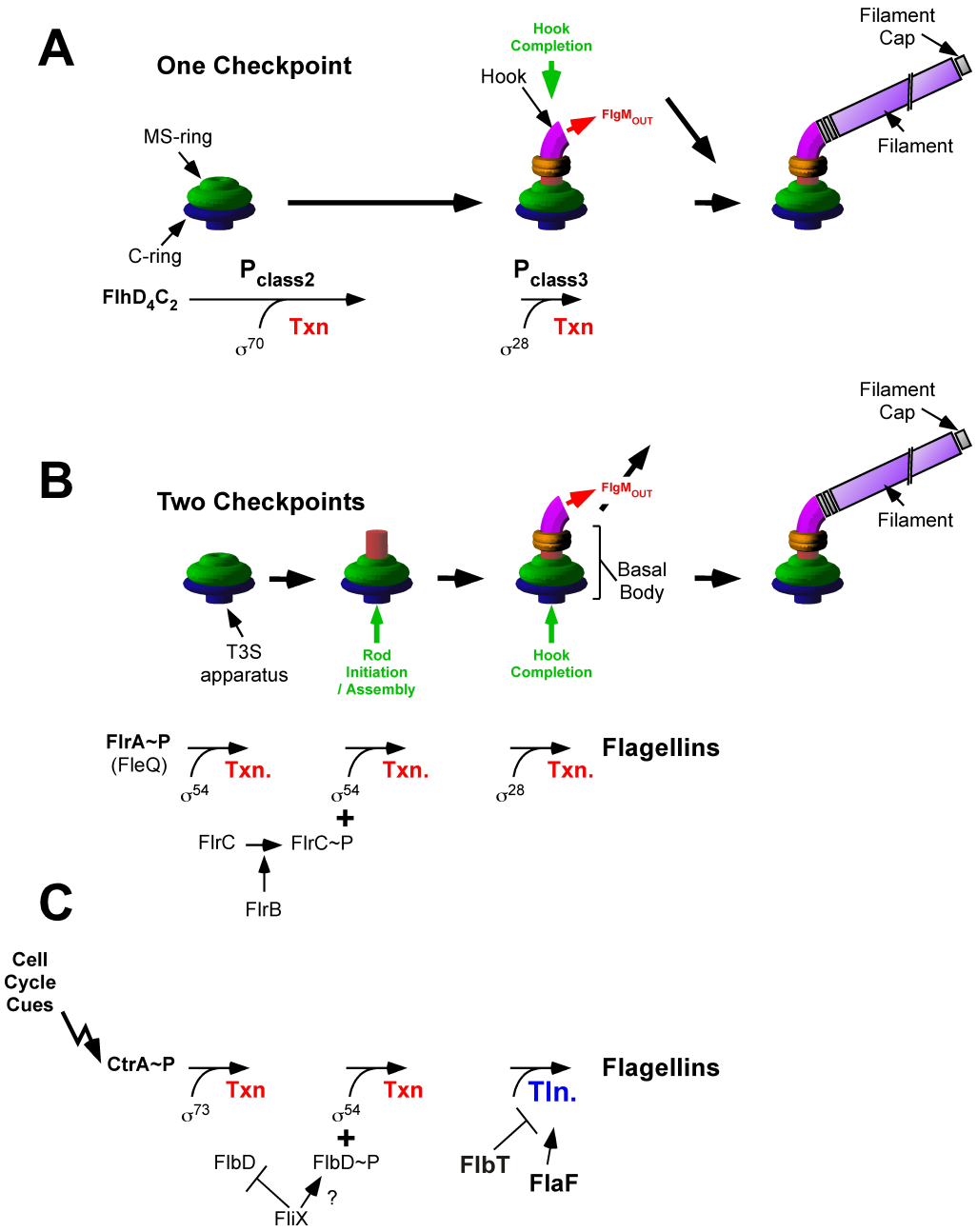

Figure 11: Regulation of flagellar assembly (adapted from Parsek and Aldridge, 2010)

Flagellar assembly checkpoints are utilised by bacteria in order to couple flagellar gene expression to the assembly pathway. All flagellar systems utilise the assembly checkpoint of hook completion. Others use an additional second intermediate assembly checkpoint of rod initiation/assembly. The schematics illustrate a simplified understanding of flagellar gene regulation. Key regulatory proteins are indicated. **A.** A σ^{28}-dependent system: *E. coli* and *S.* Typhimurium. **B.** A σ^{54}/σ^{28}-dependent system: *V. cholerae* and *P. aeruginosa*. **C.** σ^{28}-independent system: *C. crescentus*. Txn: Transcription. Tln: Translation

implicated in the quorum sensing regulation of motility in *E. coli* spp. (Sperandio *et al*., 2002). Quorum sensing is a bacterial cell-cell signalling mechanism that results in the regulation of gene expression in response to cell-population density; it has been highlighted as an important process occurring during biofilm development (Miller and Bassler, 2001). Two of the regulatory factors expressed by $FlhD_4C_2$ are the alternative sigma factor σ^{28} and its anti-sigma factor FlgM (Ohnishi *et al.*, 1990; Gillen and Hughes, 1991). It is σ^{28} that is required to drive the expression of Class 3 promoters and the expression of late flagellar genes such as the flagellins and chemotaxis machinery (Brown *et al*., 2009; Chilcott and Hughes, 2000). However, prior to HBB completion, σ^{28} is kept inactive due to a physical interaction with the anti-sigma factor FlgM (Daughdrill *et al*., 1997; Ohnishi *et al*., 1992; Sorenson *et al*., 2004). Upon HBB completion, a T3SS substrate specificity switch results in the secretion of FlgM from the cell, freeing σ^{28} to activate late flagellar gene expression (Hughes *et al*., 1993; Minamino *et al*., 1999). FlgM secretion is actually facilitated by σ^{28} itself, which acts as the T3S-chaperone by delivering FlgM to the T3S apparatus (Aldridge *et al*., 2006).

It has been recently shown that there exists a level of endogenous negative regulation of flagellar assembly in *S.* Typhimurium in order to maintain a discrete number of flagella per cell (Aldridge *et al*., 2010). FliT is a Class II enteric flagellar-specific protein that acts as an anti-$FlhD_4C_2$ factor by inhibiting $FlhD_4C_2$ binding Class 2 promoters thus reducing their transcription rates (Yamamoto and Kutsukake, 2006). Importantly, $FlhD_4C_2$ that is already bound to DNA is resistant to FliT regulation (Aldridge *et al*., 2010). FliT acts additionally as a T3S chaperone in facilitating the secretion of the Class III HAP2 (FliD) protein by binding and delivering it to the T3SS (Fraser *et al*., 1999; Imada *et al*., 2010). Therefore when interacting with HAP2, FliT cannot regulate DNA free $FlhD_4C_2$. A model proposed by Aldridge *et al*., suggests that the endogenous negative regulation of FliT on flagellar assembly is responsive to the HAP2 secretion rate and ultimately this control ensures that the number of flagella produced is not excessive (Aldridge *et al*., 2010). This process functions to make sure that the bacterial cell does not waste energy by creating too many flagella. However, the fact that FliT cannot fully inhibit $FlhD_4C_2$ activity ensures that the system is responsive to external signals and primed ready to modulate flagellar expression accordingly (Aldridge *et al*., 2010). This provides an excellent mechanism for feedback control of flagellar assembly during steady state (i.e. after the initiation of assembly of a single flagellum); by coupling flagellar gene expression post-HBB completion to the assembly of the next flagellum.

1.8.3 σ^{54}-dependent flagellar systems

In contrast to the enteric bacteria, the majority of other flagellar systems utilise the alternative sigma factor σ^{54}. These systems, including those of *C. crescentus* and *Vibrio* spp., couple flagellar gene expression to flagellar assembly in response to two assembly checkpoints: rod assembly and HBB completion (Figure 11B and 11C). As mentioned previously σ^{54}-dependent gene expression provides a stringent level of control, as transcription cannot occur without the presence of a TCS EBP.

1.8.3.1 σ^{54}- and σ^{28}-dependent flagellar systems

P. aeruginosa and *V. cholerae* swim by the means of a single polar flagellum (McCarter, 2001). In contrast, *V. parahaemolyticus* has two distinct flagellar systems: (i) a monotrichous system which produces a single polar flagellum and (ii) a lateral flagellar system. The lateral system is utilised for swarming on solid surfaces. *P. aeruginosa* and *V. cholerae* utilise both σ^{54} and σ^{28} regulation to couple flagellar gene expression to flagellar assembly. Characterisation of both systems suggests that they are very similar, differing with the annotation of gene names. We will therefore discuss in detail only one, that of *V. cholerae*, and the *P. aeruginosa* homologs will be given in parentheses after.

The flagellar genes of *V. cholerae* can be divided into four classes with respect to the two assembly checkpoints: Class I-IV. The sole Class I promoter activates the expression of the flagellar master regulator, *flrA* (*fleQ*) (Arora *et al*., 1997; Prouty *et al*., 2001). FlrA is a σ^{54}-dependent activator (EBP) that is required for the transcription of the Class II - middle genes that include the MS-ring, switch complex, some of the T3SS and the regulatory factors: FlrB (FleS), FlrC (FleR) and σ^{28} (Figure 11B) (Dasgupta *et al*., 2003; Prouty *et al*., 2001). Interestingly, the N-terminal region of FlrA does not appear to share a high degree of similarity with classical response regulator receiver domains (Figure 1). The absence of a conserved aspartate residue suggests that phosphorylation does not play a part in the regulation of FlrA dependent activation of flagellar gene expression (Prouty *et al*., 2001).

flrBC encodes a TCS that is essential for Class III gene expression and flagellar assembly (Klose and Mekalanos, 1998). Class III - middle genes represent the distal hook basal body components, some of the T3SS and *flaA* which is the only essential flagellin in an otherwise redundant system. FlrB is a sensor kinase that phosphorylates the response regulator, FlrC which activates it to carry out σ^{54}-dependent activation of

Class III promoters (Figure 11B). Here the first assembly checkpoint appears to be coinciding with rod initiation. The expression of Class IV - late flagellar genes is σ^{28}-dependent and their transcription produces the other four flagellins, components of the flagellar motor and FlgM. Consistent with the enteric flagellar systems, it is predicted that prior to HBB completion FlgM would inactivate σ^{28} from activating Class IV promoters and upon the assembly checkpoint being passed, FlgM will be secreted from the cell freeing σ^{28} (Figure 11B). The exact mechanisms of regulation for this system still require further elucidation; as does the activation signal for FlrA. It has been suggested that *V. cholerae* may use cell cycle cues in a similar way to *C. crescentus* in order to regulate the production of a single polar flagellum.

1.8.3.2 *Caulobacter crescentus*

The temporal expression of flagellar genes in *C. crescentus* is responsive to both the progression of flagellar assembly but also the cell cycle. Furthermore, the regulatory elements controlling flagellar biogenesis are spatially regulated to ensure that construction of a single polar flagellum occurs only at the new swarmer cell pole of the pre-divisional cell. The α-proteobacteria are a unique group of bacteria that utilise only σ^{54} dependent flagellar gene expression.

The flagellar genes of *C. crescentus* can be divided into four classes with respect to the two assembly checkpoints: Classes I-IV. The expression of the early flagellar genes (Class II) encoding components of basal body and the flagellar-T3SS is regulated by the synthesis and phosphorylation of the master regulator transcription factor CtrA. The completed assembly of these structures at the swarmer cell pole is then required for the transcription of genes (Class III) encoding the rod, outer membrane rings, and the hook. Finally, only upon assembly of the Class III-encoded structures can the flagellin genes (Class IV) be translated and assembled into a functional filament. This is in contrast to the regulation of filament assembly in FlgM/σ^{28}-dependent systems where the level of control occurs only at transcription and not post-transcriptionally.

1.8.3.2.1 *Initiation of flagellar assembly*

Class I represents the flagellar master regulator, CtrA (Quon *et al.*, 1996). The activity of CtrA is controlled directly by phosphorylation and proteolysis. Phosphorylated CtrA is present in motile swarmer cells where it binds the DNA origin of replication and thus inhibits DnaA from initiating DNA replication (Quon *et al.*, 1998). However, during

swarmer cell to stalked cell transition, CtrA is dephosphorylated and also rapidly degraded by the ClpXP protease (Domian *et al.*, 1997; Jenal and Fuchs, 1998). This temporal and spatial control of the availability of active CtrA ensures correct progression of the *C. crescentus* cell cycle. In SW cells, phosphorylated CtrA drives the expression of the σ^{73}-dependent, Class II genes; that encode the proximal HBB subunits of the MS-ring, the C-ring, components of the flagellar-T3SS and some flagellar regulatory proteins (Figure 11C) (Domian *et al*., 1997; Stephens *et al*., 1997; Wu *et al*., 1998). These regulatory proteins include the alternative sigma factor σ^{54} (encoded by the *rpoN* gene), FlbD and FliX (Anderson *et al*., 1995; Laub *et al*., 2002).

The transcription of Class III and Class IV genes, which encode for components of the rod, hook, HAPs and flagellins are dependent on σ^{54}. Mutants of *rpoN* in *C. crescentus* are stalled in flagellar biogenesis and display abnormal cell division phenotypes (Brun and Shapiro, 1992). Furthermore, in *C. crescentus*, σ^{54} is also required for stalk biogenesis (Biondi *et al*., 2006). FlbD is a response regulator that belongs to NtrC family of EBPs (Ramakrishnan and Newton, 1990). It has been shown to bind to a conserved sequence upstream of Class III and Class IV promoters, called *ftr* (flagellar transcriptional regulation) (Mullin and Newton, 1989; Mullin *et al*., 1994; Davis and Viollier, 2011). A *flbD* loss of function mutation results in an absence of Class III promoter activity (Ramakrishnan and Newton, 1990). Consistent with other non-flagellar σ^{54} dependent genes, the Class IV promoters also contain a binding site for the DNA-bending protein, integration host factor (IHF) (Gober and Shapiro, 1990; Shingler, 2010). This site is located in between the promoter and the *ftr*. It is predicted that the function of IHF is to aid the looping out of the DNA between the EBP and σ^{54}-RNA polymerase during open complex formation (Shingler, 2010). A mutation in the IHF binding consensus upstream of *flgE* was shown to significantly reduce the level of transcription suggesting that IHF is required for maximal promoter activity (Gober and Shapiro, 1990).

FliX is a *trans*-acting factor that regulates FlbD-dependent transcription (Muir *et al*., 2001). In the absence of a Class II gene encoded structure, FliX functions as a negative regulator of FlbD activity. Overexpression of the *fliX* gene results in the repression of both Class III and Class IV gene expression (Muir *et al*., 2001). Interestingly, mutations in *fliX* also result in the suppression of Class III and Class IV promoter activity suggesting that FliX also acts as a positive regulator (Muir *et al*., 2005). Prior to rod completion FliX represses FlbD activity through a physical interaction thought to block FlbD from binding DNA (Figure 11C) (Muir and Gober,

2004; Xu *et al*., 2011). Upon rod completion, FliX-dependent activation of FlbD leads to σ^{54}-dependent transcription of Class III and IV flagellar genes (Muir *et al.* 2001, 2005; Muir and Gober, 2002, 2004).

Interestingly, FlbD also acts as a negative regulator of Class II expression and in doing so regulates its own expression. FlbD can bind an *ftr* site upstream of the Class II gene *fliF* and subsequently block RNA polymerase binding, and potentially CtrA binding, thus acting as a transcriptional repressor of its own operon (Wingrove and Gober, 1994). Several of the Class II promoters are organised in a way such that they diverge from a Class III promoter (Mohr *et al*., 1998). Therefore, it has been suggested that *cis*-acting elements within the region coordinately regulate both Class II and Class III flagellar gene expression (Gober and England, 2000). This regulatory mechanism is key to the generation of a single polar flagellum and not multiple flagella.

1.8.3.2.2 *Second assembly checkpoint*

Once the rod is completed, FlbD is phosphorylated switching on the expression of σ^{54}-dependent Class III and Class IV genes encoding the distal HBB components, the flagellins and the regulatory proteins FlbT and FlaF. Importantly, at this time point the flagellin genes are transcribed but not all are translated until the second assembly checkpoint of HBB completion has been passed (Mangan *et al*., 1999). As previously mentioned, the *C. crescentus* flagellar operon contains six flagellin genes; the α-flagellins: *fljJ, fljK*, *fljL* and the β-flagellins: *fljM, fljN*, *fljO* (Minnich *et al*., 1988; Nierman *et al*., 2001). Consistent with other multiple flagellin systems, the flagellins of *C. crescentus* are transcribed from mono-cistronic operons. The expression of *fljK* and *fljL* is dependent on σ^{54} and FlbD. The β-flagellins and *fljJ* lack σ^{54} consensus promoter sequences although full transcription of the b-flagellins still has a partial on σ^{54} (Ely *et al*., 2000). There is evidence available to suggest that *fljJ*, *fljM, fljN* and *fljO* are actually directly regulated by CtrA and σ^{73}, thus their temporal expression occurs higher in the flagellar hierarchy (Jones *et al*., 2001; Laub *et al*., 2000). At this point it is important that we highlight a key regulatory difference between those systems that possess FlgM/σ^{28} and those like *C. crescentus* that do not. FlgM and σ^{28} combine to regulate late flagellar gene expression in response to HBB completion at the transcriptional level. In contrast, the flagellins of *C. crescentus* are transcribed prior to HBB completion but are not translated until the checkpoint has been passed. This level of control involves the Class II post-transcriptional regulators FlbT and FlaF (Figure 11C).

Class III mutants unable to make a hook structure have been shown to lack flagellin (Mangan *et al*., 1999). However, a *flbT* mutation inserted into these mutants resulted in the restoration of flagellin protein synthesis. The half-life of *fljK* mRNA in a *flgE* (hook) mutant was reduced by approximately seven-fold when compared to wild type. However, in comparison, a *flgE flbT* double mutant exhibited an increased half-life of *fljK* mRNA that was > two-fold higher than wild type (Mangan *et al*., 1999). This was the first suggestion that *flbT* gene product functions as a negative regulator of flagellin expression prior to hook basal-body completion. More recently, FlbT has been shown to negatively regulate the translation of *fljK* mRNA by binding to 5' UTR of the molecule stopping translation and promoting its degradation (Figure 11C) (Anderson and Gober, 2000).

At HBB completion the inhibitory activity of FlbT is antagonised by FlaF and flagellin mRNA is translated (Figure 11C) (Llewellyn *et al.*, 2005). A Δ*flaF* mutant was non motile and did not synthesise detectable levels of flagellin (Llewellyn *et al*., 2005). However, a mutation in the *flbT* gene restored flagellin synthesis but not motility (Llewellyn *et al*., 2005). It is hypothesised that the FlaF protein functions in both activation of translation and flagellin secretion.

The lack of FlgM/σ^{28} in *C. crescentus* appears to be overcome by the presence of FlbT and FlaF. It is important to note that our current understanding of this system and the exact mechanisms of how flagellin gene expression is coupled to filament assembly is still unclear. Bioinformatical analysis suggests that the absence of FlgM/σ^{28} on the genome is common among the α-proteobacteria (Brown *et al*., 2009). However, those exceptions, such as *Rhodobacter sphaerioides*, that do possess FlgM/σ^{28} appear to have acquired a second flagellar system (Poggio *et al*., 2007). Strikingly, all non- α-proteobacteria flagellar systems characterised have FlgM/σ^{28} (Brown *et al*., 2009). This suggests that the α-proteobacteria are unique among other bacteria in that they have evolved to rely on signal transduction as a means of regulating flagellar gene expression. The α-proteobacteria form one of the largest and most diverse groups within the kingdom of bacteria, and are abundant colonisers of both marine/aquatic and terrestrial environments (Gupta and Mok, 2007). Members of the group are known to exhibit a wide range of nutritional requirements, including those that are phototrophic, chemolithotrophic and oligotrophic (Boutte and Crosson, 2011; Lugtu *et al*., 2009; Masepohl *et al*., 2007). There are symbiotic organisms and also those that are pathogenic (Atluri *et al*., 2011; Gonzalez and Marketon, 2003). Therefore, with the diversity of lifestyles and the evident intimate relationship with the environment, it

plausible to suggest that these bacteria potentially require an alternative mechanism to respond to environmental changes i.e. whether to be motile or sessile. The ability to control flagellar assembly using the "on/off" switch of σ^{54}-dependent gene expression and a translational activation mechanism, may allow for a better response to the environment they inhabit.

Chapter 2. Aims

The primary aim of this project was to investigate the extent to which flagellin redundancy exists in the process of flagellar filament assembly in *Caulobacter crescentus*. Creating mutants that have only a single flagellin gene and then analysing motility we will determine how *C. crescentus* utilises its six flagellins. The secondary aim was to characterise the regulation of filament assembly and determine the mechanism behind the switch from hook-basal body completion to filament assembly in *C. crescentus*.

Chapter 3. Materials and Methods

All growth media, antibiotics, growth supplements, non-commercial buffers, solutions and protein gels used are listed in Appendix A.

3.1 Bacterial Strains and Growth conditions

The bacterial strains and plasmids that were used in this study are listed in Table 1 and Table 2. *E. coli* and *A. tumefaciens* strains were grown in LB media at 37 °C. *C. crescentus* strains were grown in PYE media at 30 °C. *S. meliloti* was grown in TY media at 30 °C. Growth medium was supplemented with antibiotics and growth supplements. Bacterial growth was monitored using a spectrophotometer to measure optical density at 600 nm (OD600). All bacterial strains were frozen at -80 °C for long-term storage. DMSO, final concentration 15 % v/v, was added as a cryo-protectant.

3.2 Transformation of Plasmid DNA

3.2.1 *Preparation of chemically competent cells*

The preparation of all *E. coli* strains (DH5-α, XL1-B, BTH101, S17-1) for transformation was carried out using the same method (Cohen *et al*., 1972). A single bacterial colony was inoculated in 5 ml liquid medium and grown overnight at 37 °C with shaking. The culture was then diluted back in fresh 200 ml LB broth to OD600 0.05 and grown to OD600 0.1-0.2. The cell culture was harvested by centrifugation for 10 min at 6000 x g at 4 °C and the supernatant discarded. The pellet was resuspended in 40 ml $CaCl_2$ and incubated on ice for 40 min. The cell culture was then harvested by centrifugation for 10 min at 6000 x g at 4 °C, the supernatant discarded and the pellet resuspended in 1 ml $CaCl_2$. Glycerol was added, to a final concentration of 10 %, then 100 µl aliquots were used immediately for transformation experiments. If the cells were not required they were frozen in liquid nitrogen and stored at -80 °C.

3.2.2 *Transformation by heat shock*

Competent cells were defrosted on ice and vortexed briefly. Plasmid DNA was then added to the cells followed by incubation on ice for 15 min. The cells were heat shocked

at 42 °C for 50 sec and placed on ice for 2 min. 0.9 ml of LB broth was added to the cells, followed by incubation at 37 °C for 45 min with shaking. The appropriate dilutions were then plated out on selective agar and incubated at 37 °C overnight.

3.2.3 *Transformation by bacterial conjugation*

Plasmid DNA was transformed into *C. crescentus* strains by bacterial conjugation. *C. crescentus* possesses an outer protein surface layer (S layer) that is thought to protect the cell (Smit *et al*., 1992). The presence of the S layer is known to greatly reduce the efficiency of DNA electroporation (Gilchrist and Smit, 1991). Therefore, we utilised a conjugatable strain of *E. coli* (S17-1) for the transfer of plasmid DNA.

A single bacterial colony from a plasmid harboring S17-1 strain was inoculated in 5 ml liquid medium and grown overnight at 37 °C with shaking. A single bacterial colony from a *C. crescentus* strain was inoculated in 5 ml liquid medium and grown overnight at 30 °C with shaking. 0.9 ml *C. crescentus* culture was mixed with 100 µl S17-1 culture and harvested by centrifugation (12000 x g, 3 min, RT). The supernatant was discarded and the pellet was then resuspended in fresh 50 µl PYE liquid medium. The resuspended cells were spotted onto PYE solid medium and incubated at 30 °C overnight. The bacterial growth was then scraped off using a sterile wire loop, and resuspended in 1 ml PYE liquid medium. 1 x 10^{-1}, x 10^{-2} , x 10^{-3} dilutions for integrating plasmids and 1 x 10^{-3}, x 10^{-4} , x 10^{-5} were plated out for replicating plasmids on PYE + Naladixic acid (nal) + Kanamycin (kan) solid medium and incubated at 30 °C for 3 days. Transformants were then re-streaked on PYE + kan medium to maintain plasmid selection.

3.3 Bacterial Strain Table

Table 1: Bacterial strains used in this study

Strain No.	Strain name	Genotype or Description	Reference
E. coli			
TPA2	DH5α	λ⁻ ϕ80d*lacZ*DM15 D(*lacZYA-argF*) U169 *recA1 endA1 hsdR17*(r_K^- m_K^-) *supE44 thi-1 gyrA relA1*	New England Biolabs
TPA4	S17-1	*thi pro hsdR* mutant *hsdM*$^+$ *recA* RP4-2 (Tc::Mu-Tn*7*)	Simon *et al*., 1983

TPA2233	XL1-Blue	*recA1 endA1 gyrA96 thi-1 hsdR17 supE44 relA1 lac* [F' *proAB lacI*^{q}*ZΔM15* Tn*10* (Tet^{R})]	Stratagene
TPA2232	BTH101	F^{-} *cya*$^{-}$*99 araD139 galE15 galK16 rpsL1 (Str*^{R}*) hsdR2 mcrA1 mcrB1*	Euromedex
TPA342	BL21 (DE3)	F^{-} *ompT hsdSB dcm gal* λ(DE3)	Promega
C. crescentus			
TPA435	Wild type	Syn-1000, synchronisable derivative of a *C. crescentus* wild type strain	Evinger and Agabian, 1977
TPA439	Δ*fliF*	Δ*fliF*	Jenal and Shapiro, 1996
TPA663	Δ*fljJ*	Δ*fljJ*	Faulds-Pain *et al*., 2011
TPA599	Δ*fljK*	Δ*fljK* determined by southern blot analysis to be incorrect	Faulds-Pain[a]
TPA2234	Δ*fljK*	Δ*fljK*	This work
TPA916	Δ*fljL*	Δ*fljL*	Faulds-Pain *et al*., 2011
TPA541	Δ*fljM*	Δ*fljM*	Faulds-Pain *et al*., 2011
TPA934	Δ*fljJL*	Δ*fljJ* Δ*fljL*	Faulds-Pain *et al*., 2011
TPA933	Δ*fljJK*	Δ*fljJ* Δ*fljK*	Faulds-Pain *et al*., 2011
TPA971	Δ*fljKL*	Δ*fljK* Δ*fljL*	Faulds-Pain *et al*., 2011
TPA2099	Δ*fljJM*	Δ*fljJ* Δ*fljM*	This work
TPA1300	Δ*fljLM*	Δ*fljL* Δ*fljM*	Faulds-Pain *et al*., 2011
TPA2341	Δ*fljKM*	Δ*fljK* Δ*fljM*	This work
TPA970	Δ*fljJKL*	Δ*fljJ* Δ*fljK* Δ*fljL*	Faulds-Pain *et al*., 2011
TPA1298	Δ*fljJKM*	Δ*fljJ* Δ*fljK* Δ*fljM*	Faulds-Pain *et al*., 2011
TPA1138	Δ*fljJLM*	Δ*fljJ* Δ*fljL* Δ*fljM*	Faulds-Pain *et al*., 2011
TPA1139	Δ*fljKLM*	Δ*fljK* Δ*fljL* Δ*fljM*	Faulds-Pain *et al*., 2011
TPA1299	Δ*fljMNO*	Δ*fljM*-Δ*fljO*	Faulds-Pain *et al*., 2011
TPA1140	Δ*fljJKLM*	Δ*fljJ* Δ*fljK* Δ*fljL* Δ*fljM*	Faulds-Pain *et al*., 2011

TPA2344	Δ*fljJMNO*	Δ*fljJ* Δ*fljM*-Δ*fljO*	This work
TPA2352	Δ*fljKMNO*	Δ*fljK* Δ*fljM*-Δ*fljO*	This work
TPA2356	Δ*fljLMNO*	Δ*fljL* Δ*fljM*-Δ*fljO*	This work
TPA2346	Δ*fljJKMNO*	Δ*fljJ* Δ*fljK* Δ*fljM*-Δ*fljO*	This work
TPA2353	Δ*fljJLMNO*	Δ*fljJ* Δ*fljL* Δ*fljM*-Δ*fljO*	This work
TPA2354	Δ*fljLKMNO*	Δ*fljK* Δ*fljL* Δ*fljM*-Δ*fljO*	This work
TPA2357	Δ*fljJKLMNO*	Δ*fljJ* Δ*fljK* Δ*fljL* Δ*fljM*-Δ*fljO*	This work
TPA2582	Wild type pBX	NA1000 pBXMCS-2	This work
TPA2583	Wild type pRX	NA1000 pRXMCS-2	This work
TPA2592	Δ*fljJKLMNO* pBX	Δ*fljJ* Δ*fljK* Δ*fljL* Δ*fljM*-Δ*fljO* pBXMCS-2	This work
TPA2593	Δ*fljJKLMNO* pRX	Δ*fljJ* Δ*fljK* Δ*fljL* Δ*fljM*-Δ*fljO* pRXMCS-2	This work
TPA3202	Δ*fljJKLMNO* pBX-*fljJ*	Δ*fljJ* Δ*fljK* Δ*fljL* Δ*fljM*-Δ*fljO* pBX-*fljJ*	This work
TPA3203	Δ*fljJKLMNO* pBX-*fljK*	Δ*fljJ* Δ*fljK* Δ*fljL* Δ*fljM*-Δ*fljO* pBX-*fljK*	This work
TPA3204	Δ*fljJKLMNO* pBX-*fljL*	Δ*fljJ* Δ*fljK* Δ*fljL* Δ*fljM*-Δ*fljO* pBX-*fljL*	This work
TPA3205	Δ*fljJKLMNO* pBX-*fljM*	Δ*fljJ* Δ*fljK* Δ*fljL* Δ*fljM*-Δ*fljO* pBX-*fljM*	This work
TPA3206	Δ*fljJKLMNO* pBX-*fljN*	Δ*fljJ* Δ*fljK* Δ*fljL* Δ*fljM*-Δ*fljO* pBX-*fljN*	This work
TPA3207	Δ*fljJKLMNO* pBX-*fljO*	Δ*fljJ* Δ*fljK* Δ*fljL* Δ*fljM*-Δ*fljO* pBX-*fljO*	This work
TPA2920	Δ*fljJKLMNO* pRX-*fljJ*	Δ*fljJ* Δ*fljK* Δ*fljL* Δ*fljM*-Δ*fljO* pBX-*fljJ*	This work
TPA2870	Δ*fljJKLMNO* pRX-*fljK*	Δ*fljJ* Δ*fljK* Δ*fljL* Δ*fljM*-Δ*fljO* pBX-*fljK*	This work
TPA2589	Δ*fljJKLMNO* pRX-*fljM*	Δ*fljJ* Δ*fljK* Δ*fljL* Δ*fljM*-Δ*fljO* pBX-*fljM*	This work
TPA3265	Δ*fljLKMNO* pBX	Δ*fljK* Δ*fljL* Δ*fljM*-Δ*fljO* pBXMCS-2	This work
TPA3266	Δ*fljLKMNO* pBX-*fljJ*	Δ*fljK* Δ*fljL* Δ*fljM*-Δ*fljO* pBX-*fljJ*	This work
TPA3267	Δ*fljLKMNO* pBX-*fljK*	Δ*fljK* Δ*fljL* Δ*fljM*-Δ*fljO* pBX-*fljK*	This work
TPA3268	Δ*fljLKMNO* pBX-*fljL*	Δ*fljK* Δ*fljL* Δ*fljM*-Δ*fljO* pBX-*fljL*	This work
TPA3269	Δ*fljLKMNO* pBX-*fljM*	Δ*fljK* Δ*fljL* Δ*fljM*-Δ*fljO* pBX-*fljM*	This work
TPA3270	Δ*fljLKMNO* pBX-*fljN*	Δ*fljK* Δ*fljL* Δ*fljM*-Δ*fljO* pBX-*fljN*	This work

TPA3271	Δ*fljLKMNO* pBX-*fljO*	Δ*fljK* Δ*fljL* Δ*fljM*-Δ*fljO* pBX-*fljO*	This work
TPA2818	Δ*flaF*	Δ*flaF*	This work
TPA2708	Δ*flbT*	Δ*flbT*	This work
TPA3251	Δ*flaF* pBX	Δ*flaF* pBXMCS-2	This work
TPA3252	Δ*flaF* pBX-*flbT_flaF*	Δ*flaF* pBX-*flbT_flaF*	This work
TPA3249	Δ*flbT* pBX	Δ*flbT* pBXMCS-2	This work
TPA3250	Δ*flbT* pBX-*flbT_flaF*	Δ*flbT* pBX-*flbT_flaF*	This work
TPA3027	FLAG*fljJ1*	Δ*fljJ* FLAG*fljJ*	This work
TPA3028	FLAG*fljJ2*	Δ*fljJ* FLAG*fljJ*	This work
TPA3029	FLAG*fljJ4*	Δ*fljJ* FLAG*fljJ*	This work
TPA3030	FLAG*fljJ6*	Δ*fljJ* FLAG*fljJ*	This work
TPA3031	FLAG*fljJ7*	Δ*fljJ* FLAG*fljJ*	This work
TPA3329	Δ*flaF* pBX-*fljJ*	Δ*fljJ* FLAG*fljJ*	This work
TPA3330	Δ*flaF* pBX-*fljK*	Δ*fljJ* FLAG*fljJ*	This work
TPA3331	Δ*flaF* pBX-*fljL*	Δ*fljJ* FLAG*fljJ*	This work
TPA3332	Δ*flaF* pBX-*fljM*	Δ*fljJ* FLAG*fljJ*	This work
TPA3333	Δ*flaF* pBX-*fljN*	Δ*fljJ* FLAG*fljJ*	This work
TPA3334	Δ*flaF* pBX-*fljO*	Δ*fljJ* FLAG*fljJ*	This work
S. meliloti and *A. tumefaciens*			
TPA3224	*Sinorhizobium meliloti* 1021	Wild type	Narberhaus[b]
TPA3225	*Agrobacterium tumefaciens* C58	Wild type	Narberhaus[b]

[a], London School of Hygeine & Tropical Medicine, London, England; [b], Ruhr-University Bochum, Germany

3.4 Plasmid Table

Table 2: Plasmids/Vectors used in this study

Plasmid name	Vector	Genotype or description	Reference
Flagellin deletion mutants			
	pNPTS128	Kan^r *sacB*+ *mob*+ pLitmus28-derived cloning vector	Potocka *et al*., 2002
pDEL*fljJ*	pNPTS128	*fljJ* ATG/TAA inframe deletion construct	Faulds-Pain *et al*., 2011
pDEL*fljK*	pNPTS128	*fljK* ATG/TAA inframe deletion construct	Faulds-Pain *et al*., 2011
pDEL*fljL*	pNPTS128	*fljL* ATG/TAA inframe deletion construct	Faulds-Pain *et al*., 2011

pDEL*fljM*	pNPTS128	*fljM* ATG/TAA inframe deletion construct	Faulds-Pain *et al*., 2011
pDEL*fljM-O*	pNPTS128	*fljM-O* ATG/TAA inframe deletion construct	Faulds-Pain *et al*., 2011
Flagellin overexpression			
	pGEM-T	Amp^r cloning vector	Promega
	pBXMCS-2	Kan^r high copy replicating plasmid; contains a Xylose inducible promoter	Thanbichler *et al*., 2007
	pRXMCS-2	Amp^r Kan^r low copy replicating plasmid; contains a Xylose inducible promoter	Thanbichler *et al*., 2007
pGT-*fljJ*	pGEM-T	PCR fragment created using primers 483 & 491; contains full *fljJ* ORF	This work
pGT-*fljJ2*	pGEM-T	PCR fragment created using primers 483 & 484; contains full *fljJ* ORF	This work
pGT-*fljK*	pGEM-T	PCR fragment created using primers 485 & 492; contains full *fljK* ORF	This work
pGT-*fljM*	pGEM-T	PCR fragment created using primers 489 & 109; contains full *fljM* ORF	This work
pGT-*fljN*	pGEM-T	PCR fragment created using primer 489 & 115; contains full *fljN* ORF	This work
pGT-*fljO*	pGEM-T	PCR fragment created using primer 489 & 94; contains full *fljO* ORF	This work
pBX-*fljJ*	pBXMCS-2	1140 bp NdeI-SpeI fragment subcloned from pGT-*fljJ*	This work
pBX-*fljK*	pBXMCS-2	1132 bp NdeI-SpeI fragment subcloned from pGT-*fljK*	This work
pBX-*fljL*	pBXMCS-2	PCR fragment created using primer 487 & 493; contains full *fljL* ORF	This work
pBX-*fljM*	pBXMCS-2	1090 bp NdeI-SpeI fragment subcloned from pGT-*fljM*	This work
pBX-*fljN*	pBXMCS-2	1260 bp NdeI-SpeI fragment subcloned from pGT-*fljN*	This work
pBX-*fljO*	pBXMCS-2	1192 bp NdeI-SpeI fragment subcloned from pGT-*fljO* utilising the SpeI site in the pGEM-T polylinker.	This work
pRX-*fljJ*	pRXMCS-2	1014 bp NdeI-KpnI fragment subcloned from pGT-*fljJ2*	This work

pBX-*fljK*	pRXMCS-2	PCR fragment created using primer 485 & 486; contains full *fljK* ORF	This work
pBX-*fljM*	pRXMCS-2	PCR fragment created using primer 489 & 490; contains full *fljM* ORF	This work
C. crescentus bacterial two hybrid			
	pBluescript II KS (+)	Amp^r pUC19-derived high copy cloning vector	Stratagene. Alting-Mees and Short, 1989
	pUT18C	Amp^r pUC19-derived high copy expression vector; contains T18 (CyaA) fragment for C-terminal fusion	BACTH Euromedex
	pKT25	Kan^r pSU40-derived low copy expression vector; contains T25 (CyaA) fragment for C-terminal fusion	BACTH Euromedex
	pUT18C-zip	Amp^r pUT18C-derived high copy expression vector; carries leucine zipper of GCN4 fused to T18 fragment	BACTH Euromedex
	pKT25-zip	Amp^r pKT25-derived low copy expression vector; carries leucine zipper of GCN4 fused to T25 fragment	BACTH Euromedex
pBK-*fljL*	pBluescript II KS (+)	PCR fragment created using primer 425 & 426; contains full *fljL* ORF	This work
pBK-*fljK*	pBluescript II KS (+)	PCR fragment created using primer 427 & 428; contains full *fljK* ORF	This work
pBK-*fljJ*	pBluescript II KS (+)	PCR fragment created using primer 429 & 430; contains full *fljJ* ORF	This work
pBK-*fliX*	pBluescript II KS (+)	PCR fragment created using primer 432 & 433; contains full *fliX* ORF	This work
pBK-*flbD*	pBluescript II KS (+)	PCR fragment created using primer 434 & 435; contains full *flbD* ORF	This work
pBK-*flgL*	pBluescript II KS (+)	PCR fragment created using primer 436 & 437; contains full *flgL* ORF	This work
pBK-*flaF*	pBluescript II KS	PCR fragment created using primer 438 & 439; contains full *flaF* ORF	This work

pBK-*flbT*	pBluescript II KS (+)	PCR fragment created using primer 440 & 441; contains full *flbT* ORF	This work
pBK-*fljM*	pBluescript II KS (+)	PCR fragment created using primer 431 & 89; contains full *fljM* ORF	This work
pBK-CC1462	pBluescript II KS (+)	PCR fragment created using primer 442 & 443; contains full CC1462 ORF	This work
pUT-*fljL*	pUT18C	1104 bp BamHI-KpnI fragment subcloned from pBK-*fljL*	This work
pUT-*fljK*	pUT18C	1136 bp BamHI-KpnI fragment subcloned from pBK-*fljK*	This work
pUT-*fljJ*	pUT18C	1144 bp BamHI-KpnI fragment subcloned from pBK-*fljJ*	This work
pUT-*fliX*	pUT18C	900 bp BamHI-KpnI fragment subcloned from pBK-*fliX*	This work
pUT-*flbD*	pUT18C	1432 bp BamHI-KpnI fragment subcloned from pBK-*flbD*	This work
pUT-*flgL*	pUT18C	1308 bp BamHI-KpnI fragment subcloned from pBK-*flgL*	This work
pUT-*flaF*	pUT18C	820 bp BamHI-KpnI fragment subcloned from pBK-*flaF*	This work
pUT-*flbT*	pUT18C	562 bp BamHI-KpnI fragment subcloned from pBK-*flbT*	This work
pUT-*fljM*	pUT18C	877 bp BamHI fragment subcloned from pBK-*fljM* utilising a natural BamHI site downstream of *fljM* TAA	This work
pUT-CC1462	pUT18C	686 bp BamHI-KpnI fragment subcloned from pBK-CC1462	This work
pKT-*fljL*	pKT25	1104 bp BamHI-KpnI fragment subcloned from pBK-*fljL*	This work
pKT-*fljK*	pKT25	1136 bp BamHI-KpnI fragment subcloned from pBK-*fljK*	This work
pKT-*fljJ*	pKT25	1144 bp BamHI-KpnI fragment subcloned from pBK-*fljJ*	This work
pKT-*fliX*	pKT25	900 bp BamHI-KpnI fragment subcloned from pBK-*fliX*	This work
pKT-*flbD*	pKT25	1432 bp BamHI-KpnI fragment subcloned from pBK-*flbD*	This work
pKT-*flgL*	pKT25	1308 bp BamHI-KpnI fragment subcloned from pBK-*flgL*	This work
pKT-*flaF*	pKT25	820 bp BamHI-KpnI fragment subcloned from pBK-*flaF*	This work
pKT-*flbT*	pKT25	562 bp BamHI-KpnI fragment subcloned from pBK-*flbT*	This work
pKT-*fljM*	pKT25	877 bp BamHI fragment	This work

		subcloned from pBK-*fljM* utilising a natural BamHI site downstream of *fljM* TAA	
pKT-CC1462	pKT25	686 bp BamHI-KpnI fragment subcloned from pBK-CC1462	This work
Protein expression			
	pET-28b (+)	Kan^r N-terminal His-tag/thrombin/T7 tag plasmid	Novagen
pET28b-*fljJ*	pET-28b (+)	1150 bp BamHI-SacI fragment subcloned from pUT-*fljJ*	This work
pET28b-*flbT*	pET-28b (+)	568 bp BamHI-SacI fragment subcloned from pUT-*fljJ*	This work
pET28b-*flaF*	pET-28b (+)	826 bp BamHI-SacI fragment subcloned from pUT-*fljJ*	This work
In vivo Co-IP			
pGT-FLAG*fljJ*	pGEM-T	N-terminal 3XFLAG *fljJ* construct created by PCR overlap extension. Primers 593/594/595/596	This work
pNP-FLAG*fljJ*	pNPTS128	1807 bp SpeI-HindIII fragment subcloned from pGT-FLAG*fljJ*	This work
flbT and *flaF* deletion mutants			
pDEL-*flaF*	pNPTS128	*flaF* ATG/TAA inframe deletion. Created using primers 348/349/319/326	This work
pDEL-*flbT*	pNPTS128	*flbT* ATG/TAA inframe deletion. Created using primers 350/349/418/419	This work
pGT-*flbT_flaF*	pGEM-T	PCR fragment created using primer 579 & 580; contains the whole *flbT* and *flaF* operon including promoter region	This work
pBX-*flbT_flaF*	pBXMCS-2	936 bp NdeI-SpeI fragment subcloned from pGT-*flbT_flaF*	This work
A. tumefaciens and *S. meliloti* bacterial two hybrid			
pBK-Atu0542	pBluescript II KS (+)	PCR fragment created using primer 695 & 663; contains full ORF	This work
pBK-Atu0543	pBluescript II KS (+)	PCR fragment created using primer 696 & 665; contains full ORF	This work
pBK-Atu0545	pBluescript II KS (+)	PCR fragment created using primer 697 & 667; contains full	This work

		ORF	
pBK-Atu0567	pBluescript II KS (+)	PCR fragment created using primer 698 & 669; contains full ORF	This work
pBK-Atu0578	pBluescript II KS (+)	PCR fragment created using primer 699 & 671; contains full ORF	This work
pBK-Atu0577	pBluescript II KS (+)	PCR fragment created using primer 700 & 673; contains full ORF	This work
pBK-SMc03037	pBluescript II KS (+)	PCR fragment created using primer 701 & 675; contains full ORF	This work
pBK-SMc03038	pBluescript II KS (+)	PCR fragment created using primer 701 & 676; contains full ORF	This work
pBK-SMc03039	pBluescript II KS (+)	PCR fragment created using primer 702 & 678; contains full ORF	This work
pBK-SMc03040	pBluescript II KS (+)	PCR fragment created using primer 703 & 680; contains full ORF	This work
pBK-SMc03051	pBluescript II KS (+)	PCR fragment created using primer 704 & 706; contains full ORF	This work
pBK-SMc03050	pBluescript II KS (+)	PCR fragment created using primer 705 & 684; contains full ORF	This work
pUT-Atu0542	pUT18C	954 bp BamHI-KpnI fragment subcloned from pBK-Atu0542	This work
pUT-Atu0543	pUT18C	975 bp BamHI-EcoRI fragment subcloned from pBK-Atu0543	This work
pUT-Atu0545	pUT18C	933 bp BamHI-KpnI fragment subcloned from pBK-Atu0545	This work
pUT-Atu0567	pUT18C	1305 bp XbaI-KpnI fragment subcloned from pBK-Atu0567	This work
pUT-Atu0578	pUT18C	462 bp BamHI-KpnI fragment subcloned from pBK-Atu0578	This work
pUT-Atu0577	pUT18C	357 bp XbaI-KpnI fragment subcloned from pBK-Atu0577	This work
pUT-SMc03037	pUT18C	1197 bp BamHI-KpnI fragment subcloned from pBK-SMc03037	This work
pUT-SMc03038	pUT18C	1249 bp BamHI-KpnI fragment subcloned from pBK-SMc03038	This work
pUT-SMc03039	pUT18C	1218 bp BamHI-KpnI fragment subcloned from pBK-SMc03039	This work
pUT-SMc03040	pUT18C	977 bp BamHI-KpnI fragment subcloned from pBK-SMc03040	This work

pUT-SMc03051	pUT18C	462 bp XbaI-KpnI fragment subcloned from pBK-SMc03051	This work
pUT-SMc03050	pUT18C	360 bp XbaI-KpnI fragment subcloned from pBK-SMc03050	This work
pKT-Atu0542	pKT25	954 bp BamHI-KpnI fragment subcloned from pBK-Atu0542	This work
pKT-Atu0543	pKT25	975 bp BamHI-EcoRI fragment subcloned from pBK-Atu0543	This work
pKT-Atu0545	pKT25	933 bp BamHI-KpnI fragment subcloned from pBK-Atu0545	This work
pKT-Atu0567	pKT25	1305 bp XbaI-KpnI fragment subcloned from pBK-Atu0567	This work
pKT-Atu0578	pKT25	462 bp BamHI-KpnI fragment subcloned from pBK-Atu0578	This work
pKT-Atu0577	pKT25	357 bp XbaI-KpnI fragment subcloned from pBK-Atu0577	This work
pKT-SMc03037	pKT25	1197 bp BamHI-KpnI fragment subcloned from pBK-SMc03037	This work
pKT-SMc03038	pKT25	1249 bp BamHI-KpnI fragment subcloned from pBK-SMc03038	This work
pKT-SMc03039	pKT25	1218 bp BamHI-KpnI fragment subcloned from pBK-SMc03039	This work
pKT-SMc03040	pKT25	977 bp BamHI-KpnI fragment subcloned from pBK-SMc03040	This work
pKT-SMc03051	pKT25	462 bp XbaI-KpnI fragment subcloned from pBK-SMc03051	This work
pKT-SMc03050	pKT25	360 bp XbaI-KpnI fragment subcloned from pBK-SMc03050	This work

3.5 Primer Table

PCR primers used in this study are listed in Table 3. The information contained in each primer name is as follows: (i) the gene name e.g. *fljJ*+1131spe1R (ii) the location of the sequence e.g. *fljJ*+1131spe1R (+1131 represents 1131 bp downstream of the *fljJ* start codon) or *fljJ*-496Spe1F (-496 represents 496 bp upstream of the *fljJ* start codon) (iii) the restriction enzyme site e.g. *fljJ*-496Spe1F and (iv) the direction of the primer e.g. *fljJ*-496Spe1F (Forward) or *fljJ*+1131spe1R (Reverse). In the DNA sequence the restriction enzyme site is coloured red. Underlined sequence refers to either FLAG or T7 sequence.

Table 3: PCR primers used in this study

Primer No.	Primer Name	DNA Sequence 5' 3'	Reference
Flagellin overexpression			
483	*fljJ*+4Nde1F	GGCCATATGGCGCTTAG CGTCAACAC	This work
491	*fljJ*+1131Spe1R	GGCACTAGTCGATGATG ACTGGTCAGCCCG	This work
484	*fljJ*+1131Kpn1R	GGCGGTACCCGATGATG ACTGGTCAGCCCG	This work
485	*fljK*+4Nde1F	GGCCATATGGCGCTGAA CAGCATCAA	This work
492	*fljK*+1123Spe1R	GGCACTAGTGACCGTTA TCGACGGGCTTCTCAG	This work
489	*fljM*+4Nde1F	GGCCATATGGCGCTGAA CAGCATCAA	This work
109	*fljM*+1081Spe1R	GGACTAGTCACATTGGA TGTGGACGCG	Faulds-Pain
487	*fljL*+4Nde1F	GGCCATATGCTGAACTC GATCAACAC	This work
493	*fljL*+1091Spe1R	GGCACTAGTAGAGTCCT TTTCAAGGTG	This work
115	*fljN*+1248Spe1R	GGACTAGTGACGTTGTT CAGTTCAGAACTG	Faulds-Pain[a]
94	*fljO*+1177R	GCCGCCGACATCCGCTT CAC	Faulds-Pain[a]
486	*fljK*+1123kpn1R	GGCGGTACCGACCGTTA TCGACGGGCTTCTCAG	This work
490	*fljM*+1081kpn1R	GGCGGTACCCACATTGG ATGTGGACGCGTTGTG	This work
C. crescentus bacterial two hybrid			
425	*fljL*+1BamH1F	GGCGGATCCCATGCTGA ACTCGATCAACAC	This work
426	*fljL*+1091Kpn1R	GGCGGTACCAGAGTCCT TTTCAAGGTG	This work
427	*fljK*+1BamH1F	GGCGGATCCCATGGCGC TGAACAGCATCAA	This work
428	*fljK*+1123Kpn1R	GGCGGTACCGACCGTTA TCGACGGGCTTCTCAG	This work
429	*fljJ*+1BamH1F	GGCGGATCCCATGGCGC TTAGCGTCAACAC	This work
430	*fljJ*+1131Kpn1R	GGCGGTACCCGATGATG ACTGGTCAGCCCG	This work
432	*fliX*+1BamH1F	GGCGGATCCCATGAAGG TTTCCAGCACGGG	This work
433	*fliX*+887Kpn1R	GGCGGTACCCGATCACG	This work

		GGTACGGAGCTC	
434	*flbD*+1BamH1F	GGCGGATCCCATGCGGC TTCTGGTCGTTGG	This work
435	*flbD*+1419Kpn1R	GGCGGTACCTGAGCTTG TCGAAGGGCGAG	This work
436	CC0898+1BamH1F	GGCGGATCCCATGACCC GCGTCTCGACCGT	This work
437	CC0898+1295Kpn1R	GGCGGTACCCTCATAGT CCAGCACATAGTG	This work
438	*flaF*+1BamH1F	GGCGGATCCCATGGAGT ACCGCCTGTTCGG	This work
439	*flaF*+807Kpn1R	GGCGGTACCGGTGTCCC CTGCAGCGAGCG	This work
440	*flbT*+1BamH1F	GGCGGATCCCGTGCCTT TGAAGCTGTCGCT	This work
441	*flbT*+549Kpn1R	GGCGGTACCGACCTTGC GGTTCCAGTCCA	This work
431	*fljM*+1BamH1F	GGCGGATCCCATGGCGC TGAACAGCATCAA	This work
89	C*fljM*+1081R	CACATTGGATGTGGACG CGTTGTG	Faulds-Pain [a]
442	CC1462+1BamH1F	GGCGGATCCCATGGAAC CTAAAGCCGCACT	This work
443	CC1462+673Kpn1R	GGCGGTACCCTTGGCCG TCGAGATGGCTTC	This work
In vivo Co-IP			
595	*fljJ*FLAGN_R	TTTGTCATCGTCATCCT TGTAATCGATGTCATGA TCTTTATAATCACCGTC ATGGTCTTTGTAGTCCA TGCGCGGCCTCCGATCG GCGA	This work
596	*fljJ*FLAGN_F	ATGGACTACAAAGACCA TGACGGTGATTATAAAG ATCATGACATCGATTAC AAGGATGACGATGACAA AGCGCTTAGCGTCAACA CGAAC	This work
593	*fljJ*-496Spe1F	ACTAGTGCCGTCGAACG CCCCGGACC	This work
596	*fljJ*+1249Hind3R	AAGCTTCGGCCATCACC TCGGCGAAC	This work
flbT and *flaF* deletion mutants			
348	*flaF*-511Spe1F	ACTAGTCCTAGCTTGCC GTCCAAGCC	G. Grimaldi [b]
349	*flaF*+807Pst1R	GGTGTCCCCTGCAGCGA GCG	G. Grimaldi [b]
319	DEL*flaF*F	AGAATCCCCGTGAAATG	G. Grimaldi [b]

		GAGCAATTGGCCTGATTCTGCCTTTCGGG	
326	DEL*flaF*R	CCCGAAAGGCAGAATCAGGCCAATTGCTCCATTTCACGGGGATTCT	G. Grimaldi [b]
350	*flbT*-499Spe1F	ACTAGTGTGCAATCGCCAGGATGTGC	G. Grimaldi [b]
418	DEL*flbT*F	GGGAGCGGCATCAAGTGCCTGAATTCGGCGACGCGGGCTGAGAATC	This work
419	DEL*flbT*R	GATTCTCAGCCCGCGTCGCCGAATTCAGGCACTTGATGCCGCTCCC	This work
579	*flbT*-199Nde1F	GGCCATATGTGGCGGAGGCCTTAGACTTTGC	This work
580	*flaF*+306Spe1R	GGCACTAGTTCAGGCCGCGTCGGCGCGGC	This work
RNA experiments			
591	*fljK*-63F	GTAATACGACTCACTATAGGGCACCGAGCAAAATGCTCCCGG	This work
592	*fljK*+51R	TTGCAGGGCGATCATCGCG	This work
592	*fliF*+685F	GTAATACGACTCACTATAGGGCTCCGAGGTCGAGGCCCGCAT	This work
592	*fliF*+799R	TGGTCACGCGGTTCAGGTC	This work
A. tumefaciens and *S. meliloti* bacterial two hybrid			
695	Atu0542+1BamH1F	GGCGGATCCAATGACAAGTATTCTGACGAA	This work
663	Atu0542+942Kpn1R	GCCGGTACCTTACTGGCGGAATAGCGACA	This work
696	Atu0543+1BamH1F	GGCGGATCCTATGACGAGCATTATCACGAA	This work
665	Atu0543+963EcoR1R	GCCGAATTCTTAACGGAAGAGCGACAGGA	This work
697	Atu0545+1BamH1F	GGCGGATCCGATGGCAAGCATTCTGACCAA	This work
667	Atu0545+921Kpn1R	GCCGGTACCTTAGCGGAAGAGCGACAGGA	This work
698	Atu0567+1Xba1F	GGCTCTAGACATGACAAGCATTTTGACCAA	This work
669	Atu0567+1293Kpn1R	GCCGGTACCTTACTTGAAGAGCTGGAGGA	This work
671	Atu0578+450Kpn1R	GCCGGTACCCTACCGCCATGGTGCGATCT	This work

700	Atu0577+1Xba1F	GGCTCTAGATATGTACC AGTTTTCCTACGC	This work
673	Atu0577+345Kpn1R	GCCGGTACCTCATTTCA GTCCATCCCTGA	This work
701	SMc03037+1BamH1F	GGCGGATCCAATGACGA GCATTCTCACCAA	This work
675	SMc03037+1185Kpn1 R	GCCGGTACCTTAGCGGA AGAGCGAAAGGA	This work
676	SMc03038+1237Kpn1 R	GCCGGTACCAAGGTTCG GTCAGGGTGCGG	This work
702	SMc03039+1BamH1F	GGCGGATCCGATGACCA GCATTCTCACCAA	This work
678	SMc03039+1206Kpn1 R	GCCGGTACCTTACTGAC GGAAGAGCTGGA	This work
703	SMc03040+1BamH1F	GGCGGATCCTATGACCA GCATCATGACCAA	This work
680	SMc03040+965Kpn1R	GCCGGTACCTTATTCCT GGAACAGGCGGA	This work
704	SMc03051+1Xba1F	GGCTCTAGATATGAAGA GCACACTGCGTAT	This work
706	SMc03051+450Kpn1R	GCCGGTACCTTACCGCC ATGGCGCGATCT	This work
705	SMc03050+1Xba1F	GGCTCTAGACATGTATC AGTTTGCATACGC	This work
684	SMc03050+348Kpn1R	GCCGGTACCTCATTTCA GTCCATCCCTGA	This work

[a], London School of Hygeine & Tropical Medicine, London, England; [b] Institute of Reproductive and Developmental Biology, Imperial College London, England

3.6 Isolation of Plasmid DNA

3.6.1 *Preparation of plasmid DNA by alkaline lysis with SDS*

The following protocol is based on a published method (Sambrook and Russell, 2001). A single bacterial colony was inoculated in 3-5 ml liquid medium (with appropriate antibiotic) and grown overnight with shaking. The cell culture was harvested by centrifugation for 5 min at 12000 x g at 4 °C, the supernatant discarded and the cell pellet resuspended in 0.3 ml chilled Alkaline Lysis Solution I. The cells were then lysed with 0.6 ml Alkaline Lysis Solution II. After 5 min incubation at room temperature (RT) the cell debris was precipitated with 0.25 ml of Alkaline Lysis Solution III with vigorous mixing. The bacterial lysate was then centrifuged for 20 min at 12000 x g at RT, and the cleared lysate was transferred to a new microfuge tube. The plasmid DNA was precipitated by the addition of 0.6 ml of Isoproponal, and pelleted by centrifugation

for 15 min at 12000 x g at 4 °C. The supernatant was then discarded and the DNA pellet was washed once in 70 % Ethanol and centrifuged again for 5 min in the same conditions, before being air-dried in a 60 °C oven to remove all traces of solvent. The plasmid DNA was resuspended in 50 µl sterile water and stored at -20 °C until required.

3.6.2 *Preparation of plasmid DNA-GenElute™ HP Plasmid Miniprep Kit*

The preparation of plasmid DNA by alkaline lysis with SDS using the described method does not isolate the DNA at a purity that can be accurately quantified by UV-spectrophotometry. Furthermore, the DNA cannot be used for DNA sequencing. Therefore, a second method of isolation, a commercial kit, was utilised when increased DNA purity was essential. Other than Ethanol, Isopropanol and sterile water, all solutions used were from the kit.

A single bacterial colony was inoculated in 3-5 ml liquid medium (with appropriate antibiotic) and grown overnight with shaking. The cell culture was harvested by centrifugation for 5 min at 12000 x g at 4 °C, the supernatant discarded and the cell pellet resuspended in 0.2 ml chilled RNase A /Resuspension Solution. The cells were then lysed with 0.2 ml Lysis Buffer. After 5 min incubation at RT the cell debris was precipitated with 0.35 ml of Neutralization/Binding Buffer. The bacterial lysate was then centrifuged for 10 min at 12000 x g at RT and the cleared lysate was transferred to a new microfuge tube. A GenElute HP Miniprep Binding Column was prepared by the addition of 0.5 ml Column Preparation Solution and centrifugation for 1 min at 12000 x g at RT. The cleared lysate was transferred to the prepared column and centrifuged in the same conditions. The column was then washed with 0.75 ml Wash Solution 2 and centrifuged for 1 min at 12000 x g at RT. The binding column was given a final spin for 2 min at 12000 x g at RT in order to remove any excess Wash Solution 2 and then the column was transferred to a new microfuge tube. The plasmid DNA was eluted from the binding column with 100 µl sterile water and centrifugation at 1 min at 12000 x g at RT. DNA concentration was measured by UV-spectrophotometry (NanoDrop 1000) at an absorbance of 260 nm. The DNA was stored at -20 °C until required.

3.6.3 *Preparation of plasmid DNA-GenElute^{TM} HP Plasmid Midiprep Kit*

A scaled-up isolation method was used for low copy number vectors to ensure a maximal amount of DNA was obtained. Other than Ethanol, Isopropanol, Sodium acetate and sterile water, all solutions used were from the kit.

A single bacterial colony was inoculated in 50 ml liquid medium (with appropriate antibiotic) and grown overnight with shaking. The cell culture was harvested by centrifugation for 20 min at 3000 x g at 4 °C), the supernatant discarded and the cell pellet resuspended in 4 ml chilled RNase A/Resuspension Solution. The cells were then lysed by 5 min incubation at RT with 4 ml Lysis solution. The cell debris was precipitated with 4 ml chilled Neutralization/Binding Buffer. 3 ml Binding solution was added to the lysate before it was cleared using a filter syringe. A GenElute HP Midiprep Binding Column was prepared by the addition of 4 ml Column Preparation Solution and centrifugation for 2 min at 3000 x g at 4 °C. All of the cleared lysate was then transferred to the prepared column and centrifuged in the same conditions. The column was washed once with 4 ml Wash Solution 1 and centrifuged for 2 min at 3000 x g at 4 °C, and then washed once with 4 ml Wash Solution 2 and centrifuged as before. The binding column was transferred to a new microfuge tube and the plasmid DNA was eluted with 1 ml Elution Solution and centrifugation for 5 min at 3000 x g at 4 °C. 100 µl 3 M Sodium acetate (pH 5.2) and 0.7 ml Isopropanol were added to the recovered plasmid DNA and the solution was centrifuged for 30 min at 12000 x g at 4 °C, in order to pellet the DNA. The supernatant was then discarded and the DNA pellet was washed once in 70 % Ethanol, centrifuged for 10 min at 12000 x g at 4 °C, before being air-dried in a 60 °C oven. The plasmid DNA pellet was resuspended in 50 µl sterile water and DNA concentration was measured by UV-spectrophotometry at an absorbance of 260 nm. The DNA was stored at -20 °C until required.

3.7 Isolation of Bacterial Genomic DNA

3.7.1 *Crude preparation by boiling*

C. crescentus genomic DNA was prepared in a crude manner when needed for diagnostic PCR screens. A single bacterial colony was inoculated in 5 ml liquid medium and grown overnight at 30 °C with shaking. 0.5 ml of the overnight culture was diluted with 0.5 ml sterile water. The cells were then lysed by the following process; incubation

at -80 °C for 5 min, boiling in water for 10 min, followed by incubation on ice for 5 min. 2 µl of cells were then used in PCR reactions.

3.7.2 *Preparation of bacterial genomic DNA-GenElute™ Bacterial Genomic DNA kit*

The preparation of genomic DNA by the boiling method described does not isolate the DNA from lysed cell debris thus it cannot be used for DNA sequencing. Therefore, a second method of isolation, a commercial kit, was utilised when the DNA was to be used for sequencing. Other than Ethanol and sterile water, all solutions used were from the kit.

A single bacterial colony was inoculated in 3 ml liquid medium and grown overnight with shaking. 1.5 ml cell culture was then harvested by centrifugation for 5 min at 12000 x g at 4 °C, the supernatant discarded and the cell pellet resuspended in 0.18 ml RNase A/Lysis Solution T. After 2 min incubation at RT, 20 µl Proteinase K (1 mg/ml) was added to the cells and the suspension was incubated at 55 °C for 30 min. To completely lyse the cells, 0.2 ml Lysis solution C was added followed by a further 10 min incubation at 55 °C. A GenElute HP Miniprep Binding Column was prepared by the addition of 0.5 ml Column Preparation Solution and centrifugation for 1 min at 12000 x g at RT. 0.2 ml Ethanol was added to the cell lysate which was then transferred to the prepared column and centrifuged for 1 min at 6500 x g at RT. The column was then washed once with 0.5 ml Wash Solution 1 and centrifuged under the same conditions, followed by a wash with 0.5 ml Wash Solution Concentrate and centrifuged for 3 min at 12000 x g at RT. The DNA was eluted from the binding column with 200 µl Elution Solution and centrifugation for 1 min at 12000 x g at RT. DNA concentration was measured by UV-spectrophotometry at an absorbance of 260 nm. The DNA was stored at -20 °C until required.

3.8 Agarose Gel Electrophoresis

The DNA in all PCR and cloning experiments was visualised and assessed using agarose gel electrophoresis (see Appendix B). A typical gel had an agarose concentration of 0.8 %. For the assessment of smaller DNA fragments, an agarose concentration of 1.5 % was used. Agarose was weighed and dissolved into 1 x TAE running buffer by heating in a microwave. 1 x TAE buffer by diluting 50 x TAE buffer in water (Sigma-Aldrich). Ethidium bromide (final concentration of 0.5 µg/ml) was then

added to the molten gel and the gel was cast. 1 x DNA loading buffer was mixed with the DNA sample prior to loading in the gel. The gels were run in 1 x TAE running buffer and at 120 V. The duration of the electrophoresis was judged against the migration of a 1 Kb or 100 bp DNA ladder (Promega). The gels were visualised using ultra-violet light. Gel images were taken using Gel Documentation equipment (InGenius, Syngene).

3.9 Polymerase Chain Reaction

Oligonucleotide primers for PCR experiments were designed manually using DNA sequences deposited in the NCBI nucleotide database. PCR reactions were assessed electronically using the software Amplifx 1-1.5.4 and all primers were purchased from IDT Integrated DNA technologies. When the integrity of the PCR product was essential High fidelity TAQ polymerase was used (Rovalab GmbH). For diagnostic PCR reactions MolTaq polymerase was used (Molzym).

All PCR reactions contained the following: approx 50 ng of DNA template, 20 pM of forward primer, 20 pM of reverse primer, dNTP's at a final concentration of 250 µM, 1 x Polymerase buffer, 1 unit of DNA polymerase, 10 % DMSO, made up to final volume of 50 µl with sterile water. A standard PCR cycle program was used for all PCR reactions. However, the parameter of primer annealing temperature was varied depending on the experiment. An initial denaturation at 95 °C for 2 min then 30 cycles of: 1) 95 °C for 40 sec, 2) 58-60 °C for 40 sec, 3) 75 °C for 3 min; followed by a final extension at 75 °C for 5 min. All PCR reactions were checked using agarose gel electrophoresis.

3.10 Purification of PCR DNA

3.10.1 *Purification of PCR DNA-GenElute^{TM} PCR Clean-up Kit*

PCR DNA was purified free from excess primers, nucleotides, salts and other components of the PCR reaction using a commercial kit. Other than sterile water, all solutions used were from the kit. A GenElute HP Miniprep Binding Column was prepared by the addition of 0.5 ml Column Preparation Solution and centrifugation for 1 min at 12000 x g at RT. 5 volumes of Binding Solution were added to 1 volume of the PCR reaction and the DNA suspension was then transferred to the binding column and

centrifuged under the same conditions. The column was washed with 0.5 ml Wash Solution and centrifuged for 1 min at 12000 x g at RT. The binding column was given a final spin for 2 min at 12000 x g at RT, to remove excess Wash Solution before being transferred to a new tube. The DNA was eluted with 50 µl sterile water and centrifugation 1 min at 12000 x g at RT.

3.10.2 *Purification of PCR DNA-GenElute^{TM} Gel Extraction kit*

PCR DNA from a reaction that had multiple DNA fragments in it was gel purified using a commercial kit. Other than Isopropanol and sterile water, all solutions used were from the kit. The required DNA fragment was excised from the agarose gel and weighed in a tared microfuge tube. The gel slice was solubilised by adding 3 gel volumes (according to the slice weight) of Solubilisation Solution and incubating at 60 °C until all the agarose was dissolved. A GenElute Binding Column G was prepared by the addition of 0.5 ml Column Preparation Solution and centrifugation at 1 min at 12000 x g at RT. 1 gel volume of Isopropanol was added to the solubilised mixture and mixed to homogeneity. The mixture was then transferred to the prepared binding column and centrifuged for 1 min at 12000 x g at RT. The column was washed with 0.7 ml Wash Solution and centrifuged in the same conditions. The binding column was given a final spin for 2 min at 12000 x g at RT, to remove excess Wash Solution and then transferred to a new tube. The DNA was eluted with 25-50 µl sterile water and centrifugation 1 min at 12000 x g at RT.

3.11 Digestion of DNA by Restriction Endonucleases

Plasmid restriction maps analysis and other DNA sequence analysis was carried out using SerialCloner v2-1 software (http://serialbasics.free.fr). Restriction digests of both PCR DNA and Plasmid DNA were performed during cloning experiments using Promega Restriction Enzymes. A typical digest reaction contained: 3-6 units of Restriction Endonuclease, 1 µl BSA (1 mg/ml), 1 x Restriction buffer, and sterile water. The Restriction buffer used was chosen in accordance with the Promega Restriction enzyme buffer compatibility guide. All reactions were incubated at 37 °C for 1-3 hr and then checked using agarose gel electrophoresis. DNA was then gel purified.

3.12 Alkaline Dephosphorylation of Digested Plasmid DNA

In the cases where a vector was digested with a single restriction enzyme, the 5' phosphate group was removed from the digested DNA to prevent it from re-ligating when used in cloning experiments. After restriction digest, the DNA was purified as follows. 5 µl 3 M Sodium acetate (pH 5.2) and 140 µl Ethanol were added to the reaction. The mixture was incubated at -80 °C for 30 min and centrifuged for 15 min at 12000 x g at 4 °C, in order to pellet the DNA. The supernatant was then discarded and the DNA pellet was washed once in 70 % Ethanol, centrifuged in the same conditions, before being air-dried in a 60 °C oven to remove all traces of solvent. The DNA was resuspended in 50 µl sterile water.

The DNA was then dephosphorylated. The reaction contained: 42 µl purified digested vector DNA, 3 units Alkaline Phosphatase (CIAP, Promega) and 5 µl Alkaline Phosphatase buffer. The reaction was then incubated at 37 °C for 3 hr. In order to inactivate the Alkaline Phosphatase, 10 µl TNE buffer, 5 µl 10 % SDS, and 35 µl sterile water was added to the reaction and the mixture was incubated at 68 °C for 15 min. 10 µl 3 M Sodium acetate (pH 5.2) and 275 µl Ethanol was added to the mixture. The mixture was then incubated at -80 °C for 30 min and centrifuged for 15 min at 12000 x g at 4 °C, in order to pellet the DNA. The supernatant was discarded and the DNA pellet was washed once in 70 % Ethanol, centrifuged in the same conditions, before being air-dried in a 60 °C oven. The DNA was then resuspended in 20 µl sterile water and used in ligation reactions.

3.13 DNA Ligation Reactions

All ligation reactions were performed using freshly digested and purified DNA. The amount of vector DNA used for cloning experiments was either 1 µg (high copy number) or 2 µg (low copy number). Ligations were performed on the assumption of complete recovery of vector DNA after all stages of the cloning process. A reaction always contained the following: 15 µl insert DNA (either digested PCR fragment or digested plasmid fragment for subcloning), 2 µl digested vector DNA, 3 units of T4 DNA Ligase (Promega) and 2 µl T4 Ligase Buffer. Ligation reactions were incubated overnight at 4 °C before being transformed into *E. coli*.

3.14 Intermediate Vector Cloning Step

Some plasmids were constructed by cloning the insert DNA directly into the vector required for that experiment. However, if this was unsuccessful an intermediate cloning step was introduced and the DNA was ligated into a high copy plasmid: pBluescript II KS (+) or pGEM-T. This allowed us to obtain large amounts of digested insert to then create the final construct. Both vectors allow for blue/white screening in the identification of positive clones.

The vector pGEM-T is particularly useful as it allows for the direct cloning of PCR fragments without the need for restriction digestion. pGEM-T is a linear vector that contains 3' terminal thymidine overhangs at each end that prevent it from re-circularising. Certain DNA polymerases have terminal transferase activity and leave a single 3' deoxyadenosine on the amplified PCR product DNA during the PCR reaction in a template-independent manner. These compatible overhangs allow the amplified PCR DNA and the vector DNA to be ligated very efficiently. However, the High fidelity TAQ polymerase we used for cloning experiments does not have terminal transferase activity where as MolTaq does, therefore, we had to carry out an additional A-tailing PCR reaction using MolTaq to make a PCR fragment compatible for pGEM-T cloning.

3.14.1 *A-tailing reaction*

PCR DNA was cleaned up as described (3.5.2). The A-tailing reaction was then set up as follows: 15.5 µl of PCR fragment, 2 µl of MolTaq polymerase buffer, 2 µl of dATP (25 mM) and 0.5 units of Moltaq. The reaction was incubated at 72 °C for 30 min and then used for direct ligation into pGEM-T.

3.14.2 *pGEM-T ligations*

pGEM-T ligations were carried out according to the manufacturers instructions (Promega). Ligation reactions were incubated overnight at 4 °C before being transformed into *E. coli*.

3.14.3 *Blue/White screening*

Blue-white colony screening was used for pGEM-T and pBluescript II KS (+) cloning in order to detect positive clones. X-gal is used in the culture media as a indicator dye and it is cleaved by the production of β-galactosidase to produce a blue insoluble

pigment. However, the successful ligation of insert DNA into the MCS of the vectors, results in the absence of LacZ α-complementation and an inability to hydrolyse X-gal. Subsequently, white colonies instead of blue. Transformants were cultured on media in the presence of Ampicillin and X-gal. White colonies were then picked of and the plasmid of those clones was isolated and tested by restriction digestion for a successful ligation.

3.15 DNA Sequencing

Plasmid and PCR DNA was first quantified and then adjusted to; 30-100 ng/µl and 10-50 ng/µl respectively. 30 µl of each sample was sent to GATC Biotech for DNA sequencing. If required, 30 µl (10 pmol/µl) of our own primer was sent otherwise a universal primer provided by GATC Biotech was used. DNA sequences were received in a .ab1 file format and analysed using 4Peaks v1.7.2 software (mekentosj.com).

3.16 Preparation of Whole Cell Lysates

C. crescentus whole cell lysates were prepared for immunoblot analysis. A single bacterial colony was inoculated in 3 ml liquid medium and grown overnight at 30 °C with shaking. The overnight culture was then diluted back in fresh 5 ml liquid medium to OD600 0.05 and grown to OD600 0.6-0.8. 2 ml of the cell culture was harvested by centrifugation for 3 min at 12000 x g at 4 °C, and the supernatant discarded. The pellet was then resuspended in 50 µl 2 x SDS sample buffer. Samples were placed in boiling water for 5 min and quantified in terms of OD units using the following formula:

$$\text{OD units}/\mu\text{l} = (\text{Volume of Culture}/\text{Volume of SDS buffer}) \times \text{OD600}$$

A standard number of OD units were then used for immunoblot analysis.

3.17 Secretion Assays

C. crescentus secretion assays were set up in the same way as the preparation of whole cell lysates, only the supernatant of the 2 ml (OD600 0.6-0.8) culture was used for analysis. The 2 ml supernatant was passed through a 0.2 µm syringe filter to remove any remaining cells. The cell free supernatant was passed through a Purabind 045 filter

membrane (Whatman), which was then placed inside a sterile microfuge tube. 50µl 2x SDS sample buffer was pipetted onto the membrane and the tube was incubated for 30mins at 70ºC. The OD units/µl were calculated using the equation in 3.16 and a standard number of OD units were then used for immunoblot analysis

3.18 Protein gel electrophoresis

3.18.1 *Tricine SDS-polyacrylamide gel electrophoresis*

Protein samples mixed in 2X SDS sample buffer were placed in boiling water for 5 min before being subjected to gel electrophoresis using 12 % Tricine SDS-PAGE gels, 1 x Cathode running buffer and 1 x Anode running buffer. A current of 25 mA was applied during sample migration through the stacking gel layer. The current was then increased to 40 mA until the samples had migrated to the desired distance through the separating gel layer. A protein standard was included with every gel for analysis (SeeBlue Plus2, Invitrogen). The gels were visualised by first staining in Coomassie Blue solution for 1 hr and then in Destaining solution for 1 hr.

3.18.2 *Native-polyacrylamide gel electrophoresis*

Native-PAGE analysis was used for purified protein samples and RNA EMSA experiments (see 3.31). The separating gel layer was prepared first, covered with sterile water and allowed to set. The stacking gel layer was then set on top. 1 X Native sample buffer was added to the protein samples and they were subjected to electrophoresis in 1 x Native running buffer at a constant 80 V at 4 °C. The gels were visualised by first staining in Coomassie Blue for 1 hr and then in Destaining Solution for 1 hr.

3.19 Immunoblot Analysis

Protein samples separated by SDS-PAGE were transferred to a PVDF membrane by electroblotting for 120 min at a constant 200 V in cold Immunoblot transfer buffer. Membranes were then blocked overnight in 5 ml PMT. After washing twice in 10 ml PMT the primary antibody was added in fresh 5 ml PMT (experiment dependent concentrations) and incubated at RT for 60 min. Membranes were then washed four times in 10 ml PMT before the secondary antibody (GIBCO BRL Goat α-Rabbit) was added at a concentration of 1:10000 in fresh 10 ml PMT and incubated for 60 min.

Membranes were then washed four times in 10 ml PBS. Detection was achieved using ECL-Plus and exposing the membranes to hyperfilm (Amersham GE-Healthcare). Quantification of immunoblots was performed using ImageQuant software (GE-Healthcare) after scanning 5- 15 sec exposures using a standard Epson scanner. Statistical analysis of data sets was performed using the ANOVA analysis tool in Microsoft Excel 2004.

3.20 Motility Agar Assay

C. crescentus strains were tested for their ability to swim in low percentage agar medium. Motile cells will migrate from the initial point of involution and form chemotactic rings. A single bacterial colony was stabbed using a sterile toothpick into PYE motility medium and incubated for 5-7 days at 30 °C. For plasmid selection or expression induction the appropriate concentration of antibiotic or supplement was added to the medium. Images were then taken using Gel Documentation equipment (InGenius, Syngene).

3.21 Cloning Strategy: Flagellin Overexpression

To obtain flagellar-independent expression of flagellin: the full open reading frames, minus the 5' untranslated promoter region, of *fljJ*, *fljK*, *fljL*, *fljM*, *fljN* and *fljO* were cloned into pBXMCS-2 and pRXMCS-2 (Thanbichler *et al*., 2007). An NdeI restriction site was incorporated into the 5' primer used to generate the PCR DNA fragments. The NdeI recognition sequence (CATATG) contains an ATG codon that can be used as a transcriptional start site. pBXMCS-2 and pRXMCS-2 both contain a Xylose inducible promoter that was utilised for flagellin expression in *C. crescentus*. All constructs were confirmed by DNA sequencing. Due to the high degree of sequence similarity between the β-flagellins, the same forward primer was used to clone each individual gene. This resulted in one non-complimentary nucleotide base in the PCR generated *fljO* fragment. However, the mutation was silent and the amino acid sequence did not change form that of wild type *fljO*.

3.21.1 *Xylose induction*

A single bacterial colony was inoculated in 3 ml PYE + kan + Xylose (0.3 % final concentration) liquid medium and grown overnight at 30 °C with shaking. The

overnight culture was then diluted back in fresh 3 ml PYE + kan + Xylose liquid medium to OD600 0.05 and grown to OD600 0.6-0.8. Cells were then either checked by phase contrast microscopy for their ability to swim and their swimming speed calculated (see 3.27), or whole cell lysates were prepared for immunoblot analysis using the α-Fla antibody at 1/30000 dilution. Motility agar assays were carried out on PYE motility medium + kan + Xylose.

3.22 Cloning Strategy: Inframe Deletion Mutants

A strategy was developed to make inframe deletions of *flaF* and *flbT* similar to the method used for making the flagellin deletion mutants (Figure 12). The flagellin deletion plasmids were created prior to this project. The principle is based on allelic exchange where a mutated gene replaces the wild type by recombination. Primers were designed to amplify approximately 500 bp upstream and 500 bp downstream of the gene (Figure 12). Internal deletion primers were designed to have complimentary overhangs for each other in order to allow the two regions to be fused together in a final overlapping extension PCR. The final PCR product contained only a scar of the gene:

GTGCCTgaattcGGCGACGCGGGCTGA (*flbT)*
ATGGAGgaattcGCCTGA (*flaF)*

The EcoR1 (GAATTC) site was designed into the deletion primers to be used for an extra cloning step should the overlapping extension PCR be unsuccessful. EcoR1 cloning was utilised in this way to construct the flagellin deletion plasmids (Faulds-Pain). The PCR product was cloned into pGEM-T or pBluescript II KS(+) before being subcloned into the suicide plasmid pNPTS128 and subsequently conjugated into *C. crescentus*. pNPTS128 carries Kanamycin resistance and a *sacB* gene. *sacB* is activated by sucrose and is lethal to gram negative bacteria. The replacement of the wild type gene relies on the integration of the plasmid into the chromosome and the forcing of a double cross-over event during recombination. After conjugation the strains were replica plated onto PYE + kan and PYE + Sucrose (suc) solid medium and incubated at 30 °C for 48 hr. pNPTS128 can not replicate in *C. crescentus* and therefore Kanamycin resistant/Sucrose sensitive (Kan^r Suc^s) colonies must have gone through a single cross over event where the plasmid has integrated. The second step removes the integrated plasmid DNA during chromosomal duplication. Homologous recombination leaves

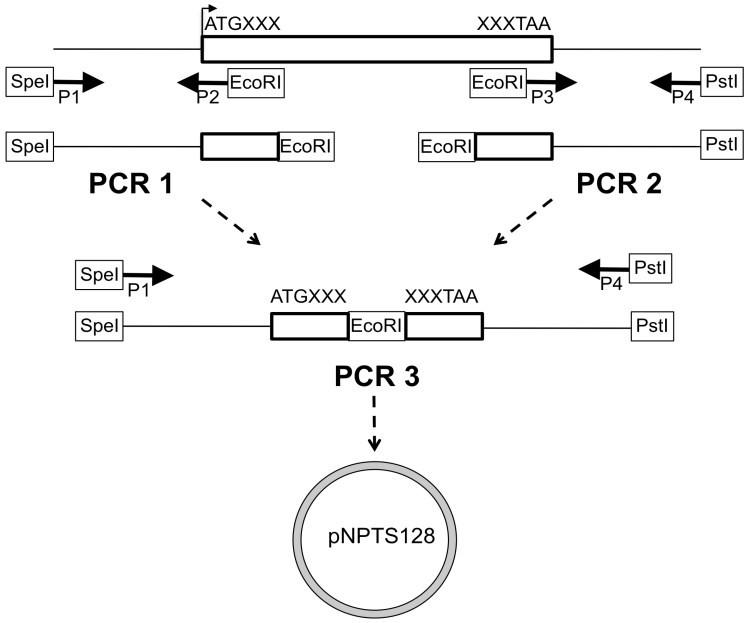

Figure 12: Cloning Strategy: Inframe Deletion Mutants

A schematic illustration of the strategy developed to make gene deletions in *C. crescentus*. DNA fragments containing the upstream and downstream sequences of the target gene were generated by PCR. The internal gene primers were designed to have complimentary ovehangs for each eachother such that they could be stiched together by overlapping extension PCR. The final PCR fragment contained a scar of the target gene. This sequence was then used to replace the wild type copy on the chromosome by recombination using the integrating vector, pNPTS128.

either the mutated gene or the wild type gene on the chromosome. To select for this step: Kan^r Suc^s colonies were cultured overnight in liquid medium without plasmid selection. 1 x 10^{-2}, x 10^{-3} and x 10^{-4} dilutions were plated out on PYE + suc solid medium and incubated at 30 °C for 48 hr. Colonies were then replica plated onto PYE + kan and PYE solid medium. Kanamycin sensitive/Sucrose resistant (Kan^s Suc^r) no longer harbor the plasmid either in or out of the chromosome. Diagnostic PCR was carried out to check for the deleted gene. Confirmation was made by DNA sequencing.

3.22.1 *Complementation of the ΔflaF and ΔflbT mutants*

To check the two deletion mutants we created a complementation plasmid that contained the containing both genes and the promoter region (Llewellyn *et al*., 2005). Primers were designed to make a pBX-*flbT_flaF* plasmid; containing the entire *flbT* and *flaF* coding sequences and 199 nucleotides upstream of the *flbT* start codon. The plasmid was confirmed to be correct by DNA sequencing. The plasmid was conjugated into both the Δ*flaF* and Δ*flbT* mutants and analysed by motility agar assays and immunoblot using α-FlbT (1/500 dilution) and α-FlaF (1/500 dilution) antibodies (Prof. James Gober). Complementation was achieved by Kanamycin selection alone and not by Xylose induction.

3.23 Isolation of Flagellar Filaments

Flagella from *C. crescentus* can be harvested relatively easily due to the fact that during the natural life cycle of the bacterium, the flagellum is ejected into the spent medium. A single bacterial colony was inoculated in 5 ml PYE liquid medium and grown overnight at 30 °C with shaking. The overnight culture was then diluted back in fresh 250-500 ml PYE liquid medium to OD600 0.05 and grown to OD600 0.6-0.8. The culture was harvested by centrifugation for 20 min at 6000 x g at 4 °C, and the supernatant was collected. The supernatant was then subjected to high-speed centrifugation for 45 min at approx 100000 x g (28000 rpm) at 4 °C, using an SW-32 Ti rotor. The subsequent pellet was resuspended in 20 ml PBS and centrifuged for 20 min at 3000 x g at 4 °C, in order to remove any remaining cells. The supernatant was then subjected to high-speed centrifugation under the same conditions on order to harvest the flagella. The protein pellet was resuspended in 50 μl PBS and stored at - 20 °C until required. Protein

samples were analysed using Tricine SDS-PAGE and Mass Spectrometry (see Appendix B).

3.24 Mass Spectroscopy Analysis of Proteins

All protein samples were processed and analysed by the in-house proteomic unit, Pinnacle. Samples were excised from Coomassie Blue stained SDS-PAGE gels, zip-tip purified and subjected to Tryptic digestion. Samples were then analysed using MALDI-TOF or LC/MS/MS.

3.25 Transmission Electron Microscopy

The electron microscopy imaging of *C. crescentus* flagellar filaments was carried out with the assistance of Dr. Wendy Smith. 5 μl of filament preparation (neat and 1 x 10^{-1} dilution) was pipetted onto the Carbon coated surface of a Copper EM grid and any excess was removed by blotting paper. The grids were then stained with 10 μl of either 3 % Uranyl acetate or 3% Phosphotungstic acid and the excess liquid removed with blotting paper. Grids were allowed to dry and then observed with a Philips CM100 TEM in the University of Newcastle upon Tyne Electron Microscopy unit (See Appendix D). Quantitative filament parameters (filament length, pitch length, pitch height) were determined using ImageJ software (rsb.info.nih.gov/ij/download.html) for between 10 and 30 filaments per mutant (Figure 13). Data and statistical analysis were performed using Microsoft Excel 2004 or the statistical software package R (www.r-project.org). The statistical significance of parameters compared to the wild type was calculated using a standard *t* test in R.

3.26 Analysis of *Caulobacter crescentus* Swimming Speeds

The measurement of *C. crescentus* swimming speeds was carried out by Dr. Shuichi Nakamura, Osaka University Japan. Free swimming cells were visualised with a phase contrast microscope (CH-40, Olympus) and recorded on VHS videotape at intervals of 1/30 seconds through a CCD camera (C5405-50, Hamamatsu Photonics). The necessary parts of the movies were captured on a computer as BMP images with video capture software (CosmoCapture, Library, Japan). The swimming speed, determined by the software, was calculated for a minimum of 25 swimming cells by tracing the centers of

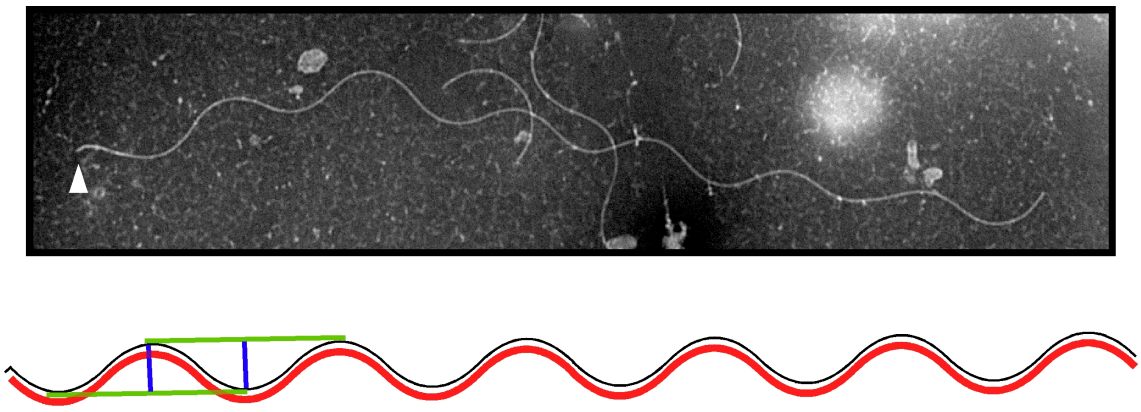

Figure 13: Measurement parameters for *Caulobacter crescentus* flagellar filaments
In order to be selected for measurement, the filament had to possess an intact hook structure (white arrow points to hook) and be completely visible. The schematic illustrates the filament parameters that were measured: filament length (red), pitch length (green), and pitch height (blue).

the cells. Statistical analysis of data sets was performed using Microsoft Excel 2004 or R using both traditional pairwise *t* tests and analysis of variance (ANOVA).

3.27 Bacterial Two-Hybrid Experiments

The BACTH system is a commercial technology that utilises the catalytic domain of Adenylate Cyclase from *Bordetella pertussis* comprising of two fragments, T18 and T25, which are inactive when separated. The fusion of the fragments to two separate interacting polypeptides results in the reconstitution of Adenylate Cyclase and the subsequent synthesis of Cyclic AMP (cAMP). Increased cAMP levels trigger the expression of the *lac* operon in *E. coli* and therefore those bacteria that are able to utilise lactose can be easily identified on selective media containing the indicator X-gal; which is cleaved in the presence of β-galactosidase (*lacZ*) to give a blue colony phenotype. Therefore, a positive result (protein-protein interaction) is blue, while a negative result (no interaction) is white.

3.27.1 *Caulobacter crescentus*

Full-length open reading frames of *fljJ*, *fljK*, *fljL*, *fljM*, *fliX*, *flbD*, *flbT*, *flaF*, *flgL* and *cc1462* were first cloned into pBluescript II KS (+) and subsequently into both pUT18c and pKT25. Genes were cloned using BamHI and KpnI restriction sites that were designed into the primers (Table 3). A natural BamHI restriction site downstream of *fljM* was utilized for cloning. All constructs were confirmed by DNA sequencing. A matrix of all possible combinations of interactions was constructed. To test an interaction, 25 ng of each plasmid was co-transformed into the test strain BTH101 by chemical transformation. Transformants were incubated on LB + kan + amp + X-gal at 37 °C for overnight. The plates were then left at RT another 24 hrs before phenotype scoring. To quantify the interactions, a standard β-galactosidase assay was performed (Sambrook and Russell, 2001).

3.27.2 *β-galactosidase activity assays*

Tests were carried out in triplicate. A single bacterial colony was inoculated in 3 ml LB + kan + amp liquid medium and grown at 30 °C with shaking until the culture reached an OD600 0.6-0.8. Cells were harvested by centrifugation for 3 min at 12000 x g at 4 °C, resuspended in 3 ml sterile saline solution, and placed on ice. In a sterile test tube,

0.5 ml cells was added to 0.55 ml Z-buffer and 100 µl chloroform. The mixture was vortexed and incubated at 30 °C for 5 min. A 4 mg/ml solution of ONPG was made in Z-buffer and 0.2 ml was added to the cells while shaking. The mixture was then incubated for 10 min before the reaction was stopped by addition of 0.5 ml 1 M $NaCO_3$. Colour was measured using a spectrophotometer at an absorbance of 420 and 550 nm. The remainder of the cell mix was used to obtain a OD650 (absorbance 650 nm) measurement. In order to calculate the activity, the following equation was used:

$$\text{Miller units} = 1000*((ABS420-(1.75*ABS550))/(ABS650*10*0.5))$$

Statistical analysis of data sets was performed using a traditional pairwise *t*-test.

3.27.3 *Agrobacterium and Sinorhizobium*

The flagellin genes, *flbT* and *flaF* from *Agrobacterium tumefaciens* C58 and *Sinorhizobium meliloti* 1021 were tested using the BACTH system. *A. tumefaciens*: *fla* (Atu0542), *flaB* (Atu0543), *flaA* (Atu0545), *flaD* (Atu0567), *flbT* (Atu0578), *flaF* (Atu0577). *S. meliloti*: *flaA* (SMc03037), *flaB* (SMc03038), *flaD* (SMc03039), *flaC* (SMc03040), *flbT* (SMc03051), *flaF* (SMc03050). Full-length open reading frames of the genes were first cloned into pBluescript II KS (+) and subsequently into both pUT18c and pKT25. The bacterial two-hybrid experiment was performed in the same way as previously mentioned (see 3.28.1).

3.28 Protein Over-Expression and Purification

Full-length open reading frames of *fljJ*, *flbT* and *flaF* were sub-cloned, using BamHI/SacI, from their corresponding pUT18C constructs into pET-28b (+). All constructs were confirmed by DNA sequencing. N-terminal histidine-tagged protein was expressed using BL21 (DE3) cells. Plasmid constructs were transformed into fresh BL21 (DE3) competent cells before very purification experiment.

A single bacterial colony was inoculated in 25 ml LB + kan liquid medium and grown overnight at 37 °C with shaking. The overnight culture was then diluted back in fresh 1 litre LB + kan liquid medium to OD600 0.05 and grown to OD600 0.6-0.8. Protein expression was then induced by the addition of IPTG (final concentration of 1 mM) and the culture was incubated for 4 hr at 30 °C with shaking. The culture was harvested by centrifugation for 20 min at 6000 x g at 4 °C, and the supernatant

discarded. The pellet was then resuspended in 20 ml His-Loading buffer and the cells were sonicated on ice (3 x 30 second pulses, with 1 min intervals). The cells were then checked for lysis using a phase contrast microscope. The cell lysate was harvested by centrifugation for 30 min at 18000 x g at 4 °C, and the supernatant containing the soluble protein fraction was discarded. The pellet was washed twice in His-Loading buffer and twice in 1 x IB wash buffer with a centrifugation under the same conditions in after each wash step. The pellet was then resuspended in 20 ml His-Loading buffer + 8 M Urea and left overnight at RT. Finally, the protein sample was centrifuged at 30 min at 18000 x g at RT, and the supernatant containing soluble protein was transferred to a sterile falcon tube.

3.28.1 *His-tag purification*

Proteins samples were subjected to nickel affinity purification using a 5 ml HiTrap Sephadex column connected to an AKTA prime purification system (GE-Healthcare) at RT. The column was first equilibrated in approximately 25 ml His-Loading buffer + 8 M Urea before the sample was loaded using a 50 ml superloop (GE-Healthcare). Bound protein was eluted in His-Elution buffer + 8 M Urea on a 50 ml gradient from 0 % to 100 % elution buffer. The elution step was monitored using a paper chart recorder plotting the detection at 280 nm. The eluted protein peaks were collected in 2 ml fractions and analysed using Tricine SDS-PAGE.

3.28.2 *Protein regeneration and gel filtration*

The fractions containing high concentrations of protein were pooled together and concentrated to 0.5 ml using a Vivaspin centrifugation column (3500 x g, RT) (Sartorius Stedim Biotech, 10 kDa MWCO). The sample was then injected into 50 ml cold Burgess Regeneration buffer. A length of dialysis membrane (10 kDa MWCO) was prepared by placing it in boiling water for 10 min. The 50 ml sample was transferred into the membrane, closed and dialysed overnight in 4 °C. The dialysed sample was then concentrated to 5 ml using a Vivaspin centrifugation column (3500 x g, 4 °C) and loaded onto a 5 ml sample loop. The sample was subjected to gel filtration using a pre-equilibrated Superdex 200 10/300 GL column (GE-Healthcare) connected to an AKTA prime purification system. This was carried out at RT using Burgess Gel Filtration buffer. Protein eluting from the column was monitored using a paper chart recorder plotting the detection at 280 nm. The eluted protein peaks were collected in 1 ml fractions and analysed using Tricine SDS-PAGE. Samples were measured by UV-

spectrophotometry at an absorbance of 280 nm, and protein concentration was calculated using the following equations:

1. Conc (mg/ml) = value from 280 nm/protein extinction coefficient

2. Conc (mM) = Conc (mg/ml)/MW (kDa)

Theoretical MW and protein extinction coefficients of the proteins were determined using the online ProtParam tool (http://web.expasy.org)

3.29 His-tag Pull Down Assay

3.29.1 *Thrombin digestion*

To test the efficiency of the Thrombin protease (Sigma) to digest and remove the N-terminal His-tag from His-FlbT and His-FlaF protein, a small-scale time course experiment was performed. Various concentrations of thrombin protease (1, 0.5, 0.2, 0.1, 0.05, and 0 units of enzyme) were incubated at RT with 10 μg of purified soluble protein overnight. At 30-60 min intervals a sample was taken and the reaction was stopped by adding 2 x SDS Sample buffer and boiling in water for 5 min. The samples were then analysed using Tricine SDS-PAGE for digestion efficiency. It was decided that the best conditions to use were 0.5 units of enzyme per 10 μg of protein and the duration of digestion to be 30 min.

3.29.2 *His-tag pull down assay*

Soluble His-FlbT and His-FlaF was digested with thrombin protease, then subjected to gel filtration to remove the protease. The collected fractions were analysed using Tricine SDS-PAGE and amount of protein in each fraction quantified. The concentrations of His-FljJ, FlbT* and FlaF* (* represents non-tagged) were normalised to approx 6 μM using His Pull Down Loading Buffer. 100 μl Ni-NTA (Qiagen) agarose was prepared by washing it four times in 500 μl sterile water and four times in 500 μl His Pull Down Loading Buffer; each time centrifuging for 10 min at 8000 x g at 4 °C, to pellet the agarose and removing the supernatant. Proteins were then incubated with the agarose overnight at 4 °C on a rotating mixer. The samples were then washed twice with 500 μl His Pull Down Loading Buffer by incubating and rotating for 2 hr at 4 °C

before being centrifuged at 10 min at 8000 x g at 4 °C, in order to pellet the agarose. Finally, proteins were eluted from the agarose using 100 µl His Pull Down Elution Buffer by incubating and rotating for 2 hr at 4 °C before being centrifuged under the same conditions. The supernatant was removed for analysis. The samples taken at various stages of the experiment were analysed by Tricine SDS-PAGE.

3.30 Cloning Strategy: FLAG Pull Down Assay

A Knock out/Knock in strategy was developed to create and place on the chromosome a N-terminal 3 x FLAG tagged *fljJ* gene under the control of its native promoter. The principle is based on the deletion of the wild type gene and the subsequent placement of a tagged version back onto the chromosome in the same place using pNPTS128 (see section 3.21). Primers were designed to amplify approximately 500 bp upstream and 500 bp downstream of *fljJ* to facilitate homologous recombination with the *C. crescentus* chromosome. Internal primers were designed to have complimentary overhangs for each other in order to allow the two regions to be fused together in a final overlapping extension PCR. These primers contained the sequence for a 3 x FLAG peptide after the *fljJ* ATG start codon. The final PCR product contained the whole *fliJ* ORF with the N-terminal tag and the upstream and downstream regions.

The PCR fragment was cloned into pNPTS128 and confirmed to be correct by DNA sequencing. The FLAG-*fljJ* containing plasmid was then conjugated into the Δ*fljJ* mutant and transformants were screened by PCR for the presence of FLAG-*fljJ*. Successful clones were confirmed by DNA sequencing. To check for FLAG-*fljJ* expression, whole cell lysates were prepared and analysed by immunoblot using an α-FLAG antibody (Sigma-Aldrich; Prof. Colin Harwood) at 1/1000 dilution.

3.30.1 *In-vivo co-immunoprecipitation*

In order to attempt to identify FljJ:FlbT/FlaF interactions *in-vivo* we decided to use the FLAG-*fljJ* expressing strain in a co-immunoprecipitation experiment. The strategy for the experiment was based on a published method (McGrath *et al*., 2006). A single bacterial colony was inoculated in 20 ml liquid medium and grown overnight at 30 °C with shaking. The overnight culture was then diluted back in 200 ml fresh liquid medium to OD600 0.05 and grown to OD600 0.6. The culture was then centrifuged for 30 min at 3500 x g at 4 °C, and the pellet washed twice in 0.5 ml CoIP buffer and

centrifuged for 5 min at 12000 x g at 4 °C, before being resuspended in 2 ml CoIP buffer. Samples were incubated with 50 mg Lysozyme (Sigma-Aldrich), 10 mM $MgCl_2$, 50 units of DNase I (Sigma-Aldrich) and 1 mM PMSF (Sigma-Aldrich) at 4 °C for 30 min. Samples were then transferred to a 2 ml tube containing glass beads then lysed using a bead beater (Bertin precellys 24 lysis and homogenizer, tubes 03961-1-004) for 3 x 30 sec at 6400 rpm). The lysates were then centrifuged for 5 min at 12000 x g at 4 °C, and the supernatant was collected. Anti-FLAG M2-agarose (Sigma-Aldrich) was prepared by washing in Co-IP buffer. Samples were incubated with 20 μl anti-FLAG M2-agarose at 4 °C overnight on a rotating mixer. Samples were then centrifuged for 10 min at 6000 x g at 4 °C, and washed three times in Co-IP Wash buffer, centrifuging under the same conditions after every wash. The supernatant was then discarded and the agarose pellet was resuspended in 50 μl 2 x SDS Sample buffer. Samples were boiled in water for 5 min before being analysed by immunoblot using the following antibodies: α-Fla (1/30000 dilution), α-FlbT (1/5000 dilution) and α-FlbT (1/5000 dilution).

3.31 RNA Electromobility Shift Assay

3.31.1 *In vitro transcription*

Primers were designed to create a DNA fragment that could be used to generate a *fljK* transcript identical in sequence to the RNA used by Anderson and Gober to show FlbT:*fljK* binding (Anderson and Gober, 2000). The transcript was a total of 115 nucleotides from the mapped transcriptional start site, which included 17 codons and 63 5' untranslated nucleotides (Figure 14) (Minnich and Newton, 1987). Primers were also designed to create a DNA fragment that could be used to generate a *fliF* transcript, that could be included in experiments as a non-specific control.

The forward primer of each DNA fragment was constructed such that it contained a T7 RNA polymerase site that could be utilised for *in-vitro* transcription. A Roche DIG-labelling (Digoxigenin) kit was used as opposed to the common method of using radiolabeled nucleotides. A DNA fragment was generated by PCR and confirmed to be correct by DNA sequencing. The PCR DNA was then incubated for 3 hr at 37 °C in a 20 μl reaction that contained the following: 10 μl DNA (approx 200 ng), 2 μl T7 buffer, 2 μl T7-RNA polymerase, 2 μl NTP-mix (DIG-UTP/UTP ATP/GTP/CTP), 3 μl Sterile water and 1 μl or 4 units of RNAse inhibitor (RNasin, Promega). After incubation, 2 μl DNase I was added to the reaction and incubated for a further 15 min at

-63 *fljK*

ACCGAGCAAAAUGCUCCCGGCAGCCAAAAUGGCGUCGGACACCUUGAAAAGGACUCUUU
CGUUAUGGCGCUGAACAGCAUCAAUACGAACGCGGGCGCGAUGAUCGCCCUGCAA

+51

+684 *fliF*

UCCGAGGUCGAGGCCCGCAUCGCCAAGACCGUCAAGGACAUGAUCGAGGGCGUGCUGGG
CCCGGGCAAGGCGCGCGUGAACGUCACCGCCGAGCUGGACCUGAACCGCGUGACCA

+799

Figure 14: RNA transcripts used in electromobility shift assays

Both RNA transcripts were created by *in vitro* transcription and labeled using DIG-UTP. The *fljK* RNA was designed to include the first 17 codons of the ORF and 63 nucleotides upstream. The *fliF* RNA was designed in a non-biased fashion. A random ORF sequence was generated and used as a non-specific control in the RNA binding experiments.

37 °C. The reaction was stopped with 2 µl EDTA (pH8.0, 0.2 M) and 2.5 µl LiCl (4 M). The RNA was then precipitated in 0.75 ml 100 % Ethanol overnight at 4 °C. The RNA was pelleted by centrifugation for 15 min at 15000 x g at 4 °C and the supernatant was discarded. The pellet was washed once in 1 ml 70 % Ethanol and centrifuged for 15 min at 12000 x g at RT. The supernatant was then discarded and the RNA pellet was air-dried in a 60 °C oven. The RNA was resuspended in 100 µl sterile water and 2 µl RNasin (4 units). RNA concentration was measured by UV-spectrophotometry at an absorbance of 260 nm and stored at -80 °C until required.

3.31.2 *RNA electromobility shift assay*

Labeled RNA was incubated with 200-fold molar excess of tRNA (Sigma-Aldrich, R4251-100UN) in RNA binding buffer for 3 min at 95 °C and then cooled on ice for 30 min. Proteins were diluted to 5 µM in RNA binding buffer, pre-mixed and incubated on ice for 30 min. The appropriate concentration of protein was then added to the appropriate concentration of labeled RNA, and 2 units of RNasin in a 15 µl reaction. After 30 min incubation on ice, 2.5 µl of 6 x loading dye (Promega) was added to each reaction and they were subjected to Native-PAGE for 4-5 hrs at constant 60 V at 4 °C. RNA was then transferred to a positively charged nylon membrane (Roche) by electroblotting for 45 min at a 200 mA in cold Native running buffer. Membranes were then dried on paper towel before being UV-crosslinked (Stratagene, UV Stratalinker 1800- Auto cross link). Membranes were washed for 5 min in 30 ml Tween washing buffer on a platform shaker under high agitation at RT. The wash buffer was then removed and the membranes were blocked for 30 min in 30 ml Blocking Buffer under gentle agitation at RT. The blocking buffer was then replaced with fresh 20 ml Blocking Buffer and 2 µl anti-DIG-AP antibody (Roche), and incubated for a further 30 min. Buffer was drained off and the membranes were washed for 90 min in 30 ml Tween washing buffer, under high agitation. The wash buffer was then removed and the membranes were incubated in 30 ml Equilibration buffer for 5 min before being dried on paper towel. 500 µl of CDP-star detection reagent (Roche- ready to use) was spread evenly over a membrane and incubated in the dark for 5 min. Membranes were then dried off and exposed to hyperfilm for approximately 5 min.

Chapter 4. Characterisation of the *Caulobacter crescentus* Flagellar Filament

4.1 Introduction

A plausible explanation for the use of multiple flagellins is that there exists a flagellin bias with respect to different environmental conditions. Bacteria inhabit many diverse ecosystems and the ability to adapt to their surroundings and survive in the most inhospitable environments is quite remarkable. The utilisation of multiple flagellin species may give a selective advantage to a bacterial cell in the avoidance of a predator or increased swimming ability in differing environments. An alternative possibility for the use of multiple flagellins is a requirement for structural integrity during filament assembly. In order to investigate the use of multiple flagellins we have focused on the flagellar system of *Caulobacter crescentus*.

4.1.1 *Caulobacter crescentus flagellins*

There are seven flagellin genes annotated in the *C. crescentus* CB15 genome (Figure 15). One, CC2976 is a designated putative flagellin gene predicted to encode a flagellin of approximately 44 kDa (Figure 15) (Nierman *et al*., 2001). Protein sequence analysis matches CC2976 with bacterial N-terminal and C-terminal flagellin helical regions (Pfam Sanger; Finn *et al*., 2010). Sequence alignment with the other six annotated flagellins shows that it shares 93 amino acids in similarity with FljM, 87 with FljK, 103 with FljL, and 95 with FljJ (CC2976 is 424 amino acids in length). A deletion of CC2976 has no obvious effect on motility (Faulds-Pain, unpublished). Therefore since it has never been isolated in filaments and is not located with other flagellar genes on the genome; CC2976 was not included in this investigation.

The other six flagellin genes are found on the genome in two unlinked loci (Figure 15). The α-flagellin cluster includes *fljJ* (29 kDa), *fljK* (25 kDa) and *fljL* (27 kDa) as well as other flagellar genes (Figure) (Nierman *et al*., 2001). The β-flagellin cluster comprises only of *fljM* (25 kDa), *fljN* (25 kDa) and *fljO* (25 kDa) (Figure 15) (Nierman *et al*., 2001). Minnich *et al*., 1988 were the first to investigate the role played by individual flagellins in the regulation and assembly of the flagellar filament in *C. crescentus* (Minnich *et al*., 1988). Previous studies had utilised large deletions of the genome incorporating flagellin genes along with other flagellar genes (Johnson and Ely,

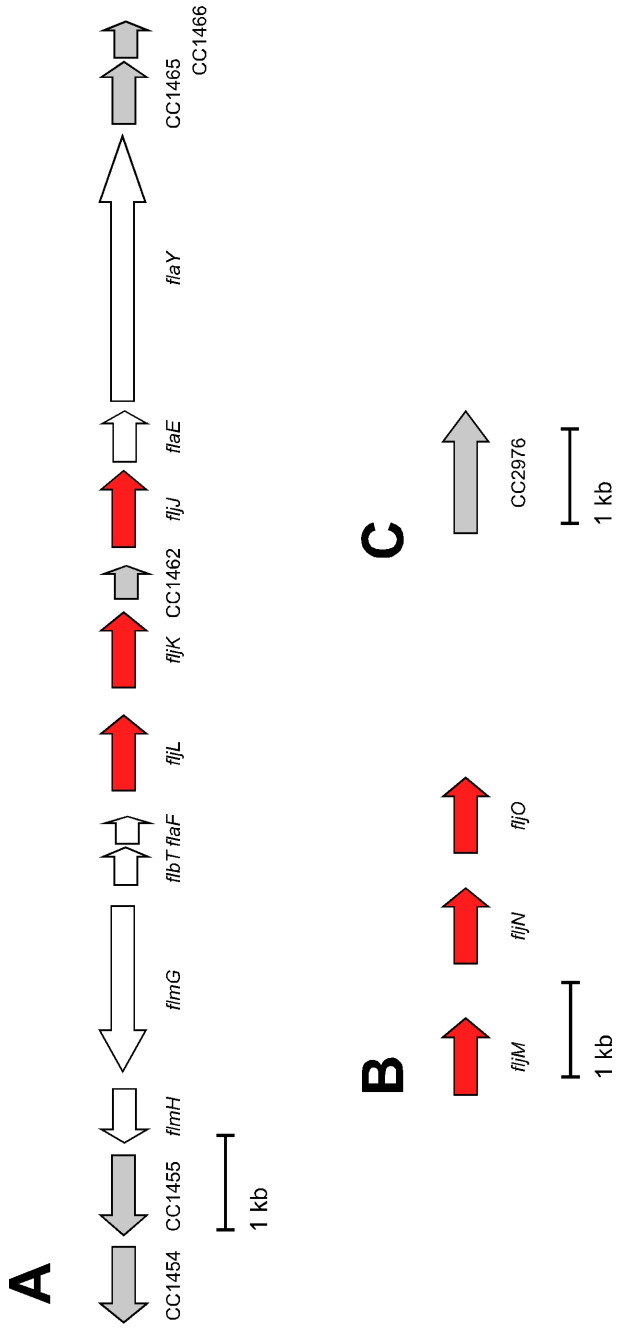

Figure 15: Genetic organisation of the α- and β-flagellin gene loci in *Caulobacter crescentus*

Flagellin genes are coloured red. Other known flagellar genes are coloured white, and hypothetical genes are grey. **A.** The three α-flagellins; *fljL*, *fljK*, and *fljJ* are found among a cluster of nine known flagellar genes. Upstream of *fljL* are two flagellar regulators: *flbT* and *flaF*. **B.** The three β-flagellins; *fljM*, *fljN* and *fljO* are located at an unlinked location on the genome. **C.** The hypothetical flagellin CC2976.

1979; Minnich *et al*., 1988). They demonstrated using a combination of insertion mutations and deletions, that the genes of the α-flagellin cluster were not essential (Minnich *et al*., 1988). However, it was concluded that FljL and FljJ were required to maintain a level of wild type motility. Importantly, they observed wild type levels of 25 kDa flagellin even when *fljK* was inactivated thus confirming the presence of the β-flagellins.

The amino acid sequences derived from the individual flagellin genes exhibit variation (Figure 16) (Ely *et al*., 2000). FljJ is the most divergent of all the flagellins exhibiting approximately 50% sequence similarity to FljM. The β-flagellins possess 94.5% sequence similarity and their divergence from FljK and FljL extends to 18% (Ely *et al*., 2000).

4.1.2 *Flagellin gene deletions*

Previous studies have shown that *fljJ* and *fljL* mutants exhibit altered motility phenotypes and a *fljK* mutant has no effect, however the extent of redundancy in the system has not been fully elucidated (Minnich *et al*., 1988; Schoenlein and Ely, 1988). Therefore this led us to investigate why *C. crescentus* maintains the use of multiple flagellins. We chose to address this question by making a complete collection of flagellin in-frame deletions.

Prior to the start of this research project, southern hybridisation analysis of the then current mutant collection, of 13 strains, revealed that the Δ*fljK* strain (TPA599) was incorrect as a result of an upstream deletion of > 5 Kb. The motility phenotype of this Δ*fljK* strain was non-motile which correlated with a statement that the 25 kDa flagellin was essential for motility (Llewellyn *et al*., 2005). In contrast, previous work had shown that a Δ*fljK* mutant should retain motility (Minnich *et al*., 1988). A number of flagellin deletion combinations were yet to be constructed in order to investigate the aspect of flagellin redundancy more rigorously. Prior to this project, attempts by our laboratory to create single deletions of *fljN* and *fljO* were not successful. The β-flagellin cluster exhibits significant homology with respect to the coding and non-coding (intergenic) regions (Figure 16). It is plausible that *fljN* and *fljO* are duplications of *fljM* or another ancestral sequence, and therefore their retention on the genome there may be due to a selective pressure to oppose genetic recombination in the region. However, deletion of the whole region and *fljM* alone was successful.

Consequently, at the beginning of this project the following 10 mutants were created: Δ*fljK,* Δ*fljKM,* Δ*fljJM,* Δ*fljJMNO,* Δ*fljKMNO,* Δ*fljLMNO,* Δ*fljJKMNO,*

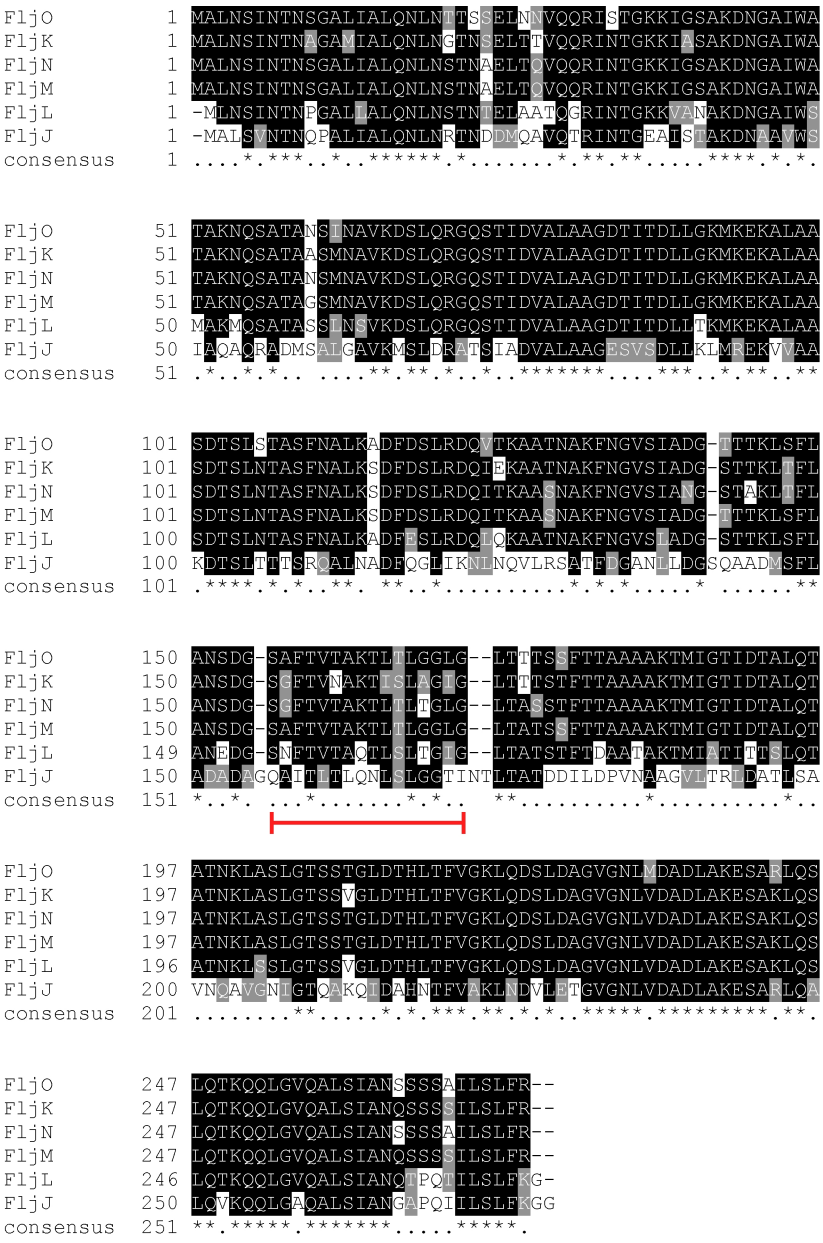

Figure 16: Primary sequence alignment of the six *Caulobacter crescentus* flagellins

The multiple alignment was assembled using ClustalW and the similarity shading was performed using BoxShade. The β-flagellins, FljM-O, possess 94.5 % sequence similarity. FljJ is the most divergent exhibiting 50 % similarity to FljM (Ely *et al*., 2000). The region marked in red indicates the sequence used to generate flagellin specific peptide-derived antibodies.

(http://www.clustal.org/) (http://www.ch.embnet.org/software/BOX_form.html)

Δ*fljJLMNO,* Δ*fljLKMNO* and Δ*fljJKLMNO*. The strains were confirmed to be correct by DNA sequencing of a PCR fragment from the region of the deleted gene(s) and southern hybridisation (Data not shown). The effect of flagellin gene deletions was measured in motility agar assays and quantified more accurately using microscopy. This results section will consider the mutants created during this project only, however some figures present data relating to strains created and analysed previously. The data from these strains are there as a reference for analysis and interpretation in the summary.

4.2 Motility Phenotypes of Flagellin Gene Deletions

The in-frame deletion mutants were tested for their ability to swim in low percentage agar motility assays (Figure 17). The newly created Δ*fljK* mutant (TPA2234) was motile, which is consistent with previous experiments (Minnich *et al*., 1988). In fact the Δ*fljK* mutant along with all single flagellin deletions showed no remarkable difference in swarm size when compared to wild type, ≤ 18 % (Table 4). This is consistent with previous studies in demonstrating that no one flagellin is essential for motility.

The double deletion mutant Δ*fljJM* produced a swarm size that was reduced by approximately 20 % when compared to wild type (Table 4). This reduction correlates to an additive effect of the two single deletions Δ*fljJ* and Δ*fljM,* which were reduced by 18 ±4 % and 7 ±7 % respectively (Table 4). However, the Δ*fljKM* mutant had a reduction in swarm size of 42 % when compared to wild type (Table 4). This intermediate motility phenotype suggests that both FljK and FljM play an important role in filament assembly.

The Δ*fljKMNO* mutant was severely impaired for motility with a reduction in swarm size of 60 % (Table 4). This large reduction correlates with the removal of 4 flagellin genes. Interestingly, two other quadruple deletion mutants (Δ*fljLMNO* and Δ*fljJMNO*) did not show a similar reduction in motility; 19 % and 23 % respectively (Table 1).

Importantly however, both the Δ*fljJLMNO* and Δ*fljJKMNO* mutants retained the ability to swim even though only one flagellin gene was present. When *fljL* was the only remaining flagellin gene (Δ*fljJKMNO*) a severely reduced phenotype was observed. In fact, on motility agar the mutant appears to be non-motile with a reduction in swarm size of 67 % compared to wild type, which is similar to that of the non-motile mutant Δ*fliF* (Table 4). However, microscopic analysis revealed that the strain is indeed motile. When *fljK* is the only remaining flagellin gene (Δ*fljJLMNO*) a much more intermediate

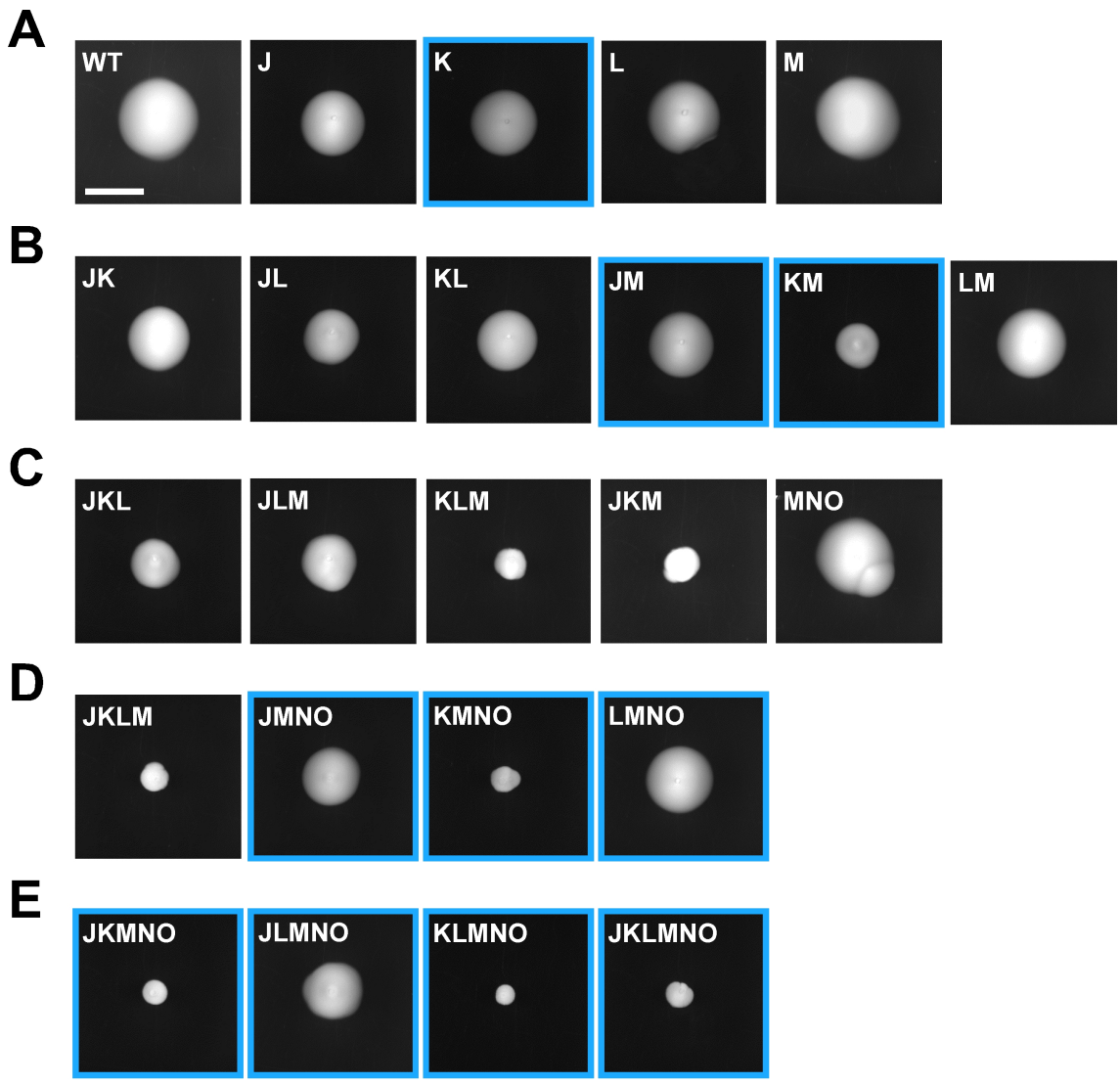

Figure 17: Motility phenotypes of wild type *Caulobacter crescentus* and flagellin gene deletion mutants

Motility agar assays were imaged after 5 days growth at 30 ºC. The genotype of the strain is indicated in white text. Strains boxed in blue were created during this project. **A.** Wild type and the single flagellin gene deletion mutants. **B.** The double flagellin gene mutants. **C.** The triple flagellin gene deletion mutants. **D.** The quadruple flagellin gene mutants. **E.** The quintuple flagellin gene mutants and the mutant with all six flagellins removed.

Genotype	Remaining Flagellins	Mot Phenotype	Relative Swarm Size %
Wild type	6	+	100 ±3
Δ*fliF*	6	-	24 ±1
Δ*fljJ*	5	+	82 ±4
Δ*fljK*	5	+	85 ±2
Δ*fljL*	5	+	85 ±4
Δ*fljM*	5	+	93 ±7
Δ*fljJL*	4	+	68 ±3
Δ*fljJK*	4	+	77 ±1
Δ*fljKL*	4	+	74 ±2
Δ*fljJM*	4	+	80 ±1
Δ*fljLM*	4	+	79 ±0
Δ*fljKM*	4	+/-	58 ±4
Δ*fljJKL*	3	+/-	59 ±3
Δ*fljJKM*	3	-/+	46 ±7
Δ*fljJLM*	3	+	63 ±1
Δ*fljKLM*	3	-/+	38 ±2
Δ*fljMNO*	3	+	88 ±7
Δ*fljJKLM*	2	-/+	32 ±2
Δ*fljJMNO*	2	+	77 ±3
Δ*fljKMNO*	2	-/+	40 ±3
Δ*fljLMNO*	2	+	81 ±4
Δ*fljJKMNO*	1	-/+	33 ±1
Δ*fljJLMNO*	1	+	61 ±2
Δ*fljLKMNO*	1	-	22 ±1
Δ*fljJKLMNO*	0	-	25 ±1

Table 4: Summary of motility phenotypes for the flagellin gene deletion mutant collection

The associated motility phenotypes of flagellin gene deletion mutants: scored and measured as compared to wild type. Phenotype scoring as follows: + (motile), +/- (intermediate motility), -/+ (severely impaired motility) and - (non-motile). The relative swarm size (as compared to wild type) was calculated by measuring the swarm size using ImageJ software (n=3 independent measurements).

motility phenotype was observed, with a reduction in swarm size of only 36 %. This further suggests that FljK plays an important role in filament assembly.

Remarkably out of the 10 strains made (and the whole mutant collection of 23 strains), a non-motile phenotype was observed for only two mutants: Δ*fljLKMNO* and Δ*fljJKLMNO*. Therefore we can define that for the *C. crescentus* flagellar system, the flagellins demonstrate extensive structural redundancy and that one flagellin is sufficient to support motility. Furthermore, it is apparent that *fljJ* alone is unable to support motility. When all six flagellins (Δ*fljJKLMNO*) were removed from the genome, *C. crescentus* is non-motile. This data strengthens the view that the putative flagellin, CC2976, is not actually utilised in flagellar assembly under normal laboratory growth conditions.

4.3 Analysis of Filament Composition

The motility analysis of the mutant collection has revealed that the flagellins of *C. crescentus* exhibit a higher degree of structural redundancy than was previously understood. However, from this type of analysis we cannot be certain if all remaining flagellins are being utilised. Previous studies had observed ordered assembly of flagellins in a wild type filament; with FljJ and FljL located at the proximal region closest to the hook and the rest of the filament made from 25 kDa flagellin (Driks *et al*., 1988; Weissborn *et al*., 1981). The hypothesis of these early investigations was that ordered assembly was a reflection of the temporal expression of the flagellin genes, but also that one particular flagellin species can only assemble next to another specific flagellin species. Therefore, it is plausible that in our mutants only a subset of flagellins are being used to make a filament.

4.3.1 *Flagellin specific peptide derived antibodies*

One method of identification of the individual species of flagellin in the mutant and wild type filament is by that of immunoblot analysis. However, this would be arduous as the only flagellin antibody available, α-Fla, recognises the six flagellins indiscriminately (Anderson and Gober, 2000). FljJ (29 kDa) and FljL (27 kDa) can be resolved using Glycine SDS-PAGE gel electrophoresis, however, the four 25 kDa flagellins cannot (Llewellyn *et al*., 2005). Therefore, in order to identify individual flagellins within the assembled filament we decided to design and generate peptide derived antibodies that would be flagellin specific. We would then use these specific

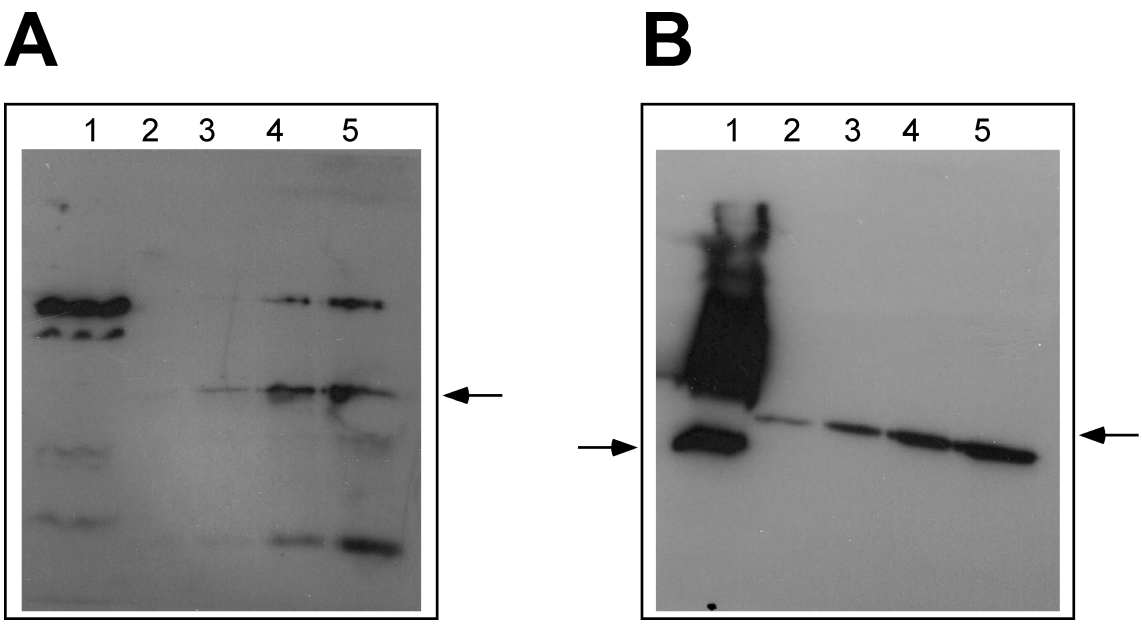

Figure 18: Immunoblot analysis of the α-FljJ peptide derived antibody

A. Analysis of the α-FljJ antibody with **(1)** wild type whole cell lysates **(2-5)** Increasing concentrations of His-FljJ protein. **B.** In comparison, analysis of the α-Fla antibody. The arrows point to flagellin protein.

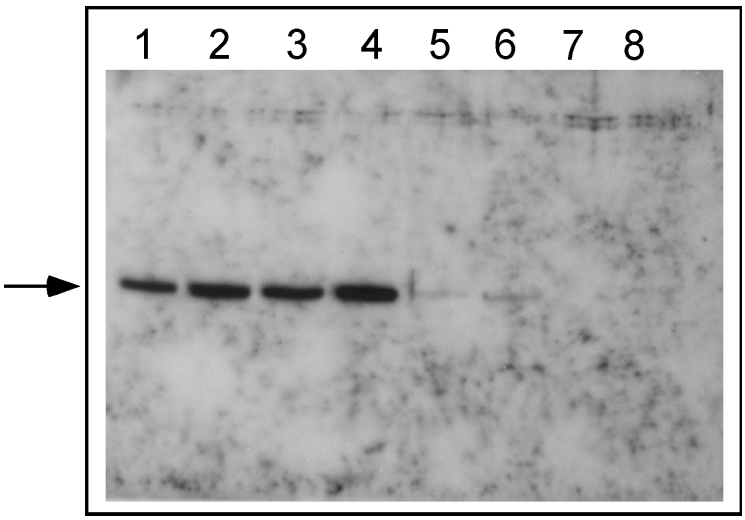

Figure 18C: Immunoblot analysis of the α-FljK peptide derived antibody

Analysis of the α-FljK antibody with **(1)** wild type whole cell lysates: 1 µg **(2)** wild type whole cell lysates: 2 µg **(3)** Δ*fljJKL* whole cell lysates: 1 µg **(4)** Δ*fljJKL* whole cell lysates: 2 µg **(5)** Δ*fljMNO* whole cell lysates: 1 µg **(6)** Δ*fljMNO* whole cell lysates: 2 µg **(7)** Δ*fljJKLMNO* whole cell lysates: 1 µg **(8)** Δ*fljJKLMNO* whole cell lysates: 2 µg. The arrow points to flagellin protein.

antibodies to test isolated filaments populations for their composition by immunoblot. We highlighted a region within the aligned primary sequences of all six flagellins that gave acceptable dissimilarity to enable specific recognition (Figure 16). Two 16 amino acid long peptides were synthesised *in vitro* and used to create specific antibodies to FljJ and FljK (Cambridge Research Biochemicals). FljJ and FljK were initially the only flagellins selected in order to establish whether or not this methodology could be a success. In addition, FljJ was included as it is the most divergent flagellin at the sequence level, thus in theory it should be easier to generate a specific antibody to. The FljJ antibody (α-FljJ) was found to react with purified His-FljJ protein (Figure 18A). It did not react with wild type whole cell lysates or isolated flagellar filaments. It is likely that the latter is a consequence of low levels of the intracellular FljJ and additional low levels of FljJ in the filament (Driks *et al*., 1989; Jones *et al*., 2001). Surprisingly, the FljK antibody (α-FljK) cross-reacted with both wild type and Δ*fljJKL* isolated filaments (Figure 18C). This suggests that α-FljK is in fact recognising one or more of the β-flagellins and not FljK exclusively. One explanation for this unexpected outcome is the possibility of post-translational modification of the flagellins in the region the peptide was designed, which would have consequences for *in vivo* recognition by the antibody (See section summary).

4.3.2 *MALDI-TOF analysis*

As the results from the peptide-derived antibodies were ambiguous we decided to analyse filament composition of the mutant collection using MALDI-TOF. Filament isolation confirmed that the only mutants not to produce a filament were the non-motile strains: Δ*fljLKMNO* and Δ*fljJKLMNO*. As the mutants, Δ*fljJLMNO* and Δ*fljJKMNO*, were motile, our initial investigation was to confirm that these two mutants were producing a filament comprising of just FljK or FljL, respectively. MALDI-TOF analysis can confirm the presence of a specific flagellin by identifying a series of signature tryptic peptides (Figure 19A); Trypsin cleaves at the C-terminal end of Arginine and Lysine residues (Olsen *et al*., 2004). For example, FljK, FljL and FljM/N can be differentiated by the N-terminal peptides: 3257 m/z (FljK), 3240 m/z (FljL) and 3296 m/z (FljM/N) (Figure 19A). Analysis of the mass spectrum confirmed that the strains Δ*fljJLMNO* and Δ*fljJKMNO* produced filaments comprised of only FljK and FljL respectively (Figure 19B).

The analysis of the outstanding motile mutants showed that all remaining flagellins were utilised in a population of filaments (See Appendix C). FljM and FljN

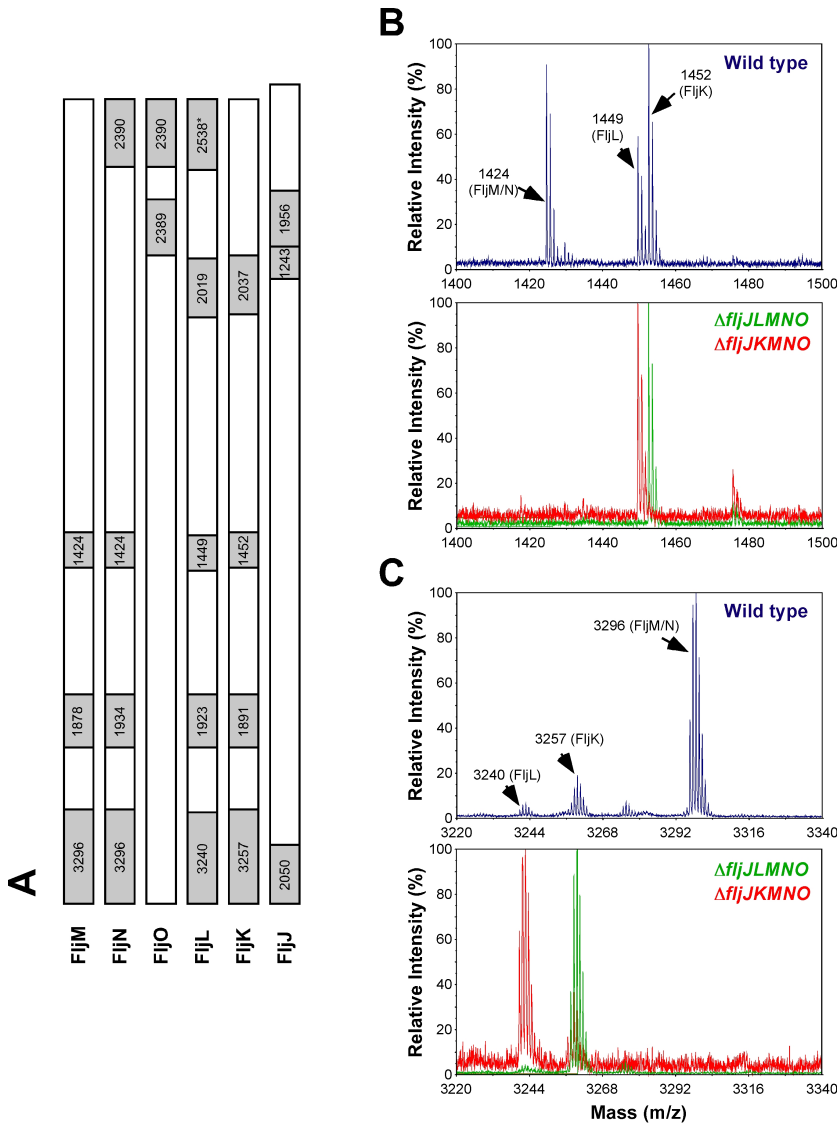

Figure 19: A summary of the MALDI-TOF analysis of wild type and mutant filaments after tryptic digestion (Faulds-Pain *et al.*, 2011)

A. A scaled schematic illustrating the signature peptides detected during MALDI-TOF analysis. The numbers stated are the approximate *m/z* values of these tryptic peptides. The 2538 peptide is predicted to possess an N-terminal pyroGlu conversion and therefore was not detected. **B.** A comparison of the MALDI-TOF analysis of central tryptic peptides from FljM/N (1424), FljL (1449), FljK (1452) from wild type (blue), Δ*fljJLMNO* (green) and Δ*fljJKMNO* (red). **C.** A comparison of the MALDI-TOF analysis of N-terminal tryptic peptides from FljM/N (3296), FljL (3240), FljK (3257) from wild type (blue), Δ*fljJLMNO* (green) and Δ*fljJKMNO* (red).

exhibit the highest level of similarity (95%) and differ only by 2 detected peptides; 1878 m/z (FljM) versus 1934 m/z (FljN), and the C-terminal FljN/O 2390 m/z peptide that is absent from FljM (Ely *et al*., 2000; Faulds-Pain *et al*., 2011). A comparison of the 3296 m/z FljM/N N-terminal peptide throughout the data set for all mutants identified a consistent drop in the intensity of this peptide in all Δ*fljM* mutants, suggesting that FljM is the major contributor to this peptide peak (Faulds-Pain *et al*., 2011). Furthermore, integration and subsequent quantification of the peptide peaks from LC/MS/MS analysis revealed that both FljM and FljK are the most abundant flagellins and that FljM always outscored FljK (C. Birchall MRes, unpublished; Faulds-Pain *et al*., 2011).

FljJ and FljO were detected with the least efficiency by MALDI-TOF (Appendix C). This is consistent with previous data on *fljJ* and *fljO* expression levels and suggests that they are present in the filament in small amounts (Jones *et al*., 2001; Laub *et al*., 2000). The only time FljJ was detected by MALDI-TOF was in the Δ*fljKL* mutant combinations i.e. when the other α-flagellins are absent (Faulds-Pain *et al*., 2011). However, utilising the more sensitive and quantitative analysis of nanospray LC/MS/MS, we were able to observe FljJ and FljO at a higher frequency (C. Birchall MRes, unpublished). Importantly, the analysis showed that for every mutant, all remaining flagellins could be identified in isolated filament populations. It therefore appears that potential effects of specific flagellin deletions on filament assembly is null, and thus, there is no preference for a subset of flagellins to be utilised during filament assembly.

4.4 Analysis of Swimming Speeds

The MALDI-TOF analysis demonstrated that all remaining flagellins are utilised to assemble the filaments of the mutant strains. Therefore, each mutant filament has a different composition; which potentially may result in alterations in the physical structure of the filament. One consequence of physical alterations could be a change in swimming speed. To determine whether a variation in swimming speed correlated with the observed motility phenotypes and loss of flagellin genes, the swimming speed of individual cells was measured (Table 5 and Figure 20). P values were calculated using ANOVA for the swimming speed of WT versus each mutant.

Consistent with the observed motility phenotypes there was no significant difference in the swimming speed of the Δ*fljK* mutant when compared to wild type; both with speeds of approximately 55 μm/sec (Table 5). The swimming speed of the

Mutant	Remaining Flagellins	Mot Phenotype	Average Filament Parameters (µm)			Swimming Speed	
			Filament Length	Pitch Length	Pitch Height	µm/sec	P-Value*
Wild type	6	+	4.15 ± 2.17	0.99 ± 0.16	0.18 ±0.05	54.78 ± 5.23	
Δ*fliF*	6	-				0	
Δ*fljJ*	5	+	4.17 ± 2.22	1.03 ± 0.16	0.26 ± 0.08	53.11 ± 7.54	0.281
Δ*fljK*	5	+	4.60 ± 1.67	0.88 ± 0.06	0.15 ± 0.04	54.66 ± 7.16	0.809
Δ*fljL*	5	+	4.63 ± 1.75	1.00 ± 0.16	0.20 ± 0.07	51.52 ± 5.96	0.006
Δ*fljM*	5	+	3.90 ± 2.04	1.08 ± 0.37	0.28 ± 0.12	57.30 ± 4.43	0.003
Δ*fljJL*	4	+	3.12 ± 1.77	0.91 ± 0.17	0.26 ± 0.11	50.27 ± 4.9	< 0.001
Δ*fljJK*	4	+	4.18 ± 1.93	1.03 ± 0.16	0.25 ± 0.11	51.31 ± 5.88	0.007
Δ*fljKL*	4	+	1.55 ± 2.08	1.02 ± 0.17	0.36 ± 0.12	47.95 ± 5.11	< 0.001
Δ*fljJM*	4	+	3.11 ± 1.48	0.96 ± 0.30	0.21 ± 0.07	52.52 ± 6.36	0.083
Δ*fljLM*	4	+	1.38 ± 1.44	1.02 ± 0.13	0.24 ± 0.08	51.25 ± 6.62	0.017
Δ*fljKM*	4	+/-	3.38 ± 0.32	0.77 ± 0.05	0.17 ± 0.04	41.86 ± 12.82	< 0.001
Δ*fljJKL*	3	+/-	4.13 ± 1.43	0.92 ± 0.16	0.26 ± 0.06	46.16 ± 10.65	< 0.001
Δ*fljJKM*	3	-/+	2.05 ± 1.17	0.94 ± 0.20	0.18 ± 0.06	27.96 ± 11.61	< 0.001
Δ*fljJLM*	3	+	1.32 ± 1.52	1.14 ± 0.13	0.24 ± 0.07	52.13 ± 9.38	0.104
Δ*fljKLM*	3	-/+	1.72 ± 1.19	0.99 ± 0.11	0.30 ± 0.10	12.40 ± 2.64	
Δ*fljMNO*	3	+	4.11 ± 2.38	1.11 ± 0.22	0.25 ± 0.06	53.74 ± 4.76	0.522
Δ*fljJKLM*	2	-/+	0.27 ± 0.32	0.07 ± 0.05	0.25 ± 0.09	18.78 ± 8.02	
Δ*fljJMNO*	2	+	3.54 ± 0.57	1.12 ± 0.23	0.29 ± 0.07	53.36 ± 5.18	0.328
Δ*fljKMNO*	2	-/+	3.02 ± 0.40	0.92 ± 0.03	0.17 ± 0.02	20.21 ± 5.84	< 0.001
Δ*fljLMNO*	2	+	3.87 ± 0.61	1.22 ± 0.08	0.28 ± 0.05	54.61 ± 8.65	0.853
Δ*fljJKMNO*	1	-/+	1.81 ± 0.44	0.80 ± 0.11	0.15 ± 0.02	19.58 ± 6.47	< 0.001
Δ*fljJLMNO*	1	+	2.99 ± 0.50	1.22 ± 0.07	0.29 ± 0.04	49.35 ± 6.57	< 0.001
Δ*fljLKMNO*	1	-				0	
Δ*fljJKLMNO*	0	-				0	

Table 5: Summary of filament parameters and swimming speeds of flagellin gene mutant combinations and the associated Mot Phenotypes

* Calculated using ANOVA for the swimming speed of WT versus each mutant. Where necessary the calculated P-value is shown.

Δ*fljKM* mutant was reduced to 41.86 μm/sec, which appears a moderate reduction but was in fact significantly lower than wild type (Table 5) ($P < 0.001$, calculated by ANOVA).

In contrast, the double deletion mutant, Δ*fljJM*, had a swimming speed of 52.52 μm/sec. The quadruple mutants, Δ*fljLMNO* and Δ*fljJMNO*, were comparable to wild type: 54.61 μm/sec and 53.36 μm/sec respectively. However, the Δ*fljKMNO* mutant was significantly reduced to 20.21 μm/sec ($P < 0.001$). This slow swimming speed correlates with the severely impaired motility phenotype observed for this mutant. The quintuple mutant, Δ*fljJLMNO*, swam at 49.35 μm/sec, which was comparable to wild type but statistically a significant change (Table 5) ($P < 0.001$). This data is further evidence that FljK plays a major role in filament assembly and functionality, as the filament produced is sufficient to generate a good swimming speed. The Δ*fljJKMNO* mutant exhibited a reduced speed, 19.58 μm/sec, which was comparable to that of the Δ*fljKMNO* mutant. However, in retaining the ability to swim this suggests that FljL does play an important role in filament assembly and function.

4.5 Analysis of the Physical Parameters of Filaments

It is plausible that changes in filament composition could affect both filament length and pitch. The pitch is a measurement of the helical packing of the flagellins into the filament (Samatey *et al*., 2001). Changes in pitch can effect the rotation of the filament and torque generation, resulting in changes in swimming speed (Magariyama *et al*., 1995). We therefore considered whether the reduced swarm size of the flagellin mutants and reduced swimming speeds correlated to any alterations in the physical properties of the filaments. The physical parameters of isolated filaments were measured from Transmission Electron Micrographs using ImageJ, and the average filament, pitch lengths and pitch heights were calculated (Table 5 and Figure 20) (Abramoff *et al*., 2004). P values were calculated using calculated by a pairwise *t*-Test for parameter measurement of WT versus each mutant. See methods for details of how the measurements were taken and Appendix D for example images.

4.5.1 *Filament length*

The filament lengths for the Δ*fljK*, Δ*fljKM* and Δ*fljJM* mutants, did not significantly change compared to wild type; 4.60 μm, 3.38 μm and 3.11 μm, compared to 4.15 μm ($P > 0.001$) (Table 5). This data is consistent with the motility phenotypes and swimming

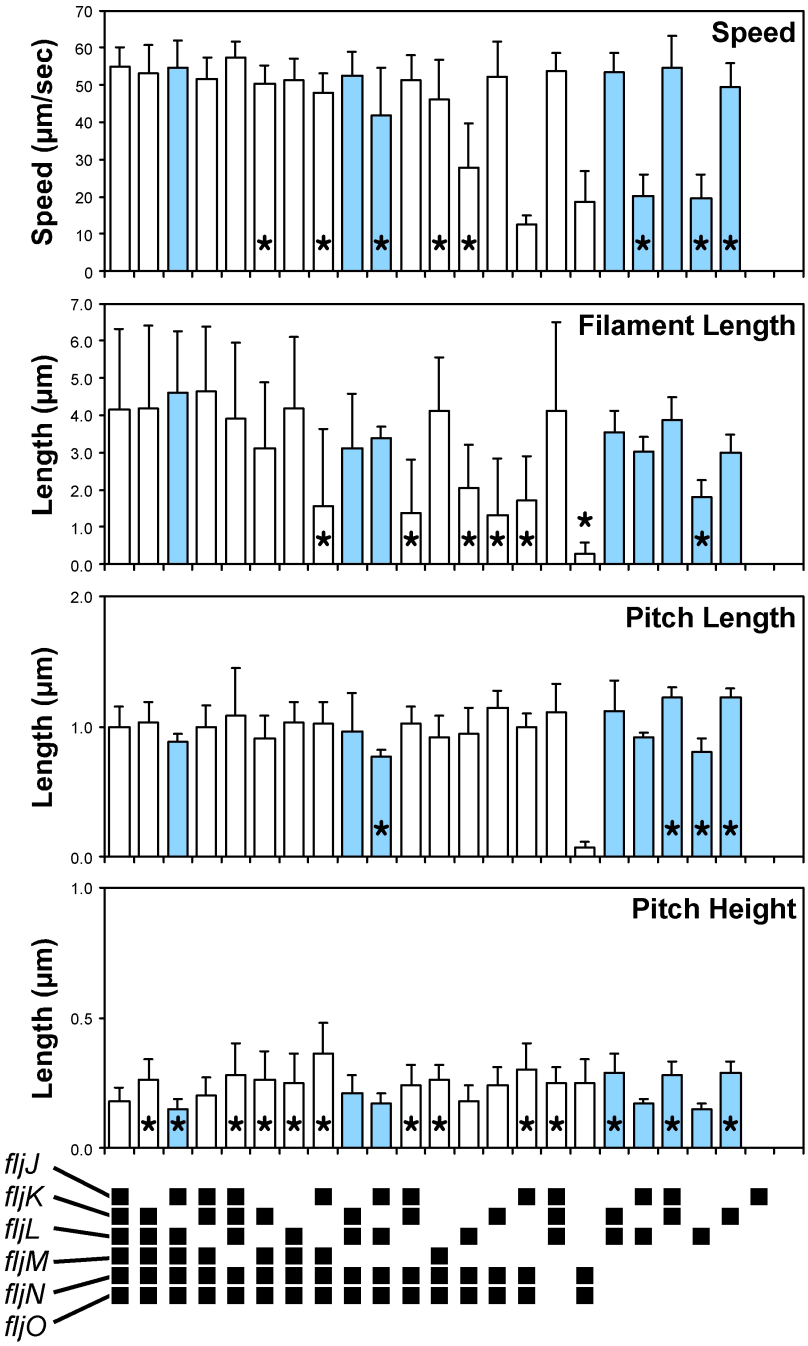

Figure 20: A comparison of the swimming speeds and the physical parameters of flagellar filaments of wild type and motile flagellin deletion mutants (Faulds-Pain *et al.*, 2011)

The average values for each strain are shown and error bars represent standard deviations. Those mutants that were significantly different when compared to wild type are marked with an asterisk ($P < 0.001$, calculated by pairwise *t*-Test). The strains created for this project are highlighted in blue. The key at the bottom represents the presence or absence of a flagellin gene. A black box indicates a gene, while a blank space indicates a gene deletion.

speed data, however, it is in contrast to the observed impaired motility phenotype for Δ*fljKM* strain. This suggests that in this mutant there could be other factors determining the ability to swim.

The quadruple mutants Δ*fljLMNO*, Δ*fljJMNO* and Δ*fljKMNO*, also did not significantly change, although the Δ*fljKMNO* mutant (3.02 μm) appeared to be considerably reduced in length (Table 5). The Δ*fljJKMNO* mutant had a filament length of 1.81 μm, which was drastically and significantly shorter than wild type ($P < 0.001$). This data correlates with the severely impaired motility phenotype and the slow swimming speed when FljL is the only remaining flagellin. The Δ*fljJLMNO* mutant was moderately reduced in filament length, however the reduction was not statistically significant. This further confirms that FljK is a major functional component of the filament.

A number of features could be observed when plotting filament parameter measurements as scatter plots (Figure 21). The whole data set exhibited a good correlation between the number of flagellins present on the genome and the distribution around the average filament length (Figure 21). For example, filaments of the two mutants with only one remaining flagellin (Δ*fljJLMNO* and Δ*fljJKMNO*) showed a lot less variation than the filaments of the single flagellin deletion mutants. In fact, the distributions only became tight when four or more flagellins were deleted. The Δ*fljMNO* mutant exhibited much more variation than the Δ*fljJKL* mutant. This potentially is a result of the clear differences between the α- and β-flagellins i.e. in regulation of the expression of, and protein stability (Faulds-Pain *et al*., 2011). The Δ*fljKL* mutant was an obvious anomaly within the data set. The majority of Δ*fljKL* filaments clustered at below 2 μm while there were a few outlying filaments at approximately 5 μm. The Δ*fljKL* mutant has a recorded swimming speed of 47 μm/s. It is plausible that these filaments are fragile and vulnerable to breaking during the isolation procedure. Furthermore, it could be possible that the mutants with few flagellins have stronger filaments, due to the better packing of flagellins into the filament, and thus have tighter distributions. The Δ*fljK* mutant exhibited a similar distribution to that of the other single flagellin deletion mutants that were created prior to this project. This is important as it demonstrates consistency in the analysis of the whole data set.

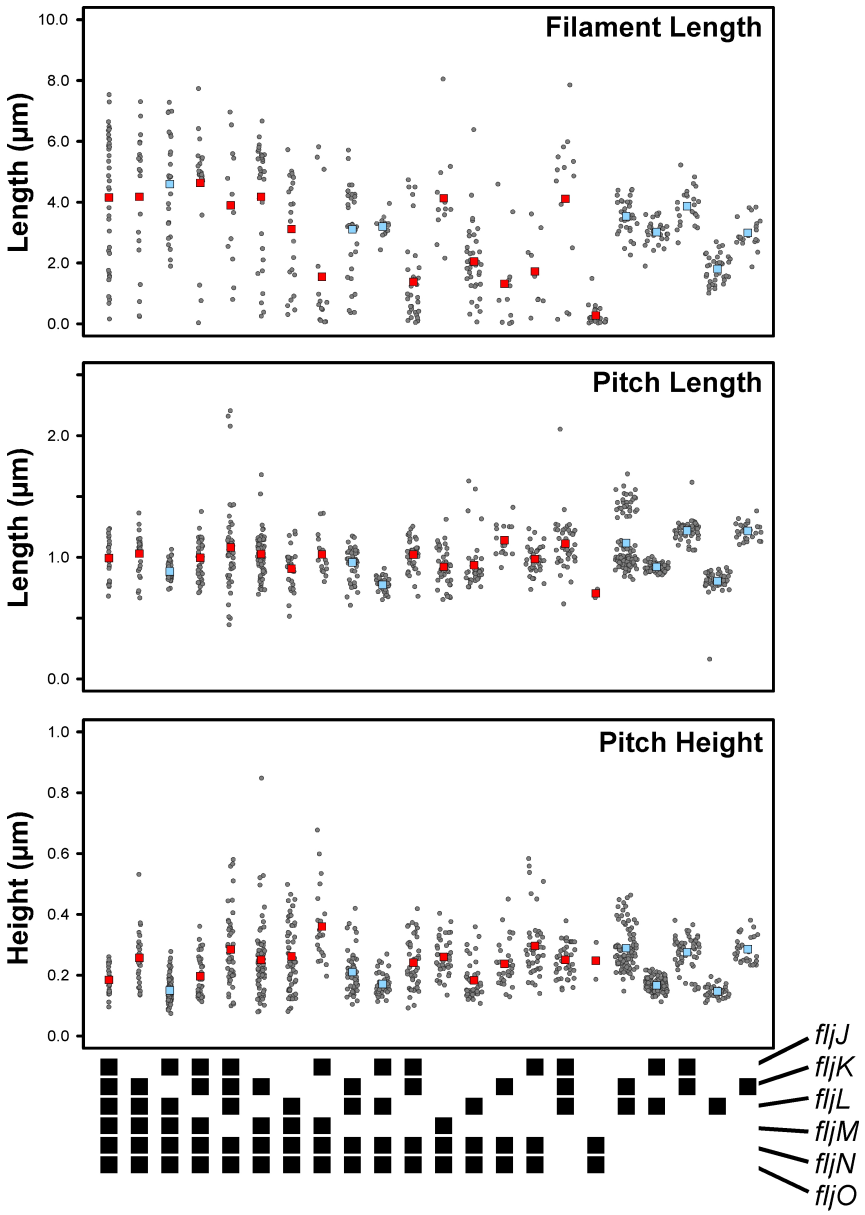

Figure 21: Distribution of filament length, pitch length and pitch height for wild type and motile flagellin deletion mutants (Faulds-Pain *et al.*, 2011)

Each grey dot represents a single measurement. The data points have been scattered on the x-axis for presentation purposes. The red and blue squares indicate the average value for each data set. The strains created for this project are highlighted blue. The key at the bottom represents the presence or absence of a flagellin gene. A black box indicates a gene, while a blank space indicates a gene deletion.

4.5.2 *Pitch length*

The average pitch length of a wild type filament was 0.99 μm, which was consistent with previous measurements (Koyasu and Shirakihara, 1984). The pitch lengths of both the Δ*fljK* and the Δ*fljJM* mutant were comparable to wild type. The pitch lengths of the Δ*fljKM* and the Δ*fljJKMNO* mutants were significantly shorter than wild type, 0.77 μm and 0.80 μm respectively ($P < 0.001$). While the Δ*fljLMNO* and the Δ*fljJLMNO* mutants both had pitch lengths of 1.22 μm, which were significantly longer than wild type ($P < 0.001$). In contrast to filament length, the distributions of pitch length for the whole flagellin gene mutant data set were much tighter (Figure 21). However, the data set was defined as significant ($P=0.006$ as calculated by ANOVA).

4.5.3 *Pitch height*

The average pitch height of a wild type filament was 0.18 μm, compared to the Δ*fljK* mutant, which was significantly reduced at 0.15 μm (Table 5) ($P < 0.001$). In contrast the pitch heights of the Δ*fljJMNO*, Δ*fljLMNO* and Δ*fljJLMNO* mutants were all significantly larger compared to wild type; 0.29 μm, 0.28 μm and 0.29 μm respectively. The Δ*fljJM*, Δ*fljKM*, Δ*fljKMNO* and Δ*fljJKMNO* mutants, were all comparable to wild type. Overall the pitch height fluctuated more and the whole data set was significant (Figure 21) ($P < 0.001$ as calculated by ANOVA).

4.6 Analysis of Flagellin Levels in Flagellin Deletion Mutants

Flagellar assembly in *C. crescentus* is integrated into the cell cycle with one polar flagellum being produced per cell division by the SW cell. The flagellum is then shed upon the differentiation from SW to ST cell. It is plausible then that this defined time limit on flagellar utilisation and thus filament assembly may be sensitive to the availability and stability of the flagellins. Mutants with shorter filaments may have reduced protein levels or the flagellins remaining may exhibit an altered stability profile. We therefore determined the concentration of flagellins by immunoblot assay in the mutant collection.

Wild type and the Δ*fliF* mutant were used as controls and the α-Fla antibody was utilised to determine the concentration of the total flagellin pool (Figure 22) (Jenal and Shapiro, 1996). A Δ*fliF* mutant should not produce flagellin protein, as the absence of the MS ring should result in no flagellar basal-body formation (Ueno *et al*., 1992).

Interestingly, however, the Δ*fliF* mutant did produce a small amount of flagellin. The transcription of both *fliF* and the β-flagellins is controlled by CtrA / σ^{73} (Laub *et al*., 2000). In contrast, expression of the ⟨-flagellins, occurs as a result of the flagellar-dependent activation of σ^{54}. Therefore, the presence of detectable levels of flagellin in the Δ*fliF* mutant can be attributed to the β-flagellins. The immunoblot analysis showed that in most mutants there were approximately wild type levels of flagellins (Figure 22). However, the Δ*fljKMNO* and the Δ*fljJKMNO* showed a significant decrease in flagellin level when compared to wild type ($P < 0.01$, calculated by pairwise *t*-Test). For the Δ*fljJKMNO* this data is consistent with a significantly shorter filament and slower swimming speed (Figure 20). No detectable levels of flagellin could be observed for the two non-motile flagellin gene deletion mutants; Δ*fljLKMNO* and Δ*fljJKLMNO*.

4.7 Flagellar-Independent Expression of Flagellin

When undertaking a mutagenesis study such as this, one should always be considerate of downstream polar effects of any gene deletions. Complementation analysis of the minus genotype is classically carried out by re-introducing the deleted gene *in trans* from an exogenous plasmid. The removal of the gene's native promoter and placing it under the control of one that is chemically-inducible would allow us to determine the effect of flagellar-independent expression of flagellin genes. Therefore, we decided to try and restore motility in the two non-motile mutants: Δ*fljLKMNO* and Δ*fljJKLMNO* as any resultant positive phenotype should be easily indentified using microscopy and motility agar assays. This would also allow us to completely answer the question of redundancy by confirming if each individual flagellin can support motility alone.

fljJ, *fljK*, *fljL*, *fljM*, *fljN* and *fljO* were individually cloned into two xylose-inducible overexpression vectors, one high copy (pBX) and one low copy (pRX) number (Thanbichler *et al*., 2007). Constructs were then transformed into the two mutants (Δ*fljLKMNO*, Δ*fljJKLMNO*) and assayed for motility, swimming speed and flagellin expression by immunoblot.

4.7.1 *Complementation of the ΔfljJKLMNO mutant*

Motility in the Δ*fljJKLMNO* mutant could be restored when the flagellins FljK, FljL, FljM, FljN and FljO were overexpressed (Figure 23). However, when the mutant was complemented with FljJ the cells remained non-motile which is consistent with the

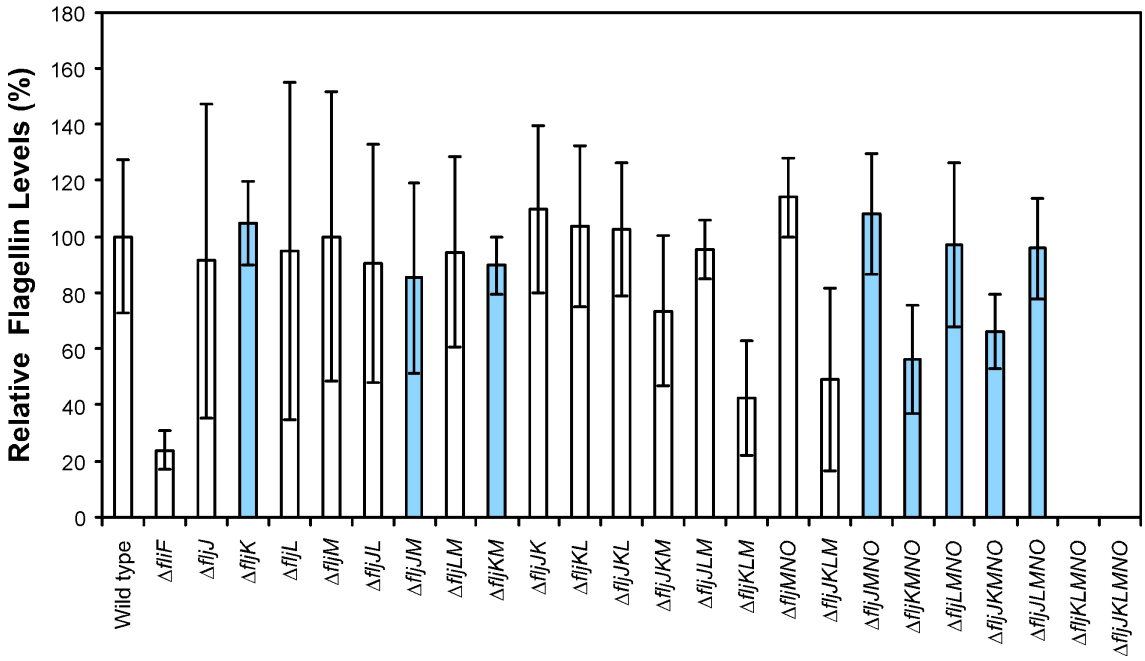

Figure 22: Quantification of flagellin protein levels in the flagellin deletion gene mutants and wild type (Faulds-Pain *et al*., 2011)

Relative flagellin levels (%) from three independent repeats of whole-cell lysate immunoblots are shown. The error bars indicate the standard deviation. A *fliF* mutant produced very low levels of what we believe to be the β-flagellins. The strains created for this project are highlighted blue.

Δ*fljLKMNO* strain. The Δ*fljJLMNO* mutant had a recorded swimming speed of 49 ±6.6 μm/sec while the Δ*fljJKLMNO* pRX-*fljK* strain swam slower at 36.9 ±7.7 μm/sec, even though there appeared to be more FljK protein expressed in the cell (Figure 23). The Δ*fljJKMNO* mutant had a swimming speed 19.6 ±6.5 μm/sec while the Δ*fljJKLMNO* pBX-*fljL* strain was swimming at 33.8 ±5.9 μm/sec, which is considerably faster and is thus reflected in an increased level of FljL production, however it is still not wild type swimming speed (Figure 23). Previously we had been unsuccessful in creating a Δ*fljJKLNO* mutant, which could possibly be due to the high intergenic homology in the β-cluster flagellin loci (Nierman *et al*., 2001). By overexpressing FljM, FljN and FljO in the Δ*fljJKLMNO* mutant we were able to show that individually each of the β-flagellins can support motility (Figure 23).

4.7.2 *Complementation of the ΔfljLKMNO mutant*

We have demonstrated that *fljJ* complementation does not result in the restoration of motility in a mutant absent of all α- and β-flagellins. Equally when *fljJ* is the only remaining flagellin on the genome, motility cannot be sustained. We asked the question: can we restore motility in the non-motile Δ*fljKLMNO* by overexpression of individual flagellins?

Motility in the Δ*fljLKMNO* mutant was restored by overexpression of the flagellins FljK, FljL, FljM, FljN, and FljO (Figure 24). However, consistent with previous observations, the overexpression of FljJ did not result in motile cells.

4.8 Summary

We now have a comprehensive flagellin deletion mutant collection comprising of 23 strains. The mutants exhibit a number of motility phenotypes on low percentage motility agar (Figure 17). These phenotypes range from wild type motility, intermediate motility, severely impaired motility and non-motile. Both the Δ*fljJLMNO* and Δ*fljJKMNO* mutants were motile while the Δ*fljLKMNO* and Δ*fljJKLMNO* mutants were non-motile. In fact, the level of observed structural redundancy is that, FljK, FljJ, FljM, FljN or FljO alone can support motility.

The flagellin FljJ is unable to form a filament by itself although mass spectrometry analysis showed that it is utilised as a structural subunit in wild type and in other mutants. Flagellar independent overexpression of FljK, FljL, FljM, FljN and

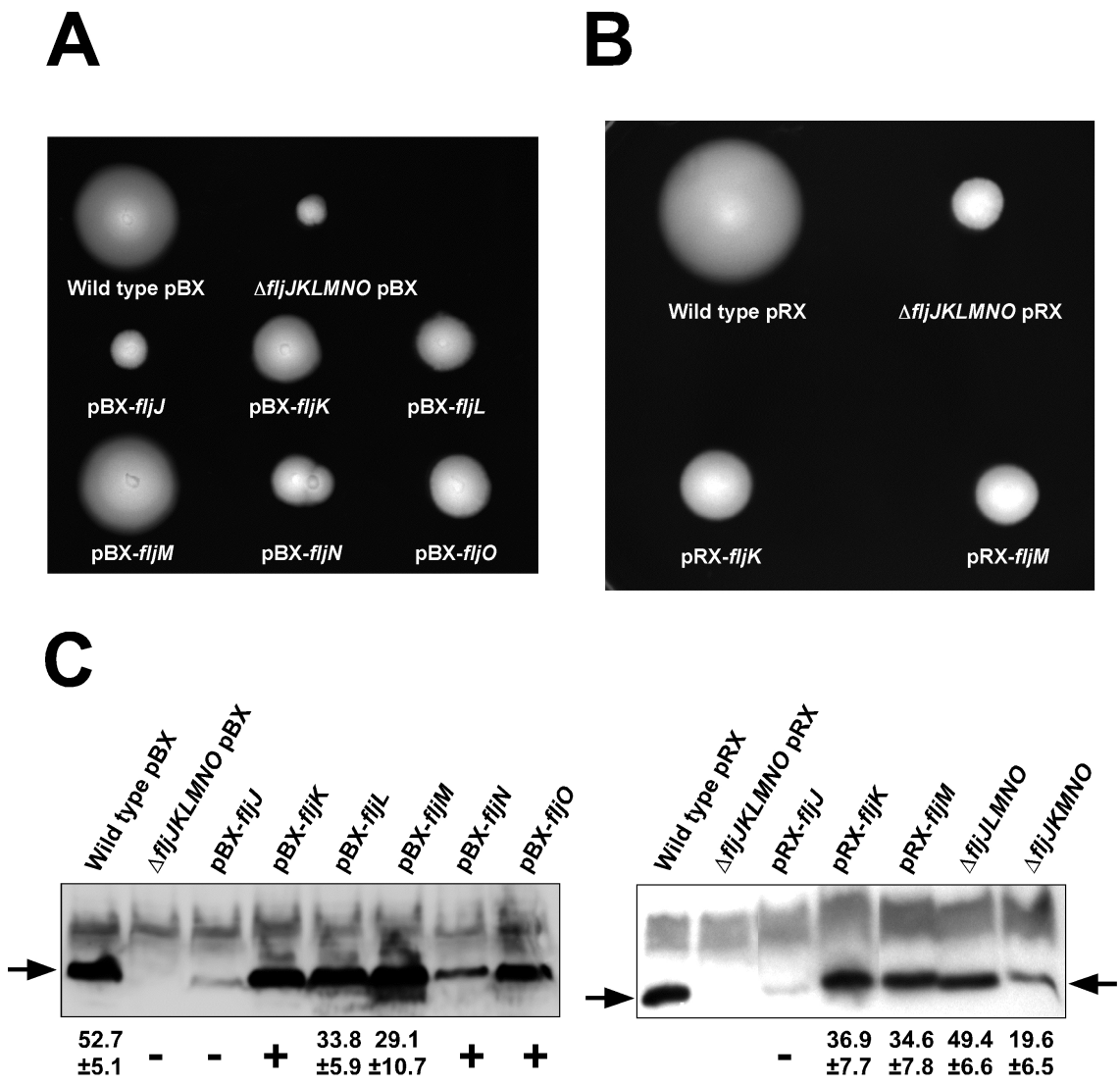

Figure 23: Flagellar independent overexpression of flagellins in the non-motile Δ*fljJKLMNO* mutant (Faulds-Pain *et al*., 2011)

The motility agar assays were inoculated on a single plate and imaged after 5 days growth at 30 ºC. The agar contained kanamycin and xylose to induce plasmid expression of flagellin. **A.** Motility swarms of Δ*fljJKLMNO* pBX- *fljJ*, *fljK*, *fljL*, *fljM*, *fljN*, *fljO*, Δ*fljJKLMNO* pBX vector control, and wild type. **B.** Motility swarms of Δ*fljJKLMNO* pRX- *fljK*, *fljM*; Δ*fljJKLMNO* pRX vector control; and wild type. **C.** Immunoblot analysis of flagellin levels in those strains used in the motility assays (α-Fla antibody). The motility phenotype of each strain is marked below. The swimming speeds of selected mutants are shown. The mutants, Δ*fljJLMNO* and Δ*fljJKMNO*, are included for comparison. The arrows point to flagellin protein.

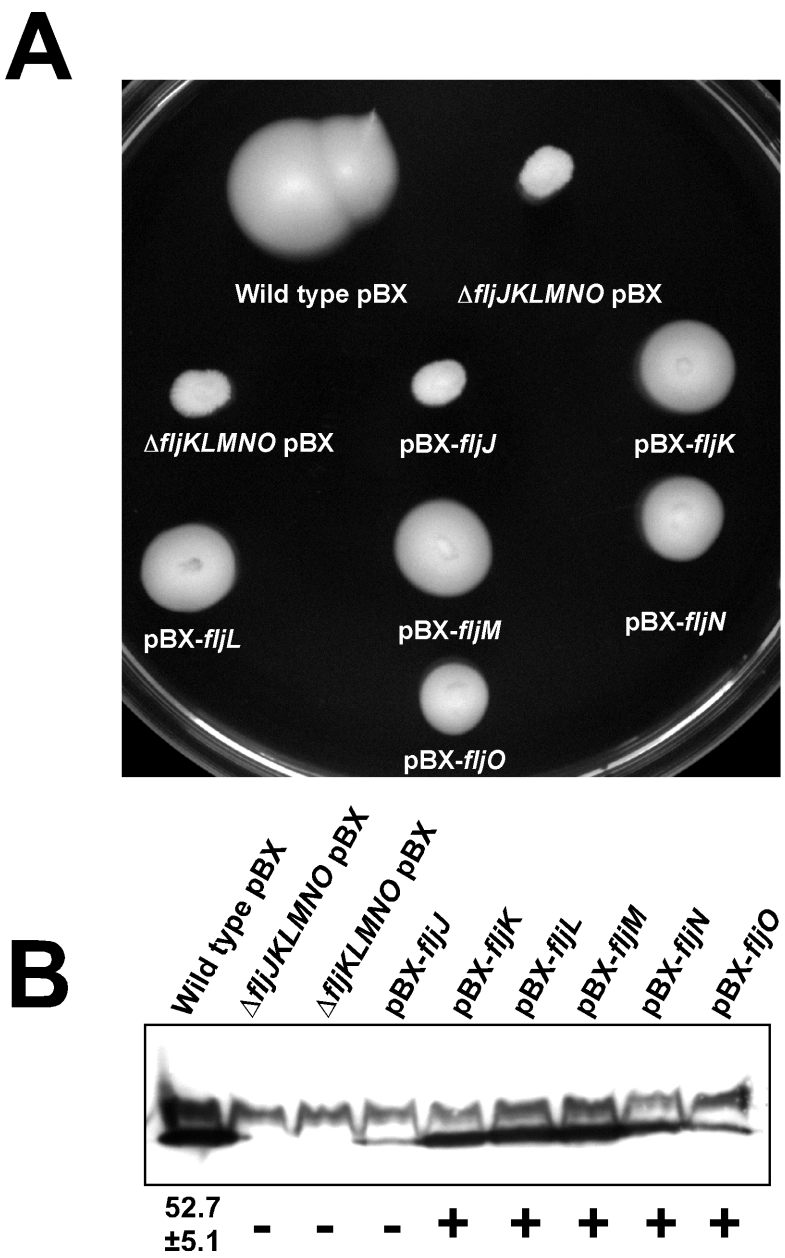

Figure 24: Flagellar independent overexpression of flagellins in the non-motile Δ*fljKLMNO* mutant

The motility agar assay was innoculated on a single plate and imaged after 5 days growth at 30 ºC. The agar contained kanamycin and xylose to induce plasmid expression of flagellin. **A.** Motility swarms of Δ*fljKLMNO* pBX- *fljJ*, *fljK*, *fljL*, *fljM*, *fljN*, *fljO*; Δ*fljJKLMNO* pBX vector control; and wild type. **B.** Immunoblot analysis of flagellin levels in those strains used in the motility assay (α-Fla antibody). The motility phenotype of each strain is marked below.

FljO could restore motility in both non-motile strains however FljJ overexpression could not (Figure 23 and 24). This suggests that FljJ is different from the other flagellins. It is plausible that the non-motile phenotype observed for both the Δ*fljLKMNO* and the Δ*fljJKLMNO* pBX-*fljJ* strains is as a result of low levels of flagellin expression. No quantifiable amounts of protein were detectable the Δ*fljLKMNO* mutant. However, overexpression of FljJ resulted in observable levels of protein that were comparable to the motile Δ*fljJKMNO* mutant. It could be that FljJ is less stable than the other flagellins. Faulds-Pain *et al*., demonstrated that as a group the α-flagellins are more stable than the β-flagellins, however, they did not investigate the stabilities of the flagellin proteins individually (Faulds-Pain *et al*., 2011). It would be interesting to examine this and furthermore whether or not the stability of FljJ is altered when in the presence of another flagellin. This could be easily achieved by pulse-chase analysis utilising Glycine SDS-PAGE in order to separate FljJ (29 kDa) from the other flagellin proteins (27 kDa, 25 kDa).

Interestingly, during flagellar-independent overexpression of flagellin, wild type swimming speeds could not be achieved, even though wild type levels of flagellin protein production were observed. This could suggest that there is a requirement by the bacterium to have more than one flagellin gene present in order to achieve wild type motility. It is plausible that this would function to achieve optimal motility in the short window available to *C. crescentus*. Equally, having flagellar-dependent expression of flagellin genes could be just as important.

MALDI-TOF analysis of mutant filaments demonstrated that all remaining flagellins are utilised in filament assembly (Faulds-Pain *et al*., 2011). These data demonstrate that the flagellins can assemble together in any order. This stochastic incorporation is in contrast to the observed ordered assembly in wild type (Driks *et al*., 1988; Weissborn *et al*., 1982). Could it be that, when order is present we are observing regulation of the system prior to or during secretion? If correct this could also explain flagellin species bias in the filament; we know that of the six flagellins it is FljK and FljM that are utilised at the highest levels (Faulds-Pain *et al*., 2011). Two likely candidates to play a role in such a regulatory mechanism are FlbT and FlaF, which are involved in the post-transcriptional regulation of *fljK* (Anderson and Gober, 2000; Llewellyn *et al*., 2005). A plausible explanation for the use of multiple flagellins is that there exists a flagellin bias with respect to different environmental conditions. Previous experiments carried out on various motile species of bacteria, demonstrated that filament pitch length and pitch height are critical determinants that influence the ability

of a bacterial cell to swim in viscous environments (Schneider and Doetsch, 1974). It was argued that on encountering higher viscosity's pitch length and height were modified to maintain swimming efficiency. Our analysis has shown that overall the pitch lengths and the pitch heights did not change dramatically, however, statistically some were significant. Importantly, there was no consistent change in both pitch height and pitch length. Therefore, it suggests that in *C. crescentus* no specific flagellin combination would present a selective advantage if the filament composition could be altered in response to environmental signals. Furthermore, no flagellin deletion mutant exhibited greater swimming speeds than that of wild type. It would, however, be interesting to observe the direct effect of viscosity on the motility of our flagellin mutants. In addition, it would also be interesting to examine the ability of the flagellar specific bacteriophage, ϕCbK, to infect the cells of each of our flagellin mutants (Guerrero-Ferreira *et al*., 2011).

A general trend throughout the whole mutant collection (23 strains) was the increase in number of flagellin deletions resulted in a greater reduction of swimming speed (Figure 20). A strong correlation was observed between the reduction in swimming speed, shorter filaments and reduced flagellin protein levels for all Δ*fljKMX* (where X stands for any other α- or β-flagellin). This indicates that FljK and FljM are major functional components of the filament. This is consistent with mass spectrometry data showing that FljM and FljK are the most abundant flagellins in a population of isolated filaments (Data not shown, C. Birchall MRes: unpublished). Interestingly, low levels of β-flagellin protein were observed in a Δ*fliF* mutant (Figure 22). The flagellar-independent production of β-flagellin suggests a possible role in the maintenance of the filament during the SW cell stage of the life cycle.

It would be interesting to look at individual filament composition rather than populations. We hoped that by designing peptide derived antibodies we would be able to achieve this, however it appears that their design and subsequent use is complicated. It is predicted that the flagellins of *C. crescentus* are glycosylated prior to secretion and their subsequent assembly into the filament (Faulds-Pain *et al*., 2011; Johnson *et al*., 1983, Leclerc *et al*., 1998). Bacteria favour O-linked modification during the addition of glycan molecules to either serine or threonine residues (Logan, 2006). The chemical synthesis of a peptide would not contain the correct post-translational modifications and thus the peptide-derived antibody would not recognise such additions. It is plausible that glycosylation in the flagellin region chosen for these experiments is affecting antibody recognition. The post-translational modification of flagellins has been shown

to be important for protein stability (Faulds-Pain *et al*., 2011). Therefore, it is likely that the observable differences in protein levels during immunoblot analysis of flagellin overexpression are a result of stability. It is possible that the flagellins of *C. crescentus* are differentially glycosylated, although this would require further experimental investigation.

Chapter 5. Subunit Feedback into the Regulation of Filament Assembly

5.1 Introduction

We have demonstrated that there is extensive structural redundancy present in the flagellins of *Caulobacter crescentus*. A working flagellum can be constructed from just one species of flagellin. However, when the only remaining flagellin is FljJ, motility cannot be sustained. FljJ is the most divergent flagellin with respect to nucleotide and amino acid sequence (Figure 16) (Ely *et al*., 2000), this therefore could suggest an alternative role for FljJ from the rest of the flagellins. In all flagellar systems there is a level of system regulation that couples gene expression with assembly utilising defined assembly checkpoints. This control is constructed from regulatory feedback loops involving flagellar-associated T3S-chaperones that couple flagellar gene expression to assembly through interactions with secretion substrates (Aldridge and Hughes, 2002). This regulation is exemplified by the canonical *Salmonella* regulatory circuit of FlgM:σ^{28}, whose combined action co-ordinates the transition from HBB completion to filament assembly. Another example is the *Salmonella* regulatory circuit of FliT:FliD:$FlhD_4C_2$ that has been recently implicated in the control of flagellar number (Aldridge *et al*., 2010). FliT is a T3S-chaperone that interacts with the filament cap protein FliD (Fraser *et al*., 1999). FliT also binds to the flagellar master transcriptional regulator $FlhD_4C_2$ and prevents it from activating early flagellar gene promoters (Yamamoto and Kutsukake, 2006). Prior to HBB completion FliD is bound to FliT however upon completion, FliD is secreted out of the cell, the action of which is facilitated by FliT in its role as a T3S-chaperone, thus freeing FliT to then bind to and negatively regulate the activity of $FlhD_4C_2$.

Filament assembly in *C. crescentus* can take place only upon HBB completion. In the majority of flagellar systems this assembly checkpoint is sensed and overcome by the secretion of FlgM. Bioinformatic analysis of bacterial flagellar systems has revealed that FlgM and σ^{28} are absent from the genomes of the majority of α-proteobacterial species (Faulds-Pain *et al*., 2011). However, when both FlgM and σ^{28} are present in an α-proteobacteria genome there is evidence to suggest that horizontal gene transfer has occurred resulting in two separate flagellar systems. For example, *Rhodobacter sphaeroides* has a second flagellar system acquired from γ-proteobacteria that is

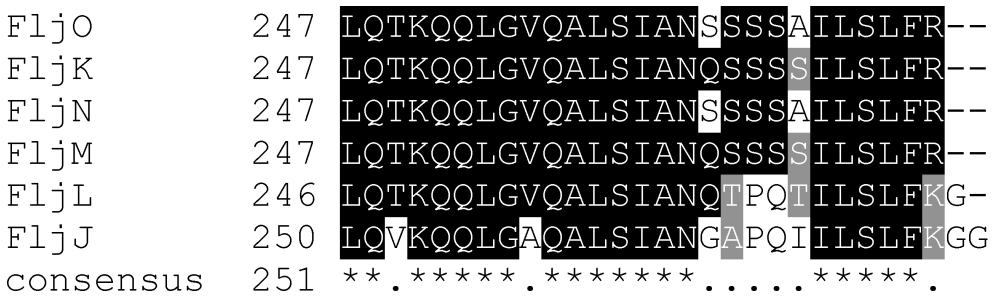

Figure 25: C-terminal primary sequence alignment of the six flagellins of *Caulobacter crescentus*

The multiple alignment was assembled using ClustalW and the similarity shading was performed using BoxShade.

induced under anaerobic growth (Poggio *et al*., 2007). Outside of the α-proteobacteria all flagellar systems characterised to date have FlgM and σ^{28} (Brown *et al*., 2009; Faulds-Pain *et al*., 2011). Interestingly, bioinformatic analysis has also highlighted the absence of FliD (filament cap) from many α-proteobacteria including *C. crescentus* (Figure 8) (Faulds-Pain *et al*., 2011). This suggests that flagellin polymerisation in those bacteria must be coordinated by a yet unidentified protein or by a different mechanism.

The absence of FlgM:σ^{28} from the *C. crescentus* genome raises an important question; how does *C. crescentus* couple the switch HBB completion to filament assembly? Two proteins have been implicated to function in this switch and they are both involved in the post-transcriptional regulation of flagellin. FlbT has been shown to be a negative regulator of *fljK* mRNA preventing translation. In contrast, FlaF acts as a positive regulator of flagellin translation (Anderson and Gober, 2000; Llewellyn *et al*., 2005; Mangan *et al*., 1999; Schoenlein and Ely, 1989). It is so far unclear as to the exact mechanisms by which these two proteins co-ordinate their regulation with HBB completion. However, it is plausible that like in other flagellar systems, HBB completion is sensed and overcome by the secretion of a flagellar-associated secretion substrate. In the absence of a filament cap and as the flagellins themselves are being secreted we asked the logical question: are the flagellins involved in subunit feedback control of the regulation of filament assembly?

5.2 Bacterial Two-Hybrid Analysis

We chose to investigate this question by looking for interactions between the flagellins and other known regulators of the system. To test this we performed a bacterial two-hybrid assay (BACTH Euromedex) using full length open reading frame constructs of *fljJ*, *fljK*, *fljL*, *fljM*, *flaF*, *flbT*, *flbD* and *fliX*. CC1462 (A hypothetical open reading frame located between *fljK* and *fljL* on the annotated genome) and *flgL* (Hook associated protein) were also included in the assay. *fljM* was the only β-flagellin gene included do to the high sequence similarity between itself and *fljN* and *fljO*. The protein-protein test interactions (transformations) were plated out individually on selective media and the phenotype scored after 48 hrs.

In flagellar systems subunit-regulator interactions often occur at the C-terminus of the subunit (Ozin *et al*., 2003). An amino acid sequence alignment of the six flagellins suggests some variability at the C-terminus, particularly in FljJ (Figure 25). Therefore, we constructed N-terminal fusions of all candidate proteins in order to leave

A

	pKT25	25-ZIP	FljL	FljK	FljJ	FliX	FlbD	FlgL	FlaF	FlbT	CC1462	FljM
pUT18c	-	-	-	-	-	-	-	-	-	-	-	-
18c-ZIP	-	+	-	-	-	-	-	-	-	-	-	-
FljL	-	-	-	-	-	-	-	-	-	-	-	-
FljK	-	-	-	-	-	-	-	-	-	-	-	-
FljJ	-	-	-	-	-	-	-	-	+	+	-	-
FliX	-	-	-	-	-	-	+	-	-	-	-	-
FlbD	-	-	-	-	-	+	+	-	-	-	-	-
FlgL	-	-	-	-	-	-	-	-	-	-	-	-
FlaF	-	-	-	-	+	-	-	-	-	-	-	-
FlbT	-	-	-	-	+	-	-	-	-	-	-	-
CC1462	-	-	-	-	-	-	-	-	-	-	-	-
FljM	-	-	-	-	-	-	-	-	-	-	-	-

B

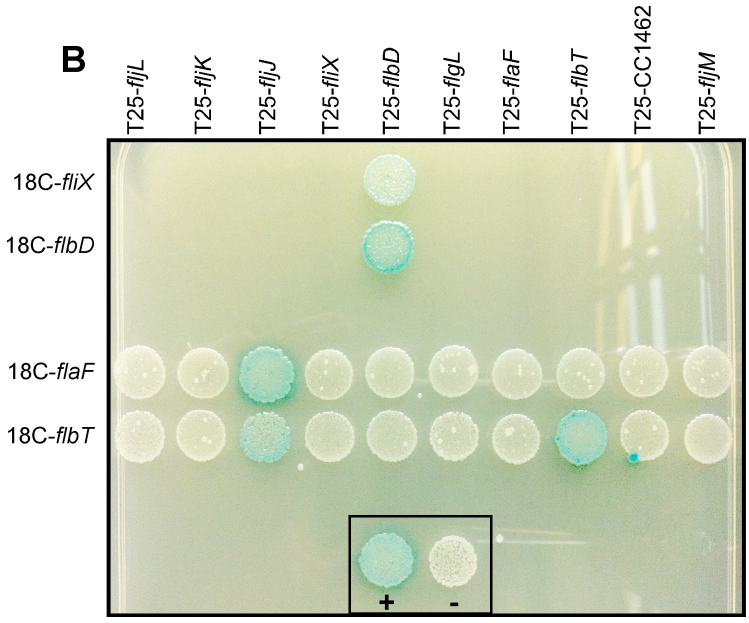

Figure 26: Bacterial two hybrid analysis of *Caulobacter crescentus* flagellar genes

A. A schematic presentation of the results from all possible interaction combinations tested (144 in total). pKT25 constructs are labeled along the top and pUT18C constructs are labeled up the side. A white box with a minus symbol represents a negative interaction. A blue box with a plus symbol represents a positive interaction. **B.** A summary of the interactions tested. FljJ interacted with both FlbT and FlaF. The internal positive control of FlbD:FliX is included. The BACTH controls are shown in the black box.

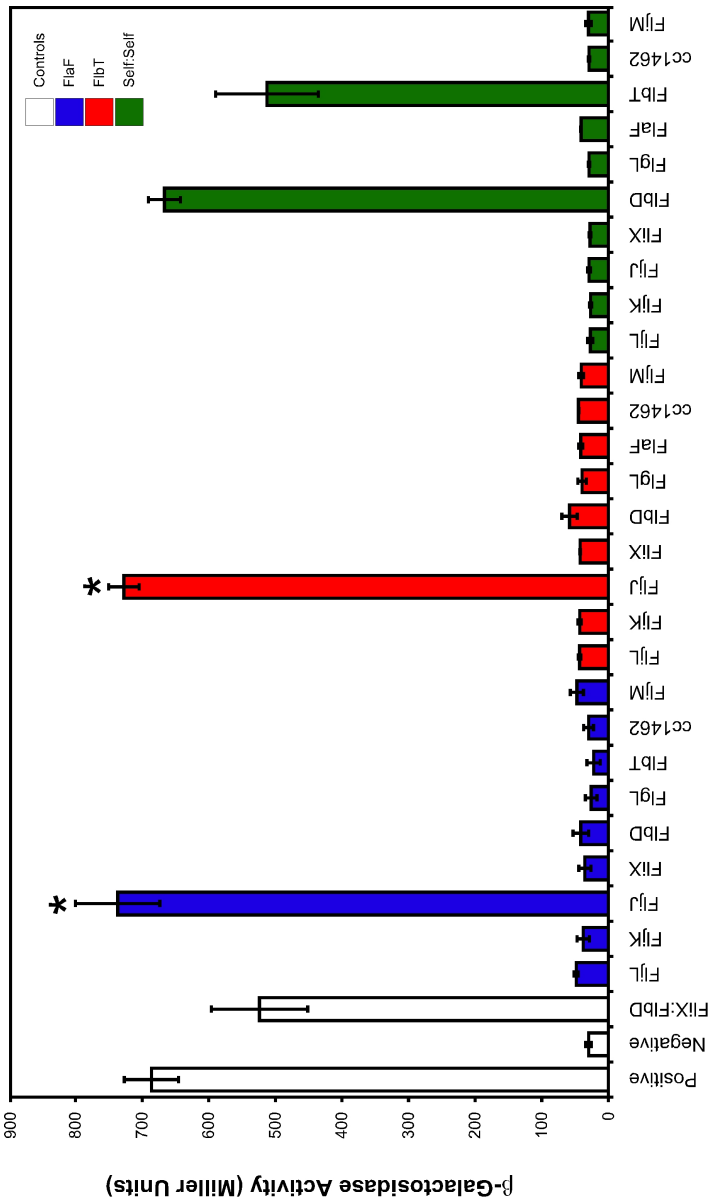

Figure 27: A summary of the β-galactosidase activities of a subset of *Caulobacter crescentus* flagellin interactions tested by bacterial two-hybrid analysis (BACTH)

The data presented is an average measurement calculated from three independent repeats. Error bars represent the standard deviations. An asterisks above a data point indicates that the measurement was significant when compared to the negative control ($P < 0.001$, calculated by pairwise *t*-Test). **White data set:** Internal BACTH controls and the known interaction between the *C. crescentus* flagellar proteins FliX and FlbD. **Blue data set:** pUT18C-*flaF* tested against all other pKT25- constructs. **Red data set:** pUT18C-*flbT* tested against all other pKT25- constructs. **Green data set:** Self:Self.

the C-termini free. The plasmids pUT18C and pKT25 both allow in-frame fusions to the C-termini of the T18 and T25 fragments. The known interaction of FlbD and FliX was used as an internal positive control alongside the controls of the system (BACTH Euromedex; Muir *et al*., 2005). 144 interactions in total were tested including all possible combinations of plasmid constructs (Figure 26). Both system controls behaved as expected; pUT18C-zip:pKT25-zip produced a positive result due to the presence of the leucine zipper region of the yeast protein GCN4 (Figure 26). The empty vectors pUT18C:pKT25 produced a negative result. We identified a number of previously unknown interactions (Figure 26). FlbT was found to interact with itself suggesting it may function as a protein dimer. FlbD also interacted with itself, which confirms what is currently predicted in the literature (Benson *et al*., 1994). However, to our surprise we observed a positive interaction between the flagellin FljJ, and both FlbT and FlaF (Figure 26). All other interactions tested resulted in a negative white colony phenotype.

5.2.1 *β-galactosidase quantification*

The observed interactions were quantified by measuring β-galactosidase in 3 independent liquid cultures using ONPG as a colorimetric substrate (Miller 1972). pUT18C-zip:pKT25-zip had an average measurement of 657 ±62 miller units where as pUT18C:pKT25 was 27 ±1 (Figure 27). The internal control of FliX:FlbD gave a measurement of 575 ±82 miller units which was comparable to the positive zip system control. FlbD:FlbD and FlbT:FlbT gave measurements of 666 ±24 and 513 ±77 respectively. FlaF:FljJ and FlbT:FljJ gave measurements of 737 ±63 and 727 ±23 respectively. Slightly higher activities than the positive zip system control suggests strong interactions. The positive interactions were significant when compared to the negative zip system control ($P < 0.01$, calculated by a pairwise *t*-Test). All other interactions were comparable to the negative system control. These data suggest that FljJ is playing both a structural and regulatory role in the feedback control of flagellin translation. As the other flagellins did not interact with FlbT or FlaF it would suggest that they are only structural components of the filament.

5.3 Biochemical Characterisation of Protein-Protein Interactions

It is possible for false positive results to occur when using a bacterial two-hybrid assay. These can occur for a variety of different reasons such as; mis-folded proteins or non-specific spurious binding to DNA leading to alterations of transcriptional activation.

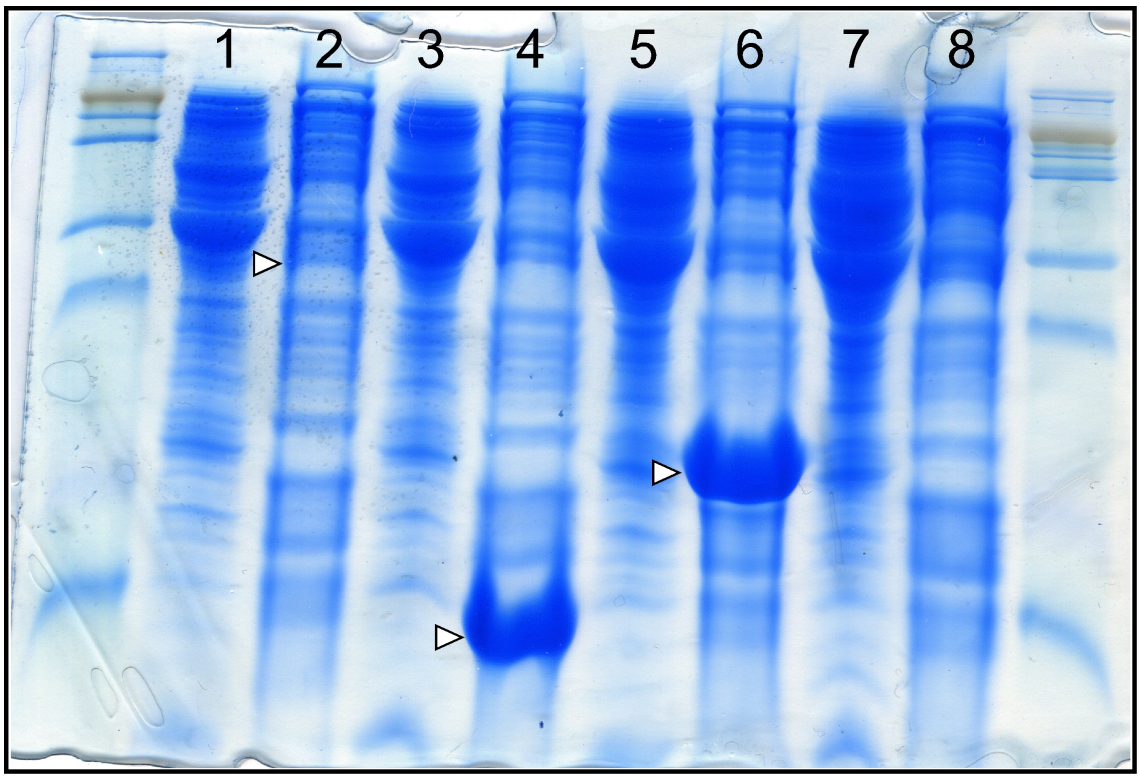

Figure 28: Small-scale overexpression of FljJ, FlbT and FlaF

pET28b constructs of *fljJ*, *flbT* and *flaF* were overexpressed in BL21 (DE3). Samples were run on a 12 % tricine SDS-PAGE gel and visualised using Coomassie Blue stain. The white arrows indicate unique protein bands. **(1)** FljJ soluble fraction. **(2)** FljJ insoluble fraction. **(3)** FlaF soluble fraction. **(4)** FlaF insoluble fraction. **(5)** FlbT soluble fraction. **(6)** FlbT insoluble fraction. **(7)** BL21 (DE3) soluble fraction. **(8)** BL21 (DE3) insoluble fraction.

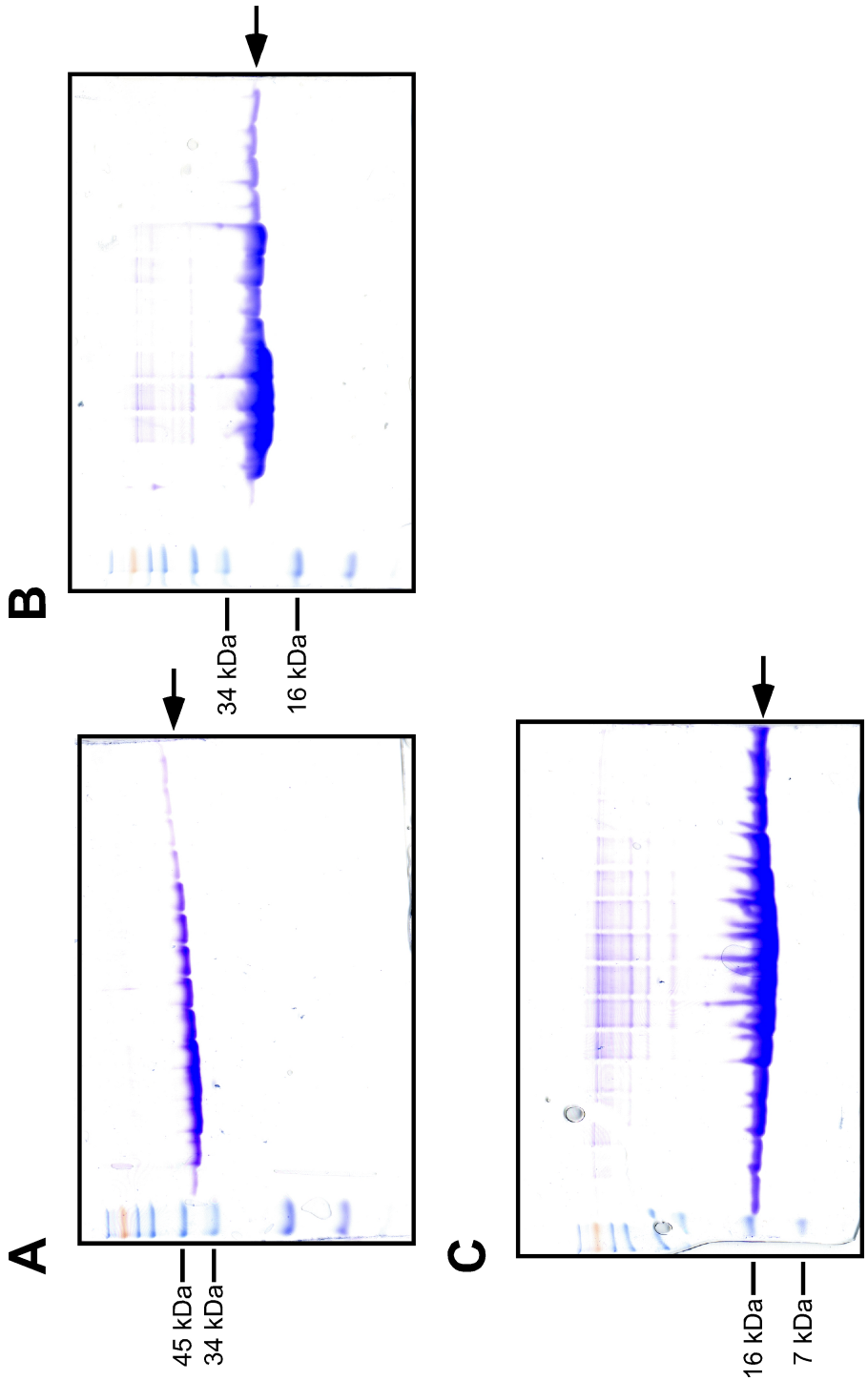

Figure 29: Large-scale (1L) purification of FljJ, FlbT and FlaF by nickel affinity chromatography

Protein samples were collected using an AKTA purification system, run on a 12 % tricine SDS-PAGE gel and visualised using Coomassie Blue stain. The approximate MW of protein marker is indicated. The arrows point to the correct protein band identified by MALDI-TOF. **A.** FljJ. **B.** FlbT. **C.** FlaF.

Because of this, it was important to confirm the FljJ:FlaF/FlbT interactions biochemically by other methods. Full length N-terminal 6 x histidine-tagged constructs of FljJ, FlbT and FlaF were created utilising the vector pET28b by subcloning gene fragments from the corresponding pUT18C plasmids. Small-scale overexpression tests revealed that all three proteins were insoluble (Figure 28). Both FlbT and FlaF expressed to a high level when compared to the BL21 (DE3) background (Figure 28). In contrast, overexpression of FljJ resulted in a low level protein visible as a small band in the insoluble fraction (Figure 28). Additional attempts to gain solubility were unsuccessful (data not shown). Therefore, a denaturing purification protocol was attempted.

Briefly, overexpression of all three proteins was carried out in 1 litre culture, then under denaturing conditions of 8 M urea samples were purified by nickel affinity chromatography (Figure 29). The denatured proteins were then refolded using an adaption of a published method (Hager and Burgess, 1980; Lowe *et al*., 1979). This refolding protocol was based on original work carried out by Richard Burgess and colleagues on the purification of insoluble sigma factors from E. coli. Protein samples were purified further and tested for interactions using gel filtration. Identification of the protein was confirmed by MALDI-TOF (See Appendix E). A high salt concentration (500 mM NaCl) was maintained in the mobile phase gel filtration buffer throughout all experiments, as the solubilised proteins were un-stable (degradation after approximately 48 hrs). All experiments were carried out at room temperature.

5.3.1 *Gel filtration analysis*

FljJ is predicted to have a molecular weight of 29 kDa and it eluted as a single narrow peak (Figure). FlbT is predicted to have a molecular weight of approximately 16 kDa and it eluted as two consecutive peaks (Figure 30). This could be explained by the observation that in the bacterial two-hybrid experiment FlbT interacted with itself. Under the conditions used in this experiment it is possible that FlbT was present in both a dimeric and monomeric form. Theoretically a dimer of FlbT should have a molecular weight of approximately 32 kDa. The first FlbT peak, however, appeared to have a similar retention time to that of FljJ (Figure 30). It is possible that under the mobile phase conditions used, and resolution of the column, we are unable differentiate a difference of 2-3 kDa. FlaF is the smallest of the three proteins with a predicted molecular weight of 11 kDa and it eluted as a single peak with a longer retention time than that of FljJ indicative of its smaller size (Figure 31).

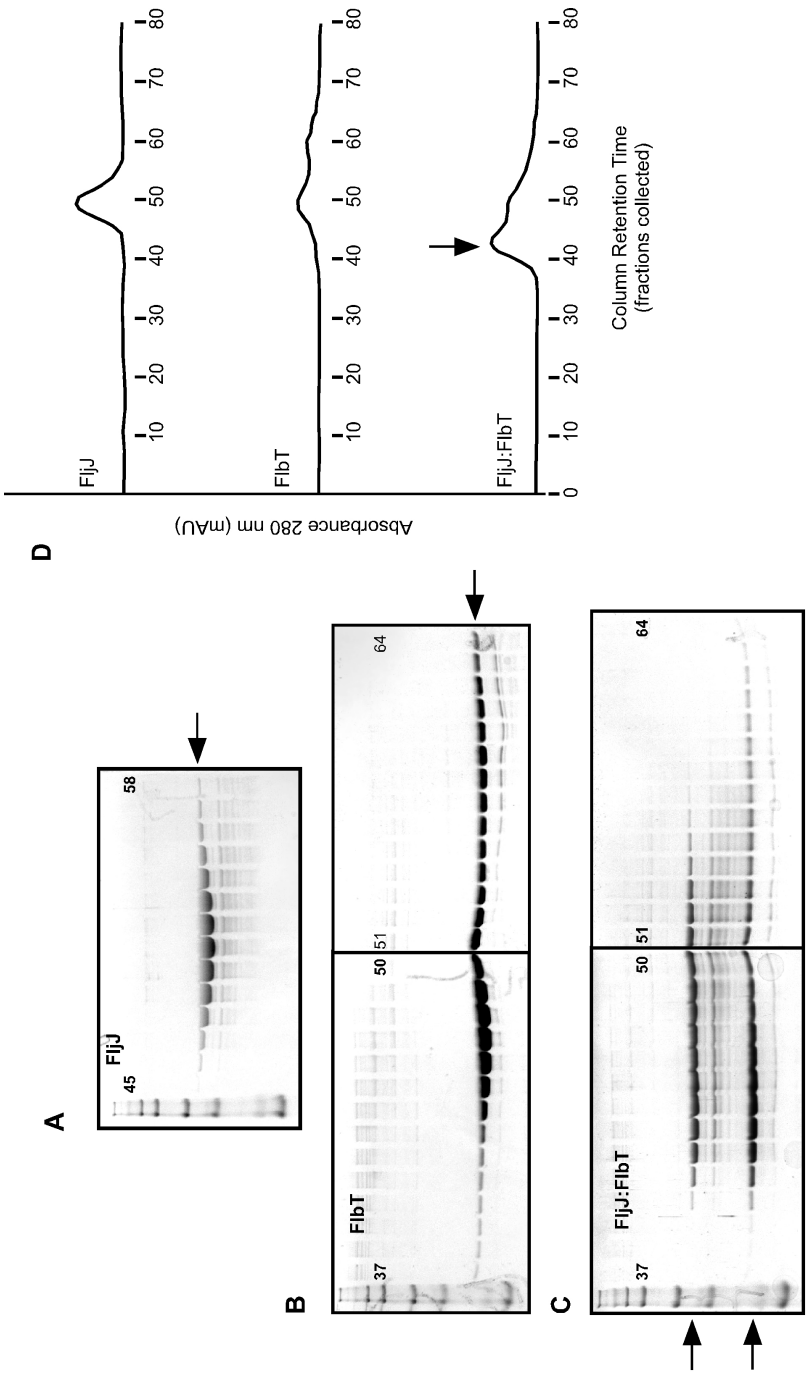

Figure 30: Gel filtration analysis of FljJ and FlbT

Protein fractions were collected using an AKTA purification system, run on a 12 % tricine SDS-PAGE gel and visualised using Coomassie Blue stain. For comparison, gels are aligned vertically by fraction number. The arrows point to the correct protein band. The total protein concentration in each sample is 13 µM. **A.** FljJ. **B.** FlbT **C.** FljJ:FlbT mixed in a 1:1 molar ratio. **D.** Gel filtration trace aligned vertically by fraction number for comparison. The arrow indicates a unique protein peak.

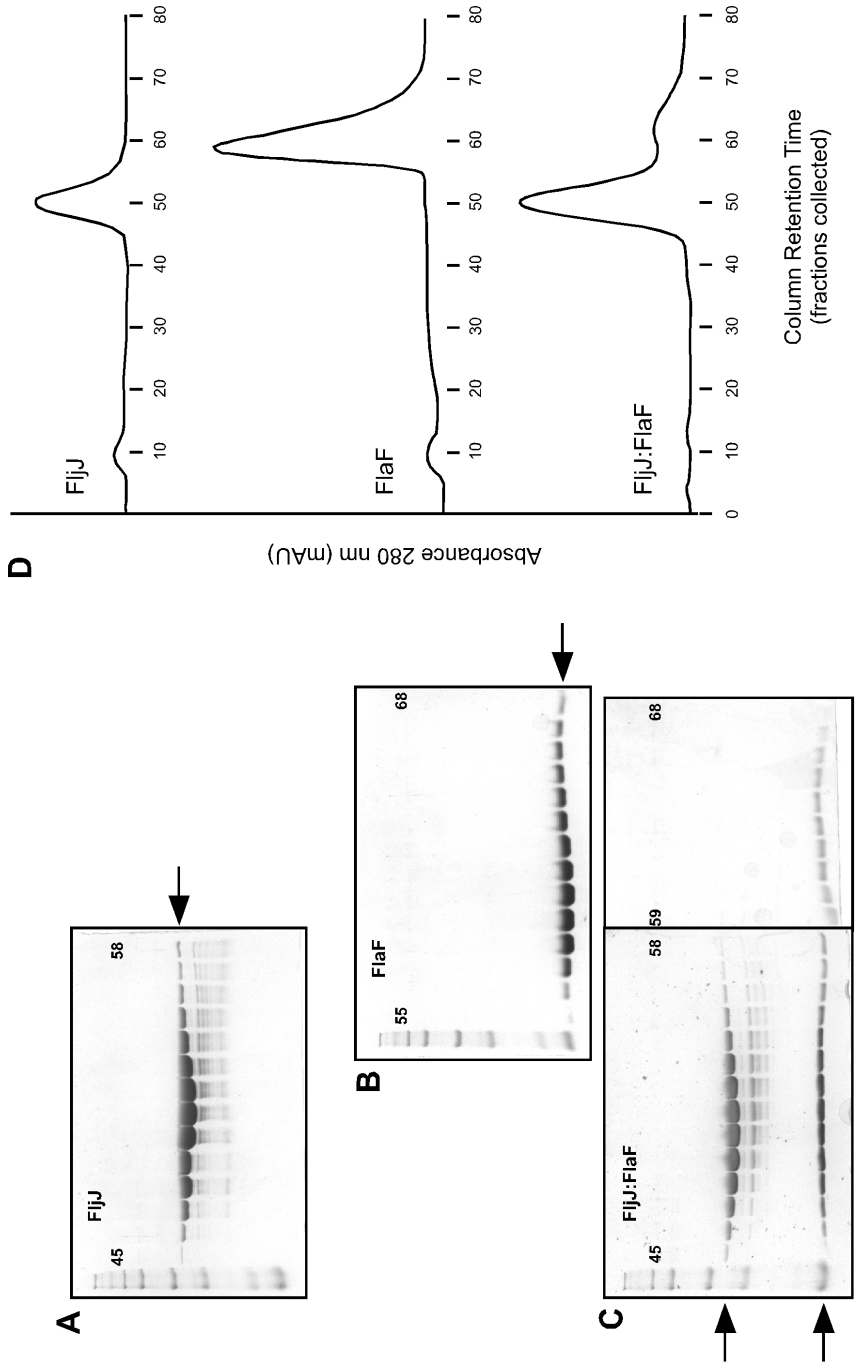

Figure 31: Gel filtration analysis of FljJ and FlaF

Protein fractions were collected using an AKTA purification system, run on a 12 % tricine SDS-PAGE gel and visualised using Coomassie Blue stain. For comparison, gels are aligned vertically by fraction number. The arrows point to the correct protein band. The total protein concentration in each sample is 23 μM. **A.** FljJ. **B.** FlaF **C.** FljJ:FlaF mixed in a 1:1 molar ratio. **D.** Gel filtration trace aligned vertically by fraction number for comparison.

5.3.1.1 Gel filtration analysis of protein-protein interactions

To confirm the interactions observed in the bacterial two-hybrid screen, FljJ was mixed with both FlbT and FlaF in a molar ratio of 1:1 and subjected to gel filtration under native conditions. The experiments demonstrated that FljJ could co-elute with FlbT and FlaF. When FljJ and FlbT were mixed together, a new peak with a shorter retention time was observed (Figure 30). The peak contained both FljJ and FlbT. A longer tail following the peak suggests the presence of a smaller species or possibly protein degradation. It is difficult to say whether or not FljJ was interacting with a FlbT dimer. If this was true then we would have expected to observe an even shorter retention time due to a large complex.

When FljJ and FlaF were mixed, the FlaF peak almost completely disappeared and the FljJ peak increased proportionally (Figure 31). Surprisingly, the retention time of the FljJ-FlaF complex did not change when compared to FljJ alone (Figure 31). An explanation for this observation could be that the binding of FlaF does not significantly change the overall shape of FljJ enough to be resolved on the gel filtration column used. However, confirmation of this would require the use of other analytical methods such as; Circular Dichroism, Dynamic Light Scattering and Analytical Ultra-centrifugation. Although the data strongly suggests that both FlbT and FlaF can interact with FljJ it is clear that a more quantitative experimental approach is needed in order to understand the stoichiometry and dynamics of the interactions.

5.3.2 *Native-PAGE analysis*

The analytical spectroscopic methods mentioned above require the analyte to be in strict buffer conditions. One such requirement is that of a low concentration of chloride ions (NaCl) as these show high absorbance in the far UV region, consequently reducing the size of the available spectra. Attempts to dialyse the protein samples into more suitable buffers were however unsuccessful. Therefore, in order to indirectly test that the proteins had refolded correctly and were functional, Native-PAGE was performed. This would confirm whether the proteins had intrinsic charge indicative of tertiary structure and also confirm whether they could interact and form a complex with each other. The theoretical pI's of FljJ, FlbT and FlaF were calculated to be: 4.68, 7.01 and 4.86 respectively (Table 6). Therefore, a Native-PAGE gel with a > pH 7 was used to allow all three proteins to migrate in the same direction during electrophoresis.

All three proteins individually migrated at different positions within the gel (Figure 32). FlaF moved the furthest distance away from the wells, then next was FljJ

followed by FlbT, which moved the shortest distance. As FlbT is predicted to possess a smaller MW than FljJ, it would suggest that FlbT is forming a dimer, which is consistent with the gel filtration profile. When FljJ and FlbT were mixed in a 1:1 molar ratio, both the individual protein bands disappeared and a new one appeared that could not migrate into the gel (Figure 32). This indicated that a FljJ:FlbT complex had formed. However, from this data we are unable to confirm whether FljJ is interacting with a FlbT dimer or monomer. When FljJ and FlaF were mixed in a 1:1 molar ratio, a new protein band appeared and the bands corresponding to the individual proteins disappeared (Figure 32). The new band migrated differently to the individual proteins indicating an interaction had occurred. These data would suggest that FljJ interacts with FlaF in a stoichiometry of 1:1.

5.3.3 *His-FljJ pull down assay*

Further confirmation was sought by removing the N-terminal his-tag of FlbT and FlaF, thus ensuring that the tag was not influencing any interaction. FlbT and FlaF were subjected to Thrombin protease digestion and tested for their ability to bind to immobilized FljJ using Ni-NTA agarose. Following incubation with Thrombin, both FlbT* and FlaF* (* refers to non-tagged protein) were subjected to gel filtration to remove the protease. SDS-PAGE analysis of the collected fractions revealed that the digestion was successful (Figure 33).

After incubation with Ni-NTA agarose, FljJ was bound by the N-terminal His-tag and could not be removed by washing. However, upon incubation with 500 mM imidazole, FljJ was eluted from the agarose (Figure 34). In contrast, after incubation with the agarose, FlaF*, was still present in the supernatant and any bound protein was removed by washing alone (Figure 34). This confirmed the absence of a His-tag. FljJ and FlaF* were then mixed in a molar ratio of 1:1 and incubated with the Ni-NTA agarose. Surprisingly, FljJ was prevented from binding to the agarose suggesting that a FljJ:FlaF complex had formed but also that FlaF* had interfered with the ability of FljJ to bind the agarose (Figure 34). This is however, consistent with the bacterial two-hybrid data and other biochemical data that FljJ can interact with FlaF. Unfortunately, FlbT* bound strongly to the agarose and could not be removed by washing, even though the incubation and washing steps were carried out in the presence of 10 mM imidazole (Figure 34) (in order to prevent non-specific interactions). This suggests that

Protein	Theoretical pI
FljJ	4.68
FljK	8.75
FljL	7.86
FljM	9.07
FljN	9.27
FljO	9.10
FlbT	7.01
FlaF	4.86

Table 6: Theoretical isoelectric point (pI) of *Caulobacter crescentus* flagellar proteins

Amino acid sequences were taken from the NCBI database and analysed using the ProtParam software tool (http://expasy.org/tools/).

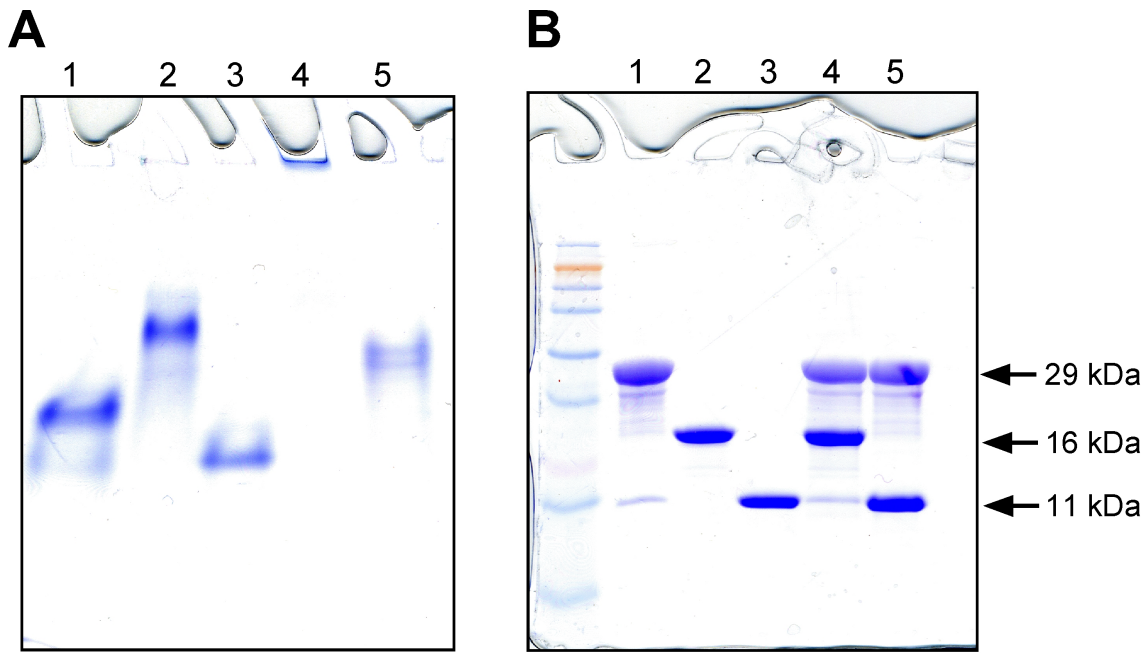

Figure 32: Native-PAGE analysis of FljJ, FlbT and FlaF

Protein samples were first gel filtrated and then used for Native-PAGE analysis. A total protein concentration of 10 µM was present in each sample. The gels were visualised using Coomassie Blue stain. **A.** 7.5 % Native-PAGE gel. **(1)** FljJ. **(2)** FlbT. **(3)** FlaF. **(4)** FljJ:FlbT mixed in a 1:1 molar ratio. **(5)** FljJ:FlaF mixed in a 1:1 molar ratio. **B.** 12 % tricine SDS-PAGE gel analysis of the same protein samples for comparison.

FlbT* binds strongly in a non-specific way to the Ni-NTA agarose. A reasonable explanation could be that the agarose presents a structure that is RNA-like, similar to that of heparin. Therefore, the RNA-binding domain of FlbT could be interacting with the agarose matrix. However, due to the project time constraints it was not possible to confirm this.

5.3.4 *In vivo* co-immunoprecipitation

We decided to attempt to isolate the FljJ:FlbT and FljJ:FlaF interactions in vivo using Co-immunoprecipitation (CoIP). If successful this would allow us to investigate the timing of the interactions with respect to the *C. crescentus* cell cycle. We hoped that this would help us to identify the biological function and significance of the interactions. We focused first on isolating the interactions from asynchronous culture, utilising FljJ as the 'bait' protein. A full length N-terminal 3 x FLAG tagged FljJ construct was created by overlap extension PCR. The tagged gene was placed on the genome of the Δ*fljJ* mutant by allelic exchange, under the control of the native *fljJ* promoter. Positive genetic recombinants were identified by PCR and screened for FLAG-FljJ expression by immunoblot using an α-FLAG antibody (Figure 35). Immunoprecipitation was performed on wild type cells expressing untagged FljJ and on cells expressing FLAG-FljJ using ANTI-FLAG M1 agarose affinity gel. Samples were then subjected to Tricine SDS-PAGE and immunoblot analysis using α-Fla, α-FlbT and α-FlaF antibodies (J. Gober).

Neither FlbT nor FlaF was detected in the wild type or the FLAG-FljJ sample (Figure 35). Surprisingly however, flagellin protein was detected in both samples (Figure 35). This suggests that flagellin protein is binding non-specifically to the ANTI-FLAG M1 agarose and is not removed during washing. It is also possible that flagella in the cell culture are binding to the agarose. It is plausible that this type of experiment may need to be completed in an alternative genetic background to that of wild type *C. crescentus* i.e. one with no other flagellin genes. However, due to the time constraints of this project this could not be realised. Furthermore, with additional time it would be important to investigate the functionality of the FLAG-*fljJ* allele, by testing if the hybrid protein can be secreted and interact *in vitro* with FlbT/FlaF.

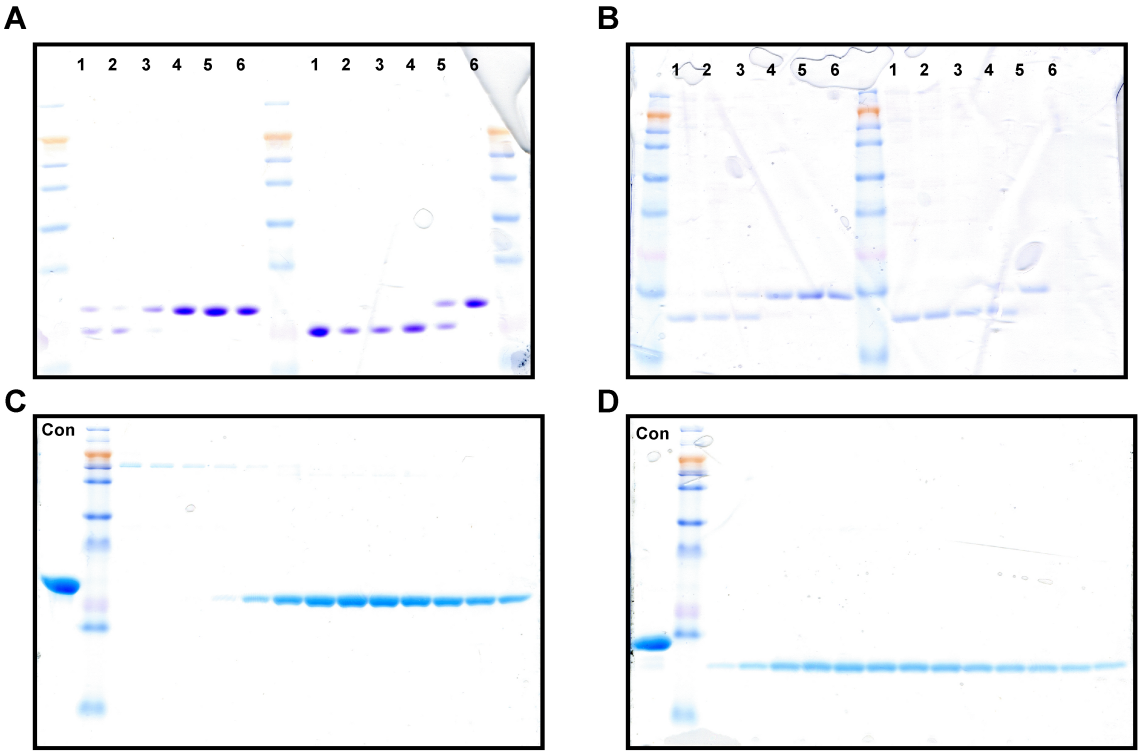

Figure 33: The removal of the his-tag from FlbT and FlaF by thrombin digestion

Tricine-SDS-PAGE analysis of protein thrombin digestion visualised using Coomassie Blue stain. Preliminary time course experiments were carried out in order to establish the amount of thrombin protease to use and the duration of the digestion reaction. **(1)** 1 unit of thrombin. **(2)** 0.5 unit **(3)** 0.2 unit **(4)** 0.1 unit **(5)** 0.05 unit **(6)** 0 unit. **A.** FlbT. The first set of six reactions (left hand side) were incubated for 0 min before the reaction was stopped. The second set of six reactions (right hand side) were incubated for 30 min. **B.** FlaF. **C.** Gel filtration of FlbT after Thrombin digestion (0.5 unit for 30 min). **D.** Gel filtration of FlaF after Thrombin digestion (0.5 unit for 30 min). **Con:** protein sample prior to digestion.

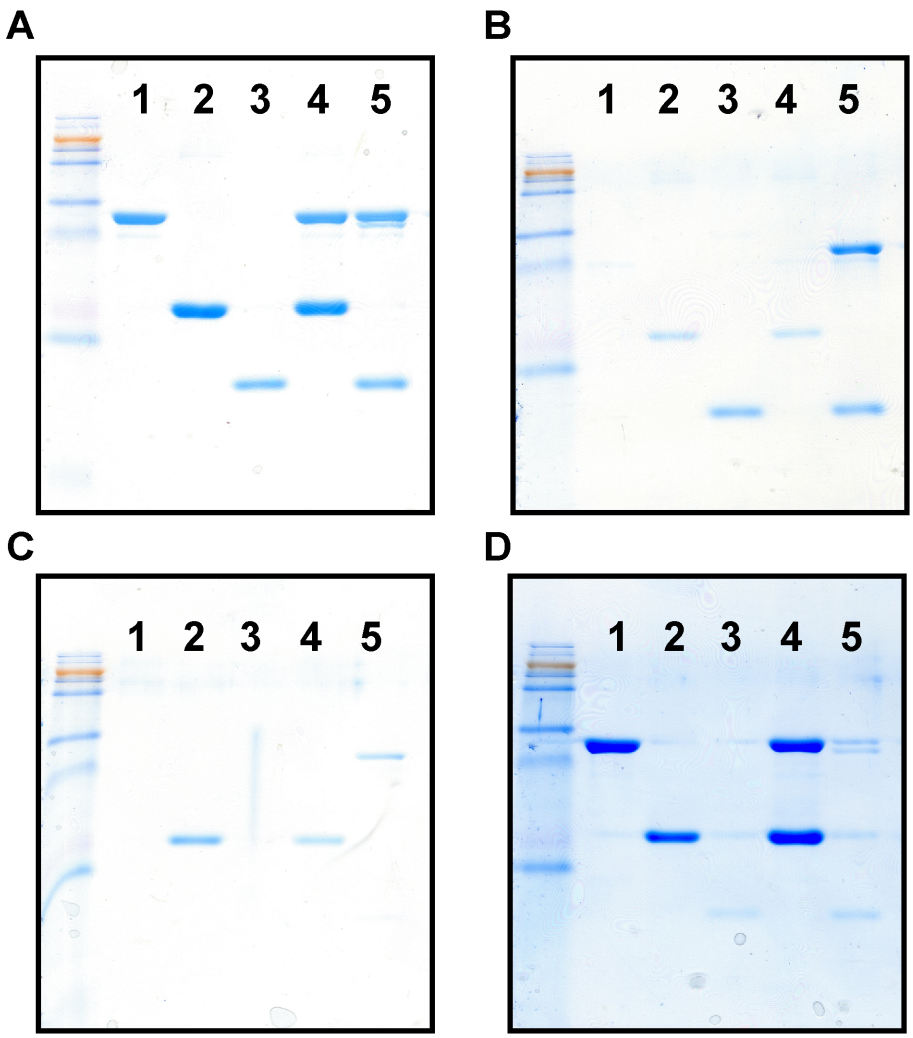

Figure 34: His-FljJ pull down assay

Tricine-SDS-PAGE analysis of the His-FljJ pull down experiment, visualised using Coomassie Blue stain. **(1)** FljJ **(2)** FlbT* **(3)** FlaF* **(4)** FljJ:FlbT* **(5)** FljJ:FlaF*. An asterisk represents a non-tagged protein. The supernatant of each sample was run on the gel. **A.** Prior to incubation with Ni-NTA agarose. **B.** After incubation. **C.** Wash. **D.** Elution.

5.4 Summary

We began by asking the question: how does *C. crescentus* couple the switch from HBB completion to filament assembly? Our rationale for investigating whether or not the flagellins were interacting with a regulatory factor was based on the following logic. In all flagellar systems, HBB completion is sensed and overcome by the secretion of FlgM. In the absence of FlgM, and an incomplete model of FlbT/FlaF regulation, our hypothesis was that one or more of the flagellins of *C. crescentus* may be involved in the switch from HBB to filament assembly. Using a bacterial two-hybrid assay we have shown to our surprise, that FljJ is the only *C. crescentus* flagellin to play a previously unknown role through interactions with the flagellin post-transcriptional regulators, FlbT and FlaF. These interactions were confirmed biochemically and the data suggests that the FljJ:FlaF could interact in a stoichiometry 1:1. How exactly FljJ, FlbT and FlaF function together to achieve this goal is still unclear. Driks *et al*., 1989 suggested that the flagellins of *C. crescentus* are assembled in an ordered fashion, by demonstrating that at FljJ and FljL are proximal components of the filament in wild type (Driks *et al*., 1989). Our flagellin deletion data however, suggests that order of flagellins is not a strict requirement for assembly and that flagellin incorporation could be stochastic. An explanation that correlates with both sets of data is that the apparent ordered assembly is a result of the system coupling flagellin synthesis to filament assembly through the secretion of FljJ.

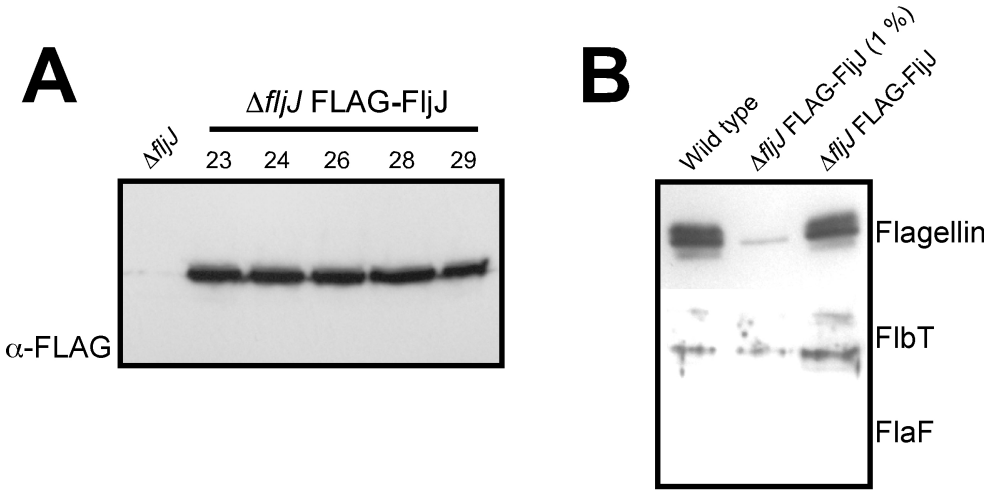

Figure 35: In-vivo co-immunoprecipitation using FLAG tagged *fljJ*

An N-terminal 3 x FLAG tag *fljJ* construct was made and placed on the chromosome of a Δ*fljJ* mutant under the control of the *fljJ* promoter. **A.** Immunoblot analysis of the screen for positive FLAG-FljJ recombinants using a commercial α-FLAG antibody. The numbers, 23, 24, 26, 28 and 29 refer to the clone number. **B.** The positive Δ*fljJ* FLAG-FljJ strain (24) was then used in a FLAG Co-IP experiment. Immunoblot analysis was carried out using α-Fla, α-FlbT, and α-FlaF antibodies. A 1 % control was performed in order to demonstrate the enrichment of protein within a sample.

Chapter 6. Mechanism of the Regulation of Filament Assembly

6.1 Introduction

Flagellar assembly in *C. crescentus* is regulated in response to two distinct checkpoints: rod completion and HBB completion. It has been previously demonstrated that not all six flagellin genes are translated until the second assembly checkpoint of HBB completion has been passed (Mangan *et al*., 1999). Therefore, the second assembly checkpoint functions to regulate flagellin expression at a post-transcriptional level. The flagellar protein FlbT has been identified as playing a critical role in the control of this assembly checkpoint. It has been shown to interact with the 5' untranslated region of the *fljK* transcript (Anderson and Gober, 2000). It is hypothesised that FlbT stabilises an RNA secondary structure that does not favour translation (Anderson and Gober, 2000). Importantly, a *fljK* RNA shift was observed in a *flbT* mutant which suggests that an additional unidentified protein may be required to allow FlbT to form a stable complex or conversely act as a positive factor in translation utilising some or all of the same 5' RNA binding site (Anderson and Gober, 2000). The mechanism of regulation has not been fully elucidated. Based on current understanding and experimental evidence, a model with respect to FljK expression has been put forward (Anderson and Gober, 2000). The post-transcriptional regulation of *fljK* mRNA is coordinated by the action of two proteins interacting with the RNA. Prior to HBB completion, when the developing flagellum structure is not ready for flagellin assembly, FlbT is bound to the RNA. When the hook structure is completed, negative repression is removed and the second protein binds to the RNA acting as a positive factor. It is currently not known how FlbT senses HBB completion or what the identity of the secondary positive factor is. Whether or not FlbT can interact with the mRNA of the other flagellins has to date, not been tested.

Downstream of *flbT* is located another flagellar gene, *flaF*. At HBB completion the inhibitory activity of FlbT is opposed by FlaF, which positively affects flagellin protein expression (Llewellyn *et al*., 2005). A Δ*flaF* mutant was shown to be non-motile and possessed only trace amounts of 25 kDa or 27 kDa flagellin. However, it did exhibit an increased rate of 29 kDa (FljJ) protein synthesis (Llewellyn *et al*., 2005; Schoenlein and Ely, 1989). It is important to note that the trace amounts of flagellin were detected using a different flagellar antibody to that of the α-Fla antibody we used in our experiments. Interestingly, a *flbT* deletion in the Δ*flaF* mutant restored protein expression but not motility (Llewellyn *et al*., 2005). Furthermore, electron microscopy

of Δ*flaF* cells showed an intact hook structure (Llewellyn *et al*., 2005). This would therefore suggest that FlaF is playing a role in filament assembly upstream of FlbT. Llewellyn *et al*., discarded the possibility that FlaF was acting as a T3S-chaperone based on protein stability experiments (Llewellyn *et al*., 2005). Instead they suggested that FlaF was required for flagellin translation and possibly for flagellin secretion. FlbT may also play a positive role in *fljK* transcription. In a *flbT* mutant, a *fljK*-lacZ transcriptional fusion exhibited approximately nine-fold lower activity when compared to wild type (Llewellyn *et al*., 2005). In comparison, it was demonstrated that *flaF* was not required for *fljK* transcription. It is hypothesised that, FlbT, when bound to the 5' *fljK* transcript functions as an antitermination factor thus promoting transcription while preventing translation (Llewellyn *et al*., 2005).

It is important to note that previous experiments in *C. crescentus* have demonstrated that not all the flagellins are regulated in the same manner. The rate of protein synthesis of the 29 kDa flagellin (FljJ) is increased in by flaF mutation and decreased in *flbT* mutant strains (Llewellyn *et al*., 2005; Schoenlein and Ely, 1989) which is in contrast to the regulation of *fljK* and *fljL*. Furthermore, there is evidence available to suggest that transcription of the FljJ and the β-flagellins is dependent on CtrA and not σ^{54} (Jones *et al*., 2001; Laub *et al*., 2002).

As we have identified FljJ:FlbT/FlaF interactions we asked the question; Does FljJ influence the regulatory activities of FlbT and FlaF via a protein-protein interaction? It is plausible that FlaF could be exerting its positive regulation by binding flagellin mRNA and thus acting as the additional unidentified positive factor. To our knowledge this has never been experimentally tested. It is important to note that Anderson and Gober could only demonstrate an interaction between FlbT and in vitro transcribed RNA in electro-mobility shift assays when using S30 cell extracted protein (Anderson and Gober, 2000). The addition of purified FlbT did not result in retardation of the RNA; therefore, it is plausible that one or both of the protein complexes are required for binding. We decided to investigate this possibility by testing the ability of FljJ, FlbT, FlaF and the protein-protein complexes to bind *fljK* transcript in vitro.

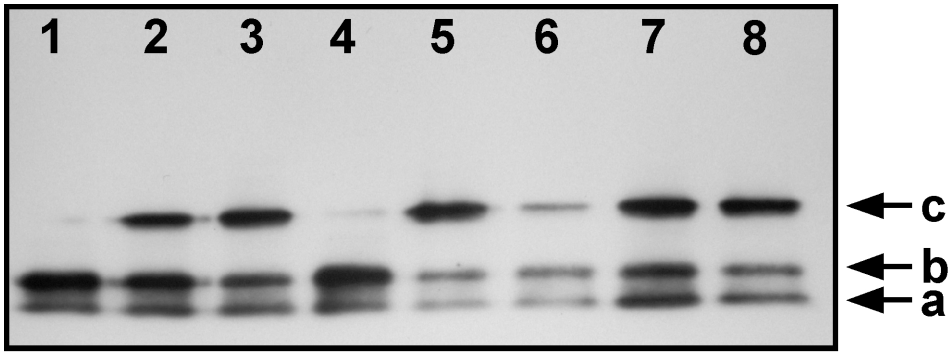

Figure 36: *fljK* transcript electromobility shift assay with FljJ, FlbT and FlaF

Native-PAGE analysis of the protein:RNA reactions. Detection of the RNA was carried out using Anti-Digoxigenin antibody. The concentration of *fljK* transcript in each reaction was 1 nM. **(1).** No protein **(2).** FljJ, 500 nM **(3).** FlbT, 500 nM **(4).** FlaF, 500 nM **(5).** FljJ:FlbT, 250 nM each **(6).** FljJ:FlaF, 250 nM each **(7).** FlbT:FlaF, 250 nM each **(8).** FljJ:FlbT:FlaF, 167 nM each. **(a)** and **(b)** points to free RNA. **(c)** points to shifted RNA (protein:RNA interaction).

6.2 RNA electro-mobility shift assays

6.2.1 *fljK transcript*

We constructed a wild type *fljK* transcript identical in sequence to that used by Anderson and Gober (Anderson and Gober, 2000). The transcript was synthesised from a DNA PCR template utilising T7 RNA polymerase and DIG-labeled UTP. The final transcript was a total of 115 nucleotides, which included 17 codons and 63 5' untranslated nucleotides (Figure 14). The RNA electromobility shift assays were carried out using Native-PAGE and RNA detection by Northern blot using Anti-Digoxigenin antibody. Preliminary experiments determined that excess of 700 nM protein in a reaction would cause precipitation (Data not shown). Therefore, in the following experiments 700 nM protein in each reaction was never exceeded. All protein-protein combinations were premixed prior to incubation with the RNA.

In all reactions, free RNA (no protein present) appeared as two bands that migrated very close to each other (Figure 36). Interestingly, when 500 nM FljJ and FlbT were incubated individually with the RNA, they produced a shifted band of similar size (Figure 36). This would suggest that both purified FljJ and FlbT can bind *fljK* transcript. However, no shift was observed in the presence of 500 nM FlaF. This data for FlbT is consistent with previous studies (Anderson and Gober, 2000). The addition of FljJ and FlbT mixed together, each at 250 nM final concentration, produced the same shifted band which suggests that a FljJ:FlbT:RNA complex had not formed under the experimental conditions used (Figure 36). Likewise, no additional shift was observed when a combination of FljJ and FlaF were added to the RNA (Figure 36). This suggests that no FjJ:FlaF:RNA complex had formed but also that FlaF had not inhibited FljJ from binding the RNA. A combination of FlbT and FlaF did not produce an additional shift, although this was not surprising considering that they did not form a protein-protein interaction in the bacterial two-hybrid experiment (see section 5.2). When all three proteins were mixed sequentially in the following order: FljJ, FlaF, FlbT; the only shifted band was that can be attributed to either FljJ:RNA or FlbT:RNA complexes, which is consistent with the other reactions (Figure 36). The observed FlbT:RNA complex using purified protein is in contrast to previous work that demonstrated FlbT binding using only S30 extract (Anderson and Gober, 2000). An explanation for this could be differences in the methodology of FlbT purification. Our method utilised a N-terminal 6-histidine tag, while in comparison, a C-terminal 6-histidine tag was previously utilised by others (Anderson and Gober, 2000).

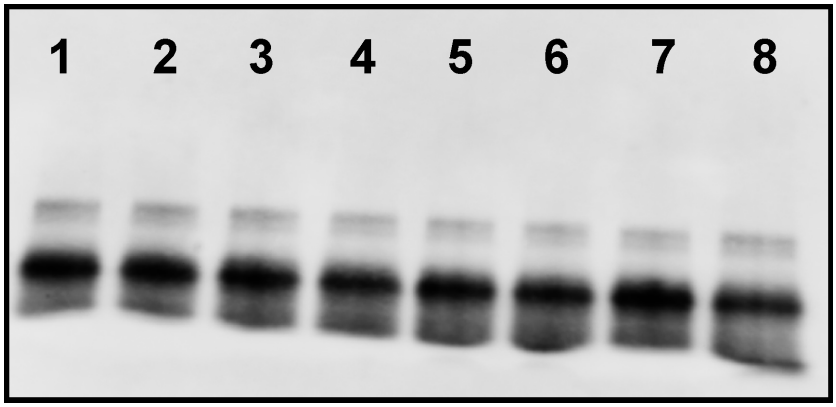

Figure 37: *fliF* transcript electromobility shift assay with FljJ, FlbT and FlaF

The concentration of *fliF* transcript in each reaction was 1 nM. **(1).** No protein **(2).** FljJ, 500 nM **(3).** FlbT, 500 nM **(4).** FlaF, 500 nM **(5).** FljJ:FlbT, 250 nM each **(6).** FljJ:FlaF, 250 nM each **(7).** FlbT:FlaF, 250 nM each **(8).** FljJ:FlbT:FlaF, 167 nM each.

6.2.2 *fliF transcript*

In order to demonstrate that the shifts were authentic, we synthesised a non-specific transcript; using a 115 nucleotide sequence from the *fliF* coding sequence (*fliF* encodes the MS-ring protein of the flagellar basal body). If the *fljK* transcript binding by FljJ and FlbT was specific then the same shift should not be produced with *fliF* transcript. Addition of all three proteins and protein-protein combinations there of, to the fliF transcript did not produce any additional bands to that of the free RNA (Figure 37). This data confirms that the binding of *fljK* transcript by FljJ and FlbT is authentic.

6.2.3 *fljK transcript concentration curve*

We next tested whether or not the interactions were RNA concentration dependent. 500 nM FljJ was added to an *fljK* RNA concentration curve of the following concentrations; 20, 10, 5, 2, 1, 0.5 nM. The same shifted band was produced in every reaction apart from free RNA (Figure 38). Importantly, for the first 3 reactions where the RNA concentration differed over a range of 4 fold, there appeared to be the same amount of RNA shifted in each reaction (Figure 38). This would suggest that in each of these reactions, the same amount of RNA is bound by FljJ. This demonstrates that if the protein is always in the presence of excess RNA the binding is dependent on protein concentration and not the amount of RNA.

6.2.4 *Quantification of protein:RNA interactions*

We next decided to examine the relationship between the observed protein-protein interactions and the protein:RNA interactions by introducing varying concentrations of protein. We hoped that this would give us quantifiable data thus allowing us to calculate binding constants between the protein:RNA interactions. A FlbT concentration dependent effect could be observed on a fixed amount of RNA, demonstrating that FlbT is binding *fljK* transcript (Figure 39A). A similar effect could be observed for FljJ, although it appears that FlbT binding of the RNA is stronger (Figure 39A). No concentrations of FlaF resulted in an RNA shift, which is consistent with our previous results (Figure 39B).

We feel that the quality of the blots is not of a standard for accurate quantification this is after numerous attempts at this experiment. The outside edges of the blots appear to have not transferred correctly. One possible alternative experiment to investigate the interactions would involve the use of Surface Plasmon Resonance, which

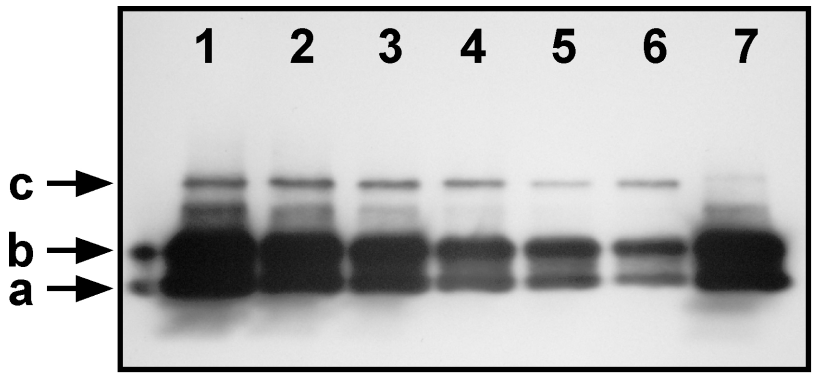

Figure 38: *fljK* transcript electromobility shift assay with FljJ

A fixed amount of FljJ (500 nM) was added to increasing concentrations of *fljK* transcript. **(1).** 20 nM **(2).** 10 nM **(3).** 5 nM **(4).** 2 nM **(5).** 1 nM **(6).** 0.5 nM **(7).** 20 nM, no FljJ. **(a)** and **(b)** points to free RNA. **(c)** points to shifted RNA (FljJ:RNA interaction).

would give more quantitative data. However, due to the time constraints of this project this could not be realised. We decided to keep a constant concentration of one protein while increasing the concentration of the other. This would allow us to investigate the potential influence of protein-protein competition with the protein:RNA complex. For example; FljJ at a constant concentration of 100 nM was tested against a concentration curve of FlaF at the following concentrations, 0, 50, 100, 250 and 500 nM. This allowed us to investigate the influence of defined molar ratios such as 2:1 and 1:5 of those interacting protein partners on the protein:RNA complex.

The addition of increasing concentrations of FlaF did not inhibit the ability of FljJ to bind the RNA (Figure 39C). Likewise, the addition of molar excess FljJ did not appear to increase or decrease the ability of FlbT to bind the RNA (Figure 39C). It is plausible that in each of the reactions, FljJ is binding the RNA, however, it is difficult to quantitate the exact amount of RNA in the shifted band. Furthermore, it is clear that FlbT binds the RNA more strongly than FljJ. When increasing concentrations of FlbT were mixed with constant FljJ; the effect of FlbT binding could still be observed due to excess RNA in the reactions (Figure 39B). When increasing concentrations of FljJ were mixed with constant FlaF; a FljJ concentration effect was observed (Figure 39D). This is consistent with our previous data in suggesting that FlaF does not inhibit the ability of FljJ to bind the RNA. Increasing concentrations of FlaF did not prevent FlbT binding the RNA (Figure 39D), which is not surprising considering we did not observe a FlaF:FlbT protein interaction in the bacterial two-hybrid assay (see section 5.2). Furthermore, when increasing concentrations of FlbT were mixed with constant FlaF; a FlbT concentration effect was observed (Figure 39E).

It is possible that in vivo, there exists interplay between all three proteins and RNA. Therefore, we decided to test the binding of *fljK* transcript in vitro by mixing all four components together (FljJ, FlbT, FlaF and *fljK* RNA). Firstly, we mixed with a fixed amount of RNA: constant FljJ, increasing concentrations of FlbT and decreasing concentrations of FlaF i.e. when the concentration of FlbT was 50 nM, the concentration of FlaF was 500 nM and when the concentration of FlbT was 100 nM, the concentration of FlaF was 250 nM (Figure 39E). FlaF did not affect the ability of FljJ and FlbT to bind the RNA, which is consistent with our previous results. Secondly, we mixed with a fixed amount of RNA: constant FlbT with increasing concentrations of FljJ and decreasing concentrations of FlaF (Figure 39F). Once again, FlaF did not affect the ability of FlbT to bind the RNA, although it was difficult to determine whether FljJ was binding, as no concentration dependent effect could be clearly seen. This is

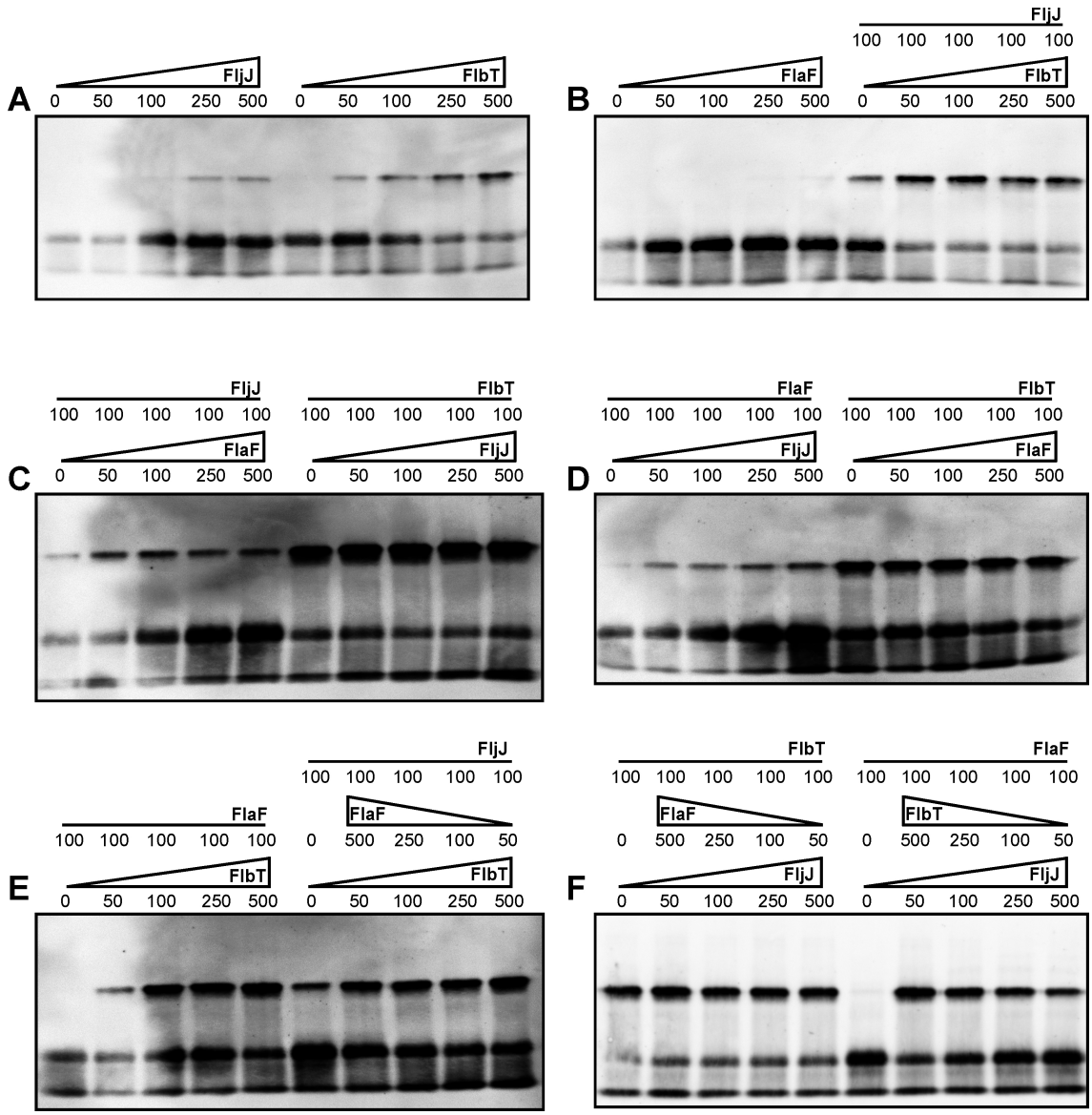

Figure 39: The dynamics of increasing protein concentrations and protein:RNA interactions

The concentration of *fljK* transcript in each reaction was 1 nM. The concentration (nM) and species of protein in each reaction is indicated above the gel.

consistent with FlbT binding the RNA more strongly than FljJ. Finally, we mixed with a fixed amount of RNA: constant FlaF with increasing concentrations of FljJ and decreasing concentrations of FlbT (Figure 39F). FlaF did not bind the RNA and a FlbT concentration effect was observed.

6.2.5 *Antibody supershift of fljK transcript*

Although we were confident that the FljJ:*fljK* and FlbT:*fljK* interactions were real; we attempted to observe a supershift of the *fljK* transcript utilising α-Fla and α-FlbT antibodies. In theory, the addition of protein antibody to the protein:RNA reaction should result in retardation of the complex thus confirming the specificity of the interaction. When α-Fla was added to a FljJ/*fljK* reaction, a supershift was observed, confirming that FljJ is bound to the RNA (Figure 40). Unfortunately, when α-FlbT was added to the FlbT/*fljK* reaction the RNA was degraded (data not shown). It is plausible that something contained within the α-FlbT plasma has RNase activity and is destroying the transcript. Importantly, this data is consistent with our previous data in demonstrating a FljJ:*fljK* interaction.

6.3 Deletion and Characterisation of *flbT* and *flaF*

We wanted to construct Δ*flbT* and Δ*flaF* mutants so that we could investigate the effect of those mutations on filament assembly in light of our protein-protein interaction data. It has been previously shown that *flbT* and *flaF* are transcribed from the same promoter, upstream of the *flbT* start codon (Llewellyn *et al*., 2005). Successful complementation of a Δ*flaF* mutant was achieved by providing a construct in trans containing both genes and the promoter region (Llewellyn *et al*., 2005). We created the same plasmid, pBX-*flbT_flaF*; containing the entire *flbT* and *flaF* coding sequences and 199 nucleotides upstream of the *flbT* start codon. In-frame deletions of the two genes were created by allelic exchange utilising the same method as the one used to create flagellin deletions.
The Δ*flaF* mutant was non-motile which is consistent with previous studies (Figure 41) (Llewellyn *et al*., 2005). Surprisingly, the Δ*flbT* mutant was also non-motile, which is in contrast to previous studies that showed a *flbT* null mutation to be weakly motile (Figure 41) (Anderson and Gober, 2000). Motility was restored in both the Δ*flaF* and the Δ*flbT* mutants upon complementation with the pBX-*flbT_flaF* plasmid (Figure 41).

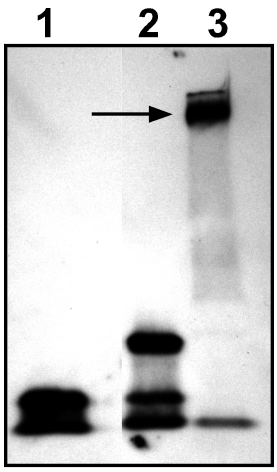

Figure 40: A FljJ:*fljK* supershift

The α-Fla antibody was added to the FljJ:*fljK* interaction in order to demonstrate that FljJ was bound to the RNA. The concentration of *fljK* transcript in each reaction was 1 nM. **(1).** no protein **(2).** 500 nM FljJ **(3).** 500 nM FljJ and α-Fla (3 μl).

As DNA sequencing confirmed both strains to be correct we decided to examine FlbT, FlaF and flagellin protein levels in both mutants by immunoblot.

6.3.1 *Immunoblot analysis of the ΔflaF and ΔflbT mutants*

FlbT and FlaF were detected in both wild type and the Δ*fljJKLMNO* mutant (Figure 42). FlbT was not detected in the non-motile Δ*flbT* mutant, and FlaF was not detected in the non-motile Δ*flaF* mutant. However, when both mutants were complemented with the pBX-*flbT_flaF* plasmid, protein levels were restored to higher than that of wild type, correlating with the observed motility phenotype (Figure 42). The amount of FlbT in the Δ*flaF* mutant was comparable to that of wild type suggesting that the absence of FlaF does not effect *flbT* expression. Also there was no detectable flagellin, which is consistent with the non-motile phenotype and previous studies (Llewellyn *et al*., 2005). Flagellin was restored to a wild type level in the complemented Δ*flaF* pBX-*flbT_flaF* strain, which correlates with the observed motile phenotype (Figure 42). Importantly, and consistent with previous experiments this demonstrates that FlaF does not effect flagellin gene transcription or mRNA stability (Llewellyn *et al*., 2005); there were higher levels of FlaF in the Δ*flaF* pBX-*flbT_flaF* strain when compared to wild type, although this did not result in higher levels of flagellin. It appeared that there were no detectable levels of FlaF in the Δ*flbT* mutant suggesting that the mutant is incorrect. Although DNA sequencing showed that the *flaF* coding and promoter sequence was correct, it is possible that as expression of the two genes is coupled, the deletion of *flbT* has somehow adversely affected the expression of FlaF. The Δ*flbT* mutant had flagellin levels comparable to wild type but also had high levels of a smaller molecular weight degradation product, which is consistent with the absence of FlaF in a double Δ*flbT* Δ*flaF* mutant (Llewellyn *et al*., 2005). On complementation with the pBX-*flbT_flaF* plasmid, the degradation product disappeared (Figure 42).

6.4 Flagellin Overexpression in a Δ*flaF* Mutant

Our data and previous studies have demonstrated that a Δ*flaF* mutant is non-motile (Llewellyn *et al*., 2005). The mutant appears to only generate trace amounts FljK, FljL or β-flagellin protein (Schoenlein and Ely, 1989). The fact that FljJ synthesis is increased in a Δ*flaF* mutant but the cells remain non-motile is consistent with both our flagellin gene deletion and flagellin over-expression data in that FljJ alone cannot

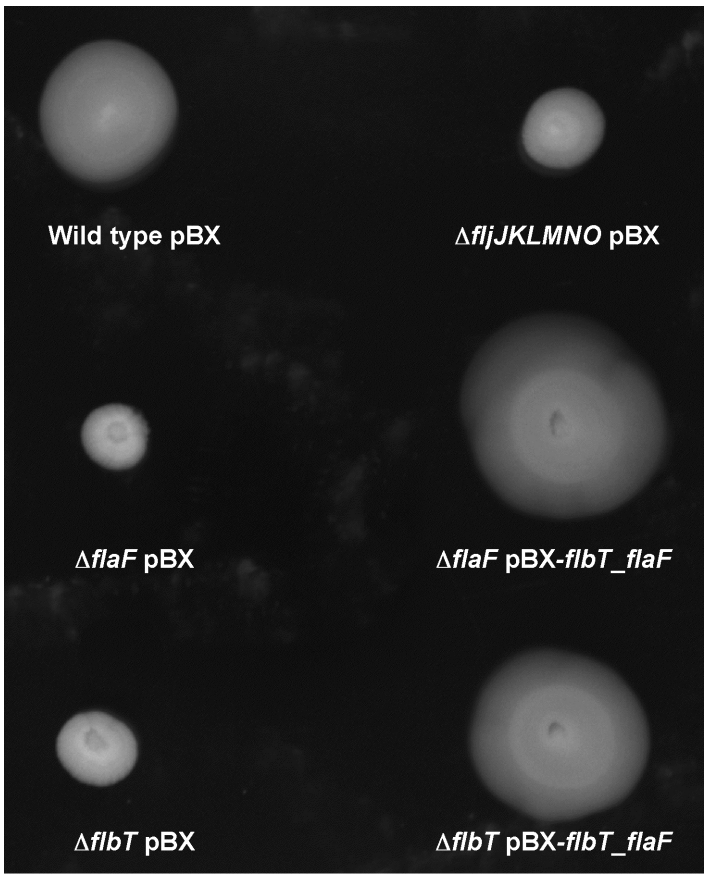

Figure 41: Complementation of a Δ*flaF* and Δ*flbT* mutant

The pBX-*flbT_flaF* plasmid containing the promoter region and full ORF's was utilised to complement a Δ*flaF* and Δ*flbT* mutant. The motility agar assay was inoculated on a single plate and imaged after 5 days growth at 30 ºC. The agar contained kanamycin to select for the plasmid, but no xylose was added. *flbT* and *flaF* expression occurred from the native promoter.

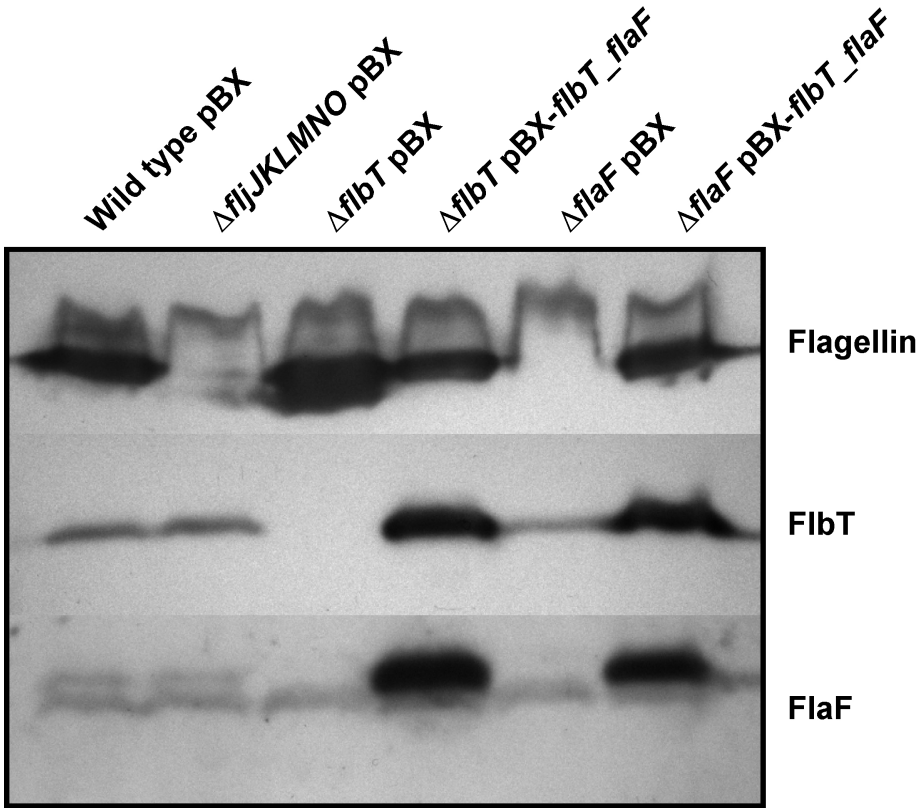

Figure 42: Immunoblot analysis of wild type, Δ*flbT* and Δ*flaF* mutant strains

Comparison of flagellin, FlbT and FlaF protein levels in *C. crescentus* strains. Using the α-flagellin, α-FlbT and α-FlaF antibodies.

support motility. It has been predicted that FlaF is somehow regulating flagellin translation either directly or indirectly or is involved in flagellin secretion (Llewellyn *et al*., 2005). The post-transcriptional regulation of FlbT on *fljK* occurs through a protein-binding site in the 5' UTR. However, our data suggests that FlaF does not bind the RNA to affect its positive activity on translation. We also now know that FlaF is interacting with a T3S substrate, FljJ, which is itself binding the *fljK* transcript. Importantly, a FljJ:FlaF:*fljK* interaction was not indentified suggesting that FlaF is not directly or indirectly affecting translation through the 5'UTR. Therefore, we decided to see what would happen if we remove flagellar assembly dependent regulation of flagellin and overexpress flagellin in a Δ*flaF* mutant using our pBX constructs. pBX-*fljJ -fljK -fljL -fljM -fljN -fljO* were conjugated into the Δ*flaF* mutant, induced with xylose and tested for motility.

Flagellar-independent overexpression of all 6 flagellins individually in the Δ*flaF* mutant did not restore motility (Figure 43A). Furthermore, no swimming cells were observed in the strains using microscopy. This is consistent with the previous observations that FlaF is required for motility (Llewellyn *et al*., 2005; Schoenlein and Ely, 1989). We then decided to analyse flagellin overexpression in the Δ*flaF* mutant by immunoblot in order to determine whether the observed non-motile phenotypes were as a result of low protein levels due to the absence of FlaF. Surprisingly, wild type levels of flagellin were observed in the Δ*flaF* pBX-*fljK -fljL -fljM -fljN* and -*flj*O strains and low levels of FljJ in the Δ*flaF* pBX-*fljJ* (Figure 43B). However, importantly all these strains were non-motile suggesting that FlaF is responsible for the secretion of all six flagellins. This is consistent with previous observations that cells of a non-motile double Δ*flbT* /Δ*flaF* mutant produce flagellin protein but do not assemble filaments (Llewellyn *et al*., 2005). FlbT does not regulate our flagellin expression constructs as they lack a 5' UTR.

6.5 Summary

Consistent with previous experiments that identified FlbT as a post-transcriptional regulator of *fljK* mRNA; we have demonstrated that FlbT can bind to the 5' leader sequence of *fljK* transcript. We have also tested our hypothesis that FljJ:FlbT, and/or FljJ:FlaF could be involved in the regulation of filament assembly by interacting with flagellin mRNA. Our results show that no protein-protein:RNA complexes were formed under the experimental conditions used. We base this conclusion on the fact that no

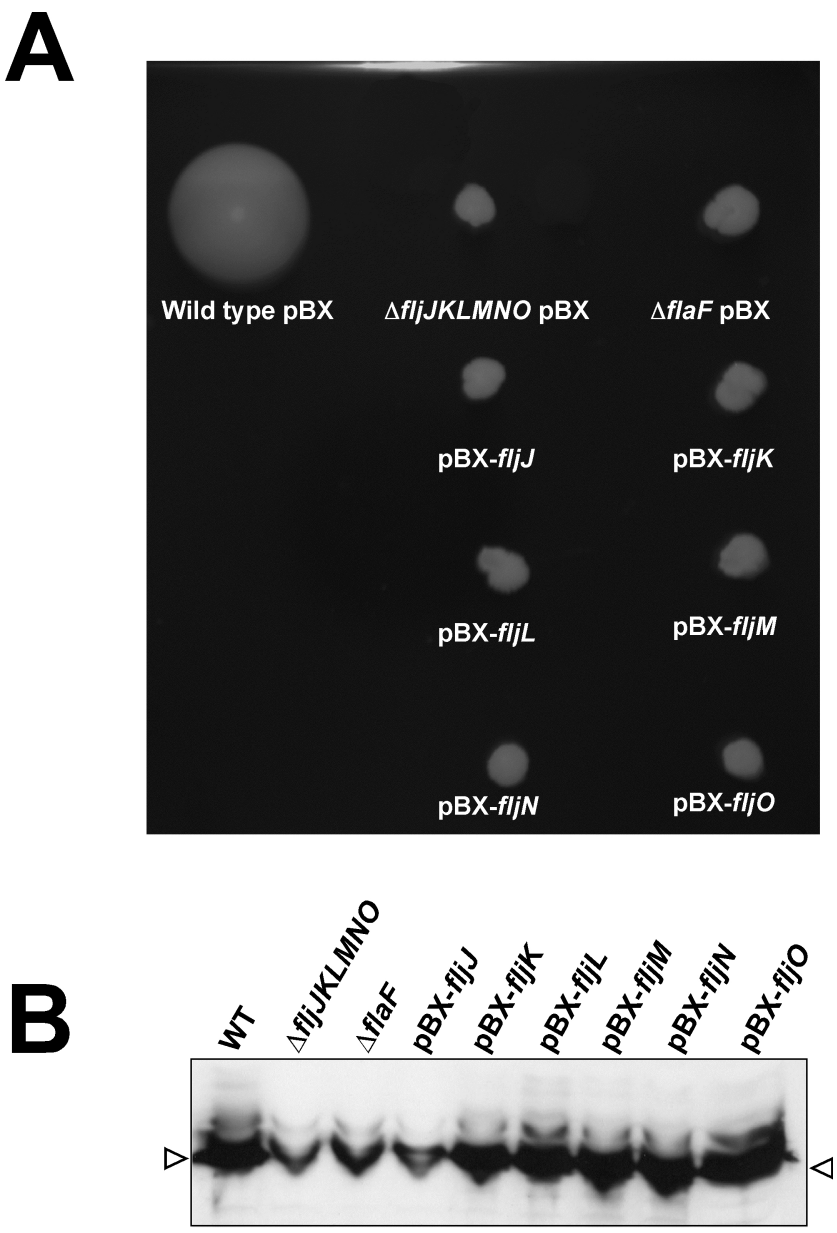

Figure 43: Flagellin overexpression in a Δ*flaF* mutant

The motility agar assays were innoculated on a single plate and imaged after 5 days growth at 30 ºC. The agar contained kanamycin and xylose to induce plasmid expression of flagellin. **A.** Motility swarms of Δ*flaF* pBX- *fljJ*, *fljK*, *fljL*, *fljM*, *fljN*, *fljO*, Δ*fljJKLMNO* pBX vector control, and wild type. **B.** Immunoblot analysis of flagellin levels in the strains used in the motility assays (α-Fla antibody). Flagellin indicated by white arrows.

unique *fljK* mRNA shifts were identified when compared to FljJ:*fljK* and FlbT:*fljK* alone. However, to our great surprise, we identified a previously unknown interaction between FljJ and the *fljK* transcript; although the affinity of FljJ for the RNA appears to be weaker than that of FlbT. Our original hypothesis was based on testing FlaF:*fljK* binding in order to establish whether or not FlaF was exerting its positive regulation through a physical interaction with the RNA transcript. We included FljJ as a control and therefore did not expect to observe a FljJ:*fljK* interaction. Anderson and Gober hypothesised that both FlbT and an unidentified secondary factor utilised the same binding site on the *fljK* transcript (Anderson and Gober, 2000). Our experimental data supports this hypothesis; when the RNA was incubated with both FljJ and FlbT, no extra shift could be observed; suggesting that only one species of protein was bound to a molecule of RNA.

FlbT and FljJ individually produced an identical shift, which was surprising due to FljJ possessing a greater molecular weight than FlbT (29 kDa and 15 kDa respectively). One plausible explanation for this discrepancy can be found in our biochemical data for both proteins: FljJ and a FlbT dimer both eluted with the exact same retention time during gel filtration. The data therefore suggests that it is a FlbT dimer and not a monomer that binds the *fljK* transcript. We will discuss the implications of FljJ binding *fljK* mRNA in the general discussion.

Due to the labeling technique of using DIG-UTP it is plausible that Digoxigenin molecules could potentially be influencing protein interaction. Given more time, it would have been satisfying to repeat these experiments using 5' end labeling of the RNA, in order to discard the possibility of an indirect effect on protein binding.

The positive regulation of flagellin translation by FlaF does not appear to be achieved through the binding of RNA; at least not *fljK* transcript. Flagellar-independent expression of flagellin in a Δ*flaF* mutant resulted in flagellin protein being produced but as the mutant remained non-motile it appears that the protein was not being secreted. This suggests that FlaF is acting as a general flagellin T3S chaperone. It is therefore surprising that in our bacterial two-hybrid experiments we observed only a protein:protein interaction between FlaF and FljJ. One plausible explanation for the two contrasting data sets is that FljK, FljL and FljM are not folding correctly when expressed in the BACTH system. This is consistent with the theoretical pI values for each *C. crescentus* flagellin protein and FlbT and FlaF (Table 6). FljJ is the only flagellin that has a low pI of 4.68, which is similar to FlaF. The other flagellins all have pI values of greater than 7.5. We did not test *fljN* and *fljO* in the BACTH system due to

high sequence similarity between the β-flagellins. However, based on their pI values and the likelihood that they would not fold correctly in the BACTH system, a negative result when tested against FlaF would not be surprising. Importantly though, this also suggests the possibility that all six flagellins could interact with FlbT: the only positive flagellin interaction observed with FlbT in the BACTH system was with FljJ.

Chapter 7. Regulation of Filament Assembly in the α-Proteobacteria

7.1 Introduction

We have identified two independent and novel protein-protein interactions in *C. crescentus*. The flagellin FljJ can bind FlbT and FlaF, both key post-transcriptional regulators involved in the regulation of flagellar filament assembly, suggesting it could be playing a regulatory feedback role within the flagellar system. We have also shown that FlaF appears to essential for the secretion of all six flagellins in *C. crescentus*. Bioinformatical analysis shows that homologues of *flbT* and *flaF* are conserved throughout the flagellated α-proteobacteria (Llewellyn *et al*., 2005). Thus far, the most extensively studied flagellar system of that group is that of *C. crescentus*. However, a recent study carried out in *Brucella melintensis* identified FlbT as a positive regulator of flagellin translation and FlaF was shown to play a negative regulatory role (Ferooz *et al*., 2011). This is in contrast to *C. crescentus*, suggesting that although the presence of *flbT* and *flaF* is conserved throughout the α-proteobacteria, their regulatory activities may not be. Interestingly, the absence of *flbT* in *B. melintensis* could be overcome by complementation with *flbT* from *Sinorhizobium meliloti* but not with *flbT* from *C. crescentus* (Ferooz *et al*., 2011). Both *B. melintensis* and *S. meliloti* are members of the α-proteobacterial order Rhizobiales where as *C. crescentus* is a member of the order Caulobacterales. This suggests that the function of the FlbT may be similar in only closely related species. Therefore, in light of our protein-protein interaction data we asked the question: Is one or more of the flagellins playing a regulatory subunit feedback role by binding FlbT and FlaF in other α-proteobacterial flagellar systems?

We chose to investigate this in two closely related bacteria; *Sinorhizobium meliloti* 1021 and *Agrobacterium tumefaciens* C58. *S. meliloti* is a soil-borne bacterium that participates in a symbiotic relationship with its legume host (Jones *et al*., 2007). *A. tumefaciens* is a soil-borne bacterium that causes tumor formation in a broad range of plant hosts (Pitzschke and Hirt, 2010). The genomes of both organisms contain *flbT*, *flaF* and four flagellin genes (Capela *et al*., 2001, Goodner *et al*., 2001). As previously mentioned, all multiple flagellin systems that have been experimentally tested possess flagellins that differ by only 2-5 kDa in size. *S. meliloti* and *A. tumefaciens* both have one flagellin that is theoretically greater than 5 kDa different in size from the other three flagellins. However, experimental studies have determined that the molecular weights of the four flagellins in each system are actually much more uniform in size (Deakin *et*

al., 1999; Scharf *et al*., 2001). The flagellin genes *flaA*, *flaB*, *flaC*, *flaD* of *S. meliloti* are all located close together on the genome and are transcribed from individual σ^{28}-dependent promoters (Scharf *et al*., 2001). The three flagellin genes *fla*, *flaB* and *flaA* of *A. tumefaciens* are clustered together while *flaD* is located on a unlinked locus (Deakin *et al*., 1999). FlaA is considered to be the major flagellin utilised during filament assembly by both species (Deakin *et al*., 1999; Scharf *et al*., 2001). In both of these flagellar systems the functions of FlbT and FlaF have not been investigated.

Therefore, we decided to utilise the bacterial two-hybrid system to screen for protein-protein interactions between flagellins, FlbT and FlaF in S. meliloti and A. tumefaciens.

7.2 Bacterial Two-Hybrid Analysis

To be consistent with the *C. crescentus* experiment we created N-terminal fusions of all candidate proteins in order to leave the C-termini free. The plasmids pUT18C and pKT25 both allow in-frame fusions to the C-termini of the T18 and T25 fragments. *C. crescentus* proteins were used as internal controls alongside the controls of the system (Euromedex). Full length open reading frame constructs of *flbT*, *flaF*, *fla*, *flaA*, *flaB*, *flaD* (*Agrobacterium tumefaciens* C58) and *flbT*, *flaF*, *flaA*, *flaB*, *flaC*, *flaD* (*Sinorhizobium meliloti* 1021) were created and tested for intra species interactions along with internal and *C. crescentus* controls. The interactions (transformations) were plated out individually on selective media and phenotype scored after 48 hrs.

Both the internal positive and negative controls behaved as expected (Figure 44). The *C. crescentus* controls were consistent with the previous experiment (See section 5.2). When FlbT was tested for a self:self interaction the result was negative (Figure 44). This is in contrast to *C. crescentus* FlbT, which produced a positive interaction. Furthermore, FlbT did not interact with any of the *A. tumefaciens* flagellin proteins. Once again this is in contrast to *C. crescentus* FlbT which interacted with the flagellin FljJ. Strikingly however, FlaF produced a positive interaction with all four flagellin proteins; Fla, FlaA, FlaB and FlaD (Figure 44). In comparison, *C. crescentus* FlaF interacted with only the flagellin FljJ. No flagellin:flagellin or FlaF:FlaF interaction was observed, which is consistent with *C. crescentus*. Consistent with *A. tumefaciens*, FlaF from *S. meliloti* interacted with all four of its flagellins, and no FlbT interaction was observed (Figure 44).

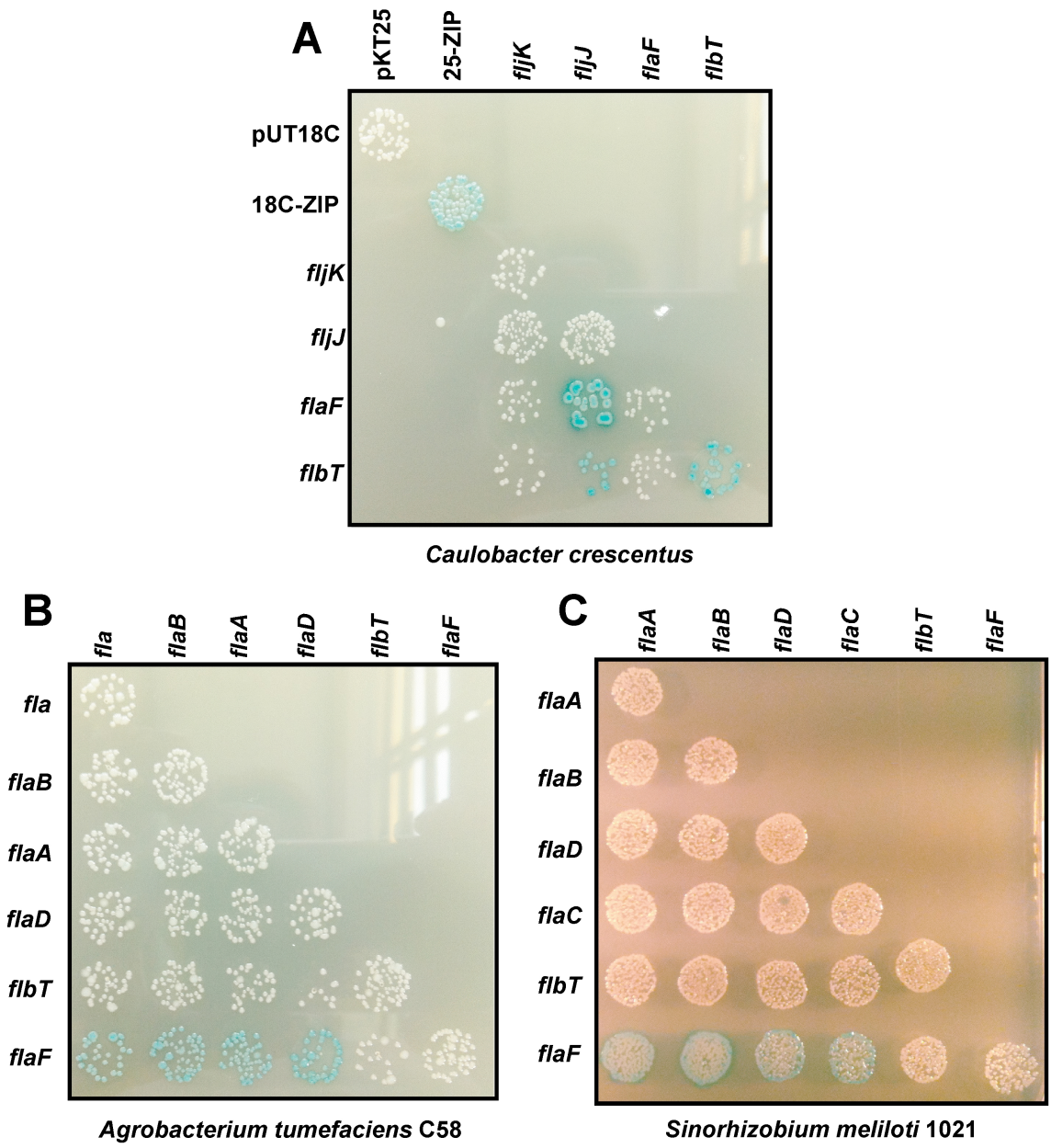

Figure 44: Bacterial two-hybrid analysis of Flagellin, FlbT and FlaF interactions

A. A summary of the *C. crescentus* interactions that were tested in Chapter 5. FljJ interacted with both FlbT and FlaF. **B.** Flagellin and FlbT/FlaF interactions in *A. tumefaciens*. **C.** Flagellin and FlbT/FlaF interactions in the *S. meliloti*. FlaF interacts with all four flagellins in both flagellar systems.

7.3 Summary

Using a bacterial two-hybrid assay we have shown that in two closely related species belonging to the α-proteobacteria, the flagellar protein FlaF binds to all flagellin proteins in the system. This is in contrast to *C. crescentus* where FlaF interacts with only one flagellin, FljJ. Importantly however, when comparing the theoretical pI values of the flagellins from *A. tumefaciens* and *S. meliloti* they are all low, similar to that of FljJ in *C. crescentus* (Table 7) (see section 5.3.2 Table 6). Therefore, the results from the bacterial two-hybrid analysis in *C. crescentus*, with respect to flagellin and FlaF interaction, appear to be mis-leading. It is more than likely that the other five flagellins of *C. crescentus* can interact with FlaF, but not, however, under the experimental conditions that were used. Based on this data and the observations that flagellin overexpression does not restore motility in a *C. crescentus* Δ*flaF* mutant, we propose the following: FlaF is playing a general regulatory role in being responsible for the secretion of flagellin in the three species of bacteria tested, and possibly throughout all the α-proteobacteria. In both *A. tumefaciens* and *S. meliloti*, no FlbT interaction was observed. It would appear that the role of FlbT in *C. crescentus* is unique among the three bacterial species investigated.

Protein	Theoretical MW kDa	Theoretical pI
Fla (Atu0542)	32864.0	4.77
FlaB (Atu0543)	32986.9	4.73
FlaA (Atu0545)	31656.4	4.75
FlaD (Atu0567)	45135.3	4.59
FlbT (Atu0578)	17058.9	8.76
FlaF (Atu0577)	13361.3	6.59
FlaA (SMc03037)	40718.0	4.19
FlaB (SMc03038)	40742.3	4.18
FlaD (SMc03039)	42040.9	4.19
FlaC (SMc03040)	33829.8	4.52
FlbT (SMc03051)	16976.8	6.74
FlaF (SMc03050)	13464.4	5.30

Table 7: Theoretical isoelectric point (pI) of *Sinorhizobium meliloti* and *Agrobacterium tumefaciens* flagellar proteins

Amino acid sequences were taken from the NCBI database and analysed using the ProtParam software tool. Atu: *Agrobacterium tumefaciens*. SMc: *Sinorhizobium meliloti*.

Chapter 8. General Discussion

8.1 Discussion

The bacterial flagellum is a complex macromolecular organelle comprised and assembled from many structural subunits together with an array of additional regulatory factors. Flagellin is the major flagellar structural protein that polymerises together to form the flagellar filament. Essential for the functionality of the flagellum, the flagellins are also a major recognition target for host defense systems or predators alike. Interestingly, approximately 45 % of annotated flagellar systems possess more than one flagellin gene; ranging between two and 15 flagellin genes per genome (Faulds-Pain *et al*., 2011). However, our current understanding of flagellar structure and assembly, combined with our knowledge of the environments inhabited by bacteria encoding multiple flagellins does not satisfactorily explain why their utilisation is an advantage. Bacterial flagellar systems couple flagellar gene expression and flagellar assembly using a regulatory network of multiple components. The assembly process is coordinated in response to a transcriptional temporal hierarchy. The α-proteobacteria are a unique group of gram-negative bacteria in that many have σ^{28}-indepenent flagellar systems. One member of this group, *Caulobacter crescentus*, utilises six flagellins during filament assembly.

In this project we have asked the question; how does *C. crescentus* manage the incorporation of six flagellins into the flagellar filament? Using flagellin gene deletion mutants we have demonstrated that the system exhibits extensive structural redundancy; to the point that one flagellin is enough to form a functional flagellum and sustain motility. However, when FljJ is alone, a filament is not made. We have shown that flagellin protein levels and filament length correlate and it is likely that in the short window of opportunity available to make a functional flagellum, this is crucial for the production of a filament of optimal length for optimal swimming speeds. We argue that FljJ is unique among the six flagellins in that it plays both a structural and regulatory role. We base this hypothesis on the experimental evidence that FljJ is the only flagellin to interact with two key post-transcriptional regulators of flagellin synthesis; FlbT and FlaF. Furthermore, our data in Chapter 4 demonstrates that in a comprehensive flagellin gene deletion mutant collection, every remaining flagellin is utilised in filament assembly. This suggests that the system has the ability to undertake stochastic incorporation of flagellin species into the growing filament. However, this is in stark

contrast to previous observations of ordered assembly, with FljJ and FljL the proximal components of a wild type filament (Driks *et al*., 1989). This strongly suggests that when order is observed it is a reflection of a regulatory input during or prior to secretion. Based on the evidence it is plausible that the system is coupling flagellin synthesis to filament assembly through the secretion of FljJ.

In Chapter 5 we tested the ability of a FljJ:FlbT complex to bind fljK mRNA, as it has been previously demonstrated that FlbT binds to the 5' leader sequence of fljK mRNA. No FljJ:FlbT:RNA complex could be isolated. However, to our surprise we identified that FlbT and FljJ can bind *fljK* mRNA individually. It would be interesting to see whether or not FljJ and FlbT can bind the mRNA of the other flagellins. It is currently not known whether FlbT regulates the expression of other flagellin mRNA in the same manner as it does with *fljK*. Three adenine bases upstream of the *fljK* ribosomal binding site have been shown to be essential for FlbT binding (Figure 45) (Anderson and Gober, 2000). It is predicted that these residues form a binding site for FlbT, which upon binding stabilises a RNA secondary structure conformation that prevents translation (Anderson and Gober, 2000). A DNA sequence alignment of all six flagellin genes highlights the conservation of the three adenine bases and surrounding sequence in the flagellins apart from *fljJ* and possibly *fljL* (Figure 45). This suggests that FlbT and plausibly FljJ could bind to the other flagellin mRNA transcripts. Importantly, both a *fljJ* mutant and a *flbT* mutant are motile. This indicates that neither gene is essential for flagellar assembly and motility. A *flbT* null mutant (*flbT*650) is however, severely impaired in motility and chemotaxis. The *flbT* mutant also exhibits a number of differing morphological defects, including: the generation of filamentous cells, abnormal or absent stalks, and the failure to eject the flagellum (Driks *et al*., 1990). In contrast, a Δ*fljJ* mutant shows only a small reduction in motility. It is plausible that the regulation of flagellin synthesis and filament assembly by FlbT and FljJ is in place to increase the efficiency of those mechanisms. This is consistent with the observation that flagellar independent overexpression of flagellin, in the absence of a 5' untranslated region, results in a 40 % reduction in swimming speed compared to wild type. It would be interesting to see if the swimming speed could be increased by flagellar independent expression of a plasmid construct possessing the 5' untranslated region. The biological function of the FljJ:FlbT interaction is still yet to be determined. It is tempting to say that somehow the complex is sensing HBB completion through the secretion of FljJ. The filaments of a *flbT* mutant do not possess FljJ, even though the protein is present inside the cell at wild type levels (Driks *et al*., 1990). This would

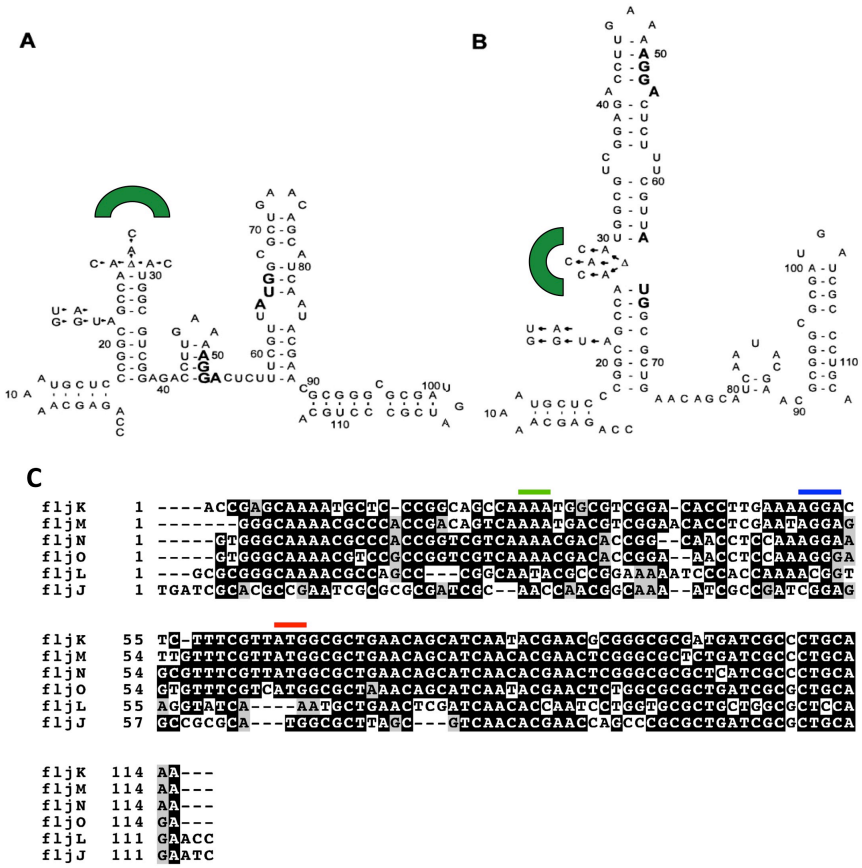

Figure 45: Regulatory features of *C. crescentus* flagellin mRNA

At the top are two predicted structures for the *fljK* transcript used in our in vitro assays (figure taken from Anderson and Gober, 2000). Each structure shows 63 nucleotides of untranslated sequence and the first 17 codons. Shown in both are the positions of site-directed mutagenesis carried out in the study (Anderson and Gober, 2000). Mutations that prevent FlbT binding are highlighted in green. **(A)** The structure is predicted to support translation due to little basepairing near the ribosome binding site (AGGA in bold). **(B)** In contrast, translation of this structure is predicted to be inefficient due to the secondary structures created around the ribosome binding site and the start codon (AUG in bold). **(C)** A DNA alignment of the *fljK* transcript region for all six flagellin genes. The nucleotides marked with a green line correspond to those marked green in (A) and (B). The ribosome-binding site is marked with a blue line. The start codon is marked with a red line. The multiple alignment was assembled using ClustalW and the similarity shading was performed using BoxShade.

suggest that the relationship between the two proteins is important and that possibly a physical protein:protein interaction is biologically relevant, however, this will require further investigation.

As *C. crescentus* FlaF is needed for the translation of 5 out of the six flagellins we decided it would be interesting to see whether or not flagellar-independent expression still falls into the grasp of FlaF regulation by testing our overexpression constructs in the Δ*flaF* mutant. Surprisingly, we observed levels of intracellular flagellin protein comparable to that of wild type, however, the cells still remained non motile. This combined with the bacterial two-hybrid data for *C. crescentus*, *A. tumefaciens* and *S. meliloti*, strongly suggests that FlaF is acting as a general flagellin T3S chaperone, and is required for flagellin secretion. In *C. crescentus* we only identified an interaction between FljJ and FlaF. It is plausible that the other FlaF:flagellin interactions were not observed due to misfolding of the flagellin proteins in the *E. coli* test strain. This would be consistent with the high theoretical PI values of FljK, FljL and FljM compared to FljJ. Alternatively, it is possible that *C. crescentus* is different among the α-proteobacteria, due to the regulation of flagellar biogenesis being tightly integrated into its cell cycle. This is consistent with the fact that a FlbT:Flagellin interaction was not observed in *A. tumefaciens* and *S. meliloti*. Furthermore, both our data and other work suggests that the exact regulatory actions of FlbT in other bacteria may differ (Anderson and Gober, 2000; Ferooz *et al*., 2011). In *C. crescentus* the cellular levels of FlaF reflect the same pattern of flagellin levels during the cell cycle, peaking in expression when flagellar assembly is initiated in a pre-divisional cell (Llewellyn *et al*., 2005). In contrast, FlbT concentrations are constant throughout the cell cycle (Llewellyn *et al*., 2005). It is therefore likely that FlaF is temporally regulated in a way such that it is made only when the flagellins need to be secreted. Importantly, we have shown that FlaF could potentially be acting as a general flagellin secretion chaperone, however; this would require further investigation.

One extremely surprising result from this investigation was the observation that FljJ can bind *fljK* mRNA. Importantly, this is consistent with previous models that suggest the possibility of localised translation of T3S substrates (Aldridge and Hughes, 2001; Cheng and Schneewind, 2000). Cheng and Schneewind proposed two models for substrate recognition by a T3SS based on YOP virulence protein secretion in pathogenic *Yersinia* spp. (Cheng and Schneewind, 2000). The first model relies on an mRNA signal to facilitate the coupling of translation and secretion. Cytosolic translation of *yop* mRNA is repressed by a negative factor and the co-translational secretion of YOP

occurs through ribosomes located near the T3SS (Cheng and Schneewind, 2000). The second model describes the utilisation of T3S chaperone that delivers the unfolded polypeptides to the T3SS for export from the cell (Cheng and Schneewind, 2000). Subsequent work investigating the YOP secretion signal established that it was an N-terminal amino acid sequence and not an mRNA signal (Lloyd *et al*., 2001). Our results appear to be consistent with the first model proposed by Cheng and Schneewind, in demonstrating that a *C. crescentus* T3S secretion protein, FljJ, is binding to the RNA transcript of another T3S substrate. However, we do not have evidence for co-translational secretion in our system. Could it be that FljJ is helping to localise flagellin mRNA to the flagellar-T3SS so that translation and secretion can occur in close proximity to each other thus increasing the efficiency of filament assembly? If this were true it would require the ribosomes to be located at the base of the flagellum. Aldridge and Hughes predicted that the space within the C-ring cavity could accommodate up to three ribosomes (Aldridge and Hughes, 2001). They propose that the ribosomes would create a gate preventing the secretion of substrates at the wrong time. During flagellar assembly, ribosomes associate with a flagellar-specific protein, which brings them near to the basal body. When the substrate specificity switch occurs the ribosomes are moved into the C-ring cavity and directly pass the actively translating polypeptide to the T3SS (Aldridge and Hughes, 2001). This process couples together translation and secretion of late flagellar subunits. Importantly, their gated model allowed chaperones to fit into the C-ring space around the ribosomes (Aldridge and Hughes, 2001). Therefore, alternatively, it could be that translation is localised and secretion occurs after the polypeptide is completed. To our knowledge these results present the first evidence for a T3SS substrate binding a secretion substrate mRNA prior to its secretion. This hypothesis requires further experimental testing but the scope for investigation of a potential mechanism of localised translation is great considering the complexity of both flagellar and virulence T3SS. If localised translation is occurring in *C. crescentus*, it would be interesting to see if FlaF can be found at the flagellar pole.

Based on the data we now have available we propose a tentative model for the regulation of filament assembly in *C. crescentus* (Figure 46). Based on the observed FljJ:FlbT protein interaction, FljJ somehow interacts with FlbT and replaces it at a specific sequence upstream of the ribosomal binding site of the flagellin mRNA. It has to be noted here that our *in vitro* data appears to suggest that FljJ has a lower affinity for *fljK* mRNA than FlbT. We therefore predict that an unknown component may be required for FljJ to replace FlbT on the mRNA. It may be a flagellar protein or the

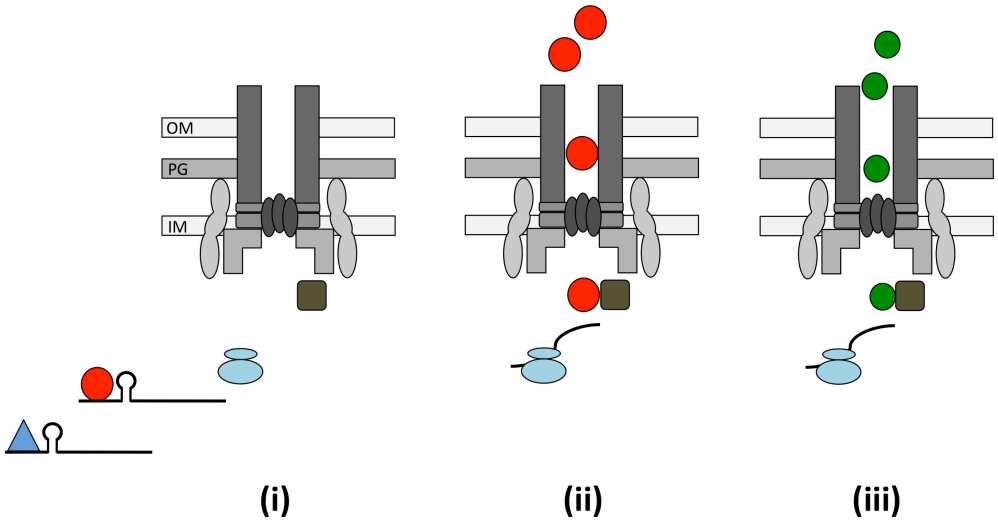

Figure 46: A proposed model for coupling flagellin expression to filament assembly in *C. crescentus*

The flagellar basal body first assembles into the inner-membrane (IM). The rod traverses across the periplasm through both the peptidoglycan (PG) and the outer-membrane (OM). Upon hook completion (hook not shown), a substrate specificity switch occurs and the system begins to secrete late flagellar subunits. Three proteins are responsible for co-ordinating the assembly of the filament. **(i)** In the cytoplasm, FlbT (dark blue triangle) binds to and prevents the translation of *fljK* mRNA. FljJ (red circle) can bind to the same sequence on the RNA displacing FlbT, and localises with the mRNA to the base of the flagellum. **(ii)** FljJ is then secreted out of the cell presumably being donated to the T3SS by FlaF (brown square). In doing so FljJ leaves behind the flagellin mRNA to be translated by ribosomes (light blue) located at the beneath the flagellum base. **(iii)** The translated flagellin polypeptide (green circle) is bound by FlaF and passed directly to the T3SS for export into the filament.

flagellar itself i.e. a functional T3SS. Therein may lay a limitation of this type of *in vitro* experiment. FljJ then localises the mRNA to the base of the flagellum, where FlaF and the ribosomes are located. FlaF binds to FljJ and passes it to the T3SS in order to be secreted out of the cell thus assembling first into the filament (Figure 46). In doing so FljJ leaves behind the mRNA, which local ribosomes process into flagellin polypeptide. The flagellin protein is then picked up by FlaF, which donates it directly to the T3SS for export (Figure 46). This way, FlaF can then exert its positive regulation in the vicinity of the ribosomes and T3SS, thus localising the process of flagellin translation and secretion. It is important to note that this model is based only on the confirmation of protein:protein interactions between FljJ and the two regulators. Likewise, we have only tested the ability of FljJ and FlbT to interact with *fljK* and have not tried other flagellin transcripts.

Llewellyn *et al*., discounted that FlaF is acting as a typical T3S chaperone based on the fact that flagellin protein stability in a double Δ*flbT*/Δ*flaF* mutant showed no difference to that of a *flbT* mutant or wild type (Llewellyn *et al*., 2005). However, the double mutant exhibited a reduced rate of 25 kDa flagellin synthesis suggesting that FlaF is required for maximal protein synthesis (Llewellyn *et al*., 2005). Importantly even though the addition of a mutation in FlbT in a Δ*flaF* mutant restored flagellin synthesis, the strain still did not make a filament and thus remained non motile. Therefore, it was concluded that FlaF is involved in both the activation of translation and secretion of flagellin.

How FlaF would function to activate flagellin translation in our model is unclear. It is tempting to suggest that the key is having FlaF localised to the flagellum pole and its absence from there is what is causing the observed reduced rate of 25 kDa synthesis in the Δ*flbT*/Δ*flaF* mutant. For example, in a Δ*flaF* background, FljJ would still localise the flagellin mRNA to the base of the flagellum however, in the absence of FlaF, cannot release the RNA for translation, which ultimately leads to its degradation. A Δ*flbT*/Δ*flaF* mutant does not express FljJ (Llewellyn *et al*., 2005). Based on our model, cells possessing this double mutant phenotype would not have the ability to localise flagellin mRNA to the flagellum for translation. However, the lack of negative regulation by FlbT would result in translation occurring regardless of this fact. Faulds-Pain *et al*., recently demonstrated that flagellin glycosylation is important for protein stability in *C. crescentus* (Faulds-Pain *et al*., 2011). A deletion of the glycosyl transferase enzyme, *flmD*, resulted in a dramatic reduction of intracellular flagellin protein (Faulds-Pain *et al*., 2011). In other bacteria, flagellin glycosylation is considered

essential for secretion (Goon *et al*., 2003). To our knowledge in these bacteria, glycosylation and flagellin stability has not been investigated. This work has led to the hypothesis that glycosylation machinery is located at the base of the flagellum (Logan, 2006). Therefore, with respect to our model of filament regulation in *C. crescentus* it is plausible that flagellin glycosylation is important. However, this will require further investigation. Our data strongly suggests that FlbT, FlaF and FljJ are coordinately regulating filament assembly in *C. crescentus*. However, it is still not exactly clear how they are doing this. Importantly, it is very likely that our in vitro assays are not completing the picture, due to the fact that they are missing an important component of the regulatory mechanism, such as an active T3SS.

The α-proteobacteria is a subdivision of bacteria that exhibits huge variation in lifestyle characteristics. A recent study into the evolution of the α-proteobacterial genome highlighted a correlation between horizontal gene transfer, deletions and duplications and bacterial lifestyle (Boussau *et al*., 2004). It has been predicted that the regulatory circuit of FlgM/σ^{28} could modulate the expression of late flagellar subunits in response flagella abundance and by doing so control flagella numbers (Saini *et al*., 2011). However if we consider the bacterial species in this project: *S. meliloti* and *A. tumefaciens* possess > 1 flagella per cell, where as *C. crescentus* has only one (Faulds-Pain *et al*., 2011; Hoang *et al*., 2008; Oberpichler *et al*., 2008). It is tempting to speculate that the α-proteobacteria have evolved to regulate filament assembly in a different manner to those bacteria that possess FlgM/σ^{28} based on differences in lifestyle, however there is currently no experimental evidence to back this notion.

We feel that our findings have opened up the door to many more lines of future investigation that are still within the scope of this project. Probably the most important of these would be to test the ability of FlbT and FljJ to bind the other flagellin mRNA's. This experiment is crucial in order to understand how the six flagellins are being regulated with respect to filament assembly. We would also like to see if FlaF can interact with components of the flagellar-T3SS in its role as a T3S chaperone. As previously mentioned it would be interesting to observe flagellar-dependent expression of flagellin in the Δ*fljJKLMNO* mutant. It is plausible that flagellin expression in this way, i.e. with constructs possessing an intact 5' transcript, would allow the system to generate wild type swimming speeds. One experiment we were unsuccessful in obtaining a result in was when trying to identify whether or not FljJ is secreted from the cell when there are no other flagellins present. Based on our data we would speculate that it is not secreted, and that for FljJ export to occur, at least one other flagellin is

required to be present. It would be possible to determine this using Mass Spectrometry to analyse the filament composition of the Δ*fljKLMNO* strain complemented with one of the other flagellins in trans. It is possible that if FljJ has no flagellin mRNA to bind to then it is not efficiently localised for secretion. Other experiments we would be interested in carrying out are (i) blocking FljJ secretion in wild type *C. crescentus* in order to investigate the secretion substrate switch to flagellin from middle to late flagellar subunits, (ii) the testing of secretion substrates in other T3SS systems for the ability to interact with mRNA (localised translation), (iii) the biochemical confirmation of FlaF:Flagellin interactions in *S. meliloti*, *A. tumefaciens*, and *C. crescentus*.

Chapter 9. Appendix A

A.1 Bacterial Growth Media

All bacterial growth media was solubilised in MilliQ water and sterilised in an autoclave. Antibiotics and growth supplements were added after, to the cooled media.

Table 8: Luria-Bertani (LB) liquid medium

Luria-Bertani (LB) liquid medium (Per litre)	
Bacto Tryptone	10 g
Bacto Yeast Extract	5 g
Sodium Chloride	5 g

Table 9: Luria-Bertani (LB) solid medium

Luria-Bertani (LB) solid medium (Per litre)	
Bacto Tryptone	10 g
Bacto Yeast Extract	5 g
Sodium Chloride	5 g
Bacto Agar	15 g

Table 10: Peptone Yeast Extract (PYE) liquid medium

Peptone Yeast Extract (PYE) liquid medium (Per litre)	
Bacto Peptone	2 g
Bacto Yeast Extract	1 g
Calcium Chloride	1 ml
MgSO47H2O	0.2 g

Table 11: Peptone Yeast Extract (PYE) solid medium

Peptone Yeast Extract (PYE) solid medium (Per litre)	
Bacto Peptone	2 g
Bacto Yeast Extract	1 g
MgSO47H2O	0.2 g
Bacto Agar	15 g

Table 12: Tryptone Yeast Extract (TY) liquid medium

Tryptone Yeast Extract (TY) liquid medium (Per litre)	
Bacto Tryptone	5 g
Bacto Yeast Extract	3 g

Table 13: Tryptone Yeast Extract (TY) solid medium

Tryptone Yeast Extract (TY) solid medium (Per litre)	
Bacto Tryptone	5 g
Bacto Yeast Extract	3 g
Bacto Agar	15 g

A.2 Antibiotics

All antibiotics were solublised according to manufacturers instructions and filter sterilised.

Table 14: Antibiotic concentrations for the growth of *Escherichia coli*

Antibiotic	Stock Concentration	Working Concentration
Kanamycin	10 mg/ml	50 µg/ml
Ampicillin	20 mg/ml	100 µg/ml

Table 15: Antibiotic concentrations for the growth of *Caulobacter crescentus*

Antibiotic	Stock Concentration	Working Concentration
Kanamycin	10 mg/ml	20 µg/ml – Solid medium
Kanamycin	10 mg/ml	5 µg/ml – Liquid medium
Naladixic Acid	2.5 mg/ml	20 µg/ml

A.3 Growth Supplements

All growth supplements were solublised according to manufacturers instructions and filter sterilised.

Table 16: Concentrations of bacterial growth supplements

Supplement	Stock Concentration	Working Concentration
Sucrose	50 %	0.2 %
Xylose	50 %	0.3 %
IPTG	1 M	1 mM
X-Gal	2 %	0.004 %

A.4 Preparation of Plasmid DNA by Alkaline Lysis with SDS

Table 17: Alkaline Lysis Solution I

Alkaline Lysis Solution I	
Glucose	50 mM
Tris.HCl (pH 8.0)	25 mM
EDTA (pH 8.0)	10 mM
RNase A	0.1 mg/ml
Sterile water	Up to 50 ml

Table 18: Alkaline Lysis Solution II

Alkaline Lysis Solution II (10 ml)		
NaOH	1 M	2 ml
SDS	10 %	1 ml
Sterile water	-	7 ml

Table 19: Alkaline Lysis Solution III

Alkaline Lysis Solution III	
Potassium Acetate	3 M
Glacial Acetic Acid	9 %
Sterile water	Up to 500 ml

A.5 Alkaline Dephosphorylation of Digested Plasmid DNA

Table 20: TNE Buffer

TNE Buffer	
Tris.HCl (pH 8.0)	10 mM
NaCl	100 mM
EDTA (pH 8.0)	1 mM
Sterile water	Up to 2 ml

Stored at 4 °C

A.6 Agarose Gel Electrophoresis

Table 21: 10 x DNA Loading Buffer

10 x DNA Loading Buffer	
Tris Acetate	200 mM
EDTA (pH 8.0)	5 mM
Glycerol	50 %
Bromophenol Blue	0.1 %
Xylene Cyanole FF	0.1 %
Orange G	0.2 %
Sterile water	Up to 50 ml

A.7 Tricine SDS-Polyacrylamide Gel Electrophoresis

Table 22: Tricine Gel Buffer

Tricine Gel Buffer	
Tris (pH 8.45)	3 M
SDS	0.3 %
Sterile water	Up to 200 ml

Solution was then filter sterilised

Table 23: 12 % Separating Gel

12 % Separating Gel (15 ml)	
Separating Acrylamide (49.5 %-16.5 % T 3% C)	3.6 ml
Tricine Gel Buffer	5 ml
Glycerol (50 %)	5 ml
Sterile water	1.4 ml
APS (10 %)	75 µl
TEMED	7.5 µl

Table 24: 3.96 % Stacking Gel

3.96 % Stacking Gel (12.5 ml)	
Stacking Acrylamide (49.5 %-4 % T 3% C)	1 ml
Tricine Gel Buffer	3.1 ml
Sterile water	8.4 ml
APS (10 %)	100 µl
TEMED	10 µl

Table 25: 10 x Cathode Running Buffer

10 x Cathode Running Buffer	
Tris (pH 8.25)	1 M
Tricine	1 M
SDS	10 %
Sterile water	Up to 1 Litre

Table 26: 10 x Anode Running Buffer

10 x Anode Running Buffer	
Tris (pH 8.9)	2 M
Sterile water	Up to 1 Litre

Table 27: 2 x SDS Sample Buffer

2 x SDS Sample Buffer	
Tris. HCl (pH 6.8-7.0)	62.5 mM
Glycerol	10 %
SDS	2 %
β-Mercaptoethanol	5 %
Bromophenol Blue	A few grains
Sterile water	Up to 50 ml

Table 28: Coomassie Blue Solution

Coomassie Blue Solution	
Ethanol	50 %
Acetic Acid	5 %
Coomassie Blue	0.02 %
Sterile water	Up to 1 litre

Table 29: Destaining Solution

Destaining Solution	
Ethanol	50 %
Acetic Acid	5 %
Sterile water	Up to 1 litre

A.8 Native-Polyacrylamide Gel Electrophoresis

Table 30: Native Separating Buffer

Native Separating Buffer	
Tris (pH 8.8)	1.5 M
Sterile water	Up to 200 ml

Solution was then filter sterilised

Table 31: Native Stacking Buffer

Native Stacking Buffer	
Tris (pH 7.5)	0.5 M
Sterile water	Up to 200 ml

Solution was then filter sterilised

Table 32: 50 x Native Running Buffer

50 x Native Running Buffer	
Tris	312.5 mM
Glycine	2.5 M
Sterile water	Up to 200 ml

Solution was then filter sterilised

Table 33: 3 x Native Sample Buffer

3 x Native Sample Buffer (10 ml)	
Glycerol	30 %
50 x Native Running Buffer	0.6 ml
Sterile water	6.4 ml
Bromophenol Blue	1 grain

Table 34: 7.5 % Separating Gel

7.5 % Separating Gel (10 ml)	
Acrylamide-Bis (40%) (29.1:0.9)	2.5 ml
Native Separating Buffer	1.875 ml
Sterile water	5 ml
APS (10 %)	50 µl
TEMED	10 µl

Table 35: 5 % Stacking Gel

5 % Stacking Gel (5 ml)	
Acrylamide-Bis (40%) (29.1:0.9)	1.25 ml
Native Stacking Buffer	0.625 ml
Sterile water	3.1 ml
APS (10 %)	30 µl
TEMED	15 µl

A.9 Immunoblot Analysis

Table 36: 10 x Phosphate Buffered Saline

10 x Phosphate Buffered Saline (PBS) (per litre)	
NaCl	80 g
KCl	2 g
Na2HPO4	14.4 g
KH2PO4	2.4 g
Sterile water	Up to 1 litre

pH 7.4 Autoclaved

Table 37: PMT

PMT	
Milk Powder	5 %
PBS	1 x
Tween 20	0.1 %
Sterile water	Up to 200 ml

Table 38: 1 x Immunoblot Transfer Buffer

1 x Immunoblot Transfer Buffer	
CAPS (pH 11.0)	10 mM
Methanol	10 %
Sterile water	Up to 2 Litre

A.10 Protein Over-Expression and Purification

Table 39: His-Loading Buffer

His-Loading Buffer	
HEPES	50 mM
NaCl	150 mM
Imidazole	20 mM
Sterile water	Up to 1 litre

pH 7.5 Filter sterilised and degassed

Table 40: His-Elution Buffer

His-Elution Buffer	
HEPES	50 mM
NaCl	150 mM
Imidazole	1 M
Sterile water	Up to 1 litre

pH 7.5 Filter sterilised and degassed

Table 41: 10 x IB Wash Solution

10 x IB Wash Solution	
Tris	200 mM
EDTA (pH 8.0)	100 mM
Trition X-100	10 %
Sterile water	Up to 1 litre

pH 7.5 Filter sterilised

Table 42: Burgess Regeneration Buffer

Burgess Regeneration Buffer	
Tris	50 mM
NaCl	15 mM
EDTA (pH 8.0)	0.1 mM
Triton X-100	0.01 %
Glycerol	20 %
DTT	2 mM
Sterile water	Up to 200 ml

pH 7.9 Filter sterilised and degassed

Table 43: Burgess Dialysis Buffer

Burgess Dialysis Buffer	
Tris	10 mM
NaCl	500 mM
EDTA (pH 8.0)	0.1 mM
Trition X-100	0.01 %
Glycerol	5 %
DTT	1 mM
Sterile water	Up to 4 litre

pH 7.9 Filter sterilised and degassed

Table 44: Burgess Gel Filtration Buffer

Burgess Gel Filtration Buffer	
Tris	10 mM
NaCl	500 mM
EDTA (pH 8.0)	0.1 mM
Triton X-100	0.01 %
Glycerol	5 %
Sterile water	Up to 2 litre

pH 7.9 Filter sterilised and degassed

A.11 His-Tag Pull Down Assay

Table 45: His Pull Down Loading Buffer

His Pull Down Loading Buffer	
Tris	10 mM
NaCl	500 mM
Triton X-100	0.01 %
Glycerol	5 %
Imidazole	20 mM
Sterile water	Up to 200 ml

pH 7.9 Filter sterilised and degassed

Table 46: His Pull Down Elution Buffer

His Pull Down Elution Buffer	
Tris	10 mM
NaCl	500 mM
Trition X-100	0.01 %
Glycerol	5 %
Imidazole	500 mM
Sterile water	Up to 200 ml

pH 7.9 Filter sterilised and degassed

A.12 In-vivo Co-Immunoprecipitation

Table 47: CoIP Buffer

CoIP Buffer	
HEPES (pH 7.5)	20 mM
NaCl	100 mM
Glycerol	20 %
Sterile water	Up to 1 litre

Table 48: CoIP Wash Buffer

CoIP Wash Buffer	
Tris.HCl (pH 7.4)	50 mM
NaCl	150 mM
Sterile water	Up to 1 litre

A.13 RNA Electromobility Shift Assay

Table 49: 10 x Buffer I

10 x Buffer I	
Maleic acid	166g
NaCl	87.66 g
NaOH	72 g
Sterile water	Up to 1 litre

pH 9.5

Table 50: Tween Washing Buffer

Tween Washing Buffer	
10 x Buffer I	100 ml
Tween 20	0.3 %
Sterile water	Up to 1 litre

Table 51: 10 % Blocking Reagent

10 % Blocking Reagent (200 ml)	
Blocking Reagent (Milk)	20 g
10 x Buffer I	200 ml

Solubilised at 65 °C

pH 7.5 adjusted using NaOH

Autoclaved and stored at 4 °C

Table 52: Blocking Buffer

Blocking Buffer (50 ml)	
10 % Blocking Reagent	5 ml
10 x Buffer I	5 ml
Sterile water	45 ml

Table 53: Equilibration Buffer

Equilibration Buffer	
Diethanol Amine	9.63 ml
Sterile water	Up to 1 litre

pH 9.5

Table 54: RNA Binding Buffer

RNA Binding Buffer	
HEPES	20 mM
KCl	100 mM
$MgCl_2$	1 mM
Glycerol	5 %

pH 7.9 Filter sterilised

A.14 β-Galactosidase Assay

Table 55: Z-Buffer

Z-Buffer (1 Litre)	
Na_2HPO_4	16.1 g
NaH_2PO_4	5.5 g
KCl	0.75 g
$MgSO_4.7H_20$	0.248 g
Sterile water	Up to 1 litre

pH 7.0 Autoclaved

Table 56: Saline

Saline (1 Litre)	
$Na_2HPO_4.7H_2O$	11 g
KH_2PO_4	3 g
NaCl	8.5 g
Sterile water	Up to 1 litre

pH 7.0 Autoclaved

A.15 Chemical Reference Table

Table 57: Chemical/Reagent suppliers and catalogue numbers

Chemical	Manufacturer	Cat/Ref number
10 x Tris Acetate Buffer (TAE)	SIGMA-ALDRICH	T9650-4L
Acetic Acid	VWR	20103.330
Acetic Acid (Glacial)	SIGMA-ALDRICH	64-19-7
Acrylamide-Bis (40%) (29.1:0.9)	MERCK	1.00641.1000
Agarose	PEQLAB	35-1020
Ammonium Persulfate (APS)	SIGMA-ALDRICH	A9164-100G
Ampicillin (Sodium salt)	SIGMA-ALDRICH	A-9518100G
Bacto Agar	BD	214030
Bacto Peptone	DIFCO	0118-07-2
Bacto Tryptone	BD	211699
Bacto Yeast Extract	BD	212720
Bromo-Chloro-Indolyl-Galactopyranoside (X-Gal)	MELFORD	MB1001
Bromophenol Blue	BDH	443053A
Calcium Chloride ($CaCl_2$)	MELFORD	C1103
CDP-Star® Reagent	NEB	N7001S
Chloroform	SIGMA-ALDRICH	24216
Coomassie Blue	FLUKA	27816
Diethanol Amine	SIGMA-ALDRICH	D8,330-3
DIG RNA Labeling Kit (SP6/T7)	ROCHE	11175025910
Dimethylformamide	VWR	23470.293
Dithiothreitol (DTT)	MELFORD	MB1015
ECL-Plus	AMWESHAM	RPN2132
Ethanol	UNIVERSITY STORES	-
Ethylenediaminetetraacetic acid (EDTA)	SIGMA-ALDRICH	EDS-500G
Glucose (D-Glucose)	MELFORD	G1400
Glycerol	SIGMA-ALDRICH	15523-5L-R
Glycine	MELFORD	
Hydrochloric Acid (HCl)	VWR	285074V
Imidazole	SIGMA-ALDRICH	I0125-1KG
Isopropyl β-D-1-thiogalactopyranoside (IPTG)	MELFORD	K0126
Kanamycin (Mono-sulphate)	MELFORD	K0126
Magnesium Sulphate Heptahydrate (MgSO47H2O)	BDH	101514Y
Maleic Acid	CARL ROTH	K304.1
Methanol	UNIVERSITY STORES	-
Milk Powder	NESTLE	Carnation instant nonfat dry milk
Blocking Reagent (Milk)	ROCHE	11886600
N-2-Hydroxy ethayolpiperazine-N'-2 (HEPES)	BDH	441475K

N-cyclohexyl-3-aminopropanesulfonic acid (CAPS)	MELFORD	B4016
Naladixic Acid (Sodium salt)	SIGMA-ALDRICH	N4382-25G
Orange G	BDH	43725Q
Ortho-Nitrophenyl-β-Galactoside (ONPG)	MELFORD	M1202
Potasium Acetate (CH3CO2K)	FLUKA	60035
Potassium di-hydrogen Orthophosphate (KH2PO4)	BDH	102034B
Potassium Chloride (KCl)	FLUKA	60132
Propanol-2 (Isoproponal)	VWR	20839.322
RNase A	SIGMA-ALDRICH	R6148-1.5ML
Separating Acrylamide (49.5 %-16.5 % T 3% C)	SEVERN BIOTECH LTD	-
di-Sodium hydrogen orthophosphate (Na2HPO4)	BDH	301584L
Sodium Acetate	BDH	301045M
Sodium Chloride (NaCl)	VWR	27810.364
Sodium Dodecyl Sulfate (SDS)	SIGMA-ALDRICH	L3771-1KG
Sodium Hydroxide (NaOH)	VWR	28245.289
Stacking Acrylamide (49.5 %-4 % T 3% C)	SEVERN BIOTECH LTD	-
Sucrose	BDH	302994G
Tetramethylethylenediamine (TEMED)	BDH	303853V
Tricine	MELFORD	T2400
Tris (Base)	MELFORD	B2005
Triton X-100	SIGMA-ALDRICH	9002-93-1
Tween 20	BDH	663684B
Urea	VWR	28876.367
Xylene Cyanole FF	BDH	439612F
Xylose	MELFORD	W360600
β-Mercaptoethanol	VWR	80501-154

Chapter 10. Appendix B

B.1 A Typical Example of DNA Agarose Gel Electrophoresis

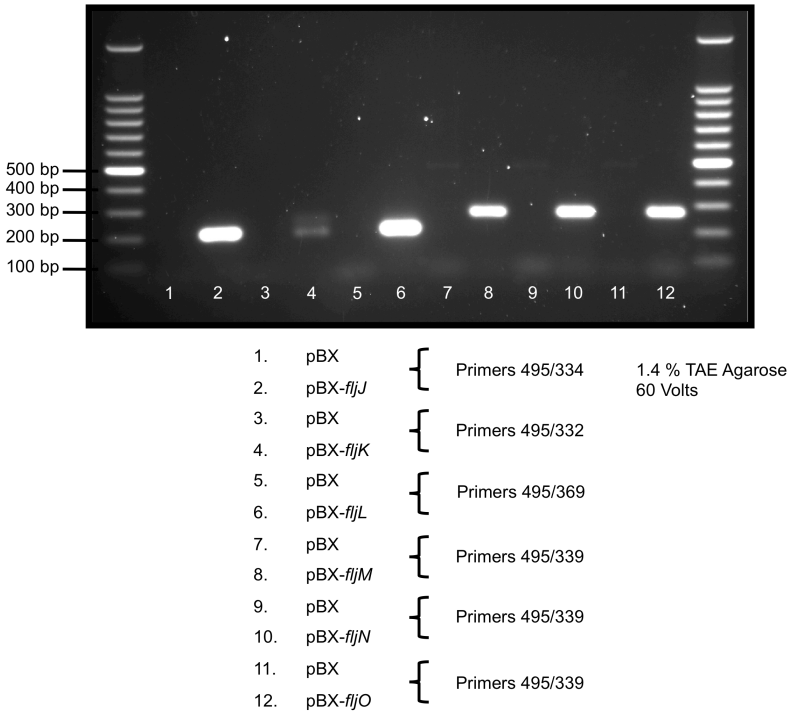

Figure 47: PCR confirmation of the flagellin overexpression constructs

PCR confirmation of the six flagellin overexpression (pBX) plasmids created (see section 3.21). The DNA sequences of the primers numbered can be found in the primer table (see section 3.5). The DNA was measured alonside a 100 bp marker on both ends of the gel.

B.2 Analysis of *Caulobacter crescentus* Isolated Filament Preparations

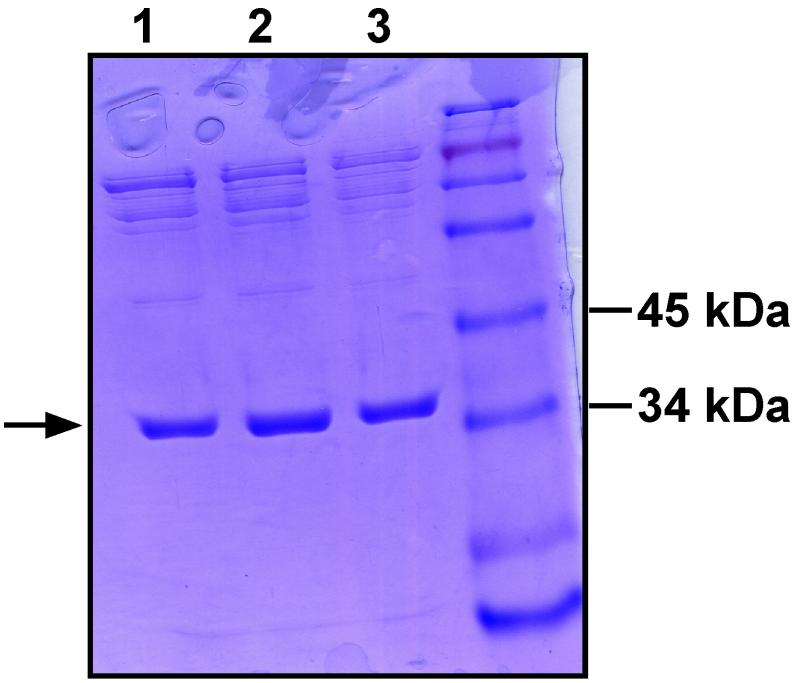

Figure 48: Isolated flagella filament preparations

All samples were run on a 12 % Tricine SDS-PAGE gel and visualised using Coomassie Blue stain. The six flagellins of *C. crescentus* migrate together when using Tricine SDS-PAGE. The approximate MW of protein marker is indicated. The arrow points to flagellin protein. **(1)** Wild type. **(2)** Δ*fljJKL*. **(3)** Δ*fljMNO*.

Chapter 11. Appendix C

C.1 Mass Spectrometry Analysis of *Caulobacter crescentus* Flagellar Filaments

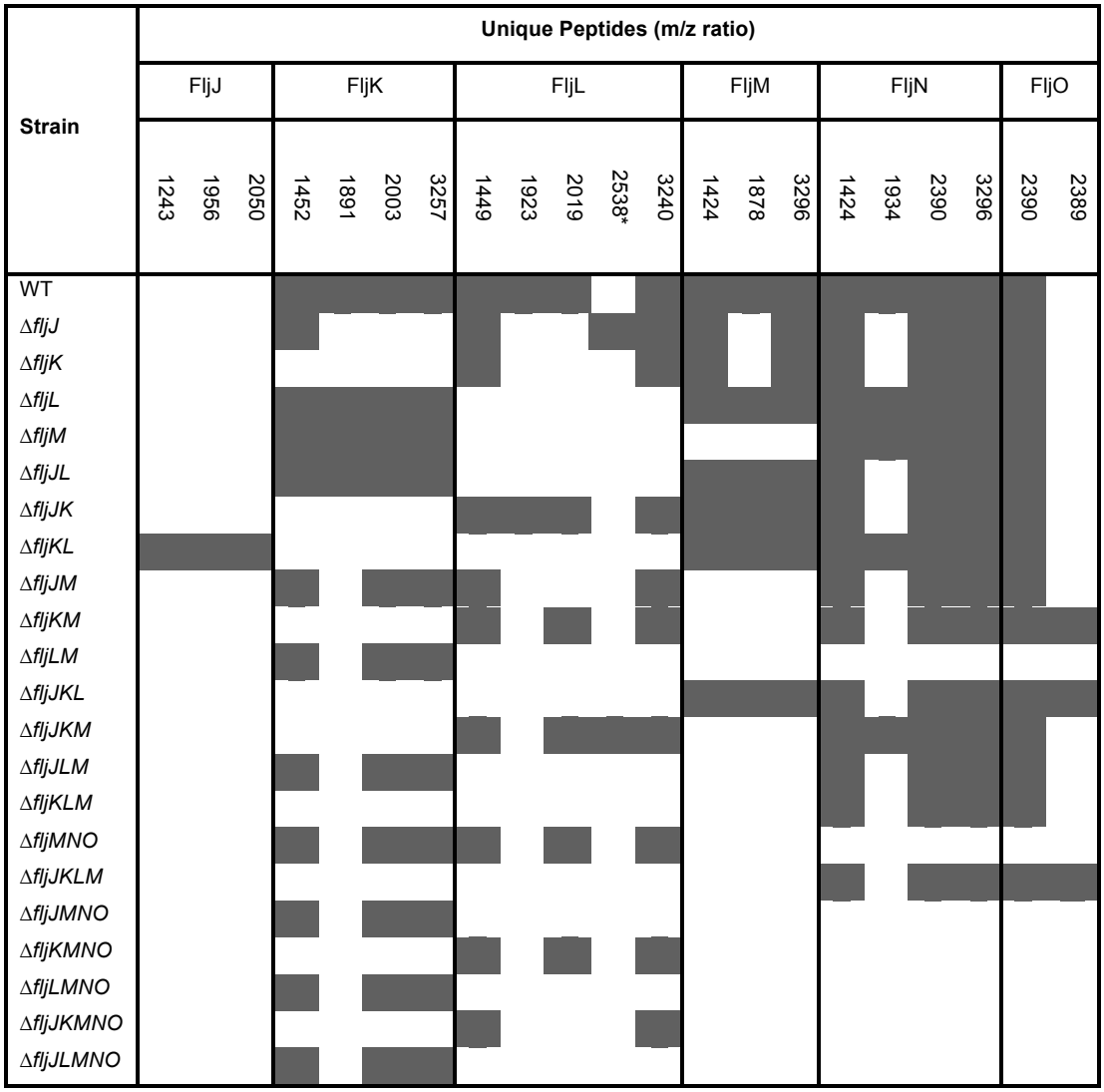

Table 58: Summary of the identification of signature peptides from the six flagellins in filament preparations of wild type and flagellin gene mutants (Faulds-Pain *et al*., 2011)

The locations of the peptides indicated can be found in Figure 19A. A grey box indicates the presence of a peptide and an empty box signifies that peptides absence. * This peptide is defined by MASCOT (MALDI-TOF analysis) as possessing an N-terminal pyroGlu conversion.

Chapter 12. Appendix D

D.1 Electron Microscopy of *Caulobacter crescentus* isolated filaments

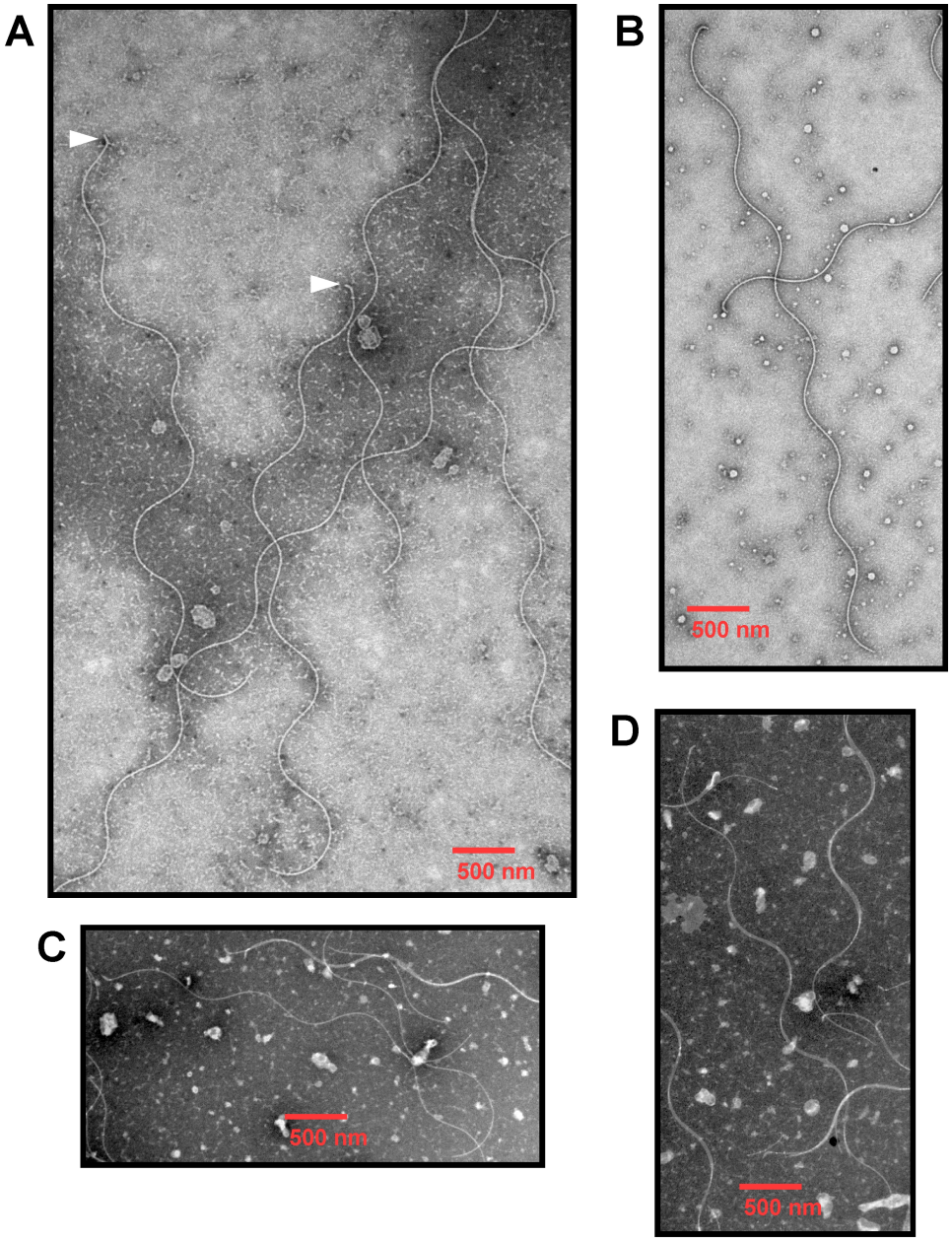

Figure 49A: Electron micrographs of isolated flagellar filaments

A. Wild type. The white arrows indicate the hook structure still attached to the filament.

B. Δ*fljK*. **C.** Δ*fljKM*. **D.** Δ*fljJMNO*

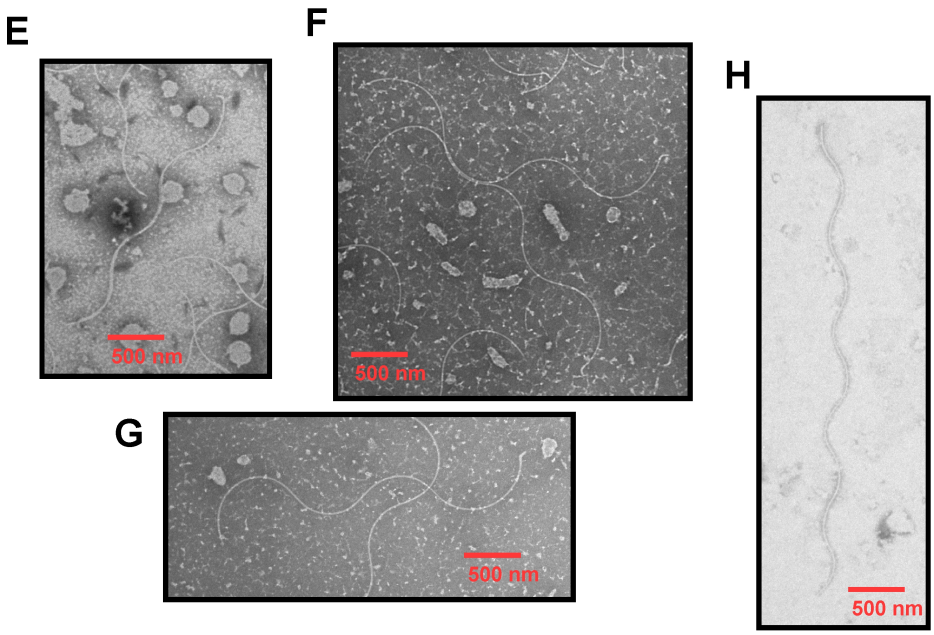

Figure 49B: Electron micrographs of isolated flagellar filaments

E. Δ*fljJKMNO*. **F.** Δ*fljLKMNO*. **G.** Δ*fljLMNO*. **H.** Δ*fljKMNO*.

Chapter 13. Appendix E

E.1 MALDI-TOF Confirmation of His-FljJ

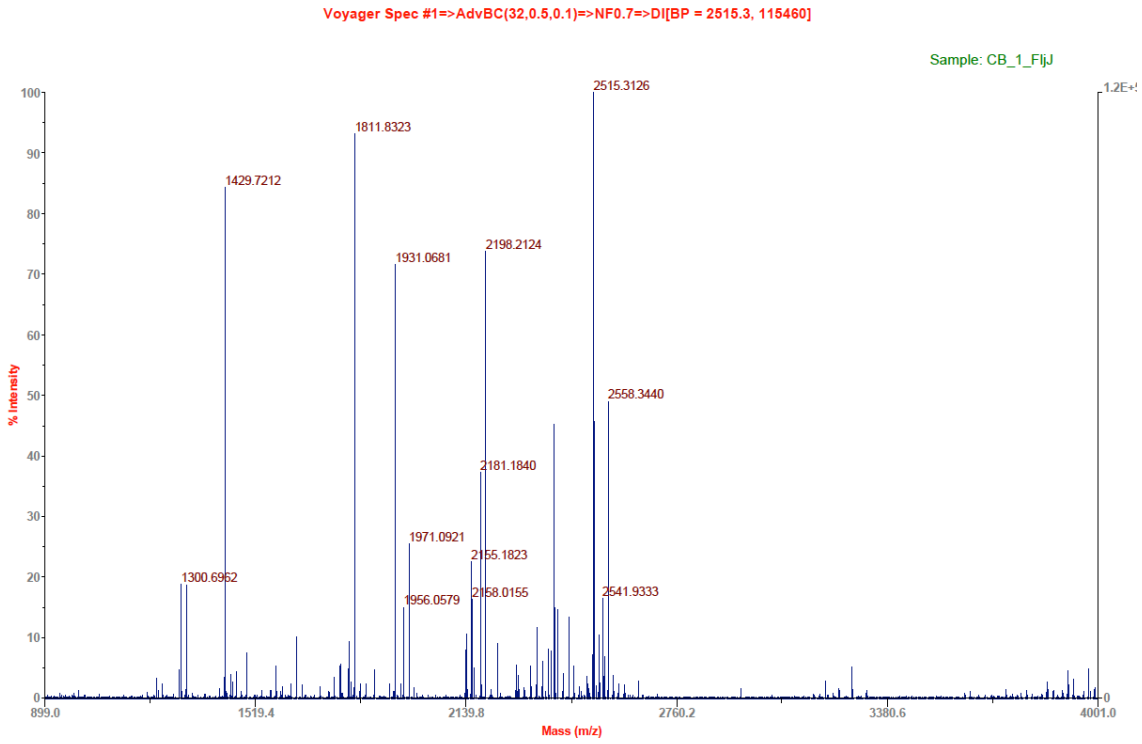

Figure 50A: Mass Spectrum of His-FljJ

Mascot Search Results

User : Joe Gray
Email : joe.gray@ncl.ac.uk
Search title : CB_1_0001.dat - SpecView
Database : MSDB 20060831 (3239079 sequences; 1079594700 residues)
Timestamp : 3 Jun 2009 at 13:47:37 GMT
Top Score : 60 for FLQL2C, flagellin, 28.5K - Caulobacter crescentus

Probability Based Mowse Score

Protein score is -10*Log(P), where P is the probability that the observed match is a random event.
Protein scores greater than 78 are significant (p<0.05).

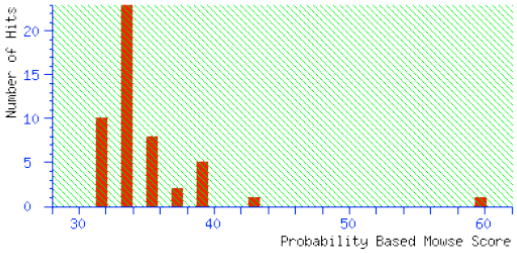

Figure 50B: Protein summary report for His-FljJ (MASCOT)

E.2 MALDI-TOF Confirmation of His-FlbT

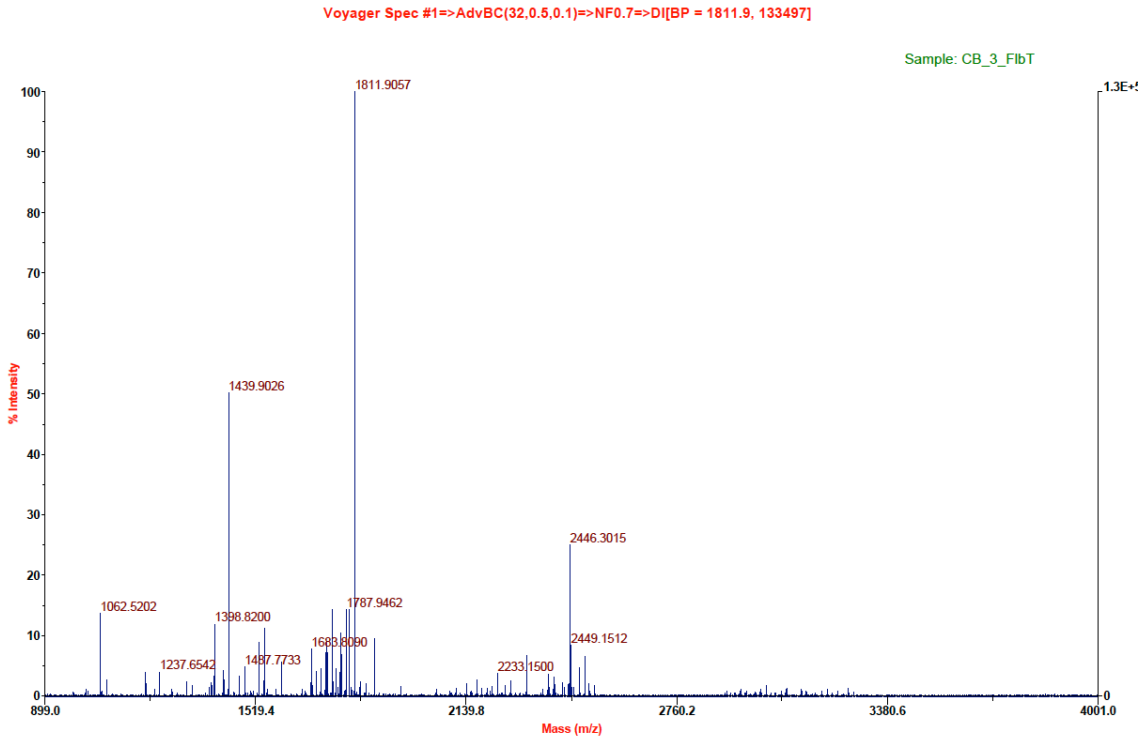

Figure 51A: Mass Spectrum of His-FlbT

Mascot Search Results

User : Joe Gray
Email : joe.gray@ncl.ac.uk
Search title : CB_3_0001.dat - SpecView
Database : MSDB 20060831 (3239079 sequences; 1079594700 residues)
Timestamp : 3 Jun 2009 at 13:35:17 GMT
Top Score : 56 for JQ0741, flbT protein - Caulobacter crescentus

Probability Based Mowse Score

Protein score is -10*Log(P), where P is the probability that the observed match is a random event.
Protein scores greater than 78 are significant (p<0.05).

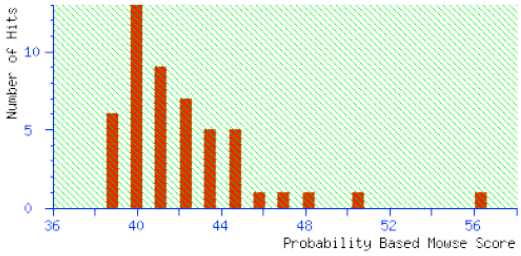

Figure 51B: Protein summary report for His-FlbT (MASCOT)

E.3 MALDI-TOF Confirmation of His-FlaF

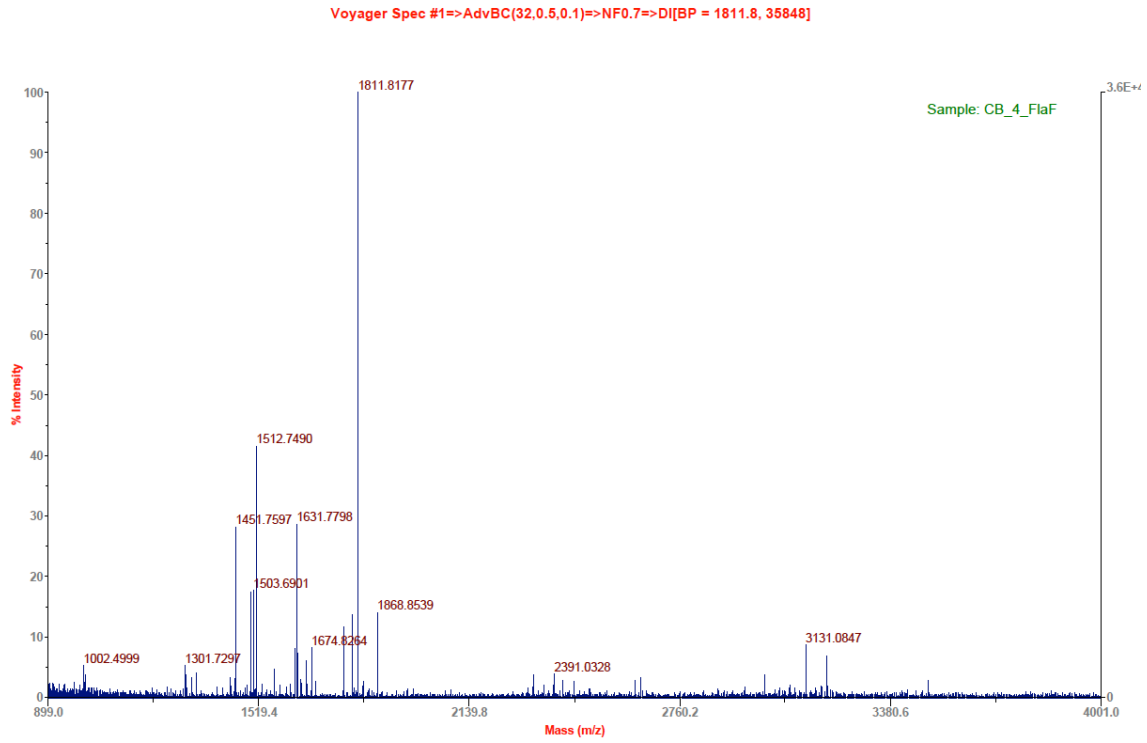

Figure 52A: Mass Spectrum of His-FlaF

Mascot Search Results

User : Joe Gray
Email : joe.gray@ncl.ac.uk
Search title : CB_4_0001.dat - SpecView
Database : NCBInr 20090528 (8915381 sequences; 3049521622 residues)
Timestamp : 3 Jun 2009 at 14:22:41 GMT
Top Score : 77 for gi|120266, RecName: Full=Protein flaF

Probability Based Mowse Score

Protein score is -10*Log(P), where P is the probability that the observed match is a random event.
Protein scores greater than 82 are significant (p<0.05).

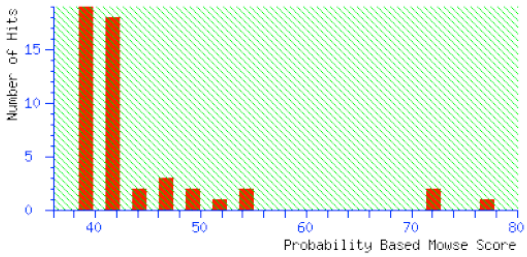

Figure 52B: Protein summary report for His-FlaF (MASCOT)

Chapter 14. References

Aizawa, S. I., G. E. Dean, C. J. Jones, R. M. Macnab & S. Yamaguchi, (1985) Purification and characterization of the flagellar hook-basal body complex of Salmonella typhimurium. *J Bacteriol* **161**: 836-849.

Aldridge, C., K. Pooncharoen, S. Saini, T. Ewen, A. Soloyva, C. V. Rao, K. Imada, T. Minamino & P. D. Aldridge, (2010) The interaction dynamics of a negative feedback loop regulates flagellar number in Salmonella enterica serovar Typhimurium. *Mol Microbiol* **78**: 1416-1430.

Aldridge, P. & K. T. Hughes, (2001) How and when are substrates selected for type III secretion? *Trends in Microbiology* **9**: 209-214.

Aldridge, P. & K. T. Hughes, (2002) Regulation of flagellar assembly. *Curr Opin Microbiol* **5**: 160-165.

Aldridge, P. & U. Jenal, (1999) Cell cycle-dependent degradation of a flagellar motor component requires a novel-type response regulator. *Mol Microbiol* **32**: 379-391.

Aldridge, P., R. Paul, P. Goymer, P. Rainey & U. Jenal, (2003) Role of the GGDEF regulator PleD in polar development of Caulobacter crescentus. *Mol Microbiol* **47**: 1695-1708.

Aldridge, P. D., J. E. Karlinsey, C. Aldridge, C. Birchall, D. Thompson, J. Yagasaki & K. T. Hughes, (2006) The flagellar-specific transcription factor, sigma28, is the Type III secretion chaperone for the flagellar-specific anti-sigma28 factor FlgM. *Genes & Development* **20**: 2315-2326.

Alting-Mees, M. A. & J. M. Short, (1989) pBluescript II: gene mapping vectors. *Nucleic Acids Res* **17**: 9494.

Anderson, D. K., N. Ohta, J. Wu & A. Newton, (1995) Regulation of the Caulobacter crescentus rpoN gene and function of the purified sigma 54 in flagellar gene transcription. *Mol Gen Genet* **246**: 697-706.

Anderson, P. E. & J. W. Gober, (2000) FlbT, the post-transcriptional regulator of flagellin synthesis in Caulobacter crescentus, interacts with the 5' untranslated region of flagellin mRNA. *Mol Microbiol* **38**: 41-52.

Antonova, E. S. & B. K. Hammer, (2011) Quorum-sensing autoinducer molecules produced by members of a multispecies biofilm promote horizontal gene transfer to Vibrio cholerae. *FEMS Microbiol Lett* **322**: 68-76.

Arora, S. K., B. W. Ritchings, E. C. Almira, S. Lory & R. Ramphal, (1997) A transcriptional activator, FleQ, regulates mucin adhesion and flagellar gene expression in Pseudomonas aeruginosa in a cascade manner. *J Bacteriol* **179**: 5574-5581.

Asai, Y., S. Kojima, H. Kato, N. Nishioka, I. Kawagishi & M. Homma, (1997) Putative channel components for the fast-rotating sodium-driven flagellar motor of a marine bacterium. *J Bacteriol* **179**: 5104-5110.

Atsumi, T., S. Sugiyama, E. J. Cragoe & Y. Imae, (1990) Specific inhibition of the Na(+)-driven flagellar motors of alkalophilic Bacillus strains by the amiloride analog phenamil. *J Bacteriol* **172**: 1634-1639.

Attmannspacher, U., B. E. Scharf & R. M. Harshey, (2008) FliL is essential for swarming: motor rotation in absence of FliL fractures the flagellar rod in swarmer cells of Salmonella enterica. *Mol Microbiol* **68**: 328-341.

Auvray, F., J. Thomas, G. M. Fraser & C. Hughes, (2001) Flagellin polymerisation control by a cytosolic export chaperone. *J Mol Biol* **308**: 221-229.

Bange, G., G. Petzold, K. Wild, R. O. Parlitz & I. Sinning, (2007) The crystal structure of the third signal-recognition particle GTPase FlhF reveals a homodimer with bound GTP. *Proceedings of the National Academy of Sciences of the United States of America* **104**: 13621-13625.

Bardy, S. L., T. Mori, K. Komoriya, S.-I. Aizawa & K. F. Jarrell, (2002) Identification and localization of flagellins FlaA and FlaB3 within flagella of Methanococcus voltae. *J Bacteriol* **184**: 5223-5233.

Barrios, H., B. Valderrama & E. Morett, (1999) Compilation and analysis of sigma(54)-dependent promoter sequences. *Nucleic Acids Research* **27**: 4305-4313.

Beatson, S. A., T. Minamino & M. J. Pallen, (2006) Variation in bacterial flagellins: from sequence to structure. *Trends Microbiol* **14**: 151-155.

Bennett, J. C. & C. Hughes, (2000) From flagellum assembly to virulence: the extended family of type III export chaperones. *Trends in Microbiology* **8**: 202-204.

Benson, A. K., G. Ramakrishnan, N. Ohta, J. Feng, A. J. Ninfa & A. Newton, (1994) The Caulobacter crescentus FlbD protein acts at ftr sequence elements both to activate and to repress transcription of cell cycle-regulated flagellar genes. *Proc Natl Acad Sci USA* **91**: 4989-4993.

Berg, H. C., (1995) Torque generation by the flagellar rotary motor. *Biophys J* **68**: 163S-166S; discussion 166S-167S.

Berleman, J. E. & J. R. Kirby, (2009) Deciphering the hunting strategy of a bacterial wolfpack. *FEMS Microbiol Rev* **33**: 942-957.

Berne, C., D. T. Kysela & Y. V. Brun, (2010) A bacterial extracellular DNA inhibits settling of motile progeny cells within a biofilm. *Molecular Microbiology*.

Biondi, E. G., S. J. Reisinger, J. M. Skerker, M. Arif, B. S. Perchuk, K. R. Ryan & M. T. Laub, (2006) Regulation of the bacterial cell cycle by an integrated genetic circuit. *Nature* **444**: 899-904.

Biondi, E. G., J. M. Skerker, M. Arif, M. S. Prasol, B. S. Perchuk & M. T. Laub, (2006) A phosphorelay system controls stalk biogenesis during cell cycle progression in Caulobacter crescentus. *Molecular Microbiology* **59**: 386-401.

Blair, D. F., (2006) Fine structure of a fine machine. *J Bacteriol* **188**: 7033-7035.

Blair, D. F. & H. C. Berg, (1990) The MotA protein of E. coli is a proton-conducting component of the flagellar motor. *Cell* **60**: 439-449.

Bocsanczy, A. M., U. C. M. Achenbach, A. Mangravita-Novo, J. Yuen & D. J. Norman, (2011) Comparative effect of low temperature on virulence and twitching motility of Ralstonia solanacearum strains present in Florida. *Phytopathology*.

Boussau, B., E. O. Karlberg, A. C. Frank, B.-A. Legault & S. G. E. Andersson, (2004) Computational inference of scenarios for alpha-proteobacterial genome evolution. *Proceedings of the National Academy of Sciences of the United States of America* **101**: 9722-9727.

Boutte, C. C. & S. Crosson, (2011) The complex logic of stringent response regulation in Caulobacter crescentus: starvation signalling in an oligotrophic environment. *Mol Microbiol* **80**: 695-714.

Bowers, L. M., E. B. Shapland & K. R. Ryan, (2008) Who's in charge here? Regulating cell cycle regulators. *Curr Opin Microbiol* **11**: 547-552.

Boyd, C. H. & J. W. Gober, (2001) Temporal regulation of genes encoding the flagellar proximal rod in Caulobacter crescentus. *J Bacteriol* **183**: 725-735.

Boyd, J. M., (2000) Localization of the histidine kinase PilS to the poles of Pseudomonas aeruginosa and identification of a localization domain. *Mol Microbiol* **36**: 153-162.

Branda, S. S., J. E. González-Pastor, E. Dervyn, S. D. Ehrlich, R. Losick & R. Kolter, (2004) Genes involved in formation of structured multicellular communities by Bacillus subtilis. *J Bacteriol* **186**: 3970-3979.

Bresolin, G., J. Trcek, S. Scherer & T. M. Fuchs, (2008) Presence of a functional flagellar cluster Flag-2 and low-temperature expression of flagellar genes in Yersinia enterocolitica W22703. *Microbiology (Reading, Engl)* **154**: 196-206.

Brown, J., Faulds-Pain, A., & P. Aldridge. The Coordination of flagellar gene expression and the flagellar assembly pathway. Caister Academic Press 2009. Pili and Flagella: Current Research and Future Trends, ed K. Jarrell

Brun, Y. V. & L. Shapiro, (1992) A temporally controlled sigma-factor is required for polar morphogenesis and normal cell division in Caulobacter. *Genes & Development* **6**: 2395-2408.

Buelow, D. R. & T. L. Raivio, (2010) Three (and more) component regulatory systems - auxiliary regulators of bacterial histidine kinases. *Mol Microbiol* **75**: 547-566.

Burbulys, D., K. A. Trach & J. A. Hoch, (1991) Initiation of sporulation in B. subtilis is controlled by a multicomponent phosphorelay. *Cell* **64**: 545-552.

Burnens, A. P., J. Stanley, R. Sack, P. Hunziker, I. Brodard & J. Nicolet, (1997) The flagellin N-methylase gene fliB and an adjacent serovar-specific IS200 element in Salmonella typhimurium. *Microbiology (Reading, Engl)* **143 (Pt 5)**: 1539-1547.

Capela, D., F. Barloy-Hubler, J. Gouzy, G. Bothe, F. Ampe, J. Batut, P. Boistard, A. Becker, M. Boutry, E. Cadieu, S. Dréano, S. Gloux, T. Godrie, A. Goffeau, D. Kahn, E. Kiss, V. Lelaure, D. Masuy, T. Pohl, D. Portetelle, A. Pühler, B. Purnelle, U. Ramsperger, C. Renard, P. Thébault, M. Vandenbol, S. Weidner & F. Galibert, (2001) Analysis of the chromosome sequence of the legume symbiont Sinorhizobium meliloti strain 1021. *Proceedings of the National Academy of Sciences of the United States of America* **98**: 9877-9882.

Chand, N. S., J. S.-W. Lee, A. E. Clatworthy, A. J. Golas, R. S. Smith & D. T. Hung, (2011) The sensor kinase KinB regulates virulence in acute Pseudomonas aeruginosa infection. *J Bacteriol* **193**: 2989-2999.

Chemier, J. A., Z. L. Fowler, M. A. G. Koffas & E. Leonard, (2009) Trends in microbial synthesis of natural products and biofuels. *Adv Enzymol Relat Areas Mol Biol* **76**: 151-217.

Cheng, L. W. & O. Schneewind, (2000) Type III machines of Gram-negative bacteria: delivering the goods. *Trends in Microbiology* **8**: 214-220.

Chevance, F. F. V. & K. T. Hughes, (2008) Coordinating assembly of a bacterial macromolecular machine. *Nat Rev Microbiol* **6**: 455-465.

Chilcott, G. S. & K. T. Hughes, (2000) Coupling of flagellar gene expression to flagellar assembly in Salmonella enterica serovar typhimurium and Escherichia coli. *Microbiol Mol Biol Rev* **64**: 694-708.

Christen, M., B. Christen, M. G. Allan, M. Folcher, P. Jenö, S. Grzesiek & U. Jenal, (2007) DgrA is a member of a new family of cyclic diguanosine monophosphate receptors and controls flagellar motor function in Caulobacter crescentus. *Proc Natl Acad Sci USA* **104**: 4112-4117.

Claret, L., S. R. Calder, M. Higgins & C. Hughes, (2003) Oligomerization and activation of the FliI ATPase central to bacterial flagellum assembly. *Mol Microbiol* **48**: 1349-1355.

Claret, L. & C. Hughes, (2000) Functions of the subunits in the FlhD(2)C(2) transcriptional master regulator of bacterial flagellum biogenesis and swarming. *J Mol Biol* **303**: 467-478.

Clarke, M. B. & V. Sperandio, (2005) Transcriptional regulation of flhDC by QseBC and sigma (FliA) in enterohaemorrhagic Escherichia coli. *Mol Microbiol* **57**: 1734-1749.

Cohen, S. N., A. C. Chang & L. Hsu, (1972) Nonchromosomal antibiotic resistance in bacteria: genetic transformation of Escherichia coli by R-factor DNA. *Proceedings of the National Academy of Sciences of the United States of America* **69**: 2110-2114.

Conover, M. S., M. Mishra & R. Deora, (2011) Extracellular DNA is essential for maintaining Bordetella biofilm integrity on abiotic surfaces and in the upper respiratory tract of mice. *PLoS ONE* **6**: e16861.

Correa, N. E., F. Peng & K. E. Klose, (2005) Roles of the regulatory proteins FlhF and FlhG in the Vibrio cholerae flagellar transcription hierarchy. *Journal of bacteriology* **187**: 6324-6332.

Costerton, J. W., P. S. Stewart & E. P. Greenberg, (1999) Bacterial biofilms: a common cause of persistent infections. *Science* **284**: 1318-1322.

Craig, L., R. K. Taylor, M. E. Pique, B. D. Adair, A. S. Arvai, M. Singh, S. J. Lloyd, D. S. Shin, E. D. Getzoff, M. Yeager, K. T. Forest & J. A. Tainer, (2003) Type IV pilin structure and assembly: X-ray and EM analyses of Vibrio cholerae toxin-coregulated pilus and Pseudomonas aeruginosa PAK pilin. *Mol Cell* **11**: 1139-1150.

Curtis, P. D. & Y. V. Brun, (2010) Getting in the loop: regulation of development in Caulobacter crescentus. *Microbiol Mol Biol Rev* **74**: 13-41.

Dasgupta, N., M. C. Wolfgang, A. L. Goodman, S. K. Arora, J. Jyot, S. Lory & R. Ramphal, (2003) A four-tiered transcriptional regulatory circuit controls flagellar biogenesis in Pseudomonas aeruginosa. *Molecular Microbiology* **50**: 809-824.

Daughdrill, G. W., M. S. Chadsey, J. E. Karlinsey, K. T. Hughes & F. W. Dahlquist, (1997) The C-terminal half of the anti-sigma factor, FlgM, becomes structured when bound to its target, sigma 28. *Nat Struct Biol* **4**: 285-291.

Davis, N. J. & P. H. Viollier, (2011) Probing flagellar promoter occupancy in wild-type and mutant Caulobacter crescentus by chromatin immunoprecipitation. *FEMS Microbiology Letters* **319**: 146-152.

Deakin, W. J., V. E. Parker, E. L. Wright, K. J. Ashcroft, G. J. Loake & C. H. Shaw, (1999) Agrobacterium tumefaciens possesses a fourth flagelin gene located in a large gene cluster concerned with flagellar structure, assembly and motility. *Microbiology (Reading, Engl)* **145 (Pt 6)**: 1397-1407.

Dingwall, A., J. D. Garman & L. Shapiro, (1992) Organization and ordered expression of Caulobacter genes encoding flagellar basal body rod and ring proteins. *J Mol Biol* **228**: 1147-1162.

Domian, I. J., K. C. Quon & L. Shapiro, (1997) Cell type-specific phosphorylation and proteolysis of a transcriptional regulator controls the G1-to-S transition in a bacterial cell cycle. *Cell* **90**: 415-424.

Douillard, F. P., K. A. Ryan, M. C. Lane, D. L. Caly, S. A. Moore, C. W. Penn, J. Hinds & P. W. O'Toole, (2010) The HP0256 gene product is involved in motility and cell envelope architecture of Helicobacter pylori. *BMC Microbiol* **10**: 106.

Driks, A., R. Bryan, L. Shapiro & D. J. DeRosier, (1989) The organization of the Caulobacter crescentus flagellar filament. *Journal of Molecular Biology* **206**: 627-636.

Driks, A., P. V. Schoenlein, D. J. DeRosier, L. Shapiro & B. Ely, (1990) A Caulobacter gene involved in polar morphogenesis. *J Bacteriol* **172**: 2113-2123.

Dutta, R., L. Qin & M. Inouye, (1999) Histidine kinases: diversity of domain organization. *Mol Microbiol* **34**: 633-640.

Ely, B. & T. W. Ely, (1989) Use of pulsed field gel electrophoresis and transposon mutagenesis to estimate the minimal number of genes required for motility in Caulobacter crescentus. *Genetics* **123**: 649-654.

Ely, B., T. W. Ely, W. B. Crymes & S. A. Minnich, (2000) A family of six flagellin genes contributes to the Caulobacter crescentus flagellar filament. *J Bacteriol* **182**: 5001-5004.

Erhardt, M., H. M. Singer, D. H. Wee, J. P. Keener & K. T. Hughes, (2011) An infrequent molecular ruler controls flagellar hook length in Salmonella enterica. *The EMBO Journal* **30**: 2948-2961.

Errington, J., (2010) From spores to antibiotics via the cell cycle. *Microbiology (Reading, Engl)* **156**: 1-13.

Evans, L. D. B., G. P. Stafford, S. Ahmed, G. M. Fraser & C. Hughes, (2006) An escort mechanism for cycling of export chaperones during flagellum assembly. *Proceedings of the National Academy of Sciences of the United States of America* **103**: 17474-17479.

Evinger, M. & N. Agabian, (1977) Envelope-associated nucleoid from Caulobacter crescentus stalked and swarmer cells. *J Bacteriol* **132**: 294-301.

Ewing, C. P., E. Andreishcheva & P. Guerry, (2009) Functional characterization of flagellin glycosylation in Campylobacter jejuni 81-176. *J Bacteriol* **191**: 7086-7093.

Fan, F. & R. M. Macnab, (1996) Enzymatic characterization of FliI. An ATPase involved in flagellar assembly in Salmonella typhimurium. *J Biol Chem* **271**: 31981-31988.

Faulds-Pain, A., C. Birchall, C. Aldridge, W. D. Smith, G. Grimaldi, S. Nakamura, T. Miyata, J. Gray, G. Li, J. Tang, K. Namba, T. Minamino & P. D. Aldridge, (2011) Flagellin redundancy in Caulobacter crescentus and its implications for flagellar filament assembly. *J Bacteriol*.

Ferooz, J., J. Lemaire & J.-J. Letesson, (2011) Role of FlbT in flagellin production in Brucella melitensis. *Microbiology (Reading, Engl)* **157**: 1253-1262.

Finn, R. D., J. Mistry, J. Tate, P. Coggill, A. Heger, J. E. Pollington, O. L. Gavin, P. Gunasekaran, G. Ceric, K. Forslund, L. Holm, E. L. L. Sonnhammer, S. R. Eddy & A. Bateman, (2010) The Pfam protein families database. *Nucleic Acids Research* **38**: D211-222.

Flemming, H.-C., (2011) The perfect slime. *Colloids Surf B Biointerfaces* **86**: 251-259.

Flemming, H.-C. & J. Wingender, (2010) The biofilm matrix. *Nat Rev Microbiol* **8**: 623-633.

Francis, N. R., G. E. Sosinsky, D. Thomas & D. J. DeRosier, (1994) Isolation, characterization and structure of bacterial flagellar motors containing the switch complex. *Journal of Molecular Biology* **235**: 1261-1270.

Fraser, G. M., J. C. Bennett & C. Hughes, (1999) Substrate-specific binding of hook-associated proteins by FlgN and FliT, putative chaperones for flagellum assembly. *Mol Microbiol* **32**: 569-580.

Fraser, G. M., B. González-Pedrajo, J. R. H. Tame & R. M. Macnab, (2003) Interactions of FliJ with the Salmonella type III flagellar export apparatus. *J Bacteriol* **185**: 5546-5554.

Fraser, G. M. & C. Hughes, (1999) Swarming motility. *Curr Opin Microbiol* **2**: 630-635.

Fujita, M. & R. Losick, (2003) The master regulator for entry into sporulation in Bacillus subtilis becomes a cell-specific transcription factor after asymmetric division. *Genes & Development* **17**: 1166-1174.

Fujita, M. & R. Losick, (2005) Evidence that entry into sporulation in Bacillus subtilis is governed by a gradual increase in the level and activity of the master regulator Spo0A. *Genes & Development* **19**: 2236-2244.

Galán, J. E., C. Ginocchio & P. Costeas, (1992) Molecular and functional characterization of the Salmonella invasion gene invA: homology of InvA to members of a new protein family. *J Bacteriol* **174**: 4338-4349.

Galkin, V. E., X. Yu, J. Bielnicki, J. Heuser, C. P. Ewing, P. Guerry & E. H. Egelman, (2008) Divergence of quaternary structures among bacterial flagellar filaments. *Science (New York, NY)* **320**: 382-385.

Gao, R., T. R. Mack & A. M. Stock, (2007) Bacterial response regulators: versatile regulatory strategies from common domains. *Trends Biochem Sci* **32**: 225-234.

Gilchrist, A. & J. Smit, (1991) Transformation of freshwater and marine caulobacters by electroporation. *J Bacteriol* **173**: 921-925.

Gillen, K. L. & K. T. Hughes, (1991) Molecular characterization of flgM, a gene encoding a negative regulator of flagellin synthesis in Salmonella typhimurium. *J Bacteriol* **173**: 6453-6459.

Giltner, C. L., M. Habash & L. L. Burrows, (2010) Pseudomonas aeruginosa minor pilins are incorporated into type IV pili. *Journal of Molecular Biology* **398**: 444-461.

Gober, J. W. & L. Shapiro, (1990) Integration host factor is required for the activation of developmentally regulated genes in Caulobacter. *Genes & Development* **4**: 1494-1504.

González, J. E. & M. M. Marketon, (2003) Quorum sensing in nitrogen-fixing rhizobia. *Microbiol Mol Biol Rev* **67**: 574-592.

Goodner, B., G. Hinkle, S. Gattung, N. Miller, M. Blanchard, B. Qurollo, B. S. Goldman, Y. Cao, M. Askenazi, C. Halling, L. Mullin, K. Houmiel, J. Gordon, M. Vaudin, O. Iartchouk, A. Epp, F. Liu, C. Wollam, M. Allinger, D. Doughty, C. Scott, C. Lappas, B. Markelz, C. Flanagan, C. Crowell, J. Gurson, C. Lomo, C. Sear, G. Strub, C. Cielo & S. Slater, (2001) Genome sequence of the plant pathogen and biotechnology agent Agrobacterium tumefaciens C58. *Science (New York, NY)* **294**: 2323-2328.

Goon, S., J. F. Kelly, S. M. Logan, C. P. Ewing & P. Guerry, (2003) Pseudaminic acid, the major modification on Campylobacter flagellin, is synthesized via the Cj1293 gene. *Mol Microbiol* **50**: 659-671.

Green, J., C. Kahramanoglou, A. Rahman, A. Pender, N. Charbonnel & G. Fraser, (2009) Recruitment of the Earliest Component of the Bacterial Flagellum to the Old Cell Division Pole by a Membrane-Associated Signal Recognition Particle Family GTP-Binding Protein. *J Mol Biol*.

Guerrero-Ferreira, R. C., P. H. Viollier, B. Ely, J. S. Poindexter, M. Georgieva, G. J. Jensen & E. R. Wright, (2011) Alternative mechanism for bacteriophage adsorption to the motile bacterium Caulobacter crescentus. *Proc Natl Acad Sci USA* **108**: 9963-9968.

Gupta, R. S. & A. Mok, (2007) Phylogenomics and signature proteins for the alpha proteobacteria and its main groups. *BMC Microbiol* **7**: 106.

Hager, D. A. & R. R. Burgess, (1980) Elution of proteins from sodium dodecyl sulfate-polyacrylamide gels, removal of sodium dodecyl sulfate, and renaturation of enzymatic activity: results with sigma subunit of Escherichia coli RNA polymerase, wheat germ DNA topoisomerase, and other enzymes. *Analytical Biochemistry* **109**: 76-86.

Hahnenberger, K. M. & L. Shapiro, (1987) Identification of a gene cluster involved in flagellar basal body biogenesis in Caulobacter crescentus. *J Mol Biol* **194**: 91-103.

Harris, L. A., S. M. Logan, P. Guerry & T. J. Trust, (1987) Antigenic variation of Campylobacter flagella. *J Bacteriol* **169**: 5066-5071.

Harshey, R. M., (2003) Bacterial motility on a surface: many ways to a common goal. *Annu. Rev. Microbiol.* **57**: 249-273.

Helmann, J. D., L. M. Márquez & M. J. Chamberlin, (1988) Cloning, sequencing, and disruption of the Bacillus subtilis sigma 28 gene. *J Bacteriol* **170**: 1568-1574.

Hickman, J. W. & C. S. Harwood, (2008) Identification of FleQ from Pseudomonas aeruginosa as a c-di-GMP-responsive transcription factor. *Mol Microbiol* **69**: 376-389.

Hirano, T., T. Minamino & R. M. Macnab, (2001) The role in flagellar rod assembly of the N-terminal domain of Salmonella FlgJ, a flagellum-specific muramidase. *J Mol Biol* **312**: 359-369.

Hirano, T., S. Yamaguchi, K. Oosawa & S. Aizawa, (1994) Roles of FliK and FlhB in determination of flagellar hook length in Salmonella typhimurium. *J Bacteriol* **176**: 5439-5449.

Hoang, H. H., N. Gurich & J. E. González, (2008) Regulation of motility by the ExpR/Sin quorum-sensing system in Sinorhizobium meliloti. *J Bacteriol* **190**: 861-871.

Hobbs, M., E. S. Collie, P. D. Free, S. P. Livingston & J. S. Mattick, (1993) PilS and PilR, a two-component transcriptional regulatory system controlling expression of type 4 fimbriae in Pseudomonas aeruginosa. *Mol Microbiol* **7**: 669-682.

Hoiczyk, E., (2000) Gliding motility in cyanobacterial: observations and possible explanations. *Arch Microbiol* **174**: 11-17.

Homma, M., H. Fujita, S. Yamaguchi & T. Iino, (1984) Excretion of unassembled flagellin by Salmonella typhimurium mutants deficient in hook-associated proteins. *Journal of bacteriology* **159**: 1056-1059.

Homma, M. & T. Iino, (1985) Locations of hook-associated proteins in flagellar structures of Salmonella typhimurium. *Journal of bacteriology* **162**: 183-189.

Homma, M., T. Iino, K. Kutsukake & S. Yamaguchi, (1986) In vitro reconstitution of flagellar filaments onto hooks of filamentless mutants of Salmonella typhimurium by addition of hook-associated proteins. *Proc Natl Acad Sci USA* **83**: 6169-6173.

Homma, M., Y. Komeda, T. Iino & R. M. Macnab, (1987) The flaFIX gene product of Salmonella typhimurium is a flagellar basal body component with a signal peptide for export. *J Bacteriol* **169**: 1493-1498.

Homma, M., K. Kutsukake, M. Hasebe, T. Iino & R. M. Macnab, (1990) FlgB, FlgC, FlgF and FlgG. A family of structurally related proteins in the flagellar basal body of Salmonella typhimurium. *J Mol Biol* **211**: 465-477.

Homma, M., K. Kutsukake, T. Iino & S. Yamaguchi, (1984) Hook-associated proteins essential for flagellar filament formation in Salmonella typhimurium. *Journal of bacteriology* **157**: 100-108.

Hosogi, N., H. Shigematsu, H. Terashima, M. Homma & K. Nagayama, (2011) Zernike phase contrast cryo-electron tomography of sodium-driven flagellar hook-basal bodies from Vibrio alginolyticus. *J Struct Biol* **173**: 67-76.

Hughes, K. T., K. L. Gillen, M. J. Semon & J. E. Karlinsey, (1993) Sensing structural intermediates in bacterial flagellar assembly by export of a negative regulator. *Science* **262**: 1277-1280.

Huitema, E., S. Pritchard, D. Matteson, S. Radhakrishnan & P. Viollier, (2006) Bacterial Birth Scar Proteins Mark Future Flagellum Assembly Site. *Cell* **124**: 1025-1037.

Iida, Y., L. Hobley, C. Lambert, A. K. Fenton, R. E. Sockett & S.-I. Aizawa, (2009) Roles of multiple flagellins in flagellar formation and flagellar growth post bdelloplast lysis in Bdellovibrio bacteriovorus. *Journal of Molecular Biology* **394**: 1011-1021.

Ikeda, J. S., C. K. Schmitt, S. C. Darnell, P. R. Watson, J. Bispham, T. S. Wallis, D. L. Weinstein, E. S. Metcalf, P. Adams, C. D. O'Connor & A. D. O'Brien, (2001) Flagellar phase variation of Salmonella enterica serovar Typhimurium contributes to virulence in the murine typhoid infection model but does not influence Salmonella-induced enteropathogenesis. *Infect Immun* **69**: 3021-3030.

Ikeda, T., M. Homma, T. Iino, S. Asakura & R. Kamiya, (1987) Localization and stoichiometry of hook-associated proteins within Salmonella typhimurium flagella. *Journal of bacteriology* **169**: 1168-1173.

Ikeda, T., S. Yamaguchi & H. Hotani, (1993) Flagellar growth in a filament-less Salmonella fliD mutant supplemented with purified hook-associated protein 2. *J Biochem* **114**: 39-44.

Imada, K., T. Minamino, M. Kinoshita, Y. Furukawa & K. Namba, (2010) Structural insight into the regulatory mechanisms of interactions of the flagellar type III chaperone FliT with its binding partners. *Proc Natl Acad Sci USA* **107**: 8812-8817.

Imada, K., T. Minamino, A. Tahara & K. Namba, (2007) Structural similarity between the flagellar type III ATPase FliI and F1-ATPase subunits. *Proceedings of the National Academy of Sciences of the United States of America* **104**: 485-490.

Imada, K., F. Vonderviszt, Y. Furukawa, K. Oosawa & K. Namba, (1998) Assembly characteristics of flagellar cap protein HAP2 of Salmonella: decamer and pentamer in the pH-sensitive equilibrium. *J Mol Biol* **277**: 883-891.

Imae, Y. & T. Atsumi, (1989) Na+-driven bacterial flagellar motors. *J Bioenerg Biomembr* **21**: 705-716.

Iniesta, A. A., P. T. McGrath, A. Reisenauer, H. H. McAdams & L. Shapiro, (2006) A phospho-signaling pathway controls the localization and activity of a protease complex critical for bacterial cell cycle progression. *Proceedings of the National Academy of Sciences of the United States of America* **103**: 10935-10940.

Jarrell, K. F. & M. J. McBride, (2008) The surprisingly diverse ways that prokaryotes move. *Nat Rev Microbiol* **6**: 466-476.

Jenal, U. & T. Fuchs, (1998) An essential protease involved in bacterial cell-cycle control. *EMBO J* **17**: 5658-5669.

Jenal, U. & J. Malone, (2006) Mechanisms of cyclic-di-GMP signaling in bacteria. *Annu Rev Genet* **40**: 385-407.

Jenal, U. & L. Shapiro, (1996) Cell cycle-controlled proteolysis of a flagellar motor protein that is asymmetrically distributed in the Caulobacter predivisional cell. *EMBO J* **15**: 2393-2406.

Jenal, U., J. White & L. Shapiro, (1994) Caulobacter flagellar function, but not assembly, requires FliL, a non-polarly localized membrane protein present in all cell types. *J Mol Biol* **243**: 227-244.

Jiang, M., W. Shao, M. Perego & J. A. Hoch, (2000) Multiple histidine kinases regulate entry into stationary phase and sporulation in Bacillus subtilis. *Mol Microbiol* **38**: 535-542.

Jin, S., K. S. Ishimoto & S. Lory, (1994) PilR, a transcriptional regulator of piliation in Pseudomonas aeruginosa, binds to a cis-acting sequence upstream of the pilin gene promoter. *Mol Microbiol* **14**: 1049-1057.

Johnson, R. C. & B. Ely, (1979) Analysis of nonmotile mutants of the dimorphic bacterium Caulobacter crescentus. *J Bacteriol* **137**: 627-634.

Johnson, R. C., D. M. Ferber & B. Ely, (1983) Synthesis and assembly of flagellar components by Caulobacter crescentus motility mutants. *J Bacteriol* **154**: 1137-1144.

Jones, C. J., M. Homma & R. M. Macnab, (1987) Identification of proteins of the outer (L and P) rings of the flagellar basal body of Escherichia coli. *J Bacteriol* **169**: 1489-1492.

Jones, C. J., M. Homma & R. M. Macnab, (1989) L-, P-, and M-ring proteins of the flagellar basal body of Salmonella typhimurium: gene sequences and deduced protein sequences. *J Bacteriol* **171**: 3890-3900.

Jones, K. M., H. Kobayashi, B. W. Davies, M. E. Taga & G. C. Walker, (2007) How rhizobial symbionts invade plants: the Sinorhizobium-Medicago model. *Nat Rev Micro* **5**: 619-633.

Jones, S. E., N. L. Ferguson & M. R. Alley, (2001) New members of the ctrA regulon: the major chemotaxis operon in Caulobacter is CtrA dependent. *Microbiology (Reading, Engl)* **147**: 949-958.

Journet, L., (2003) The Needle Length of Bacterial Injectisomes Is Determined by a Molecular Ruler. *Science* **302**: 1757-1760.

Kaiser, D., (2000) Bacterial motility: how do pili pull? *Curr Biol* **10**: R777-780.

Kanbe, M., S. Shibata, Y. Umino, U. Jenal & S.-I. Aizawa, (2005) Protease susceptibility of the Caulobacter crescentus flagellar hook-basal body: a possible mechanism of flagellar ejection during cell differentiation. *Microbiology (Reading, Engl)* **151**: 433-438.

Kanehisa, M., M. Araki, S. Goto, M. Hattori, M. Hirakawa, M. Itoh, T. Katayama, S. Kawashima, S. Okuda, T. Tokimatsu & Y. Yamanishi, (2008) KEGG for linking genomes to life and the environment. *Nucleic Acids Res* **36**: D480-484.

Kawai, T. & S. Akira, (2011) Toll-like receptors and their crosstalk with other innate receptors in infection and immunity. *Immunity* **34**: 637-650.

Kearns, D. B. & R. Losick, (2005) Cell population heterogeneity during growth of Bacillus subtilis. *Genes Dev* **19**: 3083-3094.

Kelly-Wintenberg, K., S. L. South & T. C. Montie, (1993) Tyrosine phosphate in a- and b-type flagellins of Pseudomonas aeruginosa. *J Bacteriol* **175**: 2458-2461.

Khambaty, F. M. & B. Ely, (1992) Molecular genetics of the flgI region and its role in flagellum biosynthesis in Caulobacter crescentus. *Journal of bacteriology* **174**: 4101-4109.

Kitao, A., K. Yonekura, S. Maki-Yonekura, F. A. Samatey, K. Imada, K. Namba & N. Go, (2006) Switch interactions control energy frustration and multiple flagellar filament structures. *Proc Natl Acad Sci USA* **103**: 4894-4899.

Kline, K. A., K. W. Dodson, M. G. Caparon & S. J. Hultgren, (2010) A tale of two pili: assembly and function of pili in bacteria. *Trends Microbiol* **18**: 224-232.

Klose, K. E. & J. J. Mekalanos, (1998) Differential regulation of multiple flagellins in Vibrio cholerae. *J Bacteriol* **180**: 303-316.

Kojima, S., K. Yamamoto, I. Kawagishi & M. Homma, (1999) The polar flagellar motor of Vibrio cholerae is driven by an Na+ motive force. *J Bacteriol* **181**: 1927-1930.

Kornacker, M. G. & A. Newton, (1994) Information essential for cell-cycle-dependent secretion of the 591-residue Caulobacter hook protein is confined to a 21-amino-acid sequence near the N-terminus. *Mol Microbiol* **14**: 73-85.

Kubori, T., S. Yamaguchi & S. Aizawa, (1997) Assembly of the switch complex onto the MS ring complex of Salmonella typhimurium does not require any other flagellar proteins. *J Bacteriol* **179**: 813-817.

Kusumoto, A., K. Kamisaka, T. Yakushi, H. Terashima, A. Shinohara & M. Homma, (2006) Regulation of polar flagellar number by the flhF and flhG genes in Vibrio alginolyticus. *J Biochem* **139**: 113-121.

Kusumoto, A., A. Shinohara, H. Terashima, S. Kojima, T. Yakushi & M. Homma, (2008) Collaboration of FlhF and FlhG to regulate polar-flagella number and localization in Vibrio alginolyticus. *Microbiology (Reading, Engl)* **154**: 1390-1399.

Kutsukake, K., (1997) Autogenous and global control of the flagellar master operon, flhD, in Salmonella typhimurium. *Mol Gen Genet* **254**: 440-448.

Kutsukake, K., Y. Ohya & T. Iino, (1990) Transcriptional analysis of the flagellar regulon of Salmonella typhimurium. *J Bacteriol* **172**: 741-747.

Lambert, C., K. J. Evans, R. Till, L. Hobley, M. Capeness, S. Rendulic, S. C. Schuster, S.-I. Aizawa & R. E. Sockett, (2006) Characterizing the flagellar filament and the role of motility in bacterial prey-penetration by Bdellovibrio bacteriovorus. *Mol Microbiol* **60**: 274-286.

Larsen, S. H., R. W. Reader, E. N. Kort, W. W. Tso & J. Adler, (1974) Change in direction of flagellar rotation is the basis of the chemotactic response in Escherichia coli. *Nature* **249**: 74-77.

Laub, M. T., S. L. Chen, L. Shapiro & H. H. McAdams, (2002) Genes directly controlled by CtrA, a master regulator of the Caulobacter cell cycle. *Proc Natl Acad Sci USA* **99**: 4632-4637.

Laub, M. T., H. H. McAdams, T. Feldblyum, C. M. Fraser & L. Shapiro, (2000) Global analysis of the genetic network controlling a bacterial cell cycle. *Science* **290**: 2144-2148.

Leclerc, G., S. P. Wang & B. Ely, (1998) A new class of Caulobacter crescentus flagellar genes. *J Bacteriol* **180**: 5010-5019.

Lee, K. K., H. B. Sheth, W. Y. Wong, R. Sherburne, W. Paranchych, R. S. Hodges, C. A. Lingwood, H. Krivan & R. T. Irvin, (1994) The binding of Pseudomonas aeruginosa pili to glycosphingolipids is a tip-associated event involving the C-terminal region of the structural pilin subunit. *Mol Microbiol* **11**: 705-713.

Levi, A. & U. Jenal, (2006) Holdfast formation in motile swarmer cells optimizes surface attachment during Caulobacter crescentus development. *J Bacteriol* **188**: 5315-5318.

Li, C., M. Sal, M. Marko & N. W. Charon, (2010) Differential regulation of the multiple flagellins in spirochetes. *J Bacteriol* **192**: 2596-2603.

Li, G. & J. X. Tang, (2006) Low flagellar motor torque and high swimming efficiency of Caulobacter crescentus swarmer cells. *Biophysical Journal* **91**: 2726-2734.

Llewellyn, M., R. J. Dutton, J. Easter, D. O'donnol & J. W. Gober, (2005) The conserved flaF gene has a critical role in coupling flagellin translation and assembly in Caulobacter crescentus. *Mol Microbiol* **57**: 1127-1142.

Lloyd, S. A., M. Norman, R. Rosqvist & H. Wolf-Watz, (2001) Yersinia YopE is targeted for type III secretion by N-terminal, not mRNA, signals. *Mol Microbiol* **39**: 520-531.

Logan, S. M., (2006) Flagellar glycosylation - a new component of the motility repertoire? *Microbiology (Reading, Engl)* **152**: 1249-1262.

López-Vidal, Y., S. Ponce-de-León, G. Castillo-Rojas, R. Barreto-Zúñiga & A. Torre-Delgadillo, (2008) High diversity of vacA and cagA Helicobacter pylori genotypes in patients with and without gastric cancer. *PLoS ONE* **3**: e3849.

Lowe, P. A., D. A. Hager & R. R. Burgess, (1979) Purification and properties of the sigma subunit of Escherichia coli DNA-dependent RNA polymerase. *Biochemistry* **18**: 1344-1352.

Lugtu, R. T., S.-C. Choi & Y.-S. Oh, (2009) Arsenite oxidation by a facultative chemolithotrophic bacterium SDB1 isolated from mine tailing. *J Microbiol* **47**: 686-692.

Macnab, R. M., (2004) Type III flagellar protein export and flagellar assembly. *Biochim Biophys Acta* **1694**: 207-217.

Macnab, R. M. & M. K. Ornston, (1977) Normal-to-curly flagellar transitions and their role in bacterial tumbling. Stabilization of an alternative quaternary structure by mechanical force. *J Mol Biol* **112**: 1-30.

Magariyama, Y., S. Sugiyama & S. Kudo, (2001) Bacterial swimming speed and rotation rate of bundled flagella. *FEMS Microbiol Lett* **199**: 125-129.

Magariyama, Y., S. Sugiyama, K. Muramoto, I. Kawagishi, Y. Imae & S. Kudo, (1995) Simultaneous measurement of bacterial flagellar rotation rate and swimming speed. *Biophysical Journal* **69**: 2154-2162.

Malakooti, J., S. P. Wang & B. Ely, (1995) A consensus promoter sequence for Caulobacter crescentus genes involved in biosynthetic and housekeeping functions. *Journal of bacteriology* **177**: 4372-4376.

Mallozzi, M., V. K. Viswanathan & G. Vedantam, (2010) Spore-forming Bacilli and Clostridia in human disease. *Future Microbiol* **5**: 1109-1123.

Mangan, E. K., J. Malakooti, A. Caballero, P. Anderson, B. Ely & J. W. Gober, (1999) FlbT couples flagellum assembly to gene expression in Caulobacter crescentus. *J Bacteriol* **181**: 6160-6170.

Márquez, L. M., J. D. Helmann, E. Ferrari, H. M. Parker, G. W. Ordal & M. J. Chamberlin, (1990) Studies of sigma D-dependent functions in Bacillus subtilis. *J Bacteriol* **172**: 3435-3443.

Masepohl, B. & P. C. Hallenbeck, (2010) Nitrogen and molybdenum control of nitrogen fixation in the phototrophic bacterium Rhodobacter capsulatus. *Adv Exp Med Biol* **675**: 49-70.

Matroule, J.-Y., H. Lam, D. T. Burnette & C. Jacobs-Wagner, (2004) Cytokinesis monitoring during development; rapid pole-to-pole shuttling of a signaling protein by localized kinase and phosphatase in Caulobacter. *Cell* **118**: 579-590.

Mattick, J. S., (2002) Type IV pili and twitching motility. *Annu. Rev. Microbiol.* **56**: 289-314.

Mauriello, E. M. F., T. Mignot, Z. Yang & D. R. Zusman, (2010) Gliding motility revisited: how do the myxobacteria move without flagella? *Microbiol Mol Biol Rev* **74**: 229-249.

McBride, M. J., (2001) Bacterial gliding motility: multiple mechanisms for cell movement over surfaces. *Annu Rev Microbiol* **55**: 49-75.

Mccarter, L., (1999) The multiple identities of Vibrio parahaemolyticus. *J Mol Microbiol Biotechnol* **1**: 51-57.

McCarter, L. L., (2001) Polar flagellar motility of the Vibrionaceae. *Microbiol Mol Biol Rev* **65**: 445-462, table of contents.

McGrath, P. T., A. A. Iniesta, K. R. Ryan, L. Shapiro & H. H. McAdams, (2006) A dynamically localized protease complex and a polar specificity factor control a cell cycle master regulator. *Cell* **124**: 535-547.

Mikkelsen, H., M. Sivaneson & A. Filloux, (2011) Key two-component regulatory systems that control biofilm formation in Pseudomonas aeruginosa. *Environ Microbiol* **13**: 1666-1681.

Miller, M. B. & B. L. Bassler, (2001) Quorum sensing in bacteria. *Annu. Rev. Microbiol.* **55**: 165-199.

Millikan, D. S. & E. G. Ruby, (2004) Vibrio fischeri flagellin A is essential for normal motility and for symbiotic competence during initial squid light organ colonization. *J Bacteriol* **186**: 4315-4325.

Minamino, T., R. Chu, S. Yamaguchi & R. M. Macnab, (2000) Role of FliJ in flagellar protein export in Salmonella. *J Bacteriol* **182**: 4207-4215.

Minamino, T., B. González-Pedrajo, K. Yamaguchi, S. I. Aizawa & R. M. Macnab, (1999) FliK, the protein responsible for flagellar hook length control in Salmonella, is exported during hook assembly. *Mol Microbiol* **34**: 295-304.

Minamino, T., K. Imada & K. Namba, (2008) Mechanisms of type III protein export for bacterial flagellar assembly. *Mol Biosyst* **4**: 1105-1115.

Minamino, T., K.-i. Kazetani, A. Tahara, H. Suzuki, Y. Furukawa, M. Kihara & K. Namba, (2006) Oligomerization of the bacterial flagellar ATPase FliI is controlled by its extreme N-terminal region. *Journal of Molecular Biology* **360**: 510-519.

Minamino, T. & R. M. Macnab, (1999) Components of the Salmonella flagellar export apparatus and classification of export substrates. *J Bacteriol* **181**: 1388-1394.

Minamino, T. & R. M. Macnab, (2000a) FliH, a soluble component of the type III flagellar export apparatus of Salmonella, forms a complex with FliI and inhibits its ATPase activity. *Mol Microbiol* **37**: 1494-1503.

Minamino, T. & R. M. Macnab, (2000b) Interactions among components of the Salmonella flagellar export apparatus and its substrates. *Mol Microbiol* **35**: 1052-1064.

Minamino, T. & R. M. Macnab, (2000c) Domain structure of Salmonella FlhB, a flagellar export component responsible for substrate specificity switching. *J Bacteriol* **182**: 4906-4914.

Minamino, T., N. Moriya, T. Hirano, K. T. Hughes & K. Namba, (2009) Interaction of FliK with the bacterial flagellar hook is required for efficient export specificity switching. *Mol Microbiol* **74**: 239-251.

Minamino, T. & K. Namba, (2008) Distinct roles of the FliI ATPase and proton motive force in bacterial flagellar protein export. *Nature* **451**: 485-488.

Minamino, T., S. Yamaguchi & R. M. Macnab, (2000) Interaction between FliE and FlgB, a proximal rod component of the flagellar basal body of Salmonella. *J Bacteriol* **182**: 3029-3036.

Minnich, S. A., N. Ohta, N. Taylor & A. Newton, (1988) Role of the 25-, 27-, and 29-kilodalton flagellins in Caulobacter crescentus cell motility: method for construction of deletion and Tn5 insertion mutants by gene replacement. *J Bacteriol* **170**: 3953-3960.

Mizuno, S., H. Amida, N. Kobayashi, S.-I. Aizawa & S.-i. Tate, (2011) The NMR structure of FliK, the trigger for the switch of substrate specificity in the flagellar type III secretion apparatus. *J Mol Biol* **409**: 558-573.

Mohr, C. D., U. Jenal & L. Shapiro, (1996) Flagellar assembly in Caulobacter crescentus: a basal body P-ring null mutation affects stability of the L-ring protein. *Journal of bacteriology* **178**: 675-682.

Mohr, C. D., J. K. MacKichan & L. Shapiro, (1998) A membrane-associated protein, FliX, is required for an early step in Caulobacter flagellar assembly. *Journal of bacteriology* **180**: 2175-2185.

Moir, A., (2006) How do spores germinate? *J Appl Microbiol* **101**: 526-530.

Morett, E. & L. Segovia, (1993) The sigma 54 bacterial enhancer-binding protein family: mechanism of action and phylogenetic relationship of their functional domains. *J Bacteriol* **175**: 6067-6074.

Morgan, D. G., R. M. Macnab, N. R. Francis & D. J. DeRosier, (1993) Domain organization of the subunit of the Salmonella typhimurium flagellar hook. *J Mol Biol* **229**: 79-84.

Moriya, N., T. Minamino, K. Hughes, R. Macnab & K. Namba, (2006) The Type III Flagellar Export Specificity Switch is Dependent on FliK Ruler and a Molecular Clock. *Journal of Molecular Biology* **359**: 466-477.

Muir, R. E., J. Easter & J. W. Gober, (2005) The trans-acting flagellar regulatory proteins, FliX and FlbD, play a central role in linking flagellar biogenesis and cytokinesis in Caulobacter crescentus. *Microbiology (Reading, Engl)* **151**: 3699-3711.

Muir, R. E. & J. W. Gober, (2002) Mutations in FlbD that relieve the dependency on flagellum assembly alter the temporal and spatial pattern of developmental transcription in Caulobacter crescentus. *Mol Microbiol* **43**: 597-615.

Muir, R. E. & J. W. Gober, (2004) Regulation of FlbD activity by flagellum assembly is accomplished through direct interaction with the trans-acting factor, FliX. *Mol Microbiol* **54**: 715-730.

Muir, R. E. & J. W. Gober, (2005) Role of integration host factor in the transcriptional activation of flagellar gene expression in Caulobacter crescentus. *J Bacteriol* **187**: 949-960.

Muir, R. E., T. M. O'Brien & J. W. Gober, (2001) The Caulobacter crescentus flagellar gene, fliX, encodes a novel trans-acting factor that couples flagellar assembly to transcription. *Mol Microbiol* **39**: 1623-1637.

Müller, V., C. J. Jones, I. Kawagishi, S. Aizawa & R. M. Macnab, (1992) Characterization of the fliE genes of Escherichia coli and Salmonella typhimurium and identification of the FliE protein as a component of the flagellar hook-basal body complex. *J Bacteriol* **174**: 2298-2304.

Mullin, D. A. & A. Newton, (1989) Ntr-like promoters and upstream regulatory sequence ftr are required for transcription of a developmentally regulated Caulobacter crescentus flagellar gene. *Journal of bacteriology* **171**: 3218-3227.

Mullin, D. A., N. Ohta, A. H. Mullin & A. Newton, (2001) Organization, expression, and function of Caulobacter crescentus genes needed for assembly and function of the flagellar hook. *Mol Genet Genomics* **265**: 445-454.

Mullin, D. A., S. M. Van Way, C. A. Blankenship & A. H. Mullin, (1994) FlbD has a DNA-binding activity near its carboxy terminus that recognizes ftr sequences involved in positive and negative regulation of flagellar gene transcription in Caulobacter crescentus. *J Bacteriol* **176**: 5971-5981.

Murray, T. S. & B. I. Kazmierczak, (2006) FlhF is required for swimming and swarming in Pseudomonas aeruginosa. *Journal of bacteriology* **188**: 6995-7004.

Nakamura, S., Y. V. Morimoto, N. Kami-ike, T. Minamino & K. Namba, (2009) Role of a conserved prolyl residue (Pro173) of MotA in the mechanochemical reaction cycle of the proton-driven flagellar motor of Salmonella. *J Mol Biol* **393**: 300-307.

Nambu, T., T. Minamino, R. M. Macnab & K. Kutsukake, (1999) Peptidoglycan-hydrolyzing activity of the FlgJ protein, essential for flagellar rod formation in Salmonella typhimurium. *J Bacteriol* **181**: 1555-1561.

Nan, B., J. Chen, J. C. Neu, R. M. Berry, G. Oster & D. R. Zusman, (2011) Myxobacteria gliding motility requires cytoskeleton rotation powered by proton motive force. *Proc Natl Acad Sci USA* **108**: 2498-2503.

Nan, B. & D. R. Zusman, (2010) Uncovering the Mystery of Gliding Motility in the Myxobacteria. *Annu Rev Genet*.

Nierman, W. C., T. V. Feldblyum, M. T. Laub, I. T. Paulsen, K. E. Nelson, J. A. Eisen, J. F. Heidelberg, M. R. Alley, N. Ohta, J. R. Maddock, I. Potocka, W. C. Nelson, A. Newton, C. Stephens, N. D. Phadke, B. Ely, R. T. DeBoy, R. J. Dodson, A. S. Durkin, M. L. Gwinn, D. H. Haft, J. F. Kolonay, J. Smit, M. B. Craven, H. Khouri, J. Shetty, K. Berry, T. Utterback, K. Tran, A. Wolf, J. Vamathevan, M. Ermolaeva, O. White, S. L. Salzberg, J. C. Venter, L. Shapiro, C. M. Fraser & J. Eisen, (2001) Complete genome sequence of Caulobacter crescentus. *Proc Natl Acad Sci USA* **98**: 4136-4141.

Nishihara, T. & E. Freese, (1975) Motility of Bacillus subtilis during growth and sporulation. *J Bacteriol* **123**: 366-371.

Nuijten, P. J., F. J. van Asten, W. Gaastra & B. A. van der Zeijst, (1990) Structural and functional analysis of two Campylobacter jejuni flagellin genes. *J Biol Chem* **265**: 17798-17804.

O'Toole, G., H. B. Kaplan & R. Kolter, (2000) Biofilm formation as microbial development. *Annu Rev Microbiol* **54**: 49-79.

O'Toole, G. A. & R. Kolter, (1998) Flagellar and twitching motility are necessary for Pseudomonas aeruginosa biofilm development. *Mol Microbiol* **30**: 295-304.

Oberpichler, I., R. Rosen, A. Rasouly, M. Vugman, E. Z. Ron & T. Lamparter, (2008) Light affects motility and infectivity of Agrobacterium tumefaciens. *Environ Microbiol* **10**: 2020-2029.

Ohnishi, K., K. Kutsukake, H. Suzuki & T. Iino, (1990) Gene fliA encodes an alternative sigma factor specific for flagellar operons in Salmonella typhimurium. *Mol Gen Genet* **221**: 139-147.

Ohnishi, K., K. Kutsukake, H. Suzuki & T. Lino, (1992) A novel transcriptional regulation mechanism in the flagellar regulon of Salmonella typhimurium: an antisigma factor inhibits the activity of the flagellum-specific sigma factor, sigma F. *Mol Microbiol* **6**: 3149-3157.

Ohnishi, K., Y. Ohto, S. Aizawa, R. M. Macnab & T. Iino, (1994) FlgD is a scaffolding protein needed for flagellar hook assembly in Salmonella typhimurium. *J Bacteriol* **176**: 2272-2281.

Ohta, N., L. S. Chen & A. Newton, (1982) Isolation and expression of cloned hook protein gene from Caulobacter crescentus. *Proc Natl Acad Sci USA* **79**: 4863-4867.

Ong, C. J., M. L. Wong & J. Smit, (1990) Attachment of the adhesive holdfast organelle to the cellular stalk of Caulobacter crescentus. *J Bacteriol* **172**: 1448-1456.

Osterberg, S., T. D. Peso-Santos & V. Shingler, (2011) Regulation of Alternative Sigma Factor Use. *Annu. Rev. Microbiol.* **65**: 37-55.

Pallen, M. J. & N. J. Matzke, (2006) From The Origin of Species to the origin of bacterial flagella. *Nat Rev Microbiol* **4**: 784-790.

Parkinson, J. S., (1993) Signal transduction schemes of bacteria. *Cell* **73**: 857-871.

Parsek, M., & P. Aldridge. Choosing the right lifestyle: Regulation of developmental pathways by cyclic di-GMP. ASM Press 2010. The second meessenger cyclic di-GMP, ed A. J. Wolfe & K. L. Visick

Paul, R., T. Jaeger, S. Abel, I. Wiederkehr, M. Folcher, E. G. Biondi, M. T. Laub & U. Jenal, (2008) Allosteric regulation of histidine kinases by their cognate response regulator determines cell fate. *Cell* **133**: 452-461.

Paul, R., S. Weiser, N. C. Amiot, C. Chan, T. Schirmer, B. Giese & U. Jenal, (2004) Cell cycle-dependent dynamic localization of a bacterial response regulator with a novel di-guanylate cyclase output domain. *Genes & Development* **18**: 715-727.

Petrova, O. E. & K. Sauer, (2009) A novel signaling network essential for regulating Pseudomonas aeruginosa biofilm development. *PLoS Pathog* **5**: e1000668.

Piekarska, I., J. Rytka & B. Rempola, (2010) Regulation of sporulation in the yeast Saccharomyces cerevisiae. *Acta Biochim Pol* **57**: 241-250.

Piggot, P. J. & D. W. Hilbert, (2004) Sporulation of Bacillus subtilis. *Curr Opin Microbiol* **7**: 579-586.

Pitzschke, A. & H. Hirt, (2010) New insights into an old story: Agrobacterium-induced tumour formation in plants by plant transformation. *EMBO J* **29**: 1021-1032.

Poggio, S., C. Abreu-Goodger, S. Fabela, A. Osorio, G. Dreyfus, P. Vinuesa & L. Camarena, (2007) A complete set of flagellar genes acquired by horizontal transfer coexists with the endogenous flagellar system in Rhodobacter sphaeroides. *J Bacteriol* **189**: 3208-3216.

POINDEXTER, J. S., (1964) BIOLOGICAL PROPERTIES AND CLASSIFICATION OF THE CAULOBACTER GROUP. *Bacteriological reviews* **28**: 231-295.

Poindexter, J. S., (1981) The caulobacters: ubiquitous unusual bacteria. *Microbiol Rev* **45**: 123-179.

Potocka, I., M. Thein, M. ØSterås, U. Jenal & M. R. K. Alley, (2002) Degradation of a Caulobacter soluble cytoplasmic chemoreceptor is ClpX dependent. *J Bacteriol* **184**: 6635-6641.

Prouty, M. G., N. E. Correa & K. E. Klose, (2001) The novel sigma54- and sigma28-dependent flagellar gene transcription hierarchy of Vibrio cholerae. *Mol Microbiol* **39**: 1595-1609.

Quon, K. C., G. T. Marczynski & L. Shapiro, (1996) Cell cycle control by an essential bacterial two-component signal transduction protein. *Cell* **84**: 83-93.

Quon, K. C., B. Yang, I. J. Domian, L. Shapiro & G. T. Marczynski, (1998) Negative control of bacterial DNA replication by a cell cycle regulatory protein that binds at the chromosome origin. *Proc Natl Acad Sci USA* **95**: 120-125.

Ramakrishnan, G. & A. Newton, (1990) FlbD of Caulobacter crescentus is a homologue of the NtrC (NRI) protein and activates sigma 54-dependent flagellar gene promoters. *Proc Natl Acad Sci USA* **87**: 2369-2373.

Reitzer, L. J., R. Bueno, W. D. Cheng, S. A. Abrams, D. M. Rothstein, T. P. Hunt, B. Tyler & B. Magasanik, (1987) Mutations that create new promoters suppress the sigma 54 dependence of glnA transcription in Escherichia coli. *J Bacteriol* **169**: 4279-4284.

Ren, C.-P., S. A. Beatson, J. Parkhill & M. J. Pallen, (2005) The Flag-2 locus, an ancestral gene cluster, is potentially associated with a novel flagellar system from Escherichia coli. *J Bacteriol* **187**: 1430-1440.

Ritchings, B. W., E. C. Almira, S. Lory & R. Ramphal, (1995) Cloning and phenotypic characterization of fleS and fleR, new response regulators of Pseudomonas aeruginosa which regulate motility and adhesion to mucin. *Infect Immun* **63**: 4868-4876.

Roberts, A. P. & P. Mullany, (2010) Oral biofilms: a reservoir of transferable, bacterial, antimicrobial resistance. *Expert Rev Anti Infect Ther* **8**: 1441-1450.

Roper, M., C. Ellison, J. W. Taylor & N. L. Glass, (2011) Nuclear and genome dynamics in multinucleate ascomycete fungi. *Curr Biol* **21**: R786-793.

Ross, C. & E. Abel-Santos, (2010) The Ger receptor family from sporulating bacteria. *Curr Issues Mol Biol* **12**: 147-158.

Ross, P., R. Mayer & M. Benziman, (1991) Cellulose biosynthesis and function in bacteria. *Microbiol Rev* **55**: 35-58.

Ruby, E. G. & L. M. Asato, (1993) Growth and flagellation of Vibrio fischeri during initiation of the sepiolid squid light organ symbiosis. *Arch Microbiol* **159**: 160-167.

Saini, S., E. Floess, C. Aldridge, J. Brown, P. D. Aldridge & C. V. Rao, (2011) Continuous control of flagellar gene expression by the σ28-FlgM regulatory circuit in Salmonella enterica. *Mol Microbiol* **79**: 264-278.

Samatey, F. A., K. Imada, S. Nagashima, F. Vonderviszt, T. Kumasaka, M. Yamamoto & K. Namba, (2001) Structure of the bacterial flagellar protofilament and implications for a switch for supercoiling. *Nature* **410**: 331-337.

Samatey, F. A., H. Matsunami, K. Imada, S. Nagashima, T. R. Shaikh, D. R. Thomas, J. Z. Chen, D. J. Derosier, A. Kitao & K. Namba, (2004) Structure of the bacterial flagellar hook and implication for the molecular universal joint mechanism. *Nature* **431**: 1062-1068.

Sambrook, J. & D. William Russell, (2001) Molecular cloning: a laboratory manual: 2100.

Sanders, L. A., S. Van Way & D. A. Mullin, (1992) Characterization of the Caulobacter crescentus flbF promoter and identification of the inferred FlbF product as a homolog of the LcrD protein from a Yersinia enterocolitica virulence plasmid. *J Bacteriol* **174**: 857-866.

Sar, N., L. Mccarter, M. Simon & M. Silverman, (1990) Chemotactic control of the two flagellar systems of Vibrio parahaemolyticus. *J Bacteriol* **172**: 334-341.

Sato, K. & M. Homma, (2000) Functional reconstitution of the Na(+)-driven polar flagellar motor component of Vibrio alginolyticus. *J Biol Chem* **275**: 5718-5722.

Scharf, B., H. Schuster-Wolff-Bühring, R. Rachel & R. Schmitt, (2001) Mutational analysis of the Rhizobium lupini H13-3 and Sinorhizobium meliloti flagellin genes: importance of flagellin A for flagellar filament structure and transcriptional regulation. *J Bacteriol* **183**: 5334-5342.

Schirm, M., E. C. Soo, A. J. Aubry, J. Austin, P. Thibault & S. M. Logan, (2003) Structural, genetic and functional characterization of the flagellin glycosylation process in Helicobacter pylori. *Mol Microbiol* **48**: 1579-1592.

Schneider, W. R. & R. N. Doetsch, (1974) Effect of viscosity on bacterial motility. *J Bacteriol* **117**: 696-701.

Schoenlein, P. V. & B. Ely, (1989) Characterization of strains containing mutations in the contiguous flaF, flbT, or flbA-flaG transcription unit and identification of a novel fla phenotype in Caulobacter crescentus. *J Bacteriol* **171**: 1554-1561.

Schreiber, S., M. Konradt, C. Groll, P. Scheid, G. Hanauer, H.-O. Werling, C. Josenhans & S. Suerbaum, (2004) The spatial orientation of Helicobacter pylori in the gastric mucus. *Proc Natl Acad Sci USA* **101**: 5024-5029.

Schröder, G. & E. Lanka, (2005) The mating pair formation system of conjugative plasmids-A versatile secretion machinery for transfer of proteins and DNA. *Plasmid* **54**: 1-25.

Schübbe, S., T. J. Williams, G. Xie, H. E. Kiss, T. S. Brettin, D. Martinez, C. A. Ross, D. Schüler, B. L. Cox, K. H. Nealson & D. A. Bazylinski, (2009) Complete genome sequence of the chemolithoautotrophic marine magnetotactic coccus strain MC-1. *Appl Environ Microbiol* **75**: 4835-4852.

Semmler, A. B., C. B. Whitchurch & J. S. Mattick, (1999) A re-examination of twitching motility in Pseudomonas aeruginosa. *Microbiology (Reading, Engl)* **145 (Pt 10)**: 2863-2873.

Shaikh, T. R., D. R. Thomas, J. Z. Chen, F. A. Samatey, H. Matsunami, K. Imada, K. Namba & D. J. Derosier, (2005) A partial atomic structure for the flagellar hook of Salmonella typhimurium. *Proc Natl Acad Sci USA* **102**: 1023-1028.

Shapiro, L., (1976) Differentiation in the Caulobacter cell cycle. *Annu Rev Microbiol* **30**: 377-407.

Sheffery, M. & A. Newton, (1979) Purification and characterization of a polyhook protein from Caulobacter crescentus. *Journal of bacteriology* **138**: 575-583.

Shingler, V., (2010) Signal sensory systems that impact σ54-dependent transcription. *FEMS Microbiology Reviews* **35**: 425-440.

Simon, L. D., B. Randolph, N. Irwin & G. Binkowski, (1983) Stabilization of proteins by a bacteriophage T4 gene cloned in Escherichia coli. *Proc Natl Acad Sci USA* **80**: 2059-2062.

Skerker, J. M. & H. C. Berg, (2001) Direct observation of extension and retraction of type IV pili. *Proceedings of the National Academy of Sciences of the United States of America* **98**: 6901-6904.

Skerker, J. M., B. S. Perchuk, A. Siryaporn, E. A. Lubin, O. Ashenberg, M. Goulian & M. T. Laub, (2008) Rewiring the specificity of two-component signal transduction systems. *Cell* **133**: 1043-1054.

Smit, G., B. A. Smit & W. J. M. Engels, (2005) Flavour formation by lactic acid bacteria and biochemical flavour profiling of cheese products. *FEMS Microbiology Reviews* **29**: 591-610.

Smit, J., H. Engelhardt, S. Volker, S. H. Smith & W. Baumeister, (1992) The S-layer of Caulobacter crescentus: three-dimensional image reconstruction and structure analysis by electron microscopy. *J Bacteriol* **174**: 6527-6538.

Smith, K. D., E. Andersen-Nissen, F. Hayashi, K. Strobe, M. A. Bergman, S. L. R. Barrett, B. T. Cookson & A. Aderem, (2003) Toll-like receptor 5 recognizes a conserved site on flagellin required for protofilament formation and bacterial motility. *Nat Immunol* **4**: 1247-1253.

Smith, K. D. & A. Ozinsky, (2002) Toll-like receptor-5 and the innate immune response to bacterial flagellin. *Curr Top Microbiol Immunol* **270**: 93-108.

Sommer, J. M. & A. Newton, (1988) Sequential regulation of developmental events during polar morphogenesis in Caulobacter crescentus: assembly of pili on swarmer cells requires cell separation. *J Bacteriol* **170**: 409-415.

Sorenson, M. K., S. S. Ray & S. A. Darst, (2004) Crystal structure of the flagellar sigma/anti-sigma complex sigma(28)/FlgM reveals an intact sigma factor in an inactive conformation. *Mol Cell* **14**: 127-138.

Sosinsky, G. E., N. R. Francis, M. J. Stallmeyer & D. J. DeRosier, (1992) Substructure of the flagellar basal body of Salmonella typhimurium. *J Mol Biol* **223**: 171-184.

Sperandio, V., A. G. Torres & J. B. Kaper, (2002) Quorum sensing Escherichia coli regulators B and C (QseBC): a novel two-component regulatory system involved in the regulation of flagella and motility by quorum sensing in E. coli. *Mol Microbiol* **43**: 809-821.

Stafford, G. P. & C. Hughes, (2007) Salmonella typhimurium flhE, a conserved flagellar regulon gene required for swarming. *Microbiology (Reading, Engl)* **153**: 541-547.

Stallmeyer, M. J., K. M. Hahnenberger, G. E. Sosinsky, L. Shapiro & D. J. DeRosier, (1989) Image reconstruction of the flagellar basal body of Caulobacter crescentus. *J Mol Biol* **205**: 511-518.

Stephens, C., C. Mohr, C. Boyd, J. Maddock, J. Gober & L. Shapiro, (1997) Identification of the fliI and fliJ components of the Caulobacter flagellar type III protein secretion system. *Journal of bacteriology* **179**: 5355-5365.

Taguchi, F. & Y. Ichinose, (2011) Role of type IV pili in virulence of Pseudomonas syringae pv. tabaci 6605: correlation of motility, multidrug resistance, and HR-inducing activity on a nonhost plant. *Mol Plant Microbe Interact* **24**: 1001-1011.

Taguchi, F., M. Yamamoto, M. Ohnishi-Kameyama, M. Iwaki, M. Yoshida, T. Ishii, T. Konishi & Y. Ichinose, (2010) Defects in flagellin glycosylation affect the

virulence of Pseudomonas syringae pv. tabaci 6605. *Microbiology (Reading, Engl)* **156**: 72-80.

Terashima, H., H. Fukuoka, T. Yakushi, S. Kojima & M. Homma, (2006) The Vibrio motor proteins, MotX and MotY, are associated with the basal body of Na-driven flagella and required for stator formation. *Mol Microbiol* **62**: 1170-1180.

Terashima, H., M. Koike, S. Kojima & M. Homma, (2010) The flagellar basal body-associated protein FlgT is essential for a novel ring structure in the sodium-driven Vibrio motor. *J Bacteriol* **192**: 5609-5615.

Terry, K., S. M. Williams, L. Connolly & K. M. Ottemann, (2005) Chemotaxis plays multiple roles during Helicobacter pylori animal infection. *Infect Immun* **73**: 803-811.

Thanbichler, M., A. A. Iniesta & L. Shapiro, (2007) A comprehensive set of plasmids for vanillate- and xylose-inducible gene expression in Caulobacter crescentus. *Nucleic Acids Research* **35**: e137.

Thormann, K. M. & A. Paulick, (2010) Tuning the flagellar motor. *Microbiology (Reading, Engl)* **156**: 1275-1283.

Tokuda, H. & T. Unemoto, (1982) Characterization of the respiration-dependent Na+ pump in the marine bacterium Vibrio alginolyticus. *J Biol Chem* **257**: 10007-10014.

Tsokos, C. G., B. S. Perchuk & M. T. Laub, (2011) A dynamic complex of signaling proteins uses polar localization to regulate cell-fate asymmetry in Caulobacter crescentus. *Dev Cell* **20**: 329-341.

Twine, S. M., C. W. Reid, A. Aubry, D. R. McMullin, K. M. Fulton, J. Austin & S. M. Logan, (2009) Motility and flagellar glycosylation in Clostridium difficile. *J Bacteriol* **191**: 7050-7062.

Uchida, K., M.-S. Jang, Y. Ohnishi, S. Horinouchi, M. Hayakawa, N. Fujita & S.-I. Aizawa, (2011) Characterization of Actinoplanes missouriensis spore flagella. *Appl Environ Microbiol* **77**: 2559-2562.

Ueno, T., K. Oosawa & S. Aizawa, (1992) M ring, S ring and proximal rod of the flagellar basal body of Salmonella typhimurium are composed of subunits of a single protein, FliF. *Journal of Molecular Biology* **227**: 672-677.

Ueno, T., K. Oosawa & S. Aizawa, (1994) Domain structures of the MS ring component protein (FliF) of the flagellar basal body of Salmonella typhimurium. *Journal of Molecular Biology* **236**: 546-555.

Van Way, S. M., E. R. Hosking, T. F. Braun & M. D. Manson, (2000) Mot protein assembly into the bacterial flagellum: a model based on mutational analysis of the motB gene. *J Mol Biol* **297**: 7-24.

Verma, A., M. Schirm, S. K. Arora, P. Thibault, S. M. Logan & R. Ramphal, (2006) Glycosylation of b-Type flagellin of Pseudomonas aeruginosa: structural and genetic basis. *J Bacteriol* **188**: 4395-4403.

Visick, K. L. & M. J. McFall-Ngai, (2000) An exclusive contract: specificity in the Vibrio fischeri-Euprymna scolopes partnership. *J Bacteriol* **182**: 1779-1787.

Wadhams, G. H. & J. P. Armitage, (2004) Making sense of it all: bacterial chemotaxis. *Nat Rev Mol Cell Biol* **5**: 1024-1037.

Wagner, J. K. & Y. V. Brun, (2007) Out on a limb: how the Caulobacter stalk can boost the study of bacterial cell shape. *Molecular Microbiology* **64**: 28-33.

Wagner, J. K., S. Setayeshgar, L. A. Sharon, J. P. Reilly & Y. V. Brun, (2006) A nutrient uptake role for bacterial cell envelope extensions. *Proc Natl Acad Sci USA* **103**: 11772-11777.

Wang, S., R. T. Fleming, E. M. Westbrook, P. Matsumura & D. B. McKay, (2006) Structure of the Escherichia coli FlhDC complex, a prokaryotic heteromeric regulator of transcription. *Journal of Molecular Biology* **355**: 798-808.

Wei, B. L., A. M. Brun-Zinkernagel, J. W. Simecka, B. M. Prüss, P. Babitzke & T. Romeo, (2001) Positive regulation of motility and flhDC expression by the RNA-binding protein CsrA of Escherichia coli. *Mol Microbiol* **40**: 245-256.

Weissborn, A., H. M. Steinmann & L. Shapiro, (1982) Characterization of the proteins of the Caulobacter crescentus flagellar filament. Peptide analysis and filament organization. *J Biol Chem* **257**: 2066-2074.

Whitchurch, C. B., T. Tolker-Nielsen, P. C. Ragas & J. S. Mattick, (2002) Extracellular DNA required for bacterial biofilm formation. *Science* **295**: 1487.

Wilhelms, M., R. Molero, J. G. Shaw, J. M. Tomás & S. Merino, (2011) Transcriptional Hierarchy of Aeromonas hydrophila Polar-Flagellum Genes. *Journal of bacteriology* **193**: 5179-5190.

Williams, A. W., S. Yamaguchi, F. Togashi, S. I. Aizawa, I. Kawagishi & R. M. Macnab, (1996) Mutations in fliK and flhB affecting flagellar hook and filament assembly in Salmonella typhimurium. *J Bacteriol* **178**: 2960-2970.

Wingrove, J. A. & J. W. Gober, (1994) A sigma 54 transcriptional activator also functions as a pole-specific repressor in Caulobacter. *Genes & Development* **8**: 1839-1852.

Wu, J., N. Ohta & A. Newton, (1998) An essential, multicomponent signal transduction pathway required for cell cycle regulation in Caulobacter. *Proc Natl Acad Sci USA* **95**: 1443-1448.

Xu, Z., R. J. Dutton & J. W. Gober, (2011) Direct interaction of FliX and FlbD is required for their regulatory activity in Caulobacter crescentus. *BMC Microbiol* **11**: 89.

Yamamoto, S. & K. Kutsukake, (2006) FliT acts as an anti-FlhD2C2 factor in the transcriptional control of the flagellar regulon in Salmonella enterica serovar typhimurium. *J Bacteriol* **188**: 6703-6708.

Yan, L., Q. Yang, J. Jiang, T. J. Michailides & Z. Ma, (2011) Involvement of a putative response regulator Brrg-1 in the regulation of sporulation, sensitivity to fungicides, and osmotic stress in Botrytis cinerea. *Appl Microbiol Biotechnol* **90**: 215-226.

Yang, L., Y. Liu, H. Wu, N. Hóiby, S. Molin & Z.-j. Song, (2011) Current understanding of multi-species biofilms. *Int J Oral Sci* **3**: 74-81.

Yokoseki, T., K. Kutsukake, K. Ohnishi & T. Iino, (1995) Functional analysis of the flagellar genes in the fliD operon of Salmonella typhimurium. *Microbiology (Reading, Engl)* **141 (Pt 7)**: 1715-1722.

Yonekura, K., S. Maki, D. G. Morgan, D. J. DeRosier, F. Vonderviszt, K. Imada & K. Namba, (2000) The bacterial flagellar cap as the rotary promoter of flagellin self-assembly. *Science* **290**: 2148-2152.

Yonekura, K., S. Maki-Yonekura & K. Namba, (2003) Complete atomic model of the bacterial flagellar filament by electron cryomicroscopy. *Nature* **424**: 643-650.

Zanen, G., H. Antelmann, H. Westers, M. Hecker, J. M. van Dijl & W. J. Quax, (2004) FlhF, the third signal recognition particle-GTPase of Bacillus subtilis, is dispensable for protein secretion. *Journal of bacteriology* **186**: 5956-5960.

Zhou, J., S. A. Lloyd & D. F. Blair, (1998) Electrostatic interactions between rotor and stator in the bacterial flagellar motor. *Proc Natl Acad Sci USA* **95**: 6436-6441.

Zhu, K., B. González-Pedrajo & R. M. Macnab, (2002) Interactions among membrane and soluble components of the flagellar export apparatus of Salmonella. *Biochemistry* **41**: 9516-9524.

Zhuang, W. Y. & L. Shapiro, (1995) Caulobacter FliQ and FliR membrane proteins, required for flagellar biogenesis and cell division, belong to a family of virulence factor export proteins. *J Bacteriol* **177**: 343-356.

Zimmer, D. P., E. Soupene, H. L. Lee, V. F. Wendisch, A. B. Khodursky, B. J. Peter, R. A. Bender & S. Kustu, (2000) Nitrogen regulatory protein C-controlled genes of Escherichia coli: scavenging as a defense against nitrogen limitation. *Proceedings of the National Academy of Sciences of the United States of America* **97**: 14674-14679.